

PROCEEDINGS

International Symposium on GeoInformatics for Spatial-Infrastructure Development in Earth and Allied Sciences

Chiang Rai, Thailand, 11-13 December 2024



CONFERENCE CHAIRS : Venkatesh RAGHAVAN & Phaisarn JEEFOO

EDITORS : Natraj VADDADI, Sittichai CHOOSUMRONG & Chaiwiwat VANSAROCHANA



Osaka
Metropolitan
University



Association of GeoInformatics Laboratories for Earth Sciences
Technical Document 1



GIS-IDEAS 2024

DECEMBER 11 to 13TH 2024

UNIVERSITY OF PHAYAO (UP)

CHIANG RAI, THAILAND

ORGANISED BY

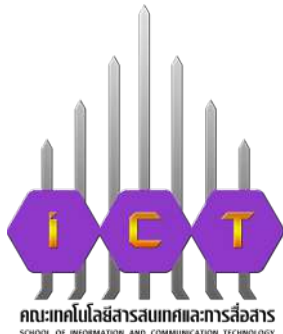
SCHOOL OF ICT, UNIVERSITY OF PHAYAO (UP)

NARESUAN UNIVERSITY (NU)

OSAKA METROPOLITAN UNIVERSITY (OMU)

ASSOCIATION OF GEOINFORMATICS LABORATORIES FOR EARTHSCIENCES (AGILE)

■ Organizers



Osaka
Metropolitan
University



■ Partners



GIS-IDEAS

GeoInformatics for Spatial - Infrastructure Development in Earth & Allied Sciences

The International Conference on GeoInformatics for Spatial-Infrastructure Development in Earth & Allied Sciences (GIS-IDEAS) provides a platform for sharing of knowledge and valuable experiences and help promote collaborations and scientific exchanges between not only between students, researchers and practitioners Japan, Vietnam and Thailand but also our other colleagues involved in developing and promoting GeoInformatics technologies. The conduct of GIS-IDEAS Conferences is based on the spirit of mutual cooperation and openness.

GIS-IDEAS is planned around a central theme which is decided in consultation with the host institution. Apart from Technical Sessions on GeoInformatics technologies and applications, Special sessions on different topics related to Geo-informatics are also held during the conference.

GIS-IDEAS is organized in collaboration with premier institutes located in Asia. GIS-IDEAS which was founded in 2002 to develop and promote Geoinformatics applications and foster cooperation in application of Information and Communication Technologies to problems and issues related to our natural and social environment. To achieve these aims, the conference aims to;

- ◆ support capacity building through organization of symposia, workshops and fieldwork.
- ◆ share information resources and know-how in Geoinformatics
- ◆ promote research collaborations and joint research in Geoinformatics
- ◆ promote exchange of information and academic publications
- ◆ develop a human resource network to support development and growth of Geoinformatics

Previous GIS-IDEAS Conferences were organized in collaboration with premier institutions like Can Tho University (VN), Danang University of Education (VN), Japan Geotechnical Consultant Association (JP), Japan Society of Geoinformatics (JP), Hanoi University of Mining and Geology (VN), Hanoi University of Natural Resources & Environment (VN), Ho Chi Minh City University of Technology (VN), Kyoto University (JP), Naresuan University Thailand, Osaka City University (JP), Osaka Metropolitan University (JP), Vietnam National University (VN) and others.

From the Conference Chairs

Our best wishes to the GIS-IDEAS Community for a Happy New Year! We are very happy to bring out this volume of the GIS-IDEAS 2024 Conference Proceedings, that was held from December 11–13 in the vibrant city of Chiang Rai, Thailand. As we look back at this exciting event, we feel immense satisfaction to continue the proud tradition of fostering global collaboration and innovation in geoinformatics that began with the establishment of the Japan-Vietnam Geoinformatics Consortium (JVGC) in 2001.

The GIS-IDEAS 2024 conference provided a unique platform to exchange ideas, share knowledge, and explore the latest advancements in spatial sciences, urban planning, and environmental sustainability. The beautiful and culturally rich Chiang Rai offered an excellent venue to discuss how Geoinformatics can address some of the most pressing global challenges. With a program that included inspiring keynote speeches, dynamic technical sessions, and hands-on workshops, GIS-IDEAS 2024 promises to deliver insights and solutions that will resonate well beyond the event.

We extend our heartfelt thanks to all the contributors whose research enriches the proceedings of this conference. Our deepest appreciation to our wonderful host the University of Phayao and to various conference committees, faculty, staff, and students who work tirelessly to ensure the event's success. Special acknowledgment is due to our sponsors and supporters, whose generous contributions enable us to create a collaborative and vibrant platform to showcase innovations and current trends in Geoinformatics research and application. We also express our thanks to the editors and manuscript reviewers and commend their hard work to bringing out the proceedings in a timely manner.

Together, we hope to kindle innovative ideas, foster meaningful collaborations, and deepen the connections that unite the Geoinformatics community worldwide. Your participation and support are integral to the success of GIS-IDEAS 2024, and we look forward to the insights, discoveries, and partnerships that this conference will inspire.

Thank you Chiang Rai!, and See you at GIS-IDEAS 2026!! Warm regards,

Phaisarn JEEFOO & Venkatesh RAGHAVAN

Chairs, GIS-IDEAS 2025

Dt: January 2025

The Committees

Conference Founders

- ◆ Late Prof. Takashi FUJITA - Japan
- ◆ Dr. Nghiem Vu KHAI - Vietnam

General Chairs

- ◆ Phaisarn JEEFOO - Thailand
- ◆ Venkatesh RAGHAVAN - Japan

General Co-Chairs

- ◆ Pornthep ROJANAVASU - Thailand
- ◆ Krittika KANTAWONG
(IEEE SPS Thailand Chapter, IEEE#94103612)
- ◆ Sittichai CHOOSUMRONG - Thailand
- ◆ Chaiwiwat VANSAROCHANA - Thailand

Financial Chair

- ◆ Jirabhorn CHAIWONGSAI - Thailand

Technical Program Chair

- ◆ Sawarin LERK-U-SUKE - Thailand

Technical Program Co-Chairs

- ◆ Punnarumol Temdee
(IEEE SPS Thailand Chapter, IEEE#94471090)
- ◆ Pradorn Sureephong
(IEEE SPS Thailand Chapter, IEEE#98063511)
- ◆ Kampanart PIYATHAMRONGCHAI - Thailand

Publication Chairs

- ◆ Sakkayaphop Pravetjit - Thailand
- ◆ Paveen Khoenkaw
- ◆ (IEEE SPS Thailand Chapter, IEEE#94052729)

Organizing Secretaries

- ◆ Tatsuya NEMOTO - Japan
- ◆ Truong Xuan QUANG - Vietnam
- ◆ Tanayaluck CHANSOMBAT - Thailand

Web And Media Committee Chairs

- ◆ Natraj VADDADI - India
- ◆ Pongsakorn SIRIKAMNOI - Thailand

Special Session Chair

- ◆ Saksit IMMAN - Thailand
- ◆ Sitthisak PINMONGKHONKUL - Thailand

Steering Committee

- ◆ Ho Dinh DUAN - Vietnam
- ◆ Huynh Thi Lan HUONG - Vietnam
- ◆ Yasuyuki KONO - Japan
- ◆ Nguyen Kim LOI - Vietnam
- ◆ Truong Xuan LUAN - Vietnam
- ◆ Lam Dao NGUYEN - Vietnam
- ◆ Le Thi TRINH - Vietnam
- ◆ Nitin TRIPATHI - Thailand
- ◆ Yasushi YAMAGUCHI - Japan
- ◆ Song XIANFENG - China
- ◆ Chalermpchai PAWATTHANA - Thailand
- ◆ Teerawong LAOSUWAN - Thailand
- ◆ Kanchana NAKHAPAKORN - Thailand
- ◆ Ornprapa P. ROBERT - Thailand
- ◆ Arisara CHAROENPANYANET - Thailand
- ◆ Kritchayan INTARAT - Thailand
- ◆ Satith SANGPRADID - Thailand
- ◆ Wirote LAONGMANEE - Thailand
- ◆ Phurith MEEPROM - Thailand
- ◆ Supaporn MANAJITPRASERT - Thailand
- ◆ Pattana RACHAWONG - Thailand

Scientific Committee

- ◆ Tran Thi AN - Vietnam
- ◆ Tran Van ANH - Vietnam
- ◆ Sanit ARUNPLOD - Thailand
- ◆ Nakarin CHAIKAEW - Thailand
- ◆ Niti IAMCHUEN - Thailand
- ◆ Atsushi KAJIYAMA - Japan
- ◆ Rangsan KET-ORD - Thailand
- ◆ Jiraporn KULSOONTORNRAT - Thailand
- ◆ Surenda Rama SITARAMAN - (US)
- ◆ Susumu NONOGAKI - Japan
- ◆ Sarawut NINSAWAT - Thailand
- ◆ Wipop PAENGWANGTHONG - Thailand
- ◆ Vinayaraj POLIYAPRAM - Japan
- ◆ Bowonsak SRISUNGSISSINTI - Thailand
- ◆ Boonsiri SUKPROMSUN - Thailand
- ◆ Pham Thi Mai THY - Vietnam
- ◆ Go YONEZAWA - Japan

The Keynote speakers

DR PAKORN PETCHPRAYOON



Dr. Pakorn Petchprayoon is the Director of the Geo-Informatics Product Innovation Office at the Geo-Informatics and Space Technology Development Agency (GISTDA). His research focuses on understanding the physical processes of energy exchange between the land and water surfaces and the atmosphere by integrating satellite data with direct field measurements. Dr. Petchprayoon has dedicated 23 years to GISTDA, contributing in various research and leadership roles. He has authored and co-authored several publications and was a lecturer on GEOG 4093 Remote Sensing of the Environment at the University of Colorado, Boulder, USA. Dr. Petchprayoon holds a B.S. from Burapha University, M.S. from Mahidol University, and M.A. and Ph.D. from the University of Colorado-Boulder, USA.

DR SUSUMU NONOGAKI



Dr. Susumu Nonogaki is a Geo-informaticist and Chief Senior Researcher at the Geological Survey of Japan, National Institute of Advanced Industrial Science and Technology (AIST). He earned his Ph.D. in Geosciences from Osaka City University in 2009 and specializes in 3D modeling and analysis of shallow subsurface geological structures in urban areas of Japan. His expertise encompasses GIS analysis, spatial interpolation, machine learning, geo-visualization, and web mapping. From 2005 to 2012, he lectured on GIS techniques for sustainable natural resource management and agricultural productivity in JICA training programs. Since 2010, he has been a member of the Scientific Committee for GIS-IDEAS. His work supports urban development and planning, contributing to safer, more sustainable cities through improved understanding of urban geological conditions.

PROF. SONG XIANFENG



Prof. Song Xianfeng is a distinguished expert in Geographic Information Sciences (GIS) and Remote Sensing Hydrology, focusing on geospatial data mining using vehicle GNSS trajectories, cellular network signalling, and DVR data. He holds an MS in Remote Sensing Geology (1995) from China University of Mining & Technology, along with a PhD in GIS from the Chinese Academy of Sciences (1998). He is presently serving as a Professor at the University of Chinese Academy of Sciences since 2011, following roles as Associate Professor and Assistant Professor there and at Kyoto University. His industry experience includes managing IT for the Chinese Investment Corporation for Sciences and Technology.

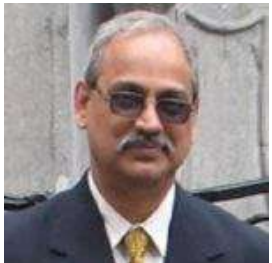
The Keynote speakers

DR TRAN VAN ANH



Dr. Tran Van Anh is a lecturer at Hanoi University of Mining and Geology (HUMG). She obtained her Master's degree in Surveying and Mapping Engineering from HUMG, Vietnam, in 2001 and her PhD degree in GeoInformatics from Osaka City University (Japan) in 2007. Her field of study is remote sensing and GIS. She has working interests in Radar Interferometry (InSAR) for land deformation detections and optical images for air pollution (PM10) determination. Besides that, she also works on geospatial data research and builds predicting models. She has had more than 50 works published in prestigious domestic and international journals.

DR NATRAJ VADDADI



Dr. Natraj Vaddadi, an Executive Member of the Governing Council at the Centre for Education & Research in Geosciences, is a geologist specializing in Urban Groundwater Recharge through Rainwater Harvesting. He holds a Master's degree in Geology from the University of Pune and a Ph.D. in Natural Resources and Environment from Naresuan University, Thailand. With over three decades of teaching experience, he serves as a Visiting Professor in Petroleum Technology at Nowrosjee Wadia College and teaches postgraduate courses in Drilling Engineering and Production Operations at the University of Pune.

Dr. Vaddadi has conducted numerous workshops on Open-Source GIS in India, Thailand, and Vietnam and is the author of the internationally acclaimed book *An Introduction to Oil Well Drilling*. As a founding member of the Centre for Education & Research in Geosciences, he advocates for geoscience education, promoting its integration into environmental conservation and sustainability initiatives.

GIS-IDEAS 2024 – CONTENTS

S. No	Title	Authors	Page #
1	Grasp of inundated areas after a tsunami disaster using satellite remote sensing data and GIS	Shouyi GAO and Mitsugu SAITO	1
2	Presenting the flood hazard analysis in Wangtong district, lower north Thailand using geo-informatics techniques with open access program: HAZMAPPER	Kittituch Naksri and Chaiwiwat Vansarochana	9
3	Assessing land use function change in urban area: a case study of Vung Tau city	Tran Duy Hung <i>et al.</i>	17
4	Climate change impacts of agricultural production in the coastal area of Thi Nai lagoon, Binh Dinh province: an analysis of the Livelihood Vulnerability Index	Vu Khac Hung	23
5	Application of GIS to build a land database in a mountainous district of son la province, Vietnam	Tran Hong Hanh <i>et al.</i>	34
6	Oil spill in the southern marine regions of Vietnam: models and simulations	Phan Minh-Thu <i>et al.</i>	47
7	Predicting land-use change using GIS and machine learning - a case study in Tuyen Quang city, Vietnam	Bui Ngoc Tu <i>et al.</i>	60
8	Investigating land subsidence by processing multi-temporal SAR time series on Google Colab: case study in Camau city, Mekong delta, Vietnam	Ha Trung Khien <i>et al.</i>	69
9	Estimate the amount of carbon emissions from deforestation and forest degradation over two decades in Kon Ha Nung plateau, Gia Lai province, Vietnam	Nguyen Huu Viet Hieu <i>et al.</i>	79
10	Extracting travel distance and slope failure height using oriented bounding boxes	Tatsuya Nemoto <i>et al.</i>	89
11	A study on the distribution of village names derived from vegetation in northeastern Thailand, Cambodia, and Laos	Nagata Yoshikatsu	95

12	Applying Geoinformatics technology for building webGIS to support drainage management in Ninh Kieu and Cai Rang districts of Can Tho city.	Nguyen Thanh Ngan <i>et al.</i>	103
13	3D urban geological information development for resilient society	Susumu Nonogaki ¹	108
14	Relationship between compound extreme indices and atmospheric circulation patterns in Thailand	Teerachai Amnuaylojaroen <i>et al.</i>	115
15	Processing and analysing multi-source, multi-resolution geospatial data on cloud platforms for some environmental and disaster applications	Tran Van Anh <i>et al.</i>	125
16	Geological consideration for development in banding island, Malaysia using remote sensing and GIS	Mohammad Firuz Ramli <i>et al.</i>	137
17	Mapping soil pollution in Camau city, Vietnam	Ho Dinh Duan	138
18	Identification of morphological features in slope failure areas due to heavy rainfall using change vector analysis and random forest classifier	Mitsunori Ueda <i>et al.</i>	139
19	Investigation of machine learning models for slope failure susceptibility zonation in parts of yen bai province, Vietnam	Tran Tung Lam <i>et al.</i>	140
20	Advancing Geoscience and Geospatial awareness through educational outreach: the CERG story	Natraj Vaddadi	141
21	Establishment of groundwater database in the coastal area of Soc Trang province by using QGIS	Nguyen Vo Chau Ngan	142

GRASP OF INUNDATED AREAS AFTER A TSUNAMI DISASTER USING SATELLITE REMOTE SENSING DATA AND GIS

Shouyi GAO¹ and Mitsugu SAITO²

¹ Design and Media Technology, Graduate School of Engineering, Iwate University
Address: 4-3-5 Ueda, Morioka, Iwate 020-8551 Japan Email: s3321003@iwate-u.ac.jp

² Design and Media Technology, Graduate School of Engineering, Iwate University
Address: 4-3-5 Ueda, Morioka, Iwate 020-8551 Japan

ABSTRACT

With the launch of high-resolution remote sensing satellites, remote sensing technology has been providing valuable information in various fields such as natural resource exploration, ecological environment protection, and meteorological disaster prediction. However, due to the influence of satellite orbit cycles and climate conditions, it is challenging to obtain sufficient time-series images with high spatial and temporal resolution. This limitation affects the accuracy of inundation area extraction after flooding disasters using remote sensing. This study investigates an analytical method to identify flood-affected areas using satellite remote sensing data and GIS systems. Focusing on the coastal areas of Miyagi Prefecture after the 2011 Great East Japan Earthquake, we conducted binarization processing of satellite image data and explored a method to accurately extract inundation areas by integrating the Normalized Difference Water Index (NDWI) and Normalized Difference Snow Index (NDSI) from Landsat 7, as well as land surface temperature (LST) from MODIS11A2.

Keywords—Satellite data; GIS systems; NDWI; LST; NDSI; Inundated Area

1. INTRODUCTION

Following a tsunami or flood disaster, large-scale collapses of forests and buildings can result in debris that obscures the inundated areas, making it difficult to accurately determine the full extent of the flooding. In situations where the disaster impacts a wide region or urgent rescue operations are required, it becomes crucial to quickly identify passable road routes. Efficient visualization of tsunami-inundated areas is essential for facilitating a swift and effective response.

With growing concern about the potential Nankai Trough megathrust earthquake, it is increasingly important to address the large-scale tsunami inundation damage that could result. Accurate identification of tsunami-inundated areas is a critical prerequisite for effective disaster management and response strategies.

In recent years, the launch of high-resolution remote sensing satellites has significantly enhanced the ability of remote sensing technology to provide valuable information in fields such as natural resource monitoring, environmental conservation, and meteorological disaster forecasting. The Japanese government has also made strides in developing systems to assess disaster conditions through satellite technology. Notably, the Cabinet Office's Strategic Innovation Promotion Program (SIP) developed a "Disaster Situation Analysis and Sharing System,¹⁾" which was completed in 2022. This system enables the rapid provision of essential satellite data to the government and local municipalities within two hours of a disaster. Satellite imagery is increasingly indispensable in visualizing disaster-affected regions and plays a crucial role in supporting relief efforts following earthquakes, tsunamis, and other natural disasters.

2. RESEARCH METHODS

2.1 Study Area

This study focuses on the coastal towns and cities of Miyagi prefecture, which were severely impacted by the widespread tsunami following the Great East Japan Earthquake on March 11, 2011. Areas highlighted in Figure. 1 have been selected as the study region for their extensive tsunami-related damage.

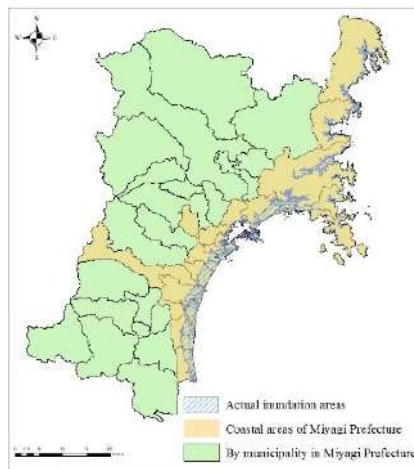


Figure 1. Miyagi Prefecture.

2.2 System

2.2.1 Hardware:

The computations have been performed on a standard PC laptop with a 12th Gen Intel (R) Core (TM) i7-12700H 2.70 GHz and 16 GB memory (MSI Vector GP76 12UH).

2.2.2 Software:

The software ArcGIS version 10.8.1.14362

2.2.3 Data Processing

- Miyagi Prefecture Tsunami Inundation Area Polygon Data After the 2011 Great East Japan Earthquake:

We confirmed the extent of tsunami inundation using GIS, referring to the tsunami inundation maps from the Geospatial Information Authority of Japan²⁾.

- Satellite Data:

We used satellite image data from Landsat 7 ETM+ (observed on March 12, 2011) and MODIS/Terra Land (observed on March 14, 2011).

- Quarry Database:

We used data from the "Current Status Survey of Quarries in the Tohoku Region" conducted by the Quarry Research Group in 2021³⁾.

- National Digital Road Map Database (Miyagi Prefecture Primary Roads) :

We used the "National Digital Road Map Database Standard, Version 3.17. 4)"

3. METHODOLOGY

3.1 Extraction of Normalized Difference Water Index (NDWI) Values

The NDWI value is expressed by equation (1):

$$NDWI = \frac{NIR - Green}{NIR + Green} \quad \dots \dots \dots \quad (1)$$

NIR: The reflectance in the 0.76-0.89 μm wavelength range

Green: The reflectance in the 0.52-0.60 μm wavelength range

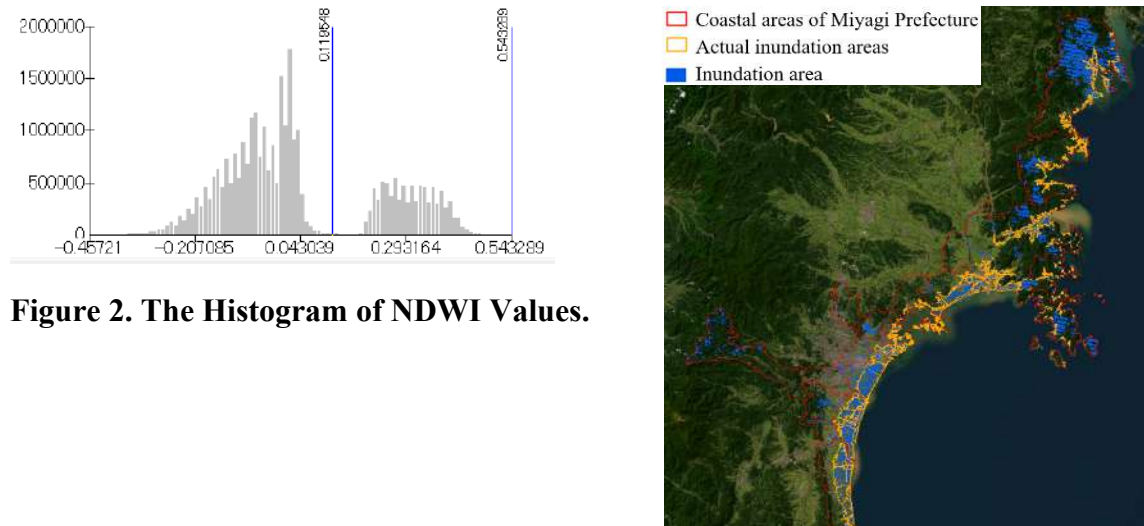


Figure 2. The Histogram of NDWI Values.

Figure 3. The Inundated Area Extracted Using NDWI Values.

Figure. 2 shows the histogram of NDWI values (x-axis) and the number of data points (y-axis) for the inundated areas along the coast of Miyagi Prefecture as of March 12, 2011.

The histogram generated by the mode method is bimodal, suggesting that the NDWI value histogram consists of both water and non-water areas. The minimum value in the valley between the two peaks was set as the threshold for NDWI values⁵⁾.

Figure. 3 shows the GIS image of the inundated area extracted using NDWI values.

3.2 Extraction of Land Surface Temperature (LST Day_1km) Values

When the land surface is covered with water, a change in land surface temperature occurs due to the presence or absence of water⁶⁾. We attempted to extract the inundated area using land surface temperature data.

The calculation of LST is performed using the Generalized Split-Window method (GSW method)⁷⁾, estimating the surface temperature from the observed brightness temperatures T31 and T32 of MODIS data Bands 31 and 32 through equation (2).

$$LST = \left(A_1 + A_2 \frac{1-\epsilon}{\epsilon} + A_3 \frac{\Delta\epsilon}{\epsilon^2} \right) \frac{T_{31}+T_{32}}{2} + \left(B_1 + B_2 \frac{1-\epsilon}{\epsilon} + B_3 \frac{\Delta\epsilon}{\epsilon^2} \right) \frac{T_{31}-T_{32}}{2} + C \quad \dots \dots \dots \quad (2)$$

A_i : Regression coefficient ($i=1,2,3$)

B_i : Observation angle ($i=1,2,3$)

C : Precipitable water

$$\epsilon = 0.5(\epsilon_{31} + \epsilon_{32}) \quad \Delta\epsilon = \epsilon_{31} - \epsilon_{32}$$

$\epsilon_{31}, \epsilon_{32}$: Surface emissivity of MODIS satellite data Band 31 and 32

Based on the distribution of LST values along the coast of Miyagi Prefecture on March 14, 2011 (Figure. 4), and the temperature distribution trends near the actual inundation line, we hypothesized a threshold of 12°C for LST values and extracted areas with LST values below 12°C as inundated areas.

Figure. 5 shows the GIS image of the inundated area extracted using LST values.

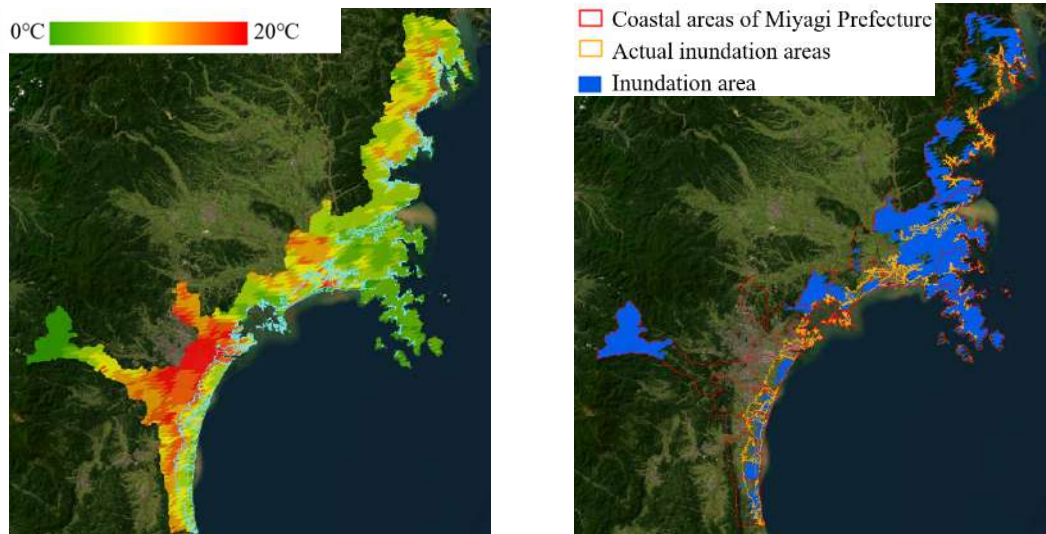


Figure 4. LST Distribution Map of the Coastal Areas of Miyagi Prefecture on March 14, 2011.

Figure 5. The Inundated Area Extracted Using LST Values.

3.3 Extraction of Inundation Areas through Integrated Analysis of NDWI and LST Values

Using the two datasets of inundation areas derived from NDWI and LST values, we integrated the extracted inundation area using the GIS Union function.

Figure. 6 shows the GIS visualization of the extracted inundation area. In ArcGIS, the area was calculated to be 1,198.28 km².

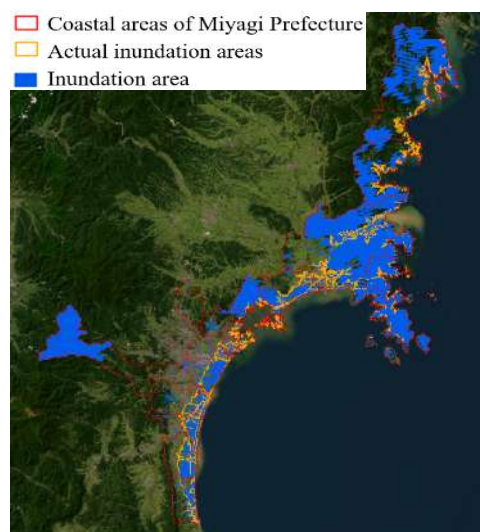


Figure 6. The Inundated Area Extracted Using NDWI and LST Values.

3.4 Extraction of Snow-Covered Areas Using the Normalized Difference Snow Index (NDSI)

To identify snow-covered surfaces, we attempted to extract NDSI values using Landsat_TM (Band 2 Green and Band 5 SWIR). Snow-covered areas exhibit high reflectance in the green band and low reflectance in the shortwave infrared (SWIR) band. NDSI values were calculated using equation (3)⁸⁾:

$$NDSI = \frac{Green - SWIR}{Green + SWIR} \quad \dots \dots \dots \quad (3)$$

Green: The pixel value of the green band

SWIR: The pixel value of the shortwave infrared band

Figure. 7 shows the histogram of NDSI values (x-axis) and the number of data points (y-axis) for the inundated areas along the coast of Miyagi Prefecture as of March 12, 2011. Given the bimodal distribution, snow-covered areas were determined to have NDSI values of 0.4 or higher⁹⁾.

Figure. 8 shows the GIS visualization of snow-covered areas extracted using NDSI values. In ArcGIS, the area was calculated to be 557.53 km².

Using the integrated analysis of NDWI and LST values to extract inundated areas, we removed the snow-covered areas identified by NDSI values.

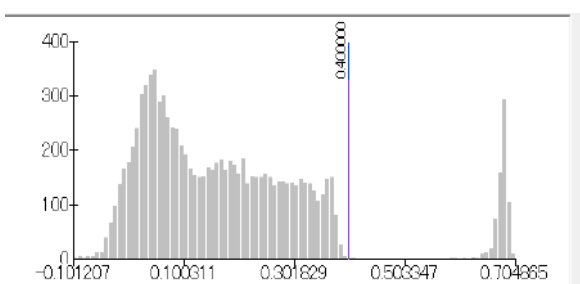


Figure 7. The Histogram of NDSI Values.

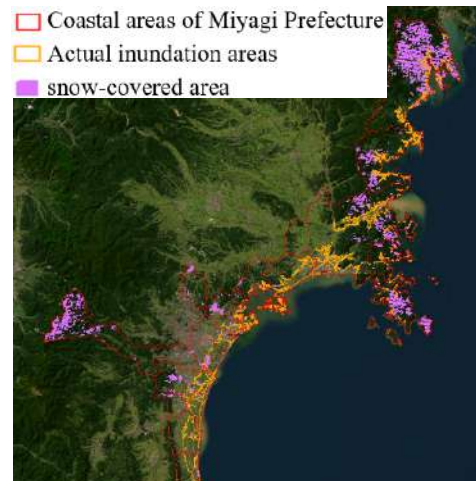


Figure 8. The Snow-Covered Area Extracted Using NDSI Values.

3.5 Removal of Snow-Covered Areas from Inundation Areas Through Integrated Analysis of NDWI and LST Values

Using the integrated analysis of NDWI and LST values to extract inundated areas, we removed the snow-covered areas identified by NDSI values.

Figure. 9 shows the integrated inundated areas, Figure. 10 shows the snow-covered areas, and Figure. 11 shows the inundated areas after removing the snow-covered areas from the integrated analysis of NDWI and LST values. In ArcGIS, the area was calculated to be 640.75 km².

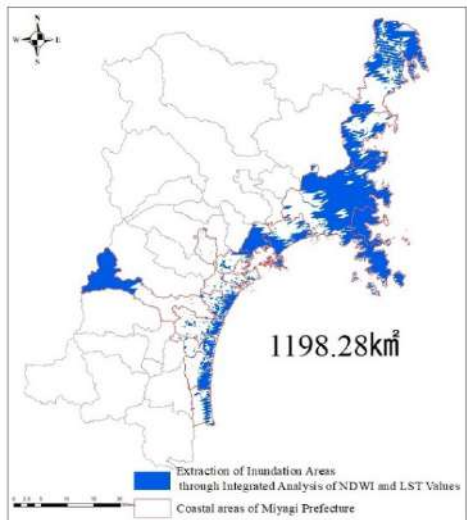


Figure 9. The Inundated Area.

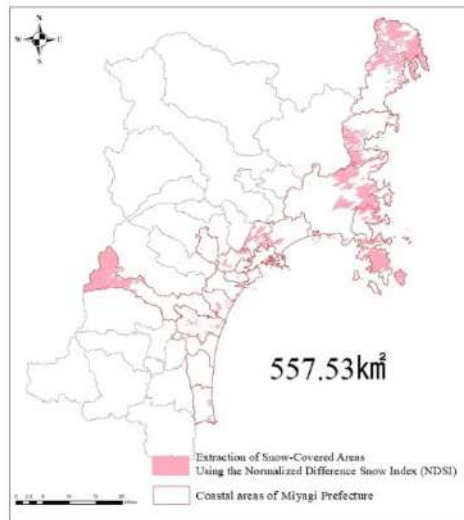


Figure 10. The Snow-Covered Area.

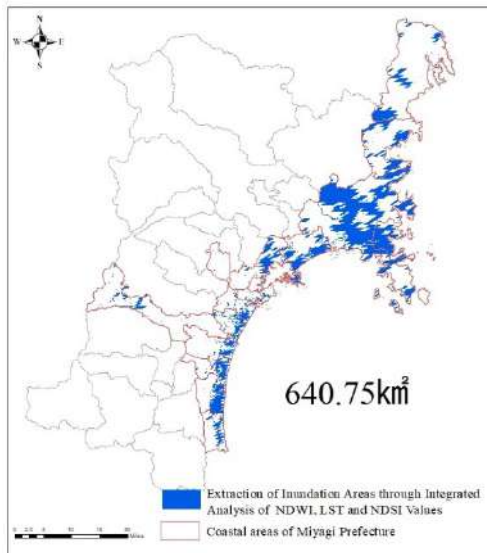


Figure 11. Detection of Inundated Areas by Excluding Snow-Covered Regions Using Integrated NDWI and LST Analysis

4. RESULTS

The results of the tsunami inundation extraction, utilizing an integrated analysis of NDWI and LST values, revealed that areas obscured by debris—such as collapsed buildings and sediment deposited by the tsunami—were inadequately identified as water zones when relying solely on NDWI data. However, the incorporation of LST data significantly enhanced the accuracy of water body extraction.

Moreover, by excluding snow-covered areas identified through the NDSI from the inundated regions extracted via the integrated NDWI and LST analysis, we effectively minimized false extractions in flood zone estimations. The area extracted from the actual inundated region was calculated to be 199.72 km², with an occupancy rate of 65% (Figure).

12./TABLE 1). Considering that the satellite images were captured several hours after the tsunami event, it is likely that some floodwaters had already receded. Overall, this methodology demonstrates significant potential as a valuable tool for accurately identifying inundated areas following a tsunami event.

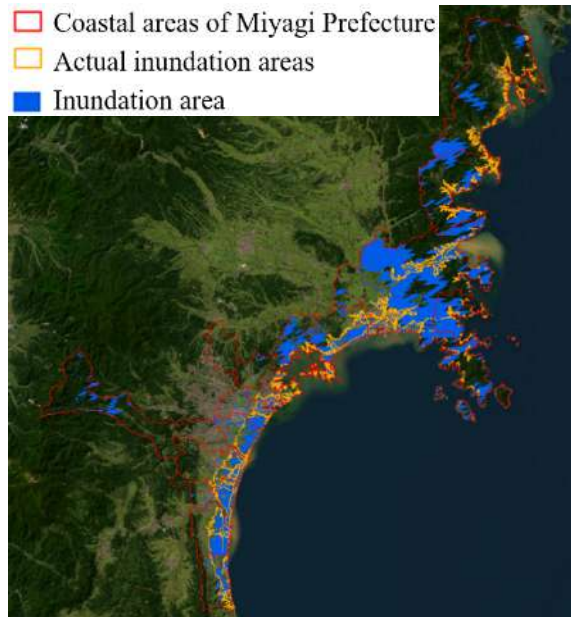


Figure 12. Detection of Inundated Areas by Excluding Snow-Covered Regions Using Integrated NDWI and LST Analysis

Table 1. Flood Zone Estimation Results and Occupancy Rates Excluding Snow-Covered Areas

Actual inundation areas:307.69 km ²	NDWI + LST – NDSI
Extracted area within the actual inundated region	199.72 km ²
Occupancy rate within the actual inundated region	65%

5. CONCLUSION

The inherent limitations of satellite data, particularly in terms of resolution and susceptibility to cloud cover during image capture, lead to frequent misidentification in flood-prone areas. These inaccuracies present challenges in constructing reliable aggregate transportation route models. To address this, future research must focus on improving the accuracy of flood zone delineation by leveraging a combination of high-resolution satellite datasets, advanced image processing techniques, and machine learning algorithms.

6. ACKNOWLEDGMENT

I would like to express my heartfelt gratitude to Professor Noritaka Endo, formerly of the Graduate School of Integrated Science at Iwate University, for providing the ArcGIS software used in this research. His generous support and invaluable guidance have been essential to the progress of this study.

7. REFERENCES

- "Satellites, Drones, and Social Media: Rapid Assessment of Damage" Kazushima Itto, Tanaka Hina, Takatsuki Yoshikazu, Nakata Atsushi, Nikkei Computer, March 2, 2021
<https://xtech.nikkei.com/atcl/nxt/mag/nc/18/022400216/022400004/>
- Crane, R. G., and Anderson, M. R., 1984, Satellite discrimination of snow/cloud surfaces. International Journal of Remote Sensing, 5(1), 213 -223.
- Dozier, J., 1984, Spectral signature of alpine snow cover from the Landsat Thematic Mapper. Remote Sensing of Environment, 28.9-22.
- Geospatial Information Authority of Japan, Ministry of Land, Infrastructure, Transport and Tourism: Details of Inundation Areas <http://fukkou.csis.u-tokyo.ac.jp/dataset/show/id/1110>
- Ichiro Tamagawa, Michio Yamada, Shuichi Ikebuchi, Yasushi Mitsuta: "On the Relationship between Surface Moisture Content and Surface Temperature Variations," Annual Report of the Disaster Prevention Research Institute, Kyoto University, No. 31B-1, 1988
- Masahito Fukumoto: "Identification of Water Intake Start Period for Paddy Fields Using Sentinel-2 Satellite Data," System Agriculture (J.JASS), 35(2): 15–23, 2019
- Nationwide Digital Road Map Database Standard Edition 3.17, January 2021 (Reiwa 3), Edited and Published by Japan Digital Road Map Association
- Takaaki Amanuma, Mitsugu Saito: "Survey on the Current Status of Quarries in the Tohoku Region" conducted by the Quarry Research Association in 2021 (Reiwa 3)
- Wan Z M and Dozier J. 1996. A generalized split-window algorithm for retrieving land-surface temperature from space. IEEE Transactions on Geoscience and Remote Sensing, 34(4): 892–905 [DOI:10.1109/36.508406]

PRESENTING THE FLOOD HAZARD ANALYSIS IN WANGTONG DISTRICT, LOWER NORTH THAILAND USING GEO-INFORMATICS TECHNIQUES WITH OPEN ACCESS PROGRAM: HAZMAPPER

Kittituch Naksri¹ and Chaiwiwat Vansarochana²

¹Master of Science Program in Geographic Information Science
Naresuan University, Phitsanulok 65000 Thailand.
E-mail: kittituchn67@nu.ac.th

²Corresponding author: Associate Professor, Faculty of Agriculture,
Natural Resources and Environment Naresuan University
E-mail: ChaiwiwatV@nu.ac.th

ABSTRACT

Flooding remains a pervasive issue in Thailand, causing significant economic losses and affecting community well-being. This study evaluates the effectiveness of the Hazmapper program in assessing flood-induced vegetation loss, in Wang Thong District, Phitsanulok, Thailand, following the flood event of October 8, 2023. The primary objective is to assess the capability of Hazmapper in detecting and quantifying vegetation changes using the relative difference NDVI (rdNDVI) approach.

The Hazmapper program utilizes Sentinel-2 satellite imagery, with a pre-event observation period of 15 days and a post-event period of 9 days, to compute rdNDVI values. This methodology involves comparing vegetation indices before and after the flood to quantify vegetation loss. Geographic data from sources such as Google Earth and Google Maps were integrated to refine spatial accuracy and context.

The rdNDVI values indicated negative values in regions where vegetation had diminished due to flooding. These results were corroborated by visual comparisons of satellite imagery taken before and after the event, demonstrating a noticeable decline in green vegetation in inundated regions.

This study also highlighted several limitations associated with the Hazmapper program. First, the rdNDVI values are computed for entire areas, including regions not directly affected by flooding, such as harvested fields and deforested lands. This broad coverage can dilute the accuracy of flood impact assessments. Second, Hazmapper's reliance on vegetation indices limits its effectiveness in detecting flooding in non-vegetated or barren areas. In short-duration floods, minimal vegetation loss may result in negligible rdNDVI values, reducing the program's sensitivity to such events.

In conclusion, this study demonstrates that Hazmapper is an effective tool for evaluating flood-induced vegetation loss, offering valuable information for disaster response and recovery efforts. The program's application of satellite imagery and vegetation indices provides significant benefits for understanding and managing the impacts of flooding on vegetation and the environment.

Keywords: NDVI, rdNDVI, Flood hazard, Repeatable analysis, Accuracy.

1. INTRODUCTION

Waterlogging and flash floods remain persistent challenges in Thailand, contributing to substantial economic losses and adversely affecting community living conditions, and the overall water management in river basins. To address these issues, local administrative organizations have increasingly integrated information technology systems for community management, including the development of Geographic Information System (GIS) databases to support a wide range of operational tasks.

Enhancing the efficiency of GIS databases requires a thorough understanding of the underlying causes of flooding and the development of proactive response plans. This can be facilitated by utilizing the Hazmapper program, a GIS tool that integrates Sentinel and Landsat

data with vegetation difference indices. Analyzed through various tools in the QGIS platform, HazMapper enables the calculation of rdNDVI values for different time periods within the same area. Moreover, it allows for combining satellite imagery with statistical data, offering a comprehensive approach to predicting the timing and severity of future disasters.

HazMapper (Hazard Mapper) is an open-access application developed within Google Earth Engine, designed to rapidly assess natural disasters. [Scheip M. C., \(2021\)](#) It caters to both scientific research and emergency management communities by monitoring landscape changes, particularly those affecting terrestrial vegetation due to natural disasters or human activities. However, the platform is currently limited to vegetated environments, restricting its application to areas without significant vegetation cover.

2. DESIGN PRINCIPLES

The Vegetation Index serves as a quantitative measure of the vegetation coverage on the Earth's surface, calculated using the ratio of specific wavelength ranges associated with vegetation. One of the most commonly employed methods for this calculation is the Normalized Difference Vegetation Index (NDVI). NDVI uses the difference in reflectance between the near-infrared (NIR) and red wavelengths, divided by their sum, to produce a normalized distribution of vegetation values.

NDVI values typically range from -1 to 1, facilitating interpretation. A value of 0 indicates the absence of green vegetation in the observed area, while values of 0.8 or 0.9 signify dense vegetation cover. When vegetation is present, the reflectance in the NIR wavelength exceeds that of the red wavelength, resulting in a positive NDVI value. Conversely, bare soil tends to reflect both wavelengths, similarly, yielding an NDVI close to 0. Water bodies, which reflect less in the NIR than in the red wavelength, often display negative NDVI values. Generally, NDVI values fall within the range of 0.1 to 0.7. [Scheip M. C., \(2021\)](#)

The formula for NDVI is expressed as follows:

$$NDVI = \left(\frac{NIR - RED}{NIR + RED} \right)$$

Where:

- NIR = Reflectance in the near-infrared wavelength (%)
- RED = Reflectance in the red visible wavelength (%)

HazMapper utilizes a variation of the NDVI technique known as the Relative Difference Normalized Difference Vegetation Index (rdNDVI). Instead of using true-color composites (i.e., red-green-blue bands) [Wegmann K., and Scheip C., \(2020\)](#), HazMapper detects changes in surface vegetation by calculating and differencing NDVI values from the greenest-pixel composite images pre- and post-event. The rdNDVI formula is as follows:

$$rdNDVI = \left(\frac{NDVI_{post} - NDVI_{pre}}{\sqrt{NDVI_{pre} + NDVI_{post}}} \right) \times 100$$

Here, NDVI_pre and NDVI_post represent the NDVI images generated from the greenest-pixel composites before and after the event, respectively. This processing routine

produces a normalized percentage reflecting the gain or loss in vegetation. The normalization includes the pre-event NDVI to account for areas where vegetation levels were already low.

The HazMapper workflow culminates in the generation of georeferenced Tagged Image File Format (GeoTIFF) files, which can be imported into GIS software for further analysis or visualization. If specific areas of interest or hazards—such as landslides, burn scars, or inundation extents—are identified, they can be digitized and exported as Keyhole Markup Language (KML) files for sharing or viewing in Google Earth.

3. CASE STUDY

An example of a flood-affected area is Wang Thong District, Phitsanulok Province, on October 8, 2023, located at a latitude of 16°49'20.5"N and a longitude of 100°25'48.7"E.

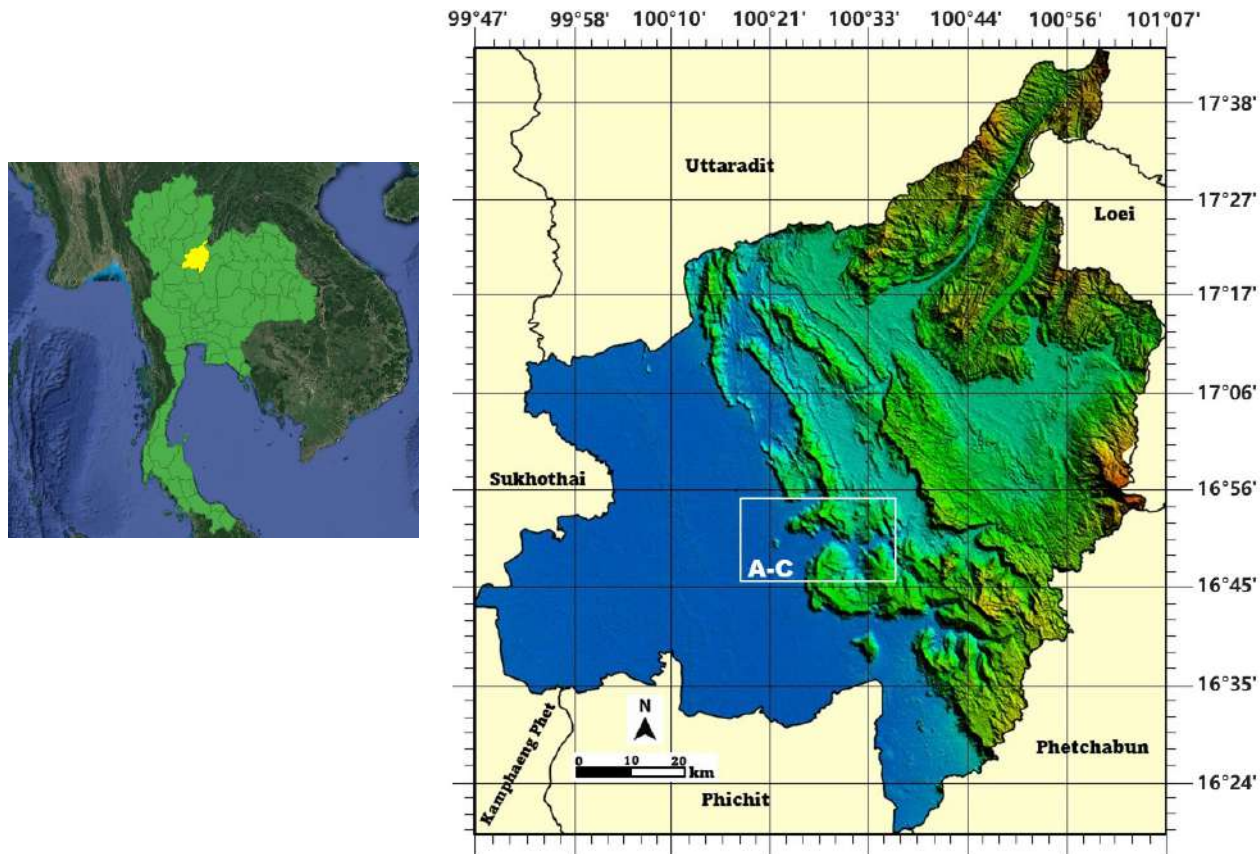


Figure 1. Topographical map of study area. <https://www.mitrearth.org/m38-phitsanulok/>

4. DATA SOURCE

The spatial data required for this study, particularly concerning natural hazards and landscape changes over a specified time period, was collected from multiple sources including Google Earth, Google Maps, and GIS databases, as well as natural disaster records. The Hazmapper program was employed to identify areas affected by flooding, utilizing analyses of vegetation index losses resulting from flood events.

5. ILLUSTRATIONS

The Hazmapper program identified areas affected by flooding in Wang Thong District, Phitsanulok Province, on October 8, 2023.

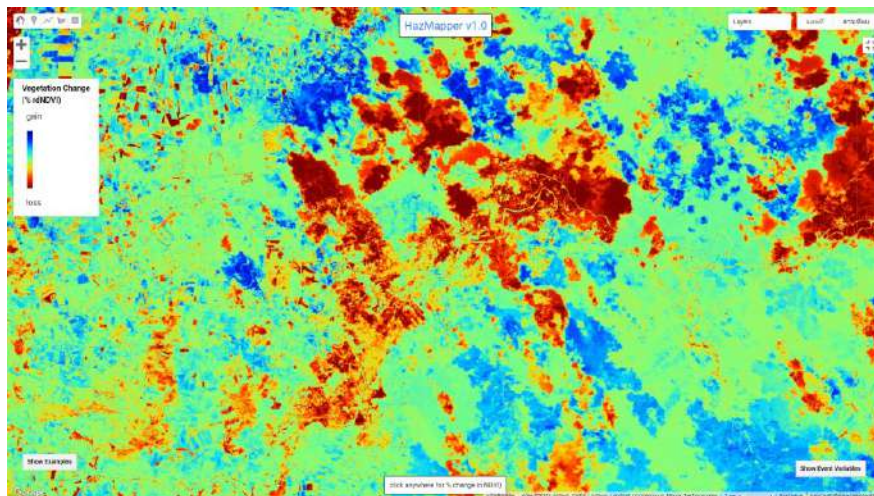


Figure 2. Vegetation Change in Hazmapper program

Use this link to view the results in Figure 2.

https://cmscheip.users.earthengine.app/view/hazmapper?fbclid=IwZXh0bgNhZW0CMTAAAR3sXZ0WPsubau0xncKjxnAH-StvTKHZWxmoxUEaqWPQfoDvVAP3ropFQLY_aem_w4a61kZ-NCSXk23moNp5pg#lon=100.47404070329924;lat=16.841299367017427;zoom=13;dataset=0;prewindow=0.5;postwindow=0.3;maxCloudCover=30;slopeThreshold=0;eventDate=20231008;

GIS data from the Hazmapper program in the study area before and after the incident.

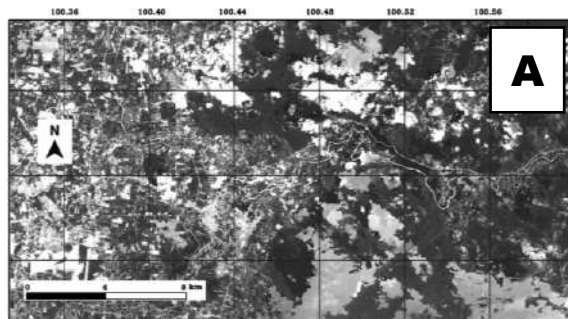


Figure 3. Pre-event, 15 days

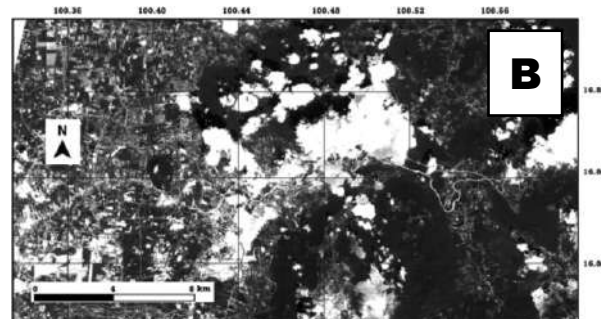


Figure 4. Post-event, 9 days

The results of the relative difference NDVI (rdNDVI) analysis indicate a loss of vegetation due to flooding. rdNDVI was employed to monitor environmental changes following the flood event on October 8, 2023, in Wang Thong District, Phitsanulok Province, Thailand. The inset map highlights the location of the flood, which posed a threat to local communities. Within three days, the water levels receded from key trade routes.

The analysis utilized Sentinel-2 data with a pre-event window of 15 days and a post-event window of 9 days, allowing for a maximum cloud cover of 30% and a slope threshold of

0° . The region experienced prolonged rainfall during the rainy season, with runoff from surrounding mountains causing the river to overflow, leading to the flood event.

The comparison of pre- and post-event images (A and B) reveals significant environmental changes. The base image (A) captures conditions after the event, while the pre-event image (B) shows the landscape dominated by relatively dense green vegetation. Nine days after the event, the post-event composite shows a noticeable decline in vegetation, primarily due to flooding. This reduction is captured by negative rdNDVI values, as illustrated in (C).

Environmental Monitoring of Vegetation Loss in Wang Thong District, Phitsanulok, Thailand, Using rdNDVI Following the Flood Event on October 8, 2023

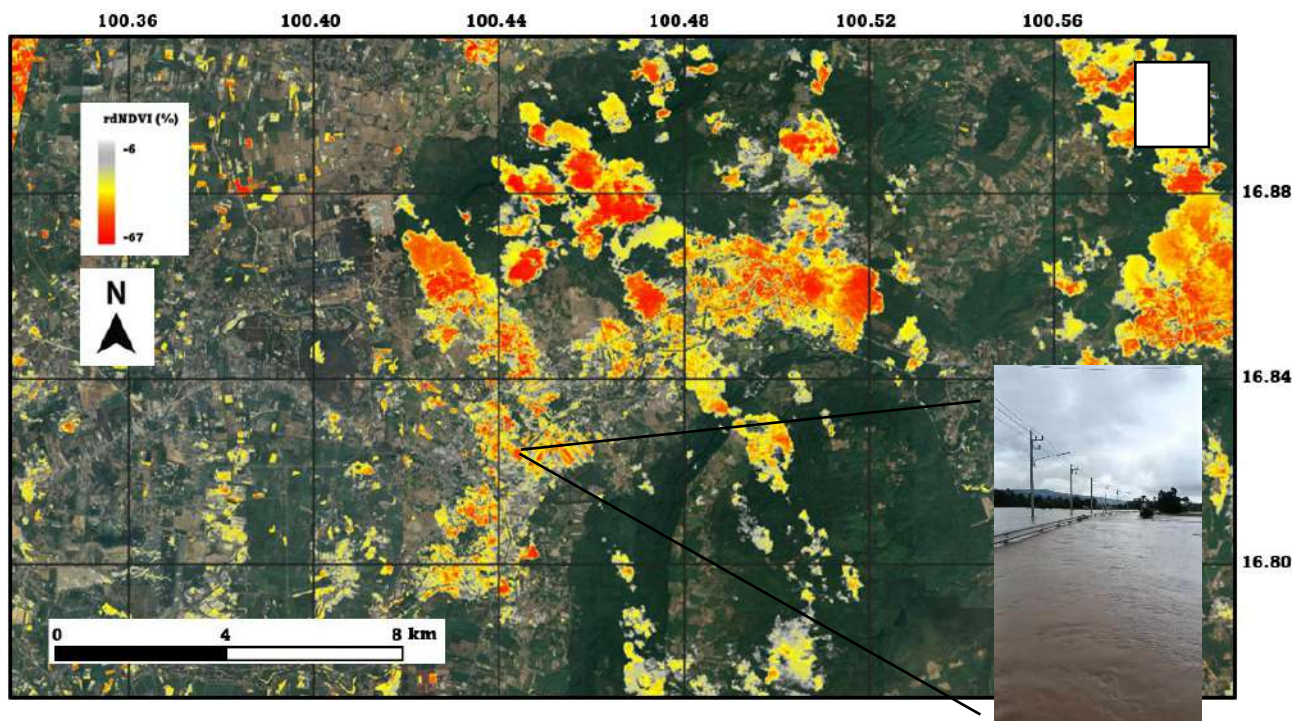


Figure 5. Environmental monitoring using rdNDVI in Wang Thong District, Phitsanulok Province, Thailand, after the flooding event on October 8, 2023. The map indicates areas affected by flooding, where vegetation loss was detected through negative rdNDVI values. The comparison between pre- and post-event images shows a decline in vegetation due to the flood. Image (A) represents conditions after the event, while image (B) illustrates the green vegetation cover before the event. The reduction in vegetation is visualized in image (C) through negative rdNDVI values.

6. TABLES 1. HazMapper input variables, definition, selected

Input variables	Definition	Selected
Dataset	Dataset to use for analysis, currently Landsat 7, Landsat 8, or Sentinel-2	Sentinel-2 (10 m) 2015+
Event date	Date of storm, earthquake, weather event, etc.	8 October 2023
Pre-event window	The number of months to use for observing the greenest pixel-by-pixel conditions prior to the event	0.5 (15 day)
Post-event window	The number of months to use for observing the greenest pixel-by-pixel conditions following the event	0.3 (9 day)
Maximum cloud cover	The maximum percentage of a scene obscured by clouds and still used in the analysis; the cloud-cover percent is embedded in the metadata for each Landsat or Sentinel scene	30
Slope threshold	A minimum topographic slope value in degrees, less than which will be omitted from the data visualization; this is helpful to remove water bodies like lakes and adjacent oceans in coastal regions	0

TABLES 2. Comparison table of advantages and disadvantages of Hazmapper program

Advantages	Disadvantages
1. Accurate Measurement of Vegetation Changes Utilizes rdNDVI to precisely analyze vegetation loss due to flooding.	1. Includes Non-Relevant Areas Hazmapper computes rdNDVI values across the entire area, including non-relevant regions such as harvested rice fields and deforested land.
2. Utilizes Sentinel-2 Satellite Data Provides high-resolution data on surface and vegetation conditions.	2. Incomplete Flood Coverage May not fully capture the extent of flooding in areas without vegetation, as rdNDVI depends on vegetation indices.
3. Facilitates Vegetation Change Monitoring Convenient for tracking and analyzing vegetation changes using satellite imagery.	3. Less Effective for Short-Duration Floods Minimal vegetation loss in short-duration floods may result in negligible rdNDVI values, making it less effective for such events.
4. Access to Data through Google Earth Engine Provides free and accessible data and tools.	4. Data Gaps from Satellite Blind Spots May result in blank areas in outputs due to gaps or blind spots in satellite imagery, depending on the data layers used.
5. Assists in Vegetation Recovery Analysis Useful for tracking and analyzing vegetation recovery post-disaster.	5. Cannot Predict Unaffected Areas Inability to measure or predict values for areas where flooding has not yet occurred, limiting pre-event analysis.

7. CONCLUSIONS

This study highlights the effectiveness of the Hazmapper program in evaluating vegetation loss due to flooding, with a specific focus on Wang Thong District, Phitsanulok Province. The application of rdNDVI through Hazmapper has proven valuable in identifying and quantifying the impact of flood events on vegetation. The use of high-resolution Sentinel-2 satellite imagery allowed for detailed analysis, revealing significant changes in vegetation cover as a result of flooding.

Nevertheless, several limitations of Hazmapper were identified. The program generates rdNDVI values across entire areas, including regions not directly affected by flooding, such as harvested rice fields and deforested lands, which can dilute the accuracy of flood impact assessments. Moreover, Hazmapper's reliance on vegetation indices means it may not effectively capture flooding in non-vegetated or barren areas. Short-duration floods, which may result in minimal vegetation loss, can also lead to negligible rdNDVI values, limiting the program's effectiveness for such events. Additionally, data gaps due to satellite blind spots and the inability to predict flooding in areas yet to be affected further constrain its application.

Despite these limitations, Hazmapper remains a useful tool for environmental monitoring and disaster management. It provides valuable insights into vegetation changes and recovery post-flood, leveraging accessible satellite data. Future enhancements and complementary analytical approaches could address these limitations, improving the program's capability to capture a more comprehensive range of flood impacts and other environmental changes.

8. REFERENCES

- Kaewthamrong, K., and Taitaku, D., (2019) Department of Landscape Architecture, Faculty of Architecture, Chulalongkorn University, Thailand, Identification of Floodplain Boundary and Relationship between Flood Pulsing and Human Adaptation: Case Study of Middle Mun River Basin <https://so05.tci-thaijo.org/index.php/sarasatr/article/view/189662>
- Kirschbaum, D., Watson, C. S., Rounce, D. R., Shugar, D. H., Kargel, J. S., Haritashya, U. K., Amatya, P., Shean, D., Anderson, E. R., and Jo, M., (2019) The State of Remote Sensing Capabilities of Cascading Hazards Over High Mountain Asia, *Front. Earth Sci.*, 7, 197, <https://www.frontiersin.org/journals/earthscience/articles/10.3389/feart.2019.00197/full>
- Opperman, J. J., P. B. Moyle, E. W. Larsen, J. L., (2018) Department of Physical and Environmental Geography, Institute of Geography and Earth Sciences, University of Pécs Pécs Hungary Florsheim and A, Manfree. Floodplains: Processes and Management for Ecosystem Services. https://www.researchgate.net/publication/326094217_Opperman_JJ_Moyle_PB_Larsen_EW_Florsheim_JL_and_Manfree_AD_Floodplains_Processes_and_Management_for_Ecosystem_Services
- Pailoplee, S., (2019). Department of Geology, Faculty of Science, Chulalongkorn University, Pathumwan, Bangkok, 38 Phitsanulok: Geography. Map. <https://www.mitrearth.org/m38-Phitsanulok/>
- Scheip M. C., and Wegmann W. K., (2021) Natural Hazards and Earth System Sciences, HazMapper: A global open-source natural hazard mapping application in Google Earth Engine. <https://nhess.copernicus.org/articles/21/1495/2021/>

Tantranee, S., (2014). Community Water Drainage Management Using Geospatial Information. Naresuan University Engineering Journal, 5(2), 1–9. <https://doi.org/10.14456/nuej.2010.4>

Wegmann K., and Scheip C., (2020) North Carolina State University, Evaluation of the HazMapper Google Earth Engine Application.

Weier J. and Herring D., (2000) Measuring Vegetation, Normalized Difference Vegetation Index. (NDVI)

ASSESSING LAND USE FUNCTION CHANGE IN URBAN AREA: A CASE STUDY OF VUNG TAU CITY

**Tran Duy Hung^{1*}, Le Hoang Tu¹, Nguyen Kim Loi¹, Vo Thi Hong Quyên²,
Ho Dinh Duan³,**

¹Nong Lam University, Ho Chi Minh city, Vietnam

²HCMC Institute of Resources Geography, Tay Nguyen Institute for Scientific Research, Ho Chi Minh city,
Vietnam

³Corresponding author, Mien Trung Institute for Scientific Research, Hue, Vietnam
Corresponding Email: duanhd@gmail.com

ABSTRACT

Vung Tau city is a class-I city of Ba Ria - Vung Tau province. The city is undergoing rapid urbanization with the expansion of the urban land, concurrent with the process of land function change. This study aimed to assess land function change in the city over the 2010-2015 and 2015-2020 periods. GIS and Markov chains techniques were applied to assess land function change of Vung Tau city. Through converting the land use code from purpose to function, the study has synthesized and identified 3 groups of land functions including civil land, non-civil land and other land. The results of assessing land function changes showed that civil and non-civil land continuously expands with an average expansion rate of +11.7% and +14.87% for the two periods. Meanwhile, other land continuously shrinks with an average rate of -5.39% for the two periods. The results of assessing land functions change in Vung Tau city can provide a basis for evaluating the local urban space development process.

Keywords. Land use, Land function, Urban transition, Markov chain, Transition matrix, Vung Tau city

1.1.1. INTRODUCTION

Land use change is a phenomenon that has been occurring worldwide. There are many causes of this change, such as urbanization, infrastructure development, population growth, deforestation, mining etc.. The common issue behind all these causes is, the changing of land use purposes. If the change is reasonable, it will contribute to effective exploitation of land resources. However, today's land use changes tend to fully exploit land resources, limiting the area of forest land and reserve land, causing degradation and affecting other factors such as floods, erosion, waste of resources [1]. Changes in land use types have great significance in affecting water flow, soil erosion, and climate change. The consequences of land degradation are floods and droughts, being very dangerous for humans and natural resources [2].

Vung Tau city in Southern Vietnam has recently undergone a strong economic restructuring process that has changed the land use structure. It also has shortcomings in the process of urban development in general and urban land use in particular. The process of arranging urban land use functions for many different purposes: urban residential areas, commercial areas, services, tourism and urban infrastructure under the pressure of development has revealed many defects, leading to fragmentation and lack of synchronization. Researching the process of land use structure transformation according to the urban spatial development structure through each stage is important to properly determine the urban development process and determine the driving factors; from which land use and implementation solutions can be proposed.

To assess land use changes over time, there are many approaches one of them is using the method of overlaying land use data at different points of time, as commonly used in GIS, while others combined with the power of Markov chains in statistics. Mundia et al [3] applied Markov

chains to forecast land use change in Nakuru city, Kenya. Similarly, Islam and Ahmed [4] used Landsat images and Markov models to determine land use changes in Dhaka city, Bangladesh. Based on the results of monitoring the evolution of land use changes from 1991 to 2008, the author has created a map predicting land use changes in 2020 and 2050. Many studies have demonstrated the application of Markov chains and GIS to evaluate effective land use changes. As a result of these novel approaches, managers have a better overview on the situation and apply appropriate methods for decision making, supporting the improvement of integrated management in the urbanization trend.

This study uses Markov chain to evaluate and predict the changes in land use functions, thereby providing an important basis in planning and adjusting urban development space projections, land use planning and urban management of Vung Tau city.

1.1.2. THE STUDY AREA

Vung Tau city has a total natural area of 15,089.60 hectares, accounting for 7.6% of the natural area of the province (198,256 hectares); Located in the south of Ba Ria - Vung Tau province, 120 km from Ho Chi Minh City and 100 km east of Bien Hoa city, there are 17 affiliated administrative units including 16 wards and one commune (Long Son). Vung Tau City has three sides bordering the sea with a total coastline length of 48.1 km [5].

The average GDP growth rate of the city is 12.5% per year. Over the past 15 years, the economic structure of Vung Tau City has shifted towards increasing trade - services, industry and handicrafts, gradually reducing the proportion in the agriculture - forestry - fishery sector [5]. The city has diverse land use types and a fast urbanization process. The city has oriented its urban structure towards a civilized - green - clean - beautiful sea city. Vung Tau City is a class 1 urban city that simultaneously functions as a tourism, port service and oil and gas exploitation centre of the country [6].

1.1.3. MATERIAL AND METHODOLOGY

1.2. Land use purposes vs land use functions

Many studies have conducted assessment of land use changes according to land use purposes [7-9]. In this study, land changes are evaluated according to land use functions. Pursuant to Article 10 of the Land Law 2013 of Vietnam [10], land use is divided according to purpose of use into the following 3 main groups: (i) Agricultural land (Land for annual crops includes Rice land and other annual crop land, perennial crop land, production forest land, etc.) are groups of land related to the purpose of use for agricultural production; (ii) Non-agricultural land (Residential land, Land for building agency headquarters, Land for defense and security purposes, etc.); and (iii) Unused land.

In addition to the above purpose-based classification urban land is furthermore classified according to land use functions [11,12]. This classification is for future planning and construction functions. Accordingly, urban construction land is land for construction of urban functional areas (including urban projected infrastructure systems). Development reserve land, agricultural and forestry land in urban areas and other types of land that do not serve urban functions are not urban construction land. Urban construction land is land arranged to build urban functional areas according to planning approved by competent state agencies. According to their functions, urban land is divided into two main groups: (i) civil land and (ii) non-civil

land [11,13]. Land for construction of civil activity includes residential, urban public facilities, public service, urban public green land space, and urban infrastructure. To obtain information for assessment of changes in land use functions, the study collected data from official land use maps of the study area in 2010, 2015, and 2020.

1.3. Assessment methods for Land use function changes in the period 2010, 2015 and 2020

This study applied the Markov chain model [15] to determine the possibility of changing the structure of land use functions based on data of land use functions in 2010, 2015, and 2020, respectively. The generation of the Markov chain is illustrated in Figure 1. The probability of change of functional soil types (γ_{ij}) is determined through the overlay technique of digital map data of functional soil types at the stated times. Specifically, functional land types at different times will be assigned different codes. Then, we use the overlay tool on the land use function map of 2010 and 2015 as well as 2015 and 2020 (Figure 2). Finally, a statistical analysis is conducted on the changes in areas of functional land types to calculate the probability of changes and evaluate the changes through the value of the probability of functional land types.

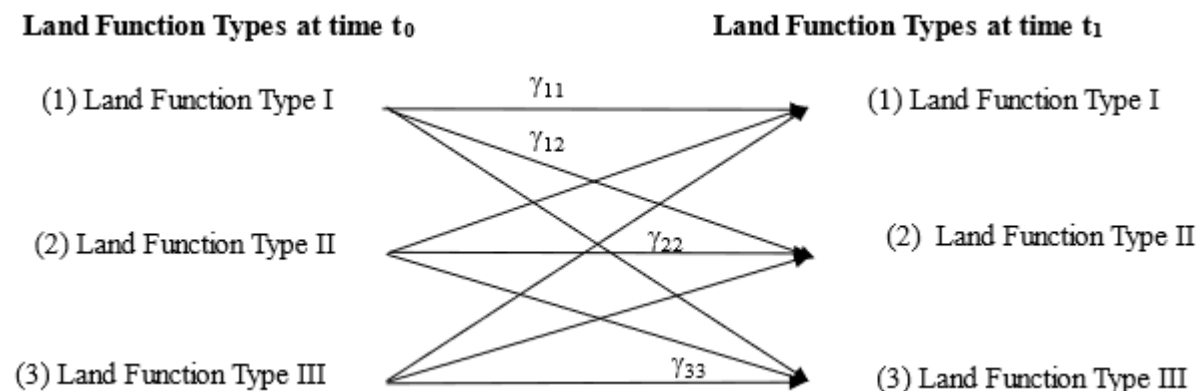
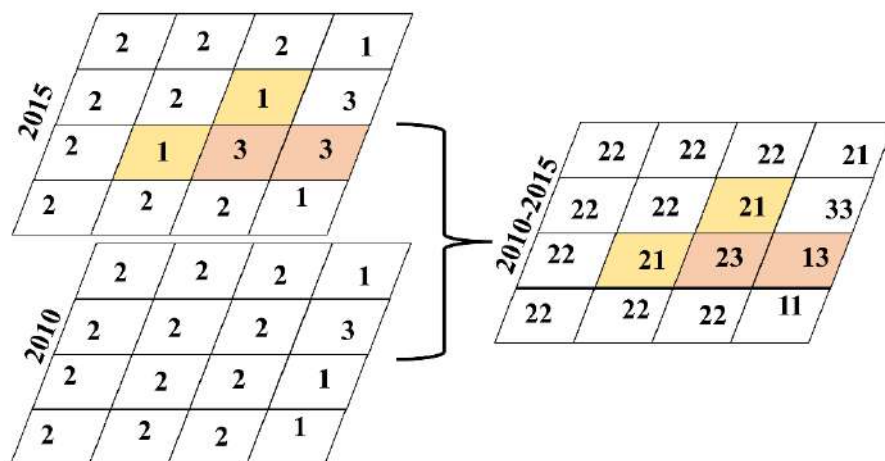


Figure 1. Illustration of Markov chain model for assessing the land function change.



Note: Land Function Type I (1); Land Function Type II (2); Land Function Type III (3)

Figure 2. Illustration of overlay technique for assessing the land functions change.

4. RESULTS AND DISCUSSIONS

4.1. Assessment of land function changes through the periods

Based on statistical analysis from digital map data of land use function types, we can see that among the types of land use functions, the “Other” types of land functions always account for a dominant percentage of the area (72.4 %, 68.33% and 64.81%) compared to other functional land types including civil and non-civilian land at the respective times of 2010, 2015 and 2020 (Table 3). Over the three periods of 2010, 2015 and 2020 in the study area, the area of civil land increased continuously from more than 2,418.1 hectares to 2,642.76 and 3,015,751 hectares. Meanwhile, non-residential land also tends to increase, in 2010 it was 1,763.16 hectares, in 2015 it was 2,156.31 and in 2020 it was 2,316.44 hectares. On the contrary, because of the stability of the natural land area of the study area (15,151.8 hectares), compared to the types of civil and non-civil functions, type “Others” tend to decrease over time. Specifically, in 2010 it was 10,970.54 hectares, then in 2015 it decreased to 10,352.73 hectares and in 2020 it was 9819.61 hectares. These trend shows that urban space is expanding and consistent with the local socio-economic development orientation.

Table 1. Statistics of areas, ratios of land function types in 2010, 2015 and 2020

Land use function type	2010		2015		2020		% of change (+/-) 2010-2015	% of change (+/-) 2015-2020
	ha	%	ha	%	ha	%		
Civil	2418.10	15.96%	2642.76	17.44%	3015.75	19.90%	+9.29%	+14.11%
Non-civil	1763.16	11.64%	2156.31	14.23%	2316.44	15.29%	+22.30%	+7.43%
Others	10970.54	72.40%	10352.73	68.33%	9819.61	64.81%	-5.63%	-5.15%
Total	15151.80	100.00%	15151.80	100.00%	15151.80	100.00%		

Table 2. Transition matrix of land function changes for 2011-2015 period (unit: %)

Land function type	Civil	Non-civil	Others
Civil	51.90%	7.20%	40.90%
Non-civil	8.62%	85.49%	5.88%
Others	11.23%	4.37%	84.41%

Table 3. Transition matrix of land function changes for 2015-2020 period (unit: %)

Land function type	Civil	Non-civil	Others
Civil	51.90%	7.20%	40.90%
Non-civil	8.62%	85.49%	5.88%
Others	11.23%	4.37%	84.41%

Tables 2 and 3 provide more detailed information about the change in land use functions over the periods 2010-2015 and 2015-2020. In the period 2010-2015, about 51.9% of civil land area was retained, the rest was converted to other groups, of which land type “others” accounted for the most with 40.9%. Nearly 85.49% of non-civil land area is retained, the rest is converted to other functional land types, with not a big difference between civil land types and other land types. Similarly, the majority of other land types are retained (84.41%), of which about 11.23% are converted to civil land and 4.27% are converted to non-civil land. In the period 2015-2020, although there was a change in the percentage of retention or conversion between functional

land types, the trend did not change. For example, the retention rate of functional land types is quite high with 86.15%, 88.5% and 91.25 respectively for civil land, non-civil land and other land. Meanwhile, compared to the previous period, this period the change in land use functions in functional land types is smaller. Specifically, if in the period 2010-2015, the civil land type was converted to other land at a rate of 40.9%, then in the period 2015-2020, the rate was only 8.51%. Thereby, one can conclude that although urbanization continues to expand over time, urbanization occurs more slowly in the period 2015-2020 than in the period 2010-2015. Map of this change in land use functions over the periods 2010-2015 and 2015-2020 is shown in Figure 3.

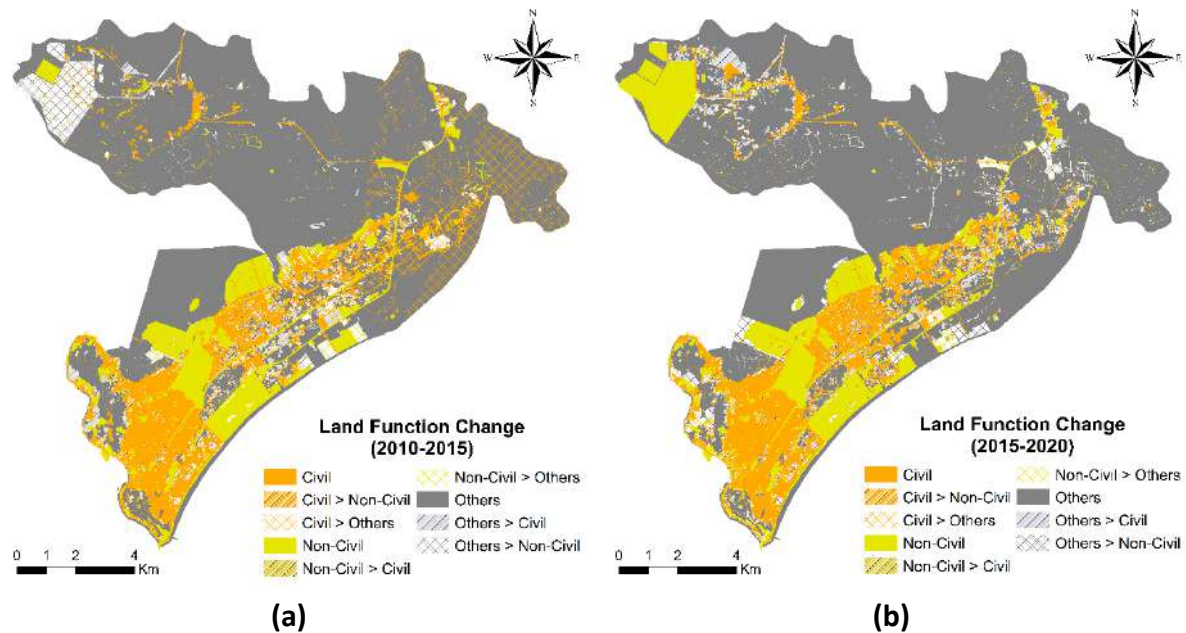


Figure 3. Land function change map over the period 2010-2015 (a) and 2015-2020 (b)

4. CONCLUSION

The study has applied GIS and Markov chains in assessing changes in land use functions for Vung Tau city through the period 2010, 2015 and 2020. The analysis and evaluation process showed that in the land use functions of the area there is a shift towards civil and non-civil functional land, which is increasingly expanding in area over time. However the rate of expansion of land with civil and non-civil functions is different across periods, faster in the period 2010-2015 and slower in the period 2015-2020. Meanwhile, land with other uses narrows in area through stages and the rate of shrinkage is also different through stages. This shows the development and expansion of the urban space of Vung Tau city through the research stages and is also consistent with the local socio-economic development orientation. Researching the process of structural transformation of land use functions also provides an important basis for planning and adjusting spatial construction planning for urban development, land use planning and urban management.

5. REFERENCES

- Alqurashi F. A. , Kumar L., 2013. Investigating the Use of Remote Sensing and GIS Techniques to Detect Land Use and Land Cover Change: A Review. Advances in Remote Sensing. 2 (2) 193-204.

-
- Aznar-Sánchez, J. A., Piquer-Rodríguez, M., Velasco-Muñoz, J. F., & Manzano-Agugliaro, F. 2019. Worldwide research trends on sustainable land use in agriculture. *Land use policy*, 87, 104069.
- Ba N.T, 1996. Construction planning and urban development. Construction Publishing House.
- Clarke, M. L., và Rendell, H. M., 2007. Climate, extreme events and land degradation. In Climate and land Degradation (pp. 137-152). Springer.
- Department of Natural Resources and Environment of Ba Ria Vung Tau province, 2021. Results of land inventory in Vung Tau City in 2019 and land statistics in 2020.
- Gidado A. K., Kamarudin M.K.A., Firdaus A. N., Aliyu Muhammad Nalado A. M., Saudi A. S. M., Md Saad M.H., Ibrahim S., 2018. Analysis of Spatiotemporal Land Use and Land Cover Changes using Remote Sensing and GIS: A Review. *International Journal of Engineering & Technology*, 7 (4.34) 159-162.
- Islam, M. S., & Ahmed, R. (2011). Land use change prediction in Dhaka city using GIS aided Markov chain modeling. *Journal of Life and Earth Science*, 6, 81-89.
- Ministry of Construction, Circular 01/2021/TT-BXD dated May 19, 2021 Promulgating QCVN 01:2021/BXD national technical regulations on Construction Planning.
- Ministry of Construction, Circular 04/2022/TT-BXD dated October 24, 2022 Regulations on dossiers of tasks and project dossiers of regional construction planning, urban planning and functional area construction planning and rural planning.
- Ministry of natural resources and environment., 2018. Circular 27/2018/TT-BTNMT dated December 14, 2018 Regulations on statistics, land inventory and mapping of current land use.
- Muller, M. R., và Middleton, J., 1994. A Markov model of land-use change dynamics in the Niagara Region, Ontario, Canada. *Landscape Ecol* 9, 151–157.
- Mundia, C. N., Mubea, K., & Ngigi, T. (2011). Assessing application of Markov Chain analysis in Nakuru. *Applied Geoinformatics for Society and Environment* 182-188.
- National Assembly of the Socialist Republic of Vietnam, 2012. Land Law 2013.
- Noszczyk T., 2028. A review of approaches to land use changes modelling. *Human and Ecological Risk Assessment: An International Journal*. 25(6) 1377-1405.
- Vung Tau City People's Committee, 2021. Report on Land Use Planning to 2030 of Vung Tau City.

CLIMATE CHANGE IMPACTS OF AGRICULTURAL PRODUCTION IN THE COASTAL AREA OF THI NAI LAGOON, BINH DINH PROVINCE: AN ANALYSIS OF THE LIVELIHOOD VULNERABILITY INDEX

Vu Khac Hung¹

¹Department of Land management

VNU University of Science, 334 Nguyen Trai, Thanh Xuan, Hanoi, Vietnam

Email: Vukhachung@hus.edu.vn

Abstract

This study identifies the vulnerability of agricultural households to climate change in the Thi Nai lagoon area, mainly concentrated in Quy Nhon city and Tuy Phuoc district. This area is assessed as vulnerable to severe climate change in Binh Dinh province. The study uses the Livelihood Vulnerability Index (LVI) calculated based on datasets from the 2024 survey of 100 households. The results showed that Tuy Phuoc showed a level of damage (LVI-IPCC = 0.11), higher than the level of damage in Quy Nhon (LVI-IPCC = 0.06). This shows the need for special support measures to improve adaptation and mitigate risks for people in Tuy Phuoc district, where the proportion of people engaged in agricultural production along the Thi Nai lagoon is higher than that of Quy Nhon city.

Keywords: LVI, Livelihood Vulnerability Index, Thi Nai lagoon, Binh Dinh, GIS.

1. INTRODUCTION

Vietnam, with over 3,000 km of coastline, is highly vulnerable to the direct impacts of climate change, particularly in coastal areas (IPCC, 2014). According to the Global Climate Report (2020), Vietnam was among the top 10 countries most affected by extreme weather events during the period from 1999 to 2018 (David ckstein et al., 2018).

Thi Nai Lagoon in Binh Dinh supports thousands of livelihoods through fishing, aquaculture, farming, and tourism. However, climate change impacts like hurricanes, coastal erosion, and saltwater intrusion are threatening these activities. Research's Phuong Huynh et al. (2021) found that saltwater intrusion and storms have disrupted fishing, reducing production and causing economic losses.

There are various approaches to assessing livelihood vulnerability. Research on livelihood vulnerability began as early as the 1990s, with notable studies by Kelly, P. M. and W. N. Adger (2000), Michael Watts and Hans-Georg Bohle (1993) and Neil Adger, W. (1999), among others. Quantitative methods, combined with qualitative approaches, are used to assess the vulnerability of people's livelihoods in various regions. In Vietnam, numerous studies on climate change assessment have been carried out (Nguyen Van Quynh Boi, Doan Thi Thanh Kieu, 2012), Nguyen Thi Vinh Ha (2016), among others. IMOLA Project (2006) applied a sustainable livelihood approach to assess the impact of various factors on the livelihoods of

people in Thua Thien Hue province. However, this approach has limitations in addressing sensitive issues and demonstrating the capacity to respond to climate change. Overall, many studies have been conducted to assess climate change, but comprehensive, in-depth studies that evaluate the impacts of climate change on all natural and socioeconomic sectors are still needed for each specific region of Vietnam.

To comprehensively assess the level of livelihood vulnerability due to climate change impacts, the Livelihood Vulnerability Index (LVI), proposed by Hahn et al. in 2009, is a comprehensive tool for evaluating the vulnerability of households and communities to climate change (Hahn, Micah B. et al., 2009). The LVI integrates various factors across different aspects, such as food security, health, and water access, to provide a detailed understanding of how climate stressors impact livelihoods. This tool has been applied globally, from the assessment of drought-stricken areas in Africa (Opiyo, Francis, 2014) to flood-prone areas in South Asia (Abawua, M. J., 2005).

Previous research in the area along the Thi Nai Lagoon has clearly demonstrated that climate change affects the livelihoods of people living near the lagoon Pham Thanh Long et al. (2015) Le Thi Thuy Trang (2021) Luong Thi Van (2021) Nguyen Nhat Minh et al. (2022) People's Committee of Binh Dinh province (2019). Salinity intrusion has directly impacted the income of aquaculture workers along the lagoon Le Thi Thuy Trang (2021). Additionally, the number and quality of mangrove forests and aquatic species in the lagoon are declining, which directly affects poor communities Luong Thi Van (2021). These studies have highlighted the impact of climate change on agricultural production along the lagoon. However, to more comprehensively assess the impact of climate change on people's livelihoods, applying the LVI index, which combines past and current climate and livelihood data, needs to be implemented.

This research applied the LVI index to assess the vulnerability of livelihoods affected by climate change in the coastal area of Thi Nai Lagoon. The research question aimed to identify the most important factors for evaluating the level of point-based livelihood damage (LVI) for communities around Thi Nai Lagoon.

2. STUDY AREA, DATA AND METHODS

2.1 Study area

Thi Nai Lagoon is one of the largest and most important lagoon ecosystems in Binh Dinh province, located in the coastal region of central Vietnam. The lagoon spans several communes and wards in Quy Nhon City and Tuy Phuoc District, covering an area of about 5,000 hectares and directly adjacent to the East Sea (Monre, 2021). Thi Nai Lagoon not only holds significant ecological value but also plays a crucial role in providing livelihoods for thousands of local households, particularly those dependent on agriculture and fisheries.

However, the coastal area of Thi Nai Lagoon is severely impacted by climate change. Phenomena such as sea-level rise, saltwater intrusion, prolonged drought, and extreme rainstorms have disrupted agricultural production. These factors not only reduce crop yields but also damage people's livelihoods (Truong Minh Duc, 2015). It is essential to analyze the LVI index for this area in order to accurately assess the extent of vulnerability and propose effective adaptation measures for the local population.

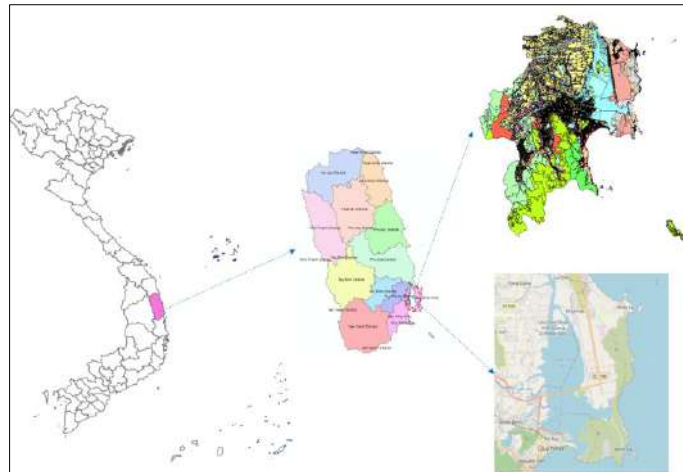


Figure 1: Location of the research area, Thi Nai Lagoon, Binh Dinh province

2.2 Data

The data in this study were collected through various methods to ensure the completeness and accuracy of the LVI index analysis for farmers in the coastal area of Thi Nai Lagoon. Both qualitative and quantitative data were used, sourced from various outlets, including household interview data, weather data such as precipitation, temperature, and extreme climatic events collected from the South Central Hydrometeorological Station, as well as socio-economic data from the statistical yearbook of Binh Dinh Province.

2.3 Methods

2.3.1. *Methods of collecting primary data*

The primary data collection method used in this study involved detailed questionnaires to gather data from households in the study area. The interview questions focused on eight main topics: Demographic Profile, Livelihood Strategies, Social Networks, Health, Water, Financial Capital, Housing and Productive Land, and Natural Disasters and Climate Change. The study sample consisted of 100 randomly selected households from communes and wards along the Thi Nai Lagoon in Quy Nhon City and Tuy Phuoc District. The sample was allocated based on population size and the degree of dependence on agricultural production (Truong Minh Duc, 2015).

Among the communes and wards adjacent to Thi Nai Lagoon, 50 households from Quy Nhon and 50 households from Tuy Phuoc were randomly selected, all of which participate in agricultural production. The interview samples were evenly distributed across the communes and wards along the Thi Nai Lagoon

2.3.2. Methodology of data analysis

Primary and secondary data were aggregated and analyzed using Microsoft Excel. The LVI method was used to assess the impact of climate change on people's livelihoods. According to Hahn et al., there are two approaches to the LVI.

First, the LVI is considered a composite index consisting of seven key factors. Each key factor includes a few sub-factors(Hahn, Micah B., Anne M. Riedereret al., 2009). However, there were a few minor changes to the key factors of the LVI to fit the study area. The LVI in this study, as a composite index, consists of eight key factors (Table 2).

Second, these eight key factors are grouped into three 'contributing' factors according to the IPCC's definition of vulnerability, which includes 'exposure,' sensitivity/vulnerability, and adaptability.

a. How to calculate LVI

Since each subfactor is measured using a different system, it is necessary to normalize it to convert it into a metric according to the formula below:

$$\text{index}_{sd} = \frac{S_d - S_{min}}{S_{max} - S_{min}}$$

In which: S_d is the root value of the sub-factor (real value) for the locality (city/district) d , and S_{min} and S_{max} are the minimum and maximum values, respectively.

Once normalized, the sub-factors were averaged to calculate the value of each major factor by applying the following formula:

$$M_d = \frac{\sum_{i=1}^n \text{index}_{sd}^i}{n}$$

In which: M_d is one of the 8 key factors for the locality (city/district) d , index_{sd}^i represents the sub-factors indexed by i , they make up each main factor, and n is the number of sub-factors in each key factor.

Once the values of the key factors were determined, the livelihood damage index at the local level (city/district) was calculated using the following formula:

$$LVI_d = \frac{\sum_{i=1}^8 M_{di} W_{Mi}}{\sum_{i=1}^8 W_{Mi}}$$

In which: LVI_d is the index of local livelihood damage (city/district) d , corresponding to the weighted average of all 8 key factors. The weight of each W_{Mi} key factor is determined by the number of sub-factors it includes.

In this research, LVI values ranged from 0 to 1. Concrete:

- LVI = 0: No damage
- $0.4 \leq LVI < 0.7$: High level of damage

- $0 < \text{LVI} < 0.4$: Moderate damage
- $0.7 \leq \text{LVI} \leq 1$: Very high level of damage

b. How to calculate LVI-IPCC

Instead of merging the key factors into the LVI in one step, this approach combines the key factors listed in Table 1 using the following formula:

$$CF_d = \frac{\sum_{i=1}^n M_{di} \cdot W_{Mi}}{\sum_{i=1}^n W_{Mi}}$$

In which:

CF_d is a "contributing" agent according to the IPCC;
 M_{di} is the main factor for the locality (city/district) d is indexed according to i;
 W_{Mi} is the weight of each major factor;
 n is the number of key factors in each contributing agent.

Table 1: Contribution of IPCC factors to key vulnerability factors

LVI - IPCC	Key factors
Exposure (E)	Natural Disasters and Climate Change
Adaptability (A)	Demographic Profile
	Livelihood strategy
	Social Networks
Vulnerability (S)	Health
	Financial capital
	Houses and production land
	Water Source

Source: Hahn, Micah B., Anne M. Riederer et al. (2009)

❖ LVI-IPCC Calculation:

LVI-IPCC = (E - A) * S	In this study, the LVI-IPCC ranged from -1 to 1. Concrete:
In which: E is Exposure S is sensitivity/vulnerability A is adaptability.	<ul style="list-style-type: none"> ▪ LVI - IPCC = -1: Undamaged ▪ $-1 < \text{LVI} - \text{IPCC} < -0.5$: Moderate damage ▪ $-0.5 \leq \text{LVI} - \text{IPCC} < 0.5$: High level of damage ▪ $0.5 \leq \text{LVI} - \text{IPCC} \leq 1$: Very high level of damage

3. RESULTS AND DISCUSSION

3.1 Analysis of vulnerability to livelihoods in the area along Thi Nai lagoon according to the LVI index

Quy Nhon had a lower vulnerability index for most factors, indicating better resilience and livelihood diversification. Factors such as Demographic Profile (0.21), Livelihood Strategy (0.16), and Water (0.00) suggest that the people of Quy Nhon are less vulnerable to the impacts of climate change (Table 2). Among the agricultural households interviewed, 50% of the surveyed households had no source of income other than agricultural production, compared to

31% in Quy Nhon. Biodiversity contributes to Quy Nhon's lower vulnerability level. Research of Neil Adger, W. (1999) points out that resilience and livelihood diversification help communities mitigate risks and better adapt to shocks from nature. This is also confirmed by Barry Smit, Johanna Wandel (2006), who emphasize that communities with diverse livelihoods are often better able to respond to climate change.

In contrast, Tuy Phuoc has a higher vulnerability index, especially for factors such as Livelihood Strategy (0.69), Water (0.27), and Natural Disasters and Climate Change (0.77). This indicates that the people of Tuy Phuoc are highly dependent on agriculture and lack access to clean water, which increases vulnerability levels when natural disasters occur.

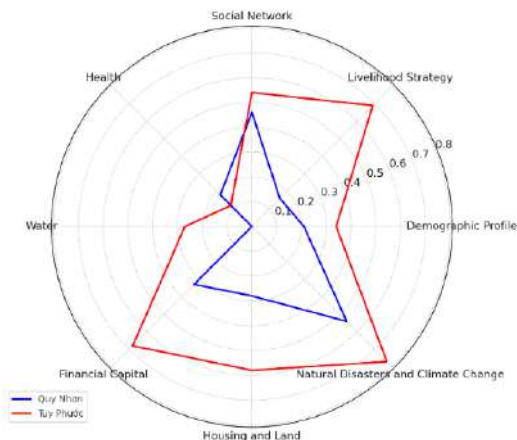


Figure 2. Spider diagram showing the main components of the Livelihood Vulnerability Index (LVI) for Quy Nhon City and Tuy Phuoc District, Binh Dinh Province

According to Kabeer, Naila (2010), households that depend on agriculture are more vulnerable to weather events. Studies from Susmita Dasgupta et al. (2009) and IPCC (2014) also emphasized that the increase in the frequency and intensity of extreme weather events due to climate change will particularly negatively impact coastal communities such as Tuy Phuoc. A similar study in the Philippines by Mastrorillo et al. (2016) showed that communities in vulnerable areas, especially those with low incomes and dependence on agriculture, tend to be more severely affected by climate change. The vulnerability index of these areas reflects the same level of vulnerability as that of Tuy Phuoc.

Quy Nhon's LVI was determined to be at a medium level (0.28), while Tuy Phuoc's LVI was at a high level (0.52). The analysis also shows that Quy Nhon has more advantages than Tuy Phuoc in many livelihood damage factors, especially in terms of Livelihood Strategy, Housing and Productive Land, and Water. Tuy Phuoc requires stronger support measures to improve resilience and adapt to the impacts of climate change. International studies have also highlighted the urgency of investing in adaptation and risk-mitigation solutions for coastal communities in the face of increasing climate change.

3.2 Analysis of livelihood vulnerability in the area along Thi Nai lagoon according to the LVI - IPCC index

The adaptability of the people of Quy Nhon was significantly lower than that of Tuy Phuoc. A low index (0.26) indicates that the people of Quy Nhon have fewer strategies and resources to cope with the impacts of climate change. **Kabeer, Naila (2010)** state that adaptability is directly related to income level and access to information. Although Tuy Phuoc has a higher index (0.52), this is still not sufficient to show that the people there are completely safe from natural shocks.

Tuy Phuoc's vulnerability index (0.44) shows that the people there are at higher risk of natural impacts than those in Quy Nhon (0.22). This may be due to their heavy dependence on agriculture and unstable sources of income. According to Neil Adger, W. (1999), high vulnerability is an indication of a deficiency in the resilience of households, especially in rural communities. Tuy Phuoc's heavy dependence on agriculture may increase its vulnerability compared to Quy Nhon. Mastorillo et al. (2016) indicate that households with diverse sources of income are often better able to recover from extreme climatic events. This highlights the need for the people of Tuy Phuoc to diversify their livelihoods.

Categories	Quy Nhon	Tuy Phuoc
Adaptive Capacity (A)	0,26	0,52
Vulnerability (S)	0,22	0,44
Exposure (E)	0,54	0,77
LVI - IPCC	0,06	0,11

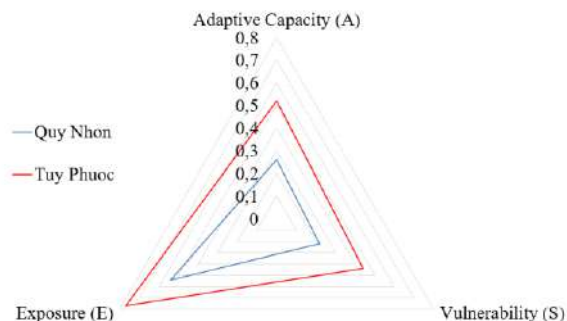


Figure 3. Vulnerability triangle diagram showing the contributing factors of the LVI- IPCC for Quy Nhon city and Tuy Phuoc district

The exposure index indicates the extent to which communities are affected by weather events. Tuy Phuoc has an index of 0.77, higher than that of Quy Nhon (0.54). This indicates that the people of Tuy Phuoc face greater risks from climate change. IPCC (2014) has shown that coastal communities are vulnerable to the increased frequency and intensity of weather events. This difference can be explained by geographical location and natural conditions. However, Tuy Phuoc, with its more vulnerable terrain and infrastructure, may be more severely affected by climate change than Quy Nhon, which is better equipped to manage and prepare for emergencies.

The damage triangle graph shows a clear difference between Quy Nhon and Tuy Phuoc in the key factors of the Livelihood Damage Index. Tuy Phuoc exhibits a high level of vulnerability (LVI-IPCC = 0.11), compared to the lower vulnerability level in Quy Nhon (LVI-IPCC = 0.06), highlighting the need for special support measures to improve resilience and mitigate risks for the people of Tuy Phuoc. Sustainable development strategies and infrastructure investments can play a crucial role in enhancing the resilience of communities.

Table 2: Values of key factors, Sub-factors and LVI index of Quy Nhon city and Tuy Phuoc district

Key Factors	Sub-factors	Units of Calculation	Greatest Value	Smallest Value	Real value in Quy Nhon city	Real value in Tuy Phuoc district	Quy Nhon City Index	Tuy Phuoc district index	Main index of Quy Nhon city	Main index of Tuy Phuoc district
Demographic Profile	Dependency Rate	%	100	0	5	36	0,05	0,36	0,21	0,34
	Percentage of households with female heads of households	%	100	0	8	12	0,08	0,12		
	Percentage of households with heads of households who do not finish primary school	%	100	0	0	8	0,00	0,08		
	Percentage of households without family members participating in climate change training classes	%	100	0	70	79	0,70	0,79		
Livelihood strategy	Percentage of households with main income from agriculture (cultivation, animal husbandry, fisheries)	%	100	0	12	78	0,12	0,78	0,16	0,69
	Percentage of households have no other source of income other than agriculture	%	100	0	31	50	0,31	0,50		
	Average Agricultural Livelihood Diversity Index	1/(Livelihood+1)	1	0,25	0,34	0,9	0,12	0,87		
	Percentage of households without members participating in a certain type of vocational training	%	100	0	10	60	0,10	0,60		
Social Media	Percentage of households do not receive support from local authorities when natural disasters occur	%	100	0	50	72	0,50	0,72	0,46	0,54
	Percentage of households with no members participating in local government organizations	%	100	0	88	82	0,88	0,82		
	Percentage of households do not have access to information sources (TV/radio/internet)	%	100	0	1	8	0,01	0,08		
Health	Number of days/year of head of household at the hospital for health check-up and monitoring	Day	45	0	18	5	0,40	0,11	0,18	0,12
	Percentage of households with family members with chronic diseases	%	100	0	8	15	0,08	0,15		

Key Factors	Sub-factors	Units of Calculation	Greatest Value	Smallest Value	Real value in Quy Nhon city	Real value in Tuy Phuoc district	Quy Nhon City Index	Tuy Phuoc district index	Main index of Quy Nhon city	Main index of Tuy Phuoc district
	Percentage of households with members taking time off work/study for 2 weeks due to illness	%	100	0	5	10	0,05	0,10		
Water	Percentage of households do not use clean tap water for daily life	%	100	0	0	38	0,00	0,38	0,00	0,27
	Percentage of households that do not meet the demand for water use in daily life	%	100	0	0	15	0,00	0,15		
Financial capital	Percentage of households borrowing money from outside	%	100	0	70	75	0,70	0,75	0,33	0,68
	Percentage of households without bank deposits	%	100	0	5	60	0,05	0,60		
	Percentage of households with no members working outside the village, in a relatively developed place	%	100	0	24	70	0,24	0,70		
Houses and production land	Percentage of households with unstable houses are easily destroyed by storms	%	100	0	89	40	0,89	0,40	0,28	0,58
	On average, the percentage of agricultural land that is vulnerable to flooding	%	100	0	11,2	56	0,11	0,56		
	On average, the percentage of agricultural land that is prone to drought	%	100	0	5	68	0,05	0,68		
	On average, the percentage of agricultural land vulnerable to saltwater intrusion	%	100	0	5	68	0,05	0,68		
Natural disasters and climate change	Percentage of households damaged by natural disasters in the past 10 years	%	100	0	25	69	0,25	0,69	0,54	0,77
	Percentage of households damaged in production due to natural disasters annually in the past 10 years	%	100	0	20	65	0,20	0,65		
	Average number of hot days ($T_{max} \geq 33^{\circ}C$) in the past 10 years	Day	80	10	80	80	1,00	1,00		
	Average number of heavy rain days ($R \geq 100mm/day$) in the past 10 years	Day	10	1	7,5	7,5	0,72	0,72		
LVI									0,28	0,52

4. CONCLUSION

The results of this study show that Thi Nai lagoon, a coastal area in the Binh Dinh province, faces many serious challenges due to climate change. Phenomena such as sea level rise, saltwater intrusion, flooding, and an increase in the frequency of storms not only reduce crop yields but also severely affect the livelihoods of local people.

The assessment factors showed a clear difference between the two areas of Quy Nhon and Tuy Phuoc. Quy Nhon has a lower vulnerability index, indicating better resilience and diversification of people's livelihoods. In contrast, Tuy Phuoc has a higher vulnerability index, especially for factors such as livelihood strategies and water resources, which underscores the need to strengthen support policies for the community.

Finally, the application of the livelihood damage index proposed by Hahn significantly affected the assessment of the impact of climate change on people's lives. Thus, this is a highly efficient and accurate method. At the same time, it is more applicable to regions affected by climate change in Vietnam.

FUNDING STATEMENT

Vu Khac Hung was funded by the Master, PhD Scholarship Programme of Vingroup Innovation Foundation (VINIF), code VINIF.2022.TS051.

5. REFERENCES

- Monre (2021), "Report on the impact of climate change in coastal areas of Vietnam. Hanoi", Science and Technology Publishing House.
- Le Thi Thuy Trang (2021), "Research on the impact of saltwater intrusion on the livelihoods of people in the Thi Nai lagoon area, Binh Dinh province", Journal of Science on Natural Resources and Environment. part 36.
- IPCC (2014), Climate Change 2014 – Impacts, Adaptation and Vulnerability: Part B: Regional Aspects: Working Group II Contribution to the IPCC Fifth Assessment Report: Volume 2: Regional Aspects, Vol. 2, Cambridge University Press, Cambridge.
- Mastrorillo et al. (2016), "Climate change and health: Vulnerability assessment in the Philippines", Environmental Science & Policy, 61, 164-175.
- Michael Watts and Hans-Georg Bohle (1993), "The Space of Vulnerability: The Causal Structure of Hunger and Famine", Progress in Human Geography - PROG HUM GEOGR. 17, tr. 43-67.
- W. Neil Adger (1999), "Social Vulnerability to Climate Change and Extremes in Coastal Vietnam", World Development. 27(2), tr. 249-269.

-
- P. M. Kelly và W. N. Adger (2000), "Theory and Practice in Assessing Vulnerability to Climate Change and Facilitating Adaptation", *Climatic Change*. 47(4), tr. 325-352.
- M. J. Abawua (2005), "Flood Risk Assessment: A Review", *Journal of Applied Sciences and Environmental Management* (ISSN: 1119-8362) Vol 9 Num 1. 9.
- Johanna Wandel Barry Smit (2006), "Adaptation, adaptive capacity and vulnerability", *Global Environmental Change*. 16(3), tr. 282-292.
- Micah B. Hahn, Anne M. Riederer và Stanley O. Foster (2009), "The Livelihood Vulnerability Index: A pragmatic approach to assessing risks from climate variability and change—A case study in Mozambique", *Global Environmental Change*. 19(1), tr. 74-88.
- Susmita Dasgupta et al. (2009), "Climate Change and the Future Impacts of Storm-Surge Disasters in Developing Countries", *Environmental Economics eJournal*.
- Naila Kabeer (2010), "Women's Empowerment, Development Interventions and the Management of Information Flows". 41(6), tr. 105-113.
- Doan Thi Thanh Kieu Nguyen Van Quynh Boi (2012), "Applying vulnerability index in livelihood research - the case of Tam Hai island commune, Nui Thanh district, Quang Nam province", *Can Tho University Journal of Science*(24b), tr. 251-260.
- Francis Opiyo (2014), Climate variability and change on vulnerability and adaptation among Turkana pastoralists in North-Western Kenya.
- Pham Thanh Long et al. (2015), "Forecasting surface sediment changes in Thi Nai lagoon, Binh Dinh province according to climate change and sea level rise scenarios", *Environmental Magazine*. 7.
- Nguyen Thi Vinh Ha (2016), "Concepts and frameworks for assessing natural disaster vulnerability in the world - Assessment of applicability in Vietnam". 32(4).
- David ckstein et al. (2018), Global climate risk index 2020, Germanwatch.
- People's Committee of Binh Dinh province (2019), "Report climate assessment of Binh Dinh province".
- Luong Thi Van (2021), "Vulnerability of poor communities in the Thi Nai lagoon area, Binh Dinh province, to the impacts of climate change", *Vietnam Studies - Proceedings of the 4th Conference*.
- Phuong Huynh et al. (2021), "Adaptive livelihood strategies among small-scale fishing households to climate change-related stressors in Central Coast Vietnam", *International Journal of Climate Change Strategies and Management*. 13(4/5), tr. 492-510.
- Nguyen Nhat Minh et al. (2022), "Assessing the impact of climate change on sustainable development goals of Binh Dinh province and recommending some response solutions", *Environmental Magazine*. 5.
- IMOLA Project (2006), "Handbook: Rapid Rural Appraisal and Sustainable Livelihood Analysis. ", Thua Thien - Hue Provincial People's Committee.
- Truong Minh Duc (2015), "Environment and Climate Change in the Central Coast of Vietnam", *Vietnam Social Sciences*.

APPLICATION OF GIS TO BUILD A LAND DATABASE IN A MOUNTAINOUS DISTRICT OF SON LA PROVINCE, VIETNAM

Tran Hong Hanh^{1,*}, Nguyen Tien Duong², Pham Thi Thanh Hoa³ and Tran Van Anh⁴

^{1,2,4} Faculty of Geomatics and Land Administration, Hanoi University of Mining and Geology, 18 Vien Street, Duc Thang Ward, Hanoi, Vietnam

Email: tranhonghanh@humg.edu.vn, phamthithanhhoa@humg.edu.vn, tranvananh@humg.edu.vn

³ Son La Department of Natural Resources and Environment
Building T2, Provincial Administrative Center, Northwest Square, Son La city, Son La
Email: tienduongmdc43@gmail.com

ABSTRACT

As a unique production resource, land is an invaluable national asset. The establishment of a database stands at the core of digital transformation. A land database consists of four key components: a cadastral database, a land statistical and inventory database, a land use planning database, and a land price database. This paper aims to create a land database to enhance the efficiency of land exploitation and management within the context of the Moc Chau mountainous district in Son La province. The study was carried out using various methodologies, including synthesis and analysis, field investigation and surveying, and notably, the integration of multiple software systems to develop the land database. Consequently, the necessary component databases have been successfully established, ensuring the requisite accuracy. These databases are compiled using the VBTLIS online software developed by Vietnam. This research holds practical significance, offering valuable insights for policymakers and aiding in effective land use planning. It establishes a robust data foundation, a crucial step towards operating within a digital government, a digital economy, and a digital society.

Keywords: Land database, GIS, VBTLIS, Moc Chau, Son La

1. INTRODUCTION

The land database is one of six national databases earmarked for prioritized implementation, aimed at enhancing state management, providing public land services, and facilitating the exchange of land information among ministries, branches, organizations, and individuals. Simultaneously, it plays a crucial role in the deployment and functioning of the e-government system.

Land serves as a unique means of production, an essential living environment, an area for residential settlements, and the foundation for economic, cultural, and national security and defense projects. The current challenges faced by the land management sector are to address the requirements for national development while concurrently ensuring the efficient and sustainable management and safeguarding of land resources.

The applications of GIS technology in land management is increasingly prevalent due to its highly effective spatial field management benefits, such as reduction in investment costs; rapid data storage and retrieval; efficient collection of large volumes of data in a short timeframe; swift and effective enhancement of the quality of public service management; increased accessibility for a wide user base, and others. The land database is systematically developed by provinces, cities, and districts, encompassing a range of components such as the cadastral database, a land statistical and inventory database, a land use planning database, and a land price database. It is structured for regular electronic accessibility, utilization, management, and updates.

The cadastral database encompasses essential information related to the establishment and modification of cadastral maps, land registration, issuance of certificates for land use rights, property ownership including houses and other assets tied to the land and associated cadastral files. The land statistical and inventory database comprises reports, tables, statistical data, land inventory, and land use maps at various administrative levels—communal, district, and provincial.

The land use planning database consists of comprehensive explanatory report data, land use maps, planning maps, land use plans, as well as adjusted land use planning and provincial and district-level plans. The land price database comprises data such as land price lists, adjusted and supplemented land price lists, land price adjustment coefficients, specific land prices, auction-winning prices for land use rights, and land price information recorded in the information collection form for land plots. All this database includes attribute and spatial database and scanned documents.

Across the globe, numerous studies address the establishment of land databases, primarily emphasizing the development of land cover and land use databases through diverse methodologies. Zahir Ali et al. meticulously outlined the constraints and challenges involved in integrating legal and geometric cadastral information to establish a novel digital cadastral system (Ali and Shakir 2012). In 2019, Benjamin Beaumont et al. conducted a consultation process to create a land cover and land use database for the Walloon region (Beaumont, Stephenne et al. 2019). In their 2022 study, Md. Zulfikar Khan and colleagues examined soil carbon stocks and documented land use changes in Italy, employing the LUCAS soil database (Khan and Chiti 2022). Matthew Mleczko et al. (2023) developed a national land use and planning database in the USA (Mleczko and Desmond 2023). Pei Yin and Jing Cheng analyzed the urban land planning database of Shanghai, China using a MySQL-based software system and proposed a conceptual model for the urban land planning database (Yin and Cheng 2023).

This multi-scale open database contains information on land use and land cover, supporting the DestinE program in creating a highly precise digital model of the Earth (Kepka, Hájek et al. 2022). Yindan Zhang et al. established the Fine-resolution, Large-area Urban Thematic information Extraction (FLUTE) framework (Zhang, Chen et al. 2022). A service-oriented GIS-based web system was developed to offer a viable solution, incorporating fundamental geographic features and benchmark land price-related information (Yang, Sun et al. 2015). A study developed a land management system using a Geographic Information System (GIS) (Yakubu and Asah 2023).

Several studies in Vietnam have explored land-related topics, employing a variety of technologies. Vo Quang Minh et al. (2004) specifically investigated land information management, integrating GIS and socioeconomic data approaches for effective land use planning (Minh, Tri et al. 2003). Huynh Van Chuong et al. (2010) conducted research to develop a database for land assessment and land use planning in Thua Thien Hue province (Chuong and Lân 2010). Nguyen The Cong and colleagues (2020) conducted research on establishing a statistical database and a land inventory in Dong Thap province (Công, Miễn et al. 2020). Tran Xuan Mien and colleagues (2022) utilized the ARCGIS API to construct a statistical land inventory database in Phu Luong district, Thai Nguyen province (Miễn, Công et al. 2022).

Mobile GIS technology has been employed in research to update market land price information in Phung town, Hanoi city (Câm 2021). Le Thi Lien established a cadastral database in Bac Kan province by utilizing Microstation and gCadas software (Liên 2022). In Long Thanh district, the land management software (DNAI.LIS) was employed to establish and extract land databases. (Thảo, Hạnh et al. 2023). Another study developed a ground spatial model and multi-objective attribute information for each land plot, emphasizing the challenges involved in creating a land database (Anh, Hải et al. 2017). The land price map database for Hoang Van Thu ward in Thai Nguyen city, along with an attribute database containing details such as the number of sheets, plots, areas, roads, state price, market price, and management system, was developed using MapInfo software (GIS) (Anh and Gâm 2020).

Building and updating the national land database is crucial, demanding completeness, accuracy, scientific rigor, and timely updates. The content, structure, and information types within the national land database follow the technical regulations outlined by the Vietnam Ministry of Natural Resources and Environment. The constituent databases within the national land system must be developed simultaneously, linked, and integrated. The organization and implementation scale of the cadastral database are determined by the administrative units at the district level.

Presently, fundamental survey data, maps, and publications related to land resources in Son La province lack uniformity, leading to cumbersome storage and difficult information retrieval. These obstacles significantly impede land management efforts at the local level, resulting in several issues and reduced effectiveness. Thus, establishing a land database for the experimental area (Moc Chau district, Son La province) becomes a matter of high urgency. This initiative will be crucial, providing essential insights to aid policymakers in formulating strategies, devising plans, and conducting land use planning to more effectively harness existing land resources for both political stability and economic development.

2. TECHNOLOGICAL PROCESSES AND SOFTWARE USED TO BUILD LAND DATABASES

2.1 Technological processes

The process of building the land database is detailed in Table 1.

Table 1. Technological process of building components of the land database.

Technological process	Steps
Cadastral Database	<ul style="list-style-type: none"> - Preparation - Collecting documents and data - Reviewing, evaluating, classifying, and organizing documents and data - Building spatial land data and cadastral spatial data - Scanning legal documents and processing files - Creating cadastral attribute data - Completing cadastral data - Checking and accepting the cadastral database - Verifying and integrating data into the system - Creating cadastral metadata
Land Statistical and Inventory Database	<ul style="list-style-type: none"> - Preparation - Collecting documents and data - Reviewing, evaluating, classifying, and organizing documents and data - Building spatial data for land inventory - Scanning legal documents and processing files

Technological process	Steps
	<ul style="list-style-type: none"> - Creating land statistical and inventory attribute data - Checking and completing land statistical and inventory data - Preparing documents for inspection and acceptance - Packaging and submitting statistical and inventory databases - Overall check and data integration into the system - Developing land statistical and inventory metadata
Land Use Planning Database	<ul style="list-style-type: none"> - Preparation - Collecting documents and data - Reviewing, evaluating, classifying, and organizing documents and data - Building spatial data - Scanning legal documents and processing files - Developing data for the land use planning database - Checking and completing land use planning data - Preparing documents for inspection and acceptance supervision - Packaging and submitting the land use planning database - Overall inspection of the land use planning database and integration into the system - Building land use planning metadata
Land Price Database	<ul style="list-style-type: none"> - Preparation - Collecting documents and data - Reviewing, evaluating, classifying, and organizing documents and data - Building spatial data for land price - Scanning legal documents and processing files - Creating land price attribute data - Checking and completing land price data - Preparing documents for supervision, inspection, and acceptance - Packaging and submitting the land price database - Overall inspection of the land price database and its integration into the system - Developing land price metadata

2.2 Main software used to build land database

The software used in the research is diverse and user-friendly. For the cadastral database, the following software and processes were employed: Microstation V8i software combined with Gcadas and LisediorTC for editing and standardizing spatial objects. Spatial data were then exported to GML.; Attributes were entered in Excel following Gcadas' Excel template; The cadastral database was packaged using ViLIS 2.0 software, encompassing space, attributes, and scanning records. Data from ViLIS 2.0 was subsequently converted to VBDLIS according to regulations. This is proprietary software developed by a IT unit in Vietnam, commissioned by the Ministry of Natural Resources and Environment for deployment across provinces and cities. Currently, only provincial land registration offices manage and access the system. In the future, local citizens may also be systematically granted access.

For other components such as land use planning, statistics and inventory, and land price databases, the primary platform used was the online VBDLIS software available at <https://vilg.vietbando.net/>. The exchange and distribution of land data were carried out using the GML geographic format language and the standard land metadata format via XML extended format language, facilitated through data storage devices and data transmission services.

MicroStation, a comprehensive geographic information system software, offers complete functionality for data acquisition, management, search, and display. Its latest version, MicroStation V8, fully supports all prevailing standard CAD formats, including AutoCAD's

DWG and MicroStation's DGN. This updated version resolves various file size limitations, enabling the integration of both 2D and 3D data within the same file while also supporting Unicode.

The advancements in MicroStation V8 are particularly significant in mapping, notably in the development of detailed topographic maps requiring grid construction and surface analysis. Notably, the previous method of dividing information layers within the 0-63 range has been replaced, allowing users to set the number of information layers according to their specific needs.

MicroStation V8 offers users enhanced flexibility, allowing for quick mounting of a 2D reference file onto a 3D terrain file. This version provides the option to display a background image for terrain from various perspectives, offering a versatile viewing experience. The introduction of Unicode support in MicroStation V8 is a significant enhancement, enabling internationalization of documents and designs, aligning with document regulations in Vietnam. MicroStation V8 now supports several Oracle database systems, including MS SQL, Sybase, Informix, and Access. Moreover, it serves as a comprehensive CAD-based application development environment by facilitating support for programming languages such as Visual Basic, MicroStation Basic, and MDL. Users can utilize the Visual C++ or .NET toolkit for coding and debugging programs.

gCadas is specialized software designed for cadastral and land management, offering a comprehensive set of tools within the Microstation V8i environment. Its functionalities include support tools for measuring and creating cadastral maps, such as registration, producing cadastral records, exporting technical records, index books, electronic cadastral books, registering for the issuance of land use rights certificates, managing land statistics and inventory, and constructing cadastral databases.

gCadas software incorporates tools that automate steps involved in creating cadastral and current status maps, significantly reducing field-work time and enhancing labor productivity. It integrates spatial processing (*.DGN) and land parcel attributes (*.GTP). For spatial data (*.DGN), gCadas software processes, detects conflicts, and offers automated tools, including converting seed files, establishing topology, editing map frames, labeling cadastral plots, and copying objects, among other functions. It supports single or multiple map files. Regarding attribute data (*.GTP), gCadas software facilitates the conversion of attribute data from software like Famis, Vilis, Elis, and TMVlis. It also enables data assignment from spatial data, direct importation into the land plot, exporting to Excel, and updating from Excel files, ensuring commonality and convenience in data management.

VBDLIS software, developed by the Viettel Military Industry and Telecommunications Group in Vietnam, is recognized by the Ministry of Natural Resources and Environment as suitable for constructing, managing, operating, and exploiting land databases. The software provides users with the capability to edit various types of maps, including traffic, urban, land, and thematic maps to highlight data models. It facilitates the connection of geometric objects with non-geometric data, enabling the editing, updating, and exploitation of digital map information. VBDLIS is a web-based software, accessible directly over the internet, offering ease and convenience in building, managing, operating, and exploiting land databases.

VBDLIS software possesses the capability to convert data from other popular GIS software, such as .mif from MapInfo and .shp from ArcGIS. Notably, VBDLIS is the sole software that

encompasses all database subsystems, including cadastral, land statistics and inventory, land use planning, and land price. The process of building a database with VBDLIS software can be accomplished in two ways: either building it online on the website or creating the database on the desktop and subsequently converting it online.

3. CHARACTERISTICS OF THE CASE STUDY

Moc Chau district is situated in the mountainous and highland region, serving as a border district in the southeast of Son La province (refer to Figure 1) (Administrative map of Moc Chau district). The central coordinates are 20°49'21 degrees North latitude and 104°43'10 degrees East longitude. The distance from Son La city center to Moc Chau along Highway 6 is approximately 115 km, while the distance from Moc Chau to Hanoi is around 195 km.

Geographically, Moc Chau district shares its borders as follows: to the east, it borders Van Ho district; to the south, it shares borders with Sop Bao district in Hua Phan province, Lao PDR, covering a common border stretch of 39,949km; to the west, it borders Yen Chau district; and to the north, it borders Phu Yen district.

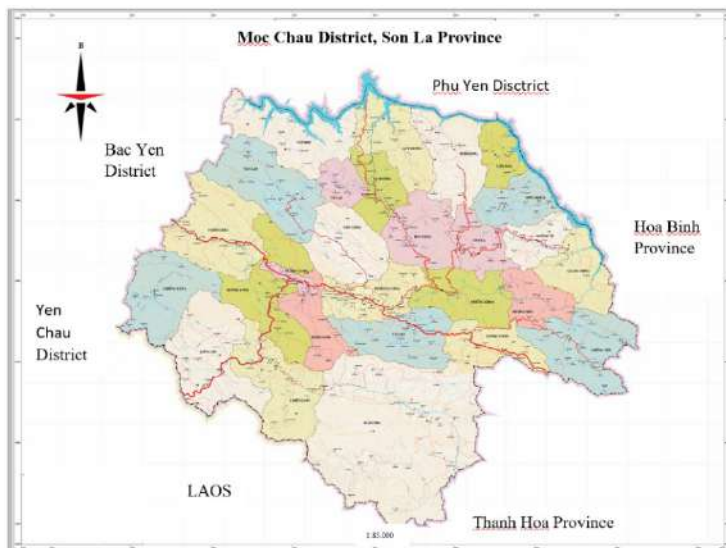


Figure 1. Administrative map of Moc Chau district, Son La province (Administrative map of Moc Chau district).

Moc Chau district comprises 15 commune-level administrative units, inclusive of two towns: Moc Chau (the district capital) and Moc Chau Farm, along with 13 communes: Chieng Hac, Chieng Khua, Chieng Son, Dong Sang, Hua Pang, Long Sap, Muong Sang, Na Muong, Phieng Luong, Quy Huong, Tan Hop, Tan Lap, and Ta Lai. The district covers a total natural land area of 1,081.66 km² and has a population of approximately 114,460 people. Among these, 42,364 reside in urban areas, while 72,096 live in rural areas, resulting in a population density of about 106 people/km² (General Statistics Office).

Moc Chau features a karst terrain dominated by limestone mountains, characterized by numerous high mountains and undulating hills resembling waves, aligning in the northwest - southeast direction. This vast plateau encompasses plains, basins, ravines, rivers, and streams, creating diverse topography. The average altitude is approximately 1,050 meters above sea level.

The region experiences a temperate monsoon climate, marked by four distinct seasons and a consistently cool highland climate. The annual average temperature hovers around 18-20°C, with yearly precipitation averaging between 1,500-1,600 mm. Air humidity maintains an average of about 85%. Noteworthy tourist destinations include Bat Cave, Muc Chau pine forest, Thai Hung waterfall, and the iconic tea hills and grasslands in Moc Chau town.

4 . RESULTS AND DISCUSSIONS

Following the sequential process outlined in Section 2.1, comprehensive results have been achieved, which include distinct databases for the experimental area. These encompass a cadastral database (Figure 2, Figure 3), a land statistical and inventory database (Figure 4), a land use planning database (Figure 5), and a land price database (Figure 6). Each stage, from preparation, document collection, review, evaluation, database construction, document scanning, to meticulous checks and quality assessments, has been meticulously conducted for every component within the land database.

* Cadastral database:

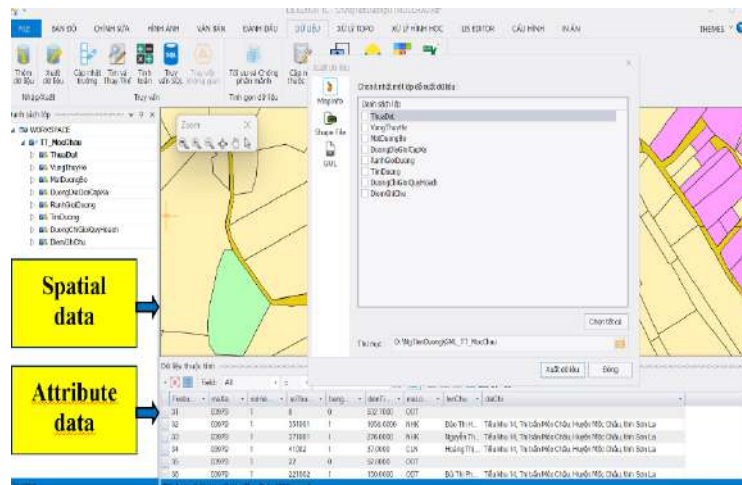


Figure 2. Building spatial cadastral database (Vietnamese language software).



Figure 3. Look up land plot information from electronic cadastral book (Vietnamese language software).

* Building and converting statistical land inventory databases

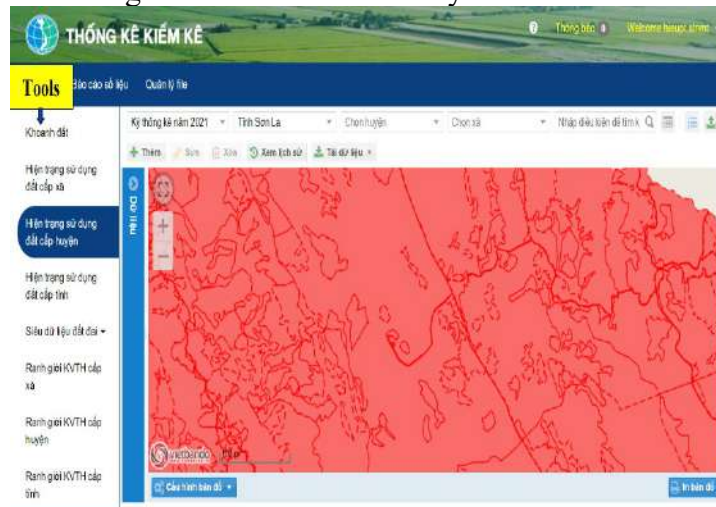


Figure 4. Result of land statistical and inventory database in the experimental area (Vietnamese language software).

* Building and converting land use planning databases:

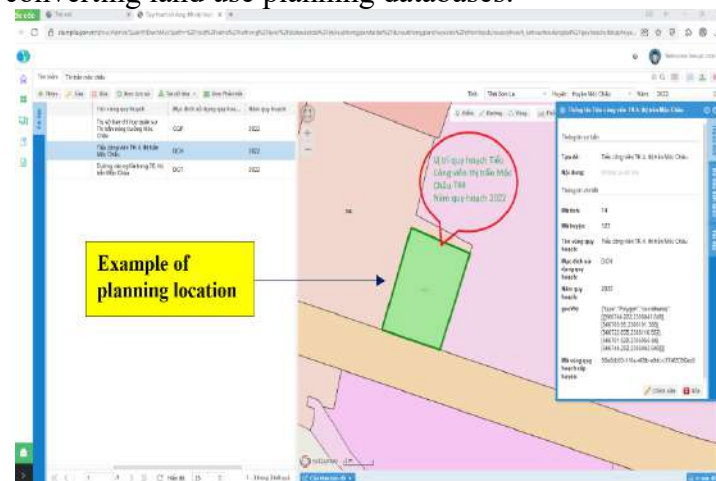


Figure 5. Result of land use planning and plan database in the case study (Vietnamese language software).

* Building and converting land price databases:

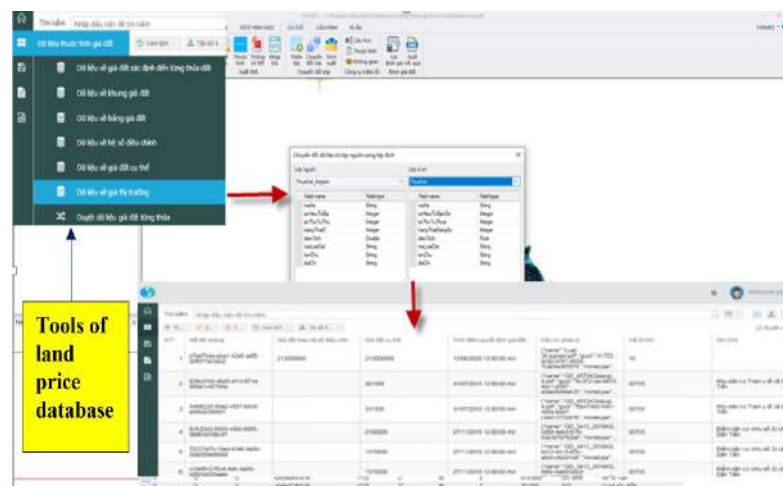


Figure 6. Build a land price database directly on VBDLIS (Vietnamese language software).

The research outcomes concerning the construction of a land database, encompassing the four components, fulfill the criteria for product quality, document completeness, input data, and operational functionality, making it fully exploitable and usable.

The quality of cadastral data is individually determined for each land plot, ensuring consistency among cadastral spatial data, cadastral attribute data, and cadastral records. The land use planning database maintains data consistency between spatial land use planning and attribute information. Land price data quality is established for each land plot, aligning with the regulations of competent state agencies and maintaining consistency with prevailing land prices. Additionally, the quality of land statistical and inventory data ensures the integration of information between statistical and attribute data.

The presentation of land attribute data aligns with the stipulations of land law regarding certificates of land use rights, property ownership, attached assets, cadastral records, land statistics and inventory, land use planning, and land pricing. The exchange and distribution of land data and metadata adhere to standard formats, specifically following the GML geographic format language and the XML extensible format language for metadata. Land data and metadata are exchanged and distributed through data storage devices and data transmission services in the form of data files.

It is evident that sustainable development necessitates well-considered planning closely aligned with local realities, avoiding indiscriminate land use, minimizing agricultural land reduction, and preventing wasteland. The district's land use planning should integrate all these aspects, thereby meeting the legal provisions and aligning with the district's natural and socio-economic conditions.

Once established, the land database will offer swift and precise land information and data, significantly enhancing state land management. It will aptly fulfill the growing demands of economic development, society, defense, security, scientific research, training, international collaboration, and the advancement of e-government in the natural resources and environment sector. Most notably, it will consistently provide essential information to the public and businesses, promoting transparency in land-related services.

The current land use data within the land database serves as the foundation for creating an updated land use map, crucial in annual planning. Leveraging the capabilities of Geographic Information Systems (GIS), spatial analysis facilitates the assessment of land use changes by overlaying map layers over specific time periods. This analysis, alongside statistical data, enables the prediction and guidance of various types of land use development. For the formulation of land use plans, quantitative evaluation of multiple criteria assists in locating optimal sites.

The land database not only supplies information for planning options and mapping but also allows for the application of multi-criteria analysis methods in conjunction with GIS to pinpoint optimal planning locations. Furthermore, it aids in evaluating the impact of land use planning on the economy, society, and the environment while providing support for compensation calculations and site clearance.

Beyond these primary functions, the land database significantly enhances the decision-making process of state management agencies, streamlines administrative services in document handling, and reduces transaction times. It ultimately improves access to land information, catering to the needs of both individuals and organizations.

Several proposed solutions aim to enhance the efficiency of land database exploitation and management within the study area and the country at large:

These include the necessity of planning a long-term strategy for the land data infrastructure, serving as the basis for implementing tailored solutions. Additionally, the proposal involves the creation and enhancement of a market-oriented land information service system. Moreover, it is essential to formulate a detailed and feasible roadmap encompassing aspects such as time, budget, and human resources for effective practical implementation.

Reform the investment policy concerning the construction of a land database by shifting from the current scattered and occasionally inconsistent investment approach to a more concentrated, definitive investment strategy. The focus should be on cultivating a diverse range of human resources, specifically individuals equipped with expertise in land data infrastructure. These professionals should possess comprehensive knowledge not only in land management but also in comprehending urban and rural infrastructure, as well as information technology and urban management.

Developing the information technology infrastructure is crucial, not only for the land management industry but also for the enhancement of the entire administrative system. Provinces and cities should conduct thorough reviews and implement necessary improvements to regulations governing the operation, exploitation, updating, and sharing of land data information under local management. Simultaneously, it is essential to establish and refine various databases, including the land database, cadastral database, land statistical and inventory database, land use planning database, and local land price database. Additional investments are required for the maintenance of connections and the operation of the land information system within the province. This system is crucial for managing, operating, exploiting, updating the land database, and ensuring its connection and sharing with the relevant departments and branches of e-government and smart cities at the local level.

Utilizing 4.0 technology in the development of land technology involves exploring and incorporating innovative technologies such as block chain in electronic transactions within the sector. Implementing open communication standards among information portals and establishing an integration platform for sharing data between information systems and land management databases aligns with cutting-edge global technology standards. Leveraging big data technology for the collection and analysis of data supports decision-making in land management. Furthermore, conducting research to provide open data for the business community encourages the development of applications that cater to the needs of the people.

Implementing robust solutions to ensure information and system security is crucial for managing and securely sharing data from the land database. One key solution involves building a new integrated land database, streamlining processes for measurements, adjusting changes in cadastral maps, and registering land while issuing certificates of use rights. This comprehensive database encompasses details related to land use, housing ownership, and other assets associated with the land.

Standardizing and converting the cadastral database into a system while developing additional component databases (planning, land use plans, land price, and statistical and inventory databases) in areas where a cadastral database already exists is essential. To achieve a cohesive national framework, it's imperative to consolidate cadastral data from provinces and cities along with land-related information provided by ministries and branches.

This consolidation includes compiling comprehensive data such as national land use planning, land price frameworks, and data on bordering areas between provinces and cities. Connecting and sharing these databases is crucial for the effective implementation of e-government initiatives and seamless integration with other national databases. This endeavor necessitates additional investments, upgrades, and the ongoing maintenance of the national land information system.

Implementing such a system would serve as an effective tool for environmental management by enabling better control over territorial planning. The modernization of the land management system represents a significant stride towards achieving the goal of establishing an electronic government through administrative reform. Moreover, a modernized land management system will facilitate an increase in financial revenues derived from land, including land use fees, rents, taxes, and associated fees. This influx of revenue will contribute not only to local budgets but also to state government budgets.

Upon the effective implementation of these solutions, the seamless connection and sharing of land data and associated information within a networked environment will serve as a foundational step towards the realization of e-government and the development of smart urban areas. Furthermore, the transparent handling of administrative procedures and land information will enhance openness and transparency. This, in turn, is poised to increase revenue, reduce costs, offer convenience for both the public and businesses, and foster greater trust among the people towards the government, thereby instilling confidence in both domestic and foreign investors. This progressive approach aims to gradually cultivate an honest government that ensures fairness for all members of society.

5. CONCLUSIONS AND PERSPECTIVES

The research applied the latest and most specialized software to build a land database, which includes components such as a cadastral database, a land statistical and inventory database, a land use planning database, and a land price database in the experimental area of Moc Chau district, Son La province. The land database is systematic and synchronous, achieving the required accuracy. Additionally, several solutions to improve the efficiency of land database exploitation and management have been proposed for localities.

The establishment of a land database in the case study of Moc Chau district offers numerous benefits, such as ensuring an accurate, secure, and transparent data system across management levels. It provides a centralized and consistent channel for accessing information, thereby preventing errors in source data management. This initiative enhances the quality of the decision-making process and advances state management in local land management. Furthermore, it improves the services of state management agencies by expediting document reception and processing, reducing transaction time, and enhancing access to land information to meet the needs of individuals and organizations.

The research's findings will be invaluable for managers, policymakers, and land use planners in an effective and scientific manner. It is recommended that the construction of land databases should continue to be carried out experimentally in various localities with diverse geographical and socio-economic characteristics, allowing the application of different methods and technologies.

For the land database of Moc Chau district and, by extension, the land database of Son La province, it's essential to further develop mechanisms and policies for information utilization. This step ensures that individuals, businesses, and organizations can conveniently, quickly, accurately, and promptly access information. Moreover, there's a need to continuously supplement, update, and refine the land database throughout its operational use and exploitation processes. Implementing clear policy mechanisms is crucial to enhancing the efficiency of use and reducing the time required for current land-related administrative procedures. People gradually gaining direct access to this database as an open-source resource would also be highly beneficial in the future.

The creation of land databases should persist across various localities with distinct characteristics, utilizing diverse methods and technologies. Effective implementation of these solutions is anticipated to facilitate the connection and sharing of land data and associated information within a networked environment. This interconnectedness serves as the foundation for implementing e-government and the development of smart urban areas. The information technology infrastructure links multiple sectors such as resources and environment, tax, banking, etc., enhancing the efficiency of information exploitation. This integration ensures accuracy, timeliness, and overall operational efficiency.

6. REFERENCES

- Administrative map of Moc Chau district, S. L. p. Retrieved 15 September 2023, from <https://mocchau.sonla.gov.vn/ban-do-hanh-chinh>.
- Ali, Z. and M. Shakir (2012). "Implementing GIS-Based cadastral and land information system in Pakistan." *Journal of Settlements and Spatial Planning* 3(1): 43-49.
- Anh, N. N. and N. T. H. Gám (2020). "Ứng dụng hệ thống thông tin địa lý (GIS) xây dựng cơ sở dữ liệu giá đất phục vụ công tác quản lý và giao dịch đất đai": 542-548.
- Anh, T. T., Đ. V. Hải, T. T. T. Thủy and H. V. Hùng (2017). "Nghiên cứu xây dựng cơ sở dữ liệu đất đai đa mục tiêu phục vụ công tác quản lý tại phường Cốc Lếu, thành phố Lào Cai" *TNU Journal of Science and Technology* 175(15): 115-120.
- Beaumont, B., N. Stephenne, L. Van de Vyvere, C. Wyard and E. Hallot (2019). Users' consultation process in building a land cover and land use database for the official Walloon Georeferential. *Joint Urban Remote Sensing Event (JURSE)*, IEEE.
- Cảm, N. B. T. (2021). "Ứng dụng công nghệ Mobile GIS cập nhật thông tin giá đất thị trường phục vụ xây dựng cơ sở dữ liệu giá đất tại thị trấn Phùng, huyện Đan Phượng, thành phố Hà Nội" *Science Journal of Natural Resources and Environment*(35): 94-102.
- Chương, H. V. and N. T. Lan (2010). "Xây dựng cơ sở dữ liệu phục vụ công tác đánh giá đất cà quy hoạch sử dụng đất tại xã Phú Sơn, huyện Hương Thủy, tỉnh Thừa Thiên Hué." 15-26.
- Công, N. T., T. X. Miễn, N. T. Dung, P. T. K. Thoa and N. T. Hiền (2020). "Building a land statistics, testing database." *Journal of Mining and Earth Sciences* 61(2): 96-105.

-
- General Statistics Office, G. S. O. Retrieved 15 September, 2023, from <https://www.gso.gov.vn/>.
- Kepka, M., P. Hájek, D. Kožuch, T. Řezník, T. Mildorf, K. Charvát, M. Kepka Vichrová and J. Chytrý (2022). "An Advanced Open Land Use Database as a Resource to Address Destination Earth Challenges." *Land* 11(9): 1-16.
- Khan, M. Z. and T. Chiti (2022). "Soil carbon stocks and dynamics of different land uses in Italy using the LUCAS soil database." *Journal of Environmental Management* 306: 1-16.
- Liên, L. T. (2022). "Xây dựng cơ sở dữ liệu địa chính xã Ân Tình, huyện Na Rì, tỉnh Bắc Kạn" *Science Journal of Natural Resources and Environment*(41): 112-121.
- Miễn, T. X., N. T. Công, P. T. K. Thoa, N. T. Dung and Đ. T. H. Nga (2022). "Ứng dụng ARCGIS API xây dựng cơ sở dữ liệu thông kê, kiểm kê đất đai tại huyện Phú Lương, tỉnh Thái Nguyên." *Tạp chí Khoa học Đo đạc và Bản đồ*(51): 56-64.
- Minh, V. Q., L. Q. Tri and R. Yamada (2003). Delineation and incorporation of socio-infrastructure database into GIS for land use planning: A case study of Tan Phu Thanh Village, Chau Thanh District, Cantho Province. *Map Asia*.
- Mleczko, M. and M. Desmond (2023). "Using natural language processing to construct a National Zoning and Land Use Database." *Urban Studies* 60(13): 2564-2584.
- Thảo, X. T. T., N. T. H. Hạnh, H. T. Lộc, P. T. Trang, P. T. Quế, Đ. T. T. Dương, N. B. Long, H. V. Hoá, N. T. Hà, N. S. Hà and T. T. Thái (2023). "Results of land database management and mining in Long Thanh district, Dong Nai province." *Journal of Science on Natural Resources and Environment*(45): 135-146.
- Yakubu, I. and R. Asah (2023). "Development of a GIS-Based Land Records Management: A Case Study." *Ghana Journal of Technology* 7(1): 19-29.
- Yang, Y., Y. Sun, S. Li, S. Zhang, K. Wang, H. Hou and S. Xu (2015). "A GIS-based web approach for serving land price information." *ISPRS International Journal of Geo-Information* 4(4): 2078-2093.
- Yin, P. and J. Cheng (2023). "A MySQL-Based Software System of Urban Land Planning Database of Shanghai in China." *CMES-Computer Modeling in Engineering & Sciences* 135(3): 2387-2405.
- Zhang, Y., G. Chen, S. W. Myint, Y. Zhou, G. J. Hay, J. Vukomanovic and R. K. Meentemeyer (2022). "UrbanWatch: A 1-meter resolution land cover and land use database for 22 major cities in the United States." *Remote Sensing of Environment* 278: 1-21.

OIL SPILL IN THE SOUTHERN MARINE REGIONS OF VIETNAM: MODELS AND SIMULATIONS

Phan Minh-Thu¹, Tran Van Chung², Ho Dinh Duan³, Le Cong Tuan⁴, Pham Thi Anh⁵

¹*Institute of Oceanography Vietnam Academy of Science and Technology, Nha Trang,
Vietnam*

²*Institute of Oceanography Vietnam Academy of Science and Technology, Nha Trang,
Vietnam*

³*HCMC Space Technology Application Center, Vietnam National Space Center, Vietnam
Academy of Science and Technology, Ho Chi Minh City, Vietnam*

⁴*University of Sciences, Hue University, Hue City, Vietnam*⁵*Civil Engineering Institute, Ho
Chi Minh City University of Transport,
Ho Chi Minh City, Vietnam*

ABSTRACT

The marine economy plays a vital role in the era of economic development in Vietnam. However, it also causes various incidents for natural resources and the environment among which oil spills have caused significant environmental and ecological harms. Therefore, rapid forecasting of the spreading process of oil makes an important influence to supporting the decision of oil spill prevention and response, as well as minimizing economic losses and negative impacts on the environment and ecology. In this paper, by integrating the Euler-Lagrange method into the 3-D hydrodynamic model-based finite element method, we build a model on simulating the spread of oil spills with scenarios occurring in different hydrometeorological conditions in the southern waters of Vietnam. The model exploited in this paper describes the horizontal composition (x,y) to reflect the preservation of heat and salt of the tangled current dynamics, and the mixing distance. Dirichlet boundary conditions are derived from tidal oscillations at the open boundary nodes, the sliding stress at the bottom and the air temperature at the surface. Our case study of oil spill was taken from the collision of the Lisa Auerbach with the My An 1 in Ba Ria - Vung Tau sea, and the My An 1 ship containing 40 tons of oil on September 14, 2021, being a severe environmental risk. Simulation results of oil spread showed that oil spills had affected ecosystems of mangroves and wetlands in the Mekong Delta.

Keywords— *Oil spill, FEM, HYCOM+NCODA, Simulation*

1. INTRODUCTION

The marine economy has become an essential pillar of economic growth in many countries, and Vietnam is no exception. Situated along the Southeast Asian coastline, Vietnam possesses a vast and diverse marine environment that serves as a critical foundation for sectors such as fishing, tourism, maritime trade, and, increasingly, energy exploitation. With a coastline stretching over 3,260 kilometers, Vietnam's territorial waters contain rich natural resources, including oil, gas, and marine biodiversity, all of which contribute significantly to the nation's economy. In recent decades, Vietnam has actively developed its marine economy, aligning with global trends in coastal and oceanic resource utilization [1]. However, this development has come at a cost, as human activities in the marine sector have introduced substantial environmental risks, among which oil spills pose one of the greatest threats to marine ecosystems and coastal communities [2].

The extraction, transport, and refining of oil have become integral components of the Vietnamese marine economy, with oil and gas exploitation forming a key part of national energy strategies. The offshore oil and gas sector has witnessed rapid growth, providing employment, fueling industrial activity, and contributing significantly to the national GDP. However, along with the economic benefits of oil exploitation comes the risk of catastrophic oil spills, which have the potential to severely damage marine environments. Oil spills release large volumes of hydrocarbons into the ocean, leading to environmental pollution, degradation of marine ecosystems, and loss of biodiversity [3-5]. The consequences of oil spills extend beyond ecological damage, also affecting economic activities dependent on clean waters, such as fisheries and tourism, as well as public health through contaminated water supplies and seafood [3, 6, 7].

The impacts of oil spills are far-reaching and multi-dimensional. First, the immediate effect of an oil spill on marine life is often devastating [4, 8, 9]. Many species, including fish, seabirds, and marine mammals, are highly susceptible to oil contamination, which disrupts their ability to feed, breed, and survive [3-5, 7, 9]. Oil that accumulates on the surface of the water can smother birds and mammals, compromising their ability to thermoregulate, while underwater contamination can devastate coral reefs, sea grasses, and other critical habitats [10]. Additionally, oil spills can cause long-term environmental damage [11], as oil residues persist in ecosystems for years, potentially altering food webs, reducing biodiversity, and hindering ecosystem recovery [10].

In Vietnam, the risk of oil spills is exacerbated by several factors. The southern waters, particularly around the continental shelf, are home to extensive oil reserves and are a focal point for offshore oil extraction [2]. Moreover, the region is a busy maritime hub, with thousands of vessels transporting goods, including oil, through its waters [1]. Accidents involving oil tankers, drilling rigs, and pipelines are not uncommon, and when such incidents occur, they can result in the release of large quantities of oil into sensitive marine and coastal areas. The combination of increasing maritime traffic, ongoing oil exploration, and unpredictable weather patterns in Vietnam's southern waters creates a high likelihood of oil spill incidents [1]. In this context, it becomes critical to develop tools and strategies that can predict the spread of oil spills and enable rapid, effective response actions.

Given the severe environmental, economic, and social consequences of oil spills, oil spill forecasting has emerged as a key area of research and development [10]. The ability to predict how oil will spread, where it will travel, and which areas it will affect is crucial for mitigating damage and informing decision-makers [8, 10, 12]. Accurate forecasting models can provide vital information to authorities, allowing them to implement preventative measures, deploy clean-up resources efficiently, and protect vulnerable ecosystems and communities. Moreover, oil spill prediction can help minimize the economic losses associated with spill incidents by reducing the time needed to respond and by targeting clean-up efforts more effectively [13].

Forecasting the behavior of oil spills is a complex process that requires an understanding of multiple environmental factors [10, 11, 14]. The movement of oil in the ocean is influenced by hydrodynamic conditions, such as currents, waves, and tides, as well as meteorological conditions, including wind speed and direction [15, 16]. Additionally, the physical and chemical properties of the oil, such as viscosity and density, determine how it interacts with the surrounding water [11], how quickly it spreads, and how it breaks down over time. To model the spread of oil spills accurately, it is necessary to integrate all of these factors into a

comprehensive simulation framework that can account for the unique conditions present in a given area [17, 18].

In the case of Vietnam's southern waters, the variability in hydrometeorological conditions poses a significant challenge to oil spill forecasting [2]. Seasonal monsoons, fluctuating ocean currents, and complex interactions between freshwater and saltwater in the region create a dynamic and unpredictable environment. These factors must be incorporated into oil spill models to ensure that predictions are accurate and applicable to real-world scenarios. Additionally, the presence of sensitive ecosystems, such as mangroves, coral reefs, and seagrass beds, further highlights the need for detailed and reliable spill prediction models that can assess the potential impact of oil on these critical habitats.

To address the challenges of oil spill forecasting in Vietnam's southern waters, this paper presents a model that integrates the Euler–Lagrange method into a 3-D hydrodynamic model based on the finite element method [19–23]. This approach allows for the simulation of oil spill scenarios under various hydrometeorological conditions, providing a robust tool for predicting the spread and impact of oil in the marine environment. The Euler–Lagrange method is well-suited to simulating the movement of particles [24–26], such as oil droplets, within a fluid medium, making it ideal for modeling the complex dynamics of oil spills. By coupling this method with a 3-D hydrodynamic model, the simulation can capture the interaction between oil and the surrounding water, accounting for factors such as current velocity, water temperature, and wave action [21]. The finite element method, in turn, allows for the creation of a detailed and flexible mesh that can represent the intricate geography of Vietnam's southern waters, ensuring that the model reflects the unique features of the region.

The model developed in this study is designed to provide decision-makers with a powerful tool for oil spill management. By simulating different spill scenarios under varying environmental conditions, the model can help authorities anticipate the trajectory of oil spills, identify areas at risk, and plan response efforts accordingly. Furthermore, the model can be used to assess the effectiveness of different prevention and response strategies, enabling more efficient allocation of resources and minimizing the environmental and economic impacts of spills.

2. THE RISK OF OIL SPILLS IN THE BIEN DONG

The Bien Dong, also known as the South China Sea, faces significant environmental threats from oil spills due to the confluence of several human activities [2]. The need to transport oil and petroleum liquids, goods between Indian and Pacific Oceans, offshore oil exploration, and fishing practices all contribute to the region's heightened risk of oil spills [1, 2]. These activities not only support the economies of numerous nations but also place immense pressure on the marine ecosystem, where a single oil spill can have catastrophic effects.

One of the primary reasons for the heightened risk of oil spills in the Bien Dong is its crude oil and petroleum liquids and role in global energy transportation. The region serves as a vital conduit for the transport of oil and gas from the Middle East to East Asia's major economies, including China, Japan, and South Korea [1]. More than half of the world's oil tankers pass through these waters, about 23.7 million barrels per day in 2023, making it one of the busiest maritime corridors on the planet. With such high traffic levels, the likelihood of collisions, groundings, and operational errors increases. Aging vessels, mechanical failures, and extreme weather conditions, such as typhoons, can all lead to accidents, resulting in oil

spills. Even small-scale, routine discharges from ships can have long-term environmental impacts by slowly poisoning marine life and ecosystems.

(https://www.eia.gov/international/analysis/special-topics/World_Oil_Transit_Chokepoints)

In addition to oil transport, the Bien Dong is a critical trade route for goods moving between Indian and Pacific Oceans. More than fifty percent of cargo ships transiting the region carries not only goods but also bunker fuel, a type of heavy oil used to power ships [1, 2]. Accidents involving these vessels, such as collisions or groundings, can result in the release of bunker oil, which is highly toxic to marine environments. With substandard shipping practices and lax enforcement of safety regulations by some nations, the risk of oil spills remains ever-present.

The oil and gas exploration and extraction activities in the Bien Dong also contribute to the risk of spills. Offshore drilling platforms in disputed areas are operated by countries including Vietnam, China, Malaysia, and the Philippines. These platforms are located in environmentally sensitive areas, where any oil spill could devastate local ecosystems. Offshore drilling is inherently risky due to the potential for blowouts, where oil gushes uncontrollably from a well, leading to large-scale spills. The deepwater nature of many of these oil fields complicates the situation, as containing a spill at such depths can be more difficult, leading to prolonged environmental damage.

Even fishing activities contribute to the risk of oil pollution in the East Sea. About 18,000 fishing vessels/boats, especially smaller or older ones, use diesel engines that are prone to leaking oil during operations [1]. In addition, fishing practices like trawling, which involve dragging heavy nets across the seafloor, can damage underwater oil pipelines, causing leaks that are challenging to detect and repair.

Therefore, the risk of oil spills in the Bien Dong is multifaceted and driven by the region's strategic importance in global energy transportation, trade, oil exploration, and fishing. These activities, while crucial to economic development, create significant environmental vulnerabilities, necessitating stronger regulations, improved safety practices, and international cooperation to minimize the risk of oil spills and protect the marine ecosystem.

3. FOUNDATION FOR MODELLING OF OIL SPILLS

The Euler–Lagrange method is applied to model the simulation of oil spill incidents, tracking the spill location and the position of particles on the edge of the oil slick [18, 24, 26–28] (Fig. 1). The combined method can fully exploit the advantages of both approaches while avoiding their disadvantages, which explains why it is widely used in solving three-dimensional hydrodynamic problems using the finite element method.

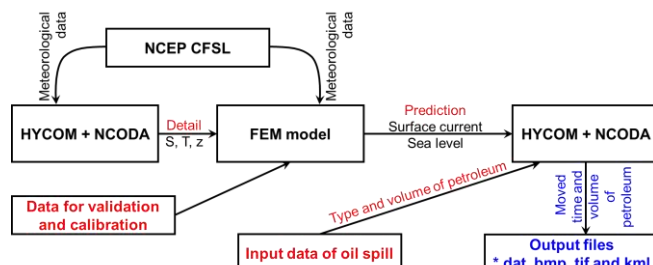


Fig. 1. Flowchart for oil spill model

3.1 The standard set of equations for the FEM (Finite Element Method) model

A three-dimensional hydrodynamic model using the finite element method (FEM) has been concentrated in the studies of references [20, 22, 23, 25], who applied this method to study the hydrodynamic and biogeochemical regime in the coastal areas of Vietnam. Initial comparisons of FEM model results with the Ecosmo model and actual measurements in the Bình Cảng – Nha Trang research area have been conducted [23], as well as comparisons with real-world data from water level stations in a study of the flow regime in the Gulf of Tonkin [29].

3.2 The dominant hydrodynamic equations

The six main variables in the 3-D model are represented in the equations below:

- Two horizontal components (x, y) of the momentum equations:

$$\frac{d\vec{v}}{dt} + \vec{f} \times \vec{v} = g\nabla_{xy}\zeta - \frac{\partial}{\partial z} \left(N_m \frac{\partial \vec{v}}{\partial z} \right) = -\frac{g}{\rho_0} \int_z^\zeta \nabla_{xy} \rho dz + \vec{F}_m + \frac{\sigma}{\rho} (\vec{v}_\sigma - \vec{v}) \quad (1)$$

- The equations for heat and salt conservation:

$$\frac{dT}{dt} - \frac{\partial}{\partial z} \left(N_h \frac{\partial T}{\partial z} \right) = F_T + \frac{\sigma}{\rho} (T_\sigma - T) \quad (2)$$

$$\frac{dS}{dt} - \frac{\partial}{\partial z} \left(N_h \frac{\partial S}{\partial z} \right) = F_S + \frac{\sigma}{\rho} (S_\sigma - S) \quad (3)$$

- The equations for turbulent kinetic energy and mixing length:

$$\frac{dq^2}{dt} - \frac{\partial}{\partial z} \left(N_q \frac{\partial q^2}{\partial z} \right) = 2 \left[N_m \left(\left(\frac{\partial u}{\partial z} \right)^2 + \left(\frac{\partial v}{\partial z} \right)^2 \right) + \frac{g}{\rho_0} N_h \frac{\partial \rho}{\partial z} \right] - 2 \left[\frac{q^3}{B_1 l} \right] + \frac{\sigma}{\rho} (q_\sigma^2 - q^2) \quad (4)$$

$$\frac{dq^2 l}{dt} - \frac{\partial}{\partial z} \left(N_q \frac{\partial q^2 l}{\partial z} \right) = l E_1 \left[N_m \left(\left(\frac{\partial u}{\partial z} \right)^2 + \left(\frac{\partial v}{\partial z} \right)^2 \right) + \frac{g}{\rho_0} N_h \frac{\partial \rho}{\partial z} \right] - l W \left[\frac{q^3}{B_1 l} \right] + \frac{\sigma}{\rho} (q_\sigma^2 l_\sigma - q^2 l) \quad (5)$$

where: E_1 and B_1 are empirical constants [30] and W is a wall proximity function [31]; $\vec{v}(x, y, z, t)$: flow velocity, with components in Cartesian coordinates (u, v, w) and time t ; $\zeta(x, y, t)$: free surface elevation; $h(x, y)$: sea depth (or depth at a constant bottom stress layer where boundary conditions are applied, typically around 1m above the seabed); $H(x, y, t)$: total depth, $H=h+\zeta$; $\rho(x, y, z, t)$: seawater density, ρ_0 taken as the average value; $T(x, y, z, t)$: seawater temperature; $S(x, y, z, t)$: seawater salinity; $q^2(x, y, z, t)/2$: turbulent kinetic energy; $l(x, y, z, t)$: turbulent mixing length; $N_m(x, y, z, t)$: vertical turbulent viscosity; $N_h(x, y, z, t)$: vertical turbulent diffusivity for temperature and salinity; $N_q(x, y, z, t)$: vertical turbulent diffusivity for q^2 and $q^2 l$; \vec{F}_m, F_T, F_S : non-geostrophic horizontal exchange terms for kinetic energy, temperature, and salinity; g : gravitational acceleration; \vec{f} : the Coriolis vector, directed vertically with magnitude f ; ∇ : the gradient operator, and ∇_{xy} is its horizontal component; d/dt : total time derivative, for three-dimensional fluid motion, $\frac{d}{dt} = \frac{\partial}{\partial t} + \vec{v} \cdot \nabla$; (x, y): horizontal Cartesian coordinates, with the positive x-axis pointing east and the positive y-axis pointing north; z : vertical coordinate, positive upwards; ; $-h \leq z \leq \zeta$; t : time; $\vec{v}_b(x, y, z, t)$:

horizontal flow velocity at the bottom of the water column; C_d : bottom drag coefficient (chosen as $C_d = 0.0026$); $\sigma(x, y, z, t)$: distributed mass source (dimension: mass/time/volume); σ/ρ : volume source (dimension: volume/time/volume); $\vec{v}_\sigma, T_\sigma, S_\sigma, q_\sigma^2, q^2 l_\sigma$: the property of the fluid source.

3.3 For oil spill dispersion

From the initially selected position x_t and y_t , the position of each assumed particle after a time interval Δt , $x_{t+\Delta t}, y_{t+\Delta t}$, is updated at each time step by the following equation:

$$x_{t+\Delta t} = x_t + [u_s(x, y, t) \Delta t + \text{Rand}(D_h)] \quad (6)$$

$$y_{t+\Delta t} = y_t + [v_s(x, y, t) \Delta t + \text{Rand}(D_h)] \quad (7)$$

where: u_s, v_s – the velocity components at the surface layer along the meridional and zonal directions (m/s); Rand - a random number between 0 and 1. The first and second terms within the brackets respectively represent the advective and diffusive displacements.

Diffusion is handled using a three-dimensional random walk technique

$$D_h = \sqrt{12A_h \Delta t} \quad (8)$$

where, A_h the horizontal diffusion coefficient (m^2/s), and Δt is the computational time step. A_h is calculated directly from the flow model and varies at different grid points. Details of the material dispersion model can be referenced in Long and Chung [20].

In the oil spill dispersion model, larger oil droplets tend to remain on the water surface and drift in the direction of the wind, while smaller droplets mix downward due to turbulence and diffuse, causing a prolonged effect in the direction of the current. Additionally, the oil will evaporate from the surface and degrade within the water column.

3.4 Boundary conditions

Tidal oscillations are incorporated at the nodes of the open boundary values to create the appropriate tidal forcing and to accurately impose Dirichlet boundary conditions. The problem is solved based on the conservation of horizontal boundary conditions. At the bottom, the typical second-order slip condition relates the bottom stress to the bottom velocity \vec{v}_b through the dimensionless second-order bottom stress drag coefficient, C_d . Air temperature is determined at the surface under "Type III" or radiation conditions with a heating rate of α and an equilibrium temperature T_0 ; at the bottom, the heat flux is assumed to be negligible. Similarly, no-flux conditions are applied to salinity at both the surface and the bottom

3.5 Input data

The study area is selected from $99^\circ E$ to $117.5^\circ E$ longitude; from $5^\circ N$ to $14^\circ N$ latitude (Fig. 2) with an unstructured mesh (triangular grid) (Fig. 3). The triangular computational grid is established with a minimum angle of 30° ; the smallest triangular element area is 35.10628

km²; the largest triangular element area is 898.4974 km²; and the average triangular element area is 491.7557 km².

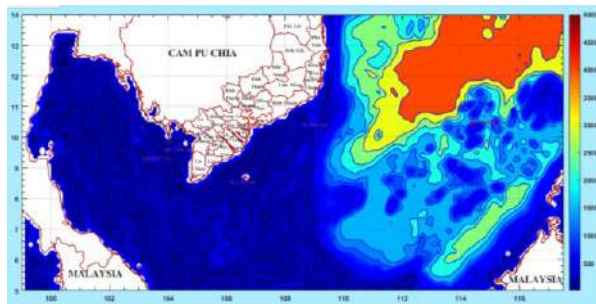


Fig. 2. Depth map in domain of modelling



Fig. 3. Triangular grid in domain of modelling

The primary data sources used for modeling are as follows the depth data, and hydrographic and ocean dynamic data sets. Depth is extracted from the GEBCO_2020 dataset (<https://www.gebco.net/>). Additionally, this data is supplemented and corrected based on in-situ measurements from the Vietnam-Germany South-Central Upwelling Project during the Sonne research vessel survey (04/2006) (with grid spacing of $\Delta x = \Delta y = 100$ m, calculated using the WGS 84 coordinate system).

Hydrographic and ocean dynamic data are collected from Tidal harmonic constants, Temperature-salinity data and Meteorological data. Tidal harmonic constants are calculated for the open boundary with 9 major tidal constituents (M4, M2, S2, N2, K2, K1, O1, Q1, P1) and this dataset was completed under the Vietnam-Germany cooperation program. Temperature-salinity are collected from the World Ocean Database 2018 (WOD18) and the World Ocean Atlas 2018 (WOA18), supplemented with normalized and reanalyzed data from HYCOM + NCODA (Hybrid Coordinate Ocean Model + Navy Coupled Ocean Data Assimilation), with horizontal grid resolution of 0.08°, and data from Russia (<http://pacificinfo.ru/>). Meteorological data (wind velocity, air temperature, relative humidity, cloud cover, precipitation, longwave radiation flux, shortwave radiation flux) is updated from the Climate Forecast System Reanalysis (CFSR) global climate model reanalysis dataset by NCEP (National Centers for Environmental Prediction) (NCEP CFSR). Some examples of input data for calculations are shown in Fig. 4.



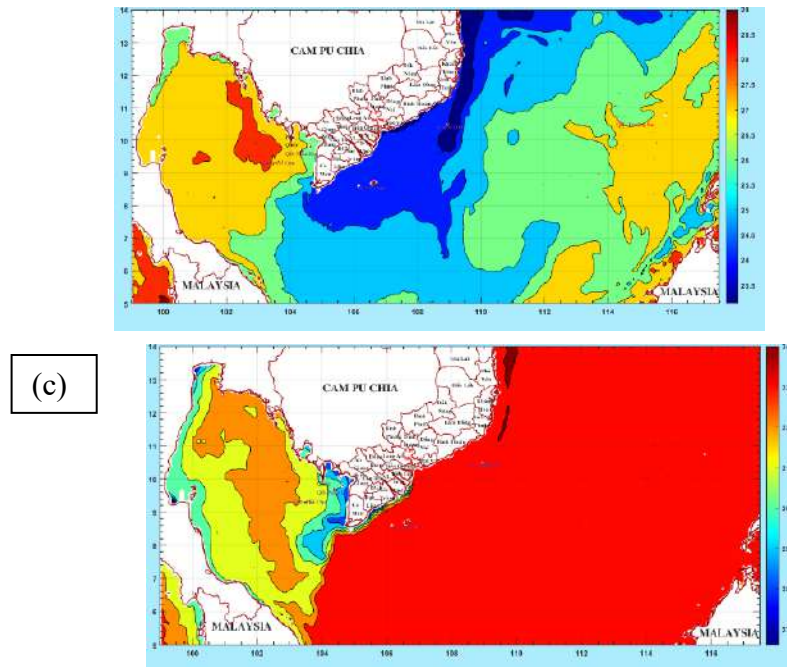


Fig. 3. Examples of input data for oil spill model. (a): monthly currents at the 2m-depth layer in January; (b) monthly seawater temperature at the 2m-depth layer in January; (c) monthly seawater salinity at the 2m-depth layer in January

3.6 Simulation of Oil Spill Incident Warning

Simulating the dispersion and spread of pollution caused by an oil spill is a crucial part of assessing the feasibility and application of the program. The case study of oil spill was taken from the collision of the Lisa Auerbach with the My An 1 in Ba Ria - Vung Tau sea, and the My An 1 ship, contained 40 tons of oil, was accidented on September 14, 2021 (Fig. 5), being a risk of spilling out into the environment. Currently, the sea was dominated by southwest wind at levels 4-5.

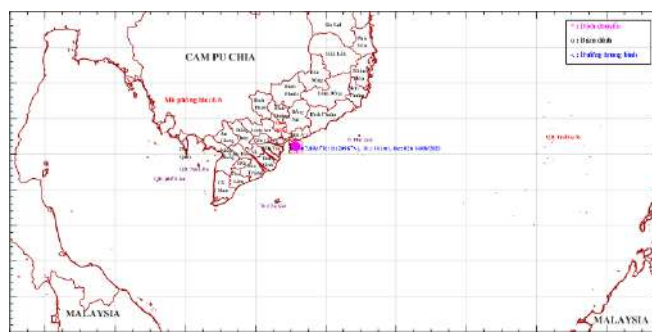


Fig. 4. The input of case study of oil spill in domain

The scenario results of forecast model show the spread of oil spills in detail of the movement path, regions and the affected area. After 150 hours of oil spills that might affected the ecosystem around Phu Quy Island and after 270 hours, the oil spill risked affecting the coral ecosystem in Spratly Islands (Fig. 6). As it continued to spread, oil spills could affect Spratly Islands after about 300 hours.

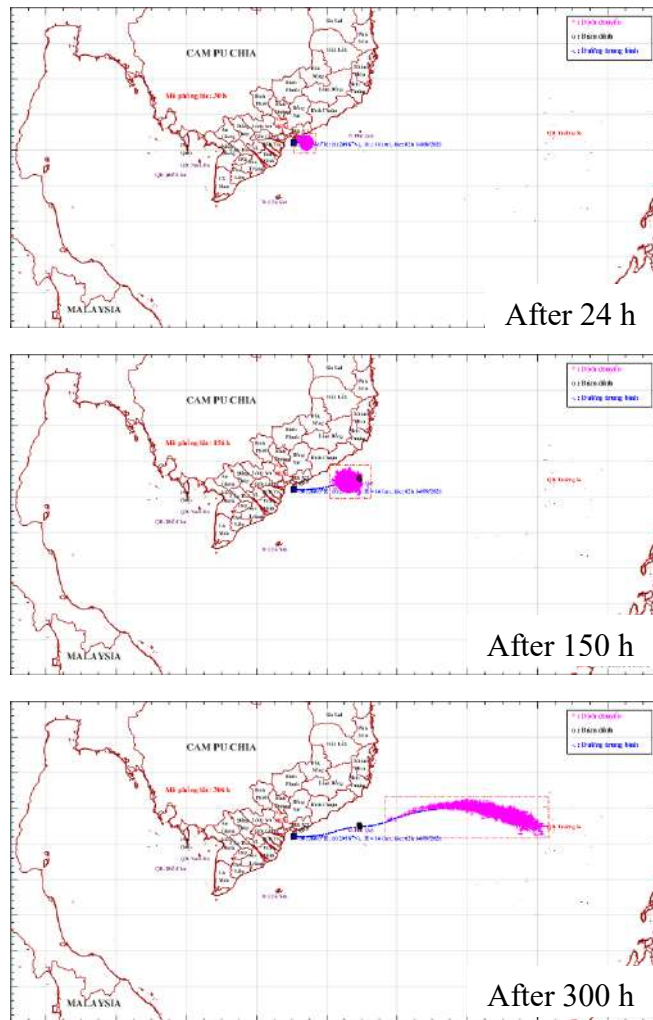
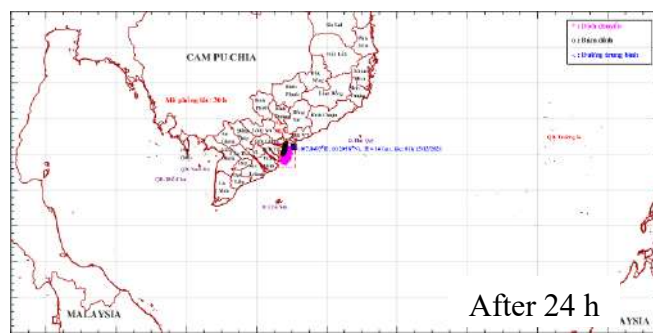


Fig. 5. Scenario results of oil spill in southwest wind at levels 4-5. Pink (+): oil moving, Black (o): oil attachment; Blue (---): moving line of oil spill

Similar to the above scenario but the weather conditions were the northeast wind at level 5-6, specifically the incident time at 12 hours on December 15, 2021. Simulation results of oil spread showed that oil spills had affected ecosystems of mangroves and wetlands in the Mekong Delta. After 264 hours, the remaining oil could pass through the Ca Mau cape and affected the environment in the Gulf of Thailand. (Fig. 7)



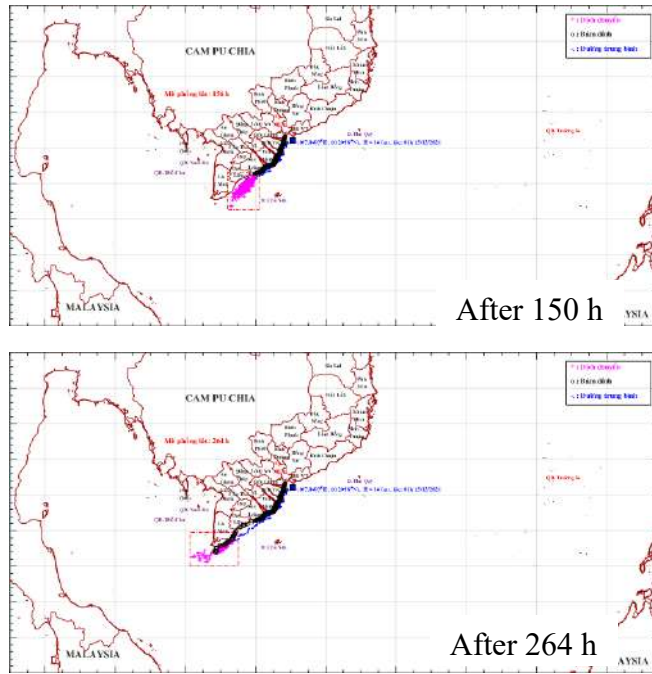


Fig. 6. Scenario results of oil spill in northeast wind at level 5-6. Pink (+): oil moving, Black (o): oil attachment; Blue (---): moving line of oil spill

From the above scenarios, the spreading process of oil spills in Southern Vietnam waters tends to spread complexly, depending on the wind regime, seasons and hydrodynamic systems. Oil spills could impact reef ecosystems in Phu Quy Island or the Spratly Islands, or mangrove forests in the Mekong Delta as well as organisms in the waters where the spilled oil passed through. Moreover, the computing time of the model in this article for an incident are ranged in 1-3 h, so the forecast result is the significant value in spreading forecast of oil spills and warning of the effects of oil spills on the surrounding environment.

4. DISCUSSIONS AND CONCLUSION

The oil spill tracking model outlined in the report presents a comprehensive and detailed method for simulating and monitoring oil spill events in coastal regions. Central to this model is its use of a three-dimensional nonlinear hydrodynamic system [3, 10, 17, 18, 21, 26, 32], which accurately captures the interactions between water currents, tides, and other environmental factors. This advanced level of detail is crucial for understanding how oil spills behave, as it reflects the inherent complexity of natural water systems.

One of the key strengths of this model lies in its rigorous validation process. By comparing the model's output with real-world data, such as tidal height, phase, and current measurements across different study areas, the researchers ensured its accuracy. This cross-validation with observational data from various sources bolsters the model's credibility, making it a dependable tool for tracking oil spill movement and predicting dispersion patterns.

The development and localization of the dispersion of oil spill and rapid warning system represents a major step forward in user interaction. Localization tailors the model to the specific environmental and geographic conditions of the region, enhancing its precision and relevance. This ease of use is particularly important in practical applications, where quick, accurate information is crucial for mitigating environmental damage during emergency responses.

This model is invaluable for decision-makers tasked with responding to pollution incidents. By providing detailed simulations of oil spill dispersion, it offers real-time insights into how an oil spill may evolve, enabling authorities to take proactive measures. Information about the spill's location, potentially affected areas, and how environmental factors like wind and water currents influence the spill aids in better resource allocation, targeted clean-up efforts, and effective environmental protection strategies.

The model's comprehensive approach is due to its integration of critical environmental variables, including flow dynamics, wind conditions, and meteorological data. These initial and boundary conditions are essential for accurately simulating oil spill behavior. By incorporating real-time data on the spill's location, size, and relevant weather conditions, the model produces highly relevant forecasts.

Ongoing model calibration and the use of annual survey data are vital for maintaining the model's accuracy. Comparing model results with real-world observations allows it to evolve continuously, adapting to new environmental knowledge or changes in coastal conditions. This feedback loop refines predictions, making the model a dynamic tool that becomes more precise with each update.

Generally, the oil spill tracking model provides a detailed and well-validated method for simulating oil spill incidents. Its ability to account for hydrodynamic interactions and adapt to local conditions makes it an essential asset in environmental monitoring and pollution response. By delivering crucial data to support timely and effective decisions, and through continuous calibration, this model remains a reliable and forward-looking solution for oil spill management.

5. ACKNOWLEDGMENT

The paper was funded by the provincial project: "Study on environmental carrying capacity for build up the master plan of sustainable development of aquaculture in Ba Ria – Vung Tau province" and also using data from the national project code of ĐTDL.CN.17/28.

6. REFERENCES

- N. T. An, P. M. Thụ, N. T. Vân, and T. P. H. Sơn, Governance and Development of Economy in Biển Đông Ha Noi, Vietnam: Publishing House for Science and Technology, 2017, p. 262.
- N. Đ. Duong, H. L. Thu, L. V. Anh, and N. K. Anh, "Oil pollution in Vietnam and neighboring Sea," Vietnam Journal of Earth Sciences, vol. 35, no. 4, pp. 424-432, 06/14 2014, doi: 10.15625/0866-7187/35/4/4130.
- Z. Asif, Z. Chen, C. An, and J. Dong, "Environmental Impacts and Challenges Associated with Oil Spills on Shorelines," Journal of Marine Science and Engineering, vol. 10, no. 6, p. 762, 2022. [Online]. Available: <https://www.mdpi.com/2077-1312/10/6/762>.
- G. Perhar and G. B. Arhonditsis, "Aquatic ecosystem dynamics following petroleum hydrocarbon perturbations: A review of the current state of knowledge," Journal of Great Lakes Research, vol. 40, pp. 56-72, 2014/01/01/ 2014, doi: <https://doi.org/10.1016/j.jglr.2014.05.013>.
- N. Andrews, N. J. Bennett, P. Le Billon, S. J. Green, A. M. Cisneros-Montemayor, S. Amongin, N. J.

- Gray, and U. R. Sumaila, "Oil, fisheries and coastal communities: A review of impacts on the environment, livelihoods, space and governance," *Energy Research & Social Science*, vol. 75, p. 102009, 2021/05/01/ 2021, doi: <https://doi.org/10.1016/j.erss.2021.102009>.
- [6] D. P. Prendergast and P. M. Gschwend, "Assessing the performance and cost of oil spill remediation technologies," *Journal of Cleaner Production*, vol. 78, pp. 233-242, 2014/09/01/ 2014, doi: <https://doi.org/10.1016/j.jclepro.2014.04.054>.
- [7] S. E. Chang, J. Stone, K. Demes, and M. Piscitelli, "Consequences of oil spills: a review and framework for informing planning," *Ecology and Society*, vol. 19, no. 2, 2014, Art no. 26, doi: 10.5751/ES-06406-190226.
- A. Jernelöv, "The Threats from Oil Spills: Now, Then, and in the Future," *AMBIO*, vol. 39, no. 5, pp. 353-366, 2010/07/01 2010, doi: 10.1007/s13280-010-0085-5.
- J. K. Keesing, A. Gartner, M. Westera, G. J. Edgar, J. Myers, N. J. Hardman-Mountford, and M. Bailey, Chapter 5: Impacts and Environmental Risks of Oil Spills on Marine Invertebrates, Algae and Seagrass: A Global Review from an Australian Perspective (*Oceanography and Marine Biology: An Annual Review*). Boca Raton, Lodon, New York: CRC Press, 2018, p. 61.
- I. Berenshtein, S. O'Farrell, N. Perlin, J. N. Sanchirico, S. A. Murawski, L. Perruso, and C. B. Paris, "Predicting the impact of future oil-spill closures on fishery-dependent communities—a spatially explicit approach," *ICES Journal of Marine Science*, vol. 76, no. 7, pp. 2276-2285, 2019, doi: 10.1093/icesjms/fsz138.
- I. Bossert, W. M. Kachel, and R. Bartha, "Fate of Hydrocarbons During Oily Sludge Disposal in Soil," *Applied and Environmental Microbiology*, vol. 47, no. 4, pp. 763-767, 1984, doi: [doi:10.1128/aem.47.4.763-767.1984](https://doi.org/10.1128/aem.47.4.763-767.1984).
- B. Zhang, E. J. Matchinski, B. Chen, X. Ye, L. Jing, and K. Lee, "Chapter 21 - Marine Oil Spills—Oil Pollution, Sources and Effects," in *World Seas: An Environmental Evaluation* (Second Edition), C. Sheppard Ed.: Academic Press, 2019, pp. 391-406.
- L. Zhong, J. Wu, Y. Wen, B. Yang, M. Grifoll, Y. Hu, and P. Zheng, "Analysis of Factors Affecting the Effectiveness of Oil Spill Clean-Up: A Bayesian Network Approach," *Sustainability*, vol. 15, no. 6, p. 4965, 2023. [Online]. Available: <https://www.mdpi.com/2071-1050/15/6/4965>.
- J. R. Nelson and T. H. Grubacic, "A repeated sampling method for oil spill impact uncertainty and interpolation," *International Journal of Disaster Risk Reduction*, vol. 22, pp. 420-430, 2017/06/01/ 2017, doi: <https://doi.org/10.1016/j.ijdrr.2017.01.014>.
- C. Kuang, J. Chen, J. Wang, R. Qin, J. Fan, and Q. Zou, "Effect of Wind-Wave-Current Interaction on Oil Spill in the Yangtze River Estuary," *Journal of Marine Science and Engineering*, vol. 11, no. 3, p. 494, 2023. [Online]. Available: <https://www.mdpi.com/2077-1312/11/3/494>.
- R. Cao, H. Chen, Z. Rong, and X. Lv, "Impact of ocean waves on transport of underwater spilled oil in the Bohai Sea," *Marine Pollution Bulletin*, vol. 171, p. 112702, 2021/10/01/ 2021, doi: <https://doi.org/10.1016/j.marpolbul.2021.112702>.
- D. Liu, L. Mu, S. Ha, S. Wang, and E. Zhao, "An innovative coupling technique for integrating oil spill prediction model with finite volume method-based ocean model," *Marine Pollution Bulletin*, vol. 185, p. 114242, 2022/12/01/ 2022, doi: <https://doi.org/10.1016/j.marpolbul.2022.114242>.
- M. De Dominicis, N. Pinardi, G. Zodiatis, and R. Archetti, "MEDSLIK-II, a Lagrangian marine surface oil spill model for short-term forecasting – Part 2: Numerical simulations and validations," *Geosci. Model Dev.*, vol. 6, no. 6, pp. 1871-1888, 2013, doi: 10.5194/gmd-6-1871-2013.
- [19] M. Cremonesi and A. Frangi, "A Lagrangian finite element method for 3D compressible flow applications," *Computer Methods in Applied Mechanics and Engineering*, vol. 311, pp. 374-392, 2016/11/01/ 2016, doi: <https://doi.org/10.1016/j.cma.2016.08.005>.
- B. H. Long and T. V. Chung, "Study on the current regime in Phan Thiet bay using 3D nonlinear finite

- element method," *Vietnam Journal of Marine Science and Technology*, vol. 12, no. 4, pp. 1-14, 11/30 2012, doi: 10.15625/1859-3097/12/4/2574.
- W. K. Liu, S. Li, and H. S. Park, "Eighty Years of the Finite Element Method: Birth, Evolution, and Future," *Archives of Computational Methods in Engineering*, vol. 29, no. 6, pp. 4431-4453, 2022/10/01 2022, doi: 10.1007/s11831-022-09740-9.
- T. V. Chung and N. H. Huan, "Calculations of current in the Vung Ro bay using the finite element method," *Vietnam Journal of Marine Science and Technology*, vol. 17, no. 2, pp. 121-131, 06/30 2017, doi: 10.15625/1859-3097/17/2/9249.
- B. H. Long and T. V. Chung, "Calculations of tidal currents in bay lagoon (Nha Trang bay) using finite element method," *Vietnam Journal of Marine Science and Technology*, vol. 14, no. 4, pp. 332-340, 12/31 2014, doi: 10.15625/1859-3097/14/4/5819.
- A. W. Visser, "Using random walk models to simulate the vertical distribution of particles in a turbulent water column," *Marine Ecology Progress Series*, vol. 158, pp. 275-281, 1997. [Online]. Available: <https://www.int-res.com/abstracts/meps/v158/p275-281/>.
- B. H. Long and T. V. Chung, "Modelling Material Transport in North Danger Reef, the Spratly Islands, Based on a Three-Dimensional Nonlinear Finite Element Model for Wind Currents," presented at the Proceedings of the Conference on the Results of the Philippines-Vietnam Joint Oceanographic and Marine Scientific Research Expedition in the South China Sea (JOMSRE-SCS I to IV), Nhatrang, Vietnam, December 11, 2008, 2008, 135-147.
- M. De Dominicis, N. Pinardi, G. Zodiatis, and R. Lardner, "MEDSLIK-II, a Lagrangian marine surface oil spill model for short-term forecasting – Part 1: Theory," *Geosci. Model Dev.*, vol. 6, no. 6, pp. 1851-1869, 2013, doi: 10.5194/gmd-6-1851-2013.
- E. Capó, A. Orfila, J. M. Sayol, M. Juza, M. G. Sotillo, D. Conti, G. Simarro, B. Mourre, L. Gómez-Pujol, and J. Tintoré, "Assessment of operational models in the Balearic Sea during a MEDESS-4MS experiment," *Deep Sea Research Part II: Topical Studies in Oceanography*, vol. 133, pp. 118-131, 2016/11/01/ 2016, doi: <https://doi.org/10.1016/j.dsr2.2016.03.009>.
- Y. C. Zeng, J. P. Yang, and C. W. Yu, "Mixed Euler–Lagrange approach to modeling fiber motion in high speed air flow," *Applied Mathematical Modelling*, vol. 29, no. 3, pp. 253-261, 2005/03/01/ 2005, doi: <https://doi.org/10.1016/j.apm.2004.09.007>.
- T. V. Chung and B. H. Long, "Some calculated results of current in the Gulf of Tonkin by using nonlinear three-dimensional (3D) model," *Vietnam Journal of Marine Science and Technology*, vol. 15, no. 4, pp. 320-333, 12/31 2015, doi: 10.15625/1859-3097/15/4/7377.
- G. L. Mellor and T. Yamada, "Development of a turbulence closure model for geophysical fluid problems," *Reviews of Geophysics and Space Physics*, vol. 20, no. 4, pp. 851-875, 1982.
- A. F. Blumberg, B. Galperin, and D. J. O'Connor, "Modeling Vertical Structure of Open-Channel Flows," *Journal of Hydraulic Engineering*, vol. 118, no. 8, pp. 1119-1134, 1992, doi: doi:10.1061/(ASCE)0733-9429(1992)118:8(1119).
- K.-H. Lee, T.-G. Kim, and Y.-H. Cho, "Influence of Tidal Current, Wind, and Wave in Hebei Spirit Oil Spill Modeling," *Journal of Marine Science and Engineering*, vol. 8, no. 2, p. 69, 2020. [Online]. Available: <https://www.mdpi.com/2077-1312/8/2/69>.

PREDICTING LAND-USE CHANGE USING GIS AND MACHINE LEARNING - A CASE STUDY IN TUYEN QUANG CITY, VIETNAM

Bui Ngoc Tu¹, Le Phuong Thuy¹, Pham Le Tuan¹, Nguyen Xuan Linh¹, Tran Quoc Binh¹

¹University of Science, Vietnam National University, 334 Nguyen Trai, Thanh Xuan, Hanoi, Vietnam

Email: buingoctu@hus.edu.vn

Email: lephuongthuy@hus.edu.vn

Email: phamletuan@hus.edu.vn

Email: nguyenxuanlinh@hus.edu.vn

Email: tranquocbinh@hus.edu.vn

ABSTRACT

The prediction of land-use change helps identify trends in land conversion and supports urban land-use planning. In this study, we utilized the Artificial neural network-Cellular automata (ANN-CA) model and random forests (RF) algorithm to predict future land-use change and analyze the contributions of each driving factor in Tuyen Quang city, Vietnam. The model incorporated land-use maps in the years 2010, 2015, 2020 and 12 driving factors, categorized into three groups: natural, transportation, public services and population factors. A comparison of the simulated and actual land-use maps for 2020 achieving a strong overall accuracy of 87.58% and a Kappa coefficient of 0.83, thereby validating the dependability of the model's predictions. Subsequently, this model was applied to predict land-use change for the years 2025 and 2030. Additionally, this study identified elevation, slope, distance to river, distance to main road and distance to trade center as the most significant factors influencing land-use change in Tuyen Quang city. This study offers urban planners useful insights to develop land use strategies and support the area's sustainable development goals.

Keywords: Machine learning, ANN-CA, Random forest, GIS, Land-use change, Driving factors.

1. INTRODUCTION

Urbanization drives land-use change, transforming rural areas into urban spaces (Weith *et al.*, 2021). Predicting land-use change is crucial for managing land resources and developing strategies for future land use management (Camara *et al.*, 2020). Additionally, anticipating land use trends helps policymakers address challenges such as urban sprawl, habitat loss, and deforestation (Hassan and Nazem, 2016; McDermott *et al.*, 2023). The change in land-use is a complex process, thus the development of models to simulate and predict land-use change is a challenging task (Samardžić-Petrović *et al.*, 2015). The Cellular Automata (CA) model is widely used to predict future land use because of its simplicity, flexibility, ability to generate spatiotemporal patterns, and effectiveness in simulating complex dynamic systems across various regions and scales (Xu *et al.*, 2023; Du *et al.*, 2020; Zhang *et al.*, 2019). The CA model represents geographic space as grids of cells, where each cell's state is determined by its prior state and the states of its neighboring cells, following specific transition rules (Santé *et al.*, 2010). However, previous studies have identified challenges in defining transition rules or transition potential, difficulty in representing the non-linear relationships between land-use change and different spatial driving factors in CA model (X. Wu *et al.*, 2022). By integrating with CA, machine learning algorithms improve the accuracy of land-use change simulations, enabling the exploration of

potential land-use patterns and the consideration of complex spatiotemporal non-linear relationships (Yue *et al.*, 2024; Yang *et al.*, 2016). The machine learning algorithms commonly integrated with CA model in land use change simulation and prediction include: the Artificial neural network-Cellular automata (ANN-CA) (Iskandar *et al.*, 2024; Karengas and Nilsonthi, 2024; Ramadhan and Hidayati, 2022; Yang *et al.*, 2016; Yue *et al.*, 2024), the random forest-cellular automata (RF-CA) (R. Wu *et al.*, 2021; Zhang *et al.*, 2019), support vector machine-cellular automata (SVM-CA) (Yang *et al.*, 2008). In these studies, the machine learning algorithms (ANN, RF, SVM) was utilized to derive transfer probabilities in land-use change for CA. In addition to predicting land-use change, it is essential to identify the contributions of driving factors to support decision-making in land-use planning (F. Wu *et al.*, 2022, Yue *et al.*, 2024).

In this study, the ANN-CA model in MOLUSCE (Modules of Land Use Change Evaluation) plug-in in the QGIS 3.34.1 software was used to fill the gap of knowledge for predicting land-use change in Tuyen Quang city (Vietnam). A novel contribution of this paper, compared to various other studies that utilized the MOLUSCE plug-in to predict land-use change, was the incorporation of the RF to explore the contributions of each driving factor.

2. METHODOLOGY

2.1 Study Area and Data collection

Tuyen Quang City is the capital and the political, economic, cultural, and social center of Tuyen Quang Province, located in the Northeast region of Vietnam, 165 km south of Hanoi. To enhance the socio-economic development area, the city explained its administrative boundary in 2020 and currently covers an area of 184.38 km², with a population of 232,230 people as of that year. Recent rapid urbanization has led to substantial population growth in the city, generating new economic development opportunities while also presenting significant challenges in land management. Due to data limitations and to ensure consistency in the spatial scope of all datasets, the study area in this paper is defined by the administrative boundary of the city according to the official land-use maps 2010 and 2015 (Fig.1).

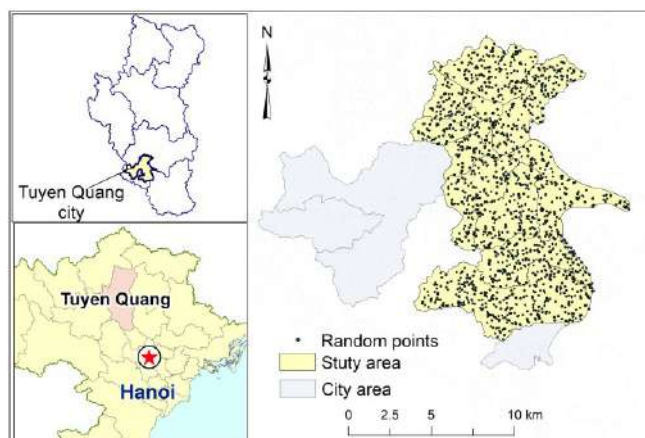


Figure 1. The location of study area

In this study, two primary types of data were utilized for model development: official land-use maps and a series of spatial driving factors data. In Vietnam, official land-use maps are made at 5-year intervals (The National Assembly of the Socialist Republic of Vietnam, 2024). The original land-use vector maps from 2010, 2015, and 2020 were obtained from the local Resources and Environmental Office. We rasterized and reclassified the original land-use maps into the seven

most representative land-use classes, which can represent the main land-use types in our study area, included: Agricultural land (AL), forest land (FL), residential land (RL), administration and public services land (APL), industrial and commercial land (ICL), water (WL), and unused land (UL). Based on previous studies (R. Wu *et al.*, 2021; X. Wu *et al.*, 2022; Zhang *et al.*, 2019), this research selected 12 spatial driving factors, categorized into three groups: natural, transportation, public services and population factors (Table 1). Natural factors are one of the key factors influencing the spatial distribution of land-use (Li *et al.*, 2018; F. Wu *et al.*, 2022). Three types of natural factors have been commonly recognized: elevation (DEM), slope (SI), distance to river (Ri). Traffic conditions significantly influence urban development and land-use dynamics (Reilly *et al.*, 2009). In this study, four determinants of transportation network accessibility were identified: Distance to main road (MRoad), distance to small road (SRoad), distance to bus station (Bus), and distance to city centre (CityC). Many studies have shown that population has a significant impact on land-use change, particularly in relation to public service facilities (Feudjio Fogang *et al.*, 2023; R. Wu *et al.*, 2021; Zhang *et al.*, 2019). Five factors related to public services and population were chosen: Distance to school (Sch), distance to hospital (Hosp), distance to trade centre (Trade), distance to government organization (Gov), population density (Pop). All land-use data and spatial driving factors data are rasterized at a spatial resolution of 20 x 20 m, includes 563,038 cells with 917 rows and 614 columns.

Table 1. Spatial driving factors

Categories	Driving factors	Tools	Source of data
Natural factors	DEM	ArcGIS's Spatial	Tuyen Quang Geographical database
	Slope	Interpolation	
	Distance to river		
Transportation factors	Distance to main road		Tuyen Quang Geographical database, land-use maps
	Distance to small road		
	Distance to bus station		
Public services and population factors	Distance to city centre	ArcGIS's Euclidean Distance	Local socioeconomic statistical report 2009, 2019
	Distance to school		
	Distance to hospital		
	Distance to trade centre		
	Distance to government organization		
	Population density	ArcGIS's Density tool	

2.2 Land-use change prediction

In this study, we used the ANN-CA model in MOLUSCE (Modules of Land Use Change Evaluation) plug-in in the QGIS 3.34.1 software to predict future land-use change based on historical data and 12 spatial driving factors (Fig. 2). This plug-in is widely employed in research on simulation and prediction of land-use change (Iskandar *et al.*, 2024; Ramadhan and Hidayati, 2022). The ANN algorithm, specifically multilayer perceptron (ANN-MLP), which is used to predict land-use change potential, consists of three distinct layers: input, hidden, and output. The input layer incorporates data obtained from land-use maps for the years 2010 and 2015, alongside driving factors, whereas the hidden layer analyzes this data to calculate the transition probabilities. The probability of land-use change is ascertained by evaluating the output layer of transition values generated by neural networks, wherein the classification is adjusted to the category

exhibiting the greatest probability. We created 1500 random points to develop the training ANN-CA model, and the ANN algorithm was executed with a neighborhood rule of 1 px, a learning rate of 0.001, a maximum of 1,000 iterations, 10 hidden layers, and a momentum of 0.050. These values are consistent with several studies and yield good results in these studies (Iskandar *et al.*, 2024; Klanreungsan and Nilsonthi, 2024; Ramadhan and Hidayati, 2022). The CA algorithm analysis is carried out to generate the simulated land-use map for 2020 based on the results from the potential transition step with one-time iteration.

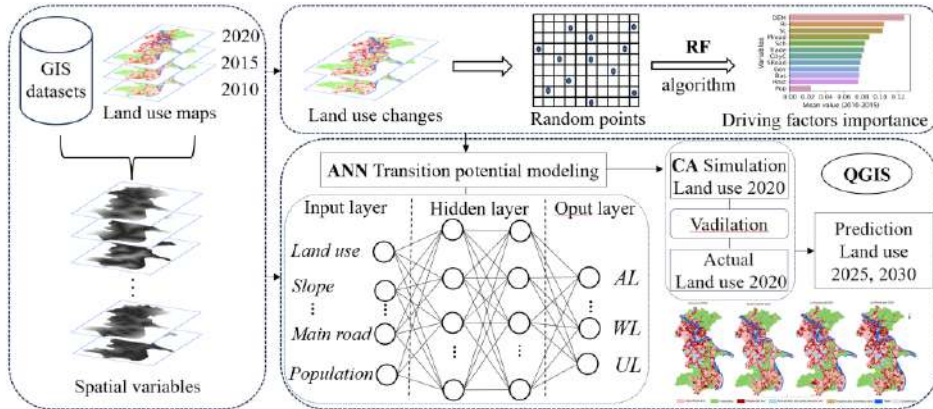


Figure 2. Methodology flowchart

The performance of the ANN-CA model is assessed by the kappa coefficient, which quantifies the alignment between the simulated and actual land-use map in 2020. The kappa coefficient is the predominant metric employed to evaluate model performance, and the kappa value was calculated using Equation 1 (Petropoulos *et al.*, 2015):

$$Kappa\ coefficient = \frac{N \sum_{i=1}^r X_{ii} - \sum_{i=1}^r X_{i+}X_{+i}}{N^2 - \sum_{i=1}^r X_{i+}X_{+i}} \quad (1)$$

Where: N is the total number of pixels, X_i is the corrected classified pixels, r is the number of rows, X_{i+} represents the marginal sum of rows, and X_{+i} represents the marginal sum of columns.

The Kappa coefficient ranges from -1 to 1. If the Kappa value exceeds 0.61, the model is evaluated as having good performance (Isinkaralar and Varol, 2023), several research studies only employ the model for predicting future land-use if the Kappa coefficient above 0.75 (Ramadhan and Hidayati, 2022). In this study, models achieving a Kappa coefficient above 0.75 will be utilized to predict land-use change for the years 2025 and 2030, using two and three iterations, respectively.

2.3 Importance of spatial driving factors

Identifying driving factors contributions in land-use change models aids urban planners in comprehending land use evolution (Lv *et al.*, 2021), which is essential for formulating effective land-use planning policies (Zhang *et al.*, 2019). The RF, which was proposed by (Breiman, 2001), which is considered to be the most accurate, simple variable importance estimator and is commonly used in many studies related to land-use change dynamics (R. Wu *et al.*, 2021). The RF is a combination algorithm using multiple decision trees for prediction (Breiman, 2001). This study utilized the Random Forest Classifier class from the Scikit-learn library to construct models and determine the contributions of each driving factor to the land-use change between the two periods: 2010–2015, 2015–2020. From the 1500 random points generated in ANN-CA model (Section 2.2),

we created a dependent variable classified with two values: random points in cells with land-use transitions were encoded as ‘1’, and those with no transitions were encoded as ‘0’. For the independent variables, the sample points will take values from corresponding cells from 12 spatial driving factors layers (Table 1). The data are divided randomly into two parts: the training dataset for training the model (80%) and the test dataset for evaluating the performance of the model (20%). Each spatial driving factor has a different impact on land-use change, which is reflected by the importance of value. In this study, we used the returned values of the feature_importances_ parameter to rank spatial driving factors by their importance in the land-use change.

3. RESULTS AND DISCUSSION

3.1 Transition matrix

The transition matrix quantifies land-use change rates and facilitates future change modeling (Muhammad *et al.*, 2022; Yue *et al.*, 2024). The values of the transition matrix range from 0 to 1, with higher values indicating a greater likelihood of that land-use type being converted into another. The diagonal values represent the stability of the land-use type, while the off-diagonal values represent transitions from one class to another (Muhammad *et al.*, 2022). Land-use data from 2010 to 2015 were used to calculate the transition matrix (Table 2), which is employed to simulate land-use in 2020 (Section 3.2). Analysis of the results in Table 3 shows that agricultural land, industrial and commercial land have the highest probability of transitioning to residential land. Water and residential land have the highest stability probabilities compared to other land-use types, with rates of 0.98 and 0.92, respectively.

Table 2. Transition matrix of land use for the period 2010–2015

	AL	FL	RL	APL	ICL	WL	UL
AL	0.73	0.03	0.15	0.03	0.02	0.04	0.00
FL	0.05	0.88	0.04	0.01	0.02	0.00	0.00
RL	0.01	0.01	0.92	0.02	0.04	0.00	0.00
APL	0.01	0.02	0.18	0.69	0.09	0.01	0.00
ICL	0.01	0.03	0.12	0.04	0.79	0.01	0.00
WL	0.02	0.00	0.00	0.00	0.00	0.98	0.00
UL	0.00	0.00	0.03	0.04	0.03	0.00	0.90

3.2 Simulation and Model validation

By using actual land-use data from 2010 to 2015 along with spatial variables, we simulated land-use for 2020. Upon comparing the simulated land-use with the actual land-use in 2020, we achieved an overall accuracy of 87.58% and a kappa value of 0.83. Based on previous studies (Isinkaralar and Varol, 2023; Iskandar *et al.*, 2024; Klanreungsan and Nilsonthi, 2024; Ramadhan and Hidayati, 2022), this model can be used to predict future land-use change. The actual and simulated land-use for 2020 are illustrated in Fig. 3a and Fig. 3b, respectively (Section 3.3).

3.3 Future land-use prediction

The CA modeling with two-time and three-time iterations resulted in land-use change predictions for 2025 and 2030 (Fig. 3c and Fig. 3d, respectively). The predictions of land-use change for 2030 predictions indicate that AL and FL will still comprise a significant portion of

the city's total area (56.43%); however, these two land-use types are expected to decline, while areas designated for RL, APL, and ICL land are projected to expand substantially (Table 3). This trend reflects the city's development strategy for the coming period, which focuses on expanding land for construction projects aimed at supporting the growth of industries, services, tourism, and urbanization. With regard to FL, the city also needs to continue prioritizing forest conservation to protect the environment and mitigate the risk of landslides in mountainous areas caused by natural disasters. The area of WL and UL has remained relatively stable; however, when compared to the actual land use from 2020, the changes in unused land (UL) still do not fully capture the current trend in reality. Simulating and predicting land-use change is a complex process (Samardžić-Petrović et al., 2015); therefore, future research should continue to thoroughly evaluate and analyze the causes of changes for each land-use type.

Table 3. Land-use area statistics for actual 2020 and predicted 2025 and 2030

	Area 2020 (km²)	Area 2020 (%)	Area 2025 (km²)	Area 2025 (%)	Area 2030 (km²)	Area 2030 (%)
AL	33.94	28.47	33.15	27.81	32.20	27.01
FL	38.03	31.90	35.92	30.13	35.07	29.42
RL	26.84	22.52	27.36	22.95	27.99	23.48
APL	8.10	6.79	8.26	6.93	8.84	7.42
ICL	4.24	3.56	5.67	4.76	6.27	5.26
WL	7.52	6.31	7.84	6.57	7.89	6.62
UL	0.54	0.45	1.01	0.85	0.95	0.80
Total	119.21	100	119.21	100	119.21	100

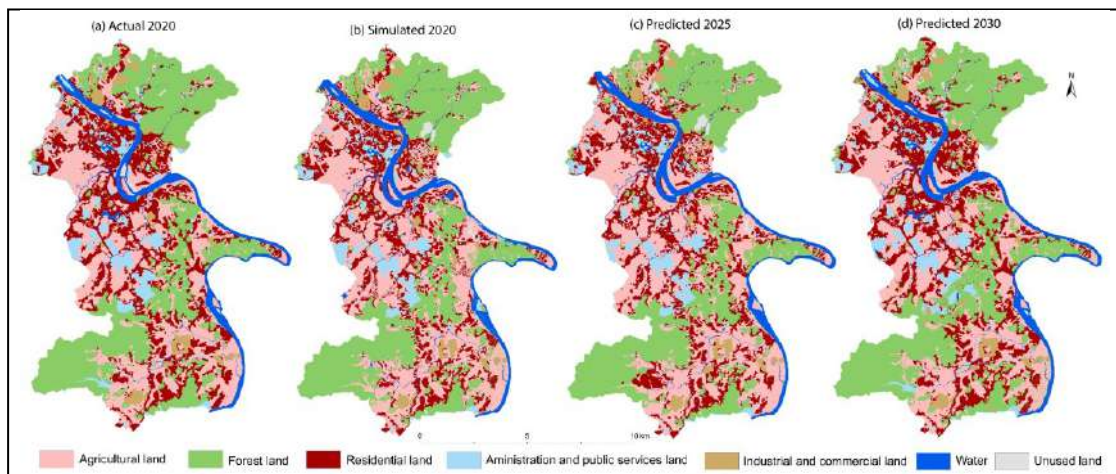


Figure 3. Actual, simulated 2020 and predicted land-use change 2025, 2030

3.4 Analysis of the driving factors in land-use change

The results of measuring the importance of spatial driving factors during the two periods, 2010–2015 (Fig. 4a) and 2015–2020 (Fig. 4b), indicate that five factors, namely DEM, Ri, SL, Mroad, and Trade, had the most significant impact on land-use change. These findings are consistent with the research of R. Wu *et al.* (2021) and X. Wu *et al.* (2022) in Huizhou (China), where DEM and SL strongly influenced forest and agricultural land changes. According to R. Wu *et al.* (2021), the factors Ri, Mroad, and Trade are commonly associated with land-use change

in RL and ICL. Interestingly, the Pop factor had the least impact on land-use change in Tuyen Quang City, which contrasts with the findings of X. Wu *et al.* (2022), W. Yue *et al.* (2024) in Huizhou and Dongguan (China). This discrepancy may be due to the lack of detailed population density data in this study, which was insufficient to clarify its impact on land-use change. Other factors contributed almost equally to land-use change in Tuyen Quang City during the period from 2010 to 2020. This study only assessed the contributions of each driving factor in overall land-use change; but did not examine their influence on each land-use type. Therefore, future research should focus on analyzing the significance of these factors for each particular land-use type.

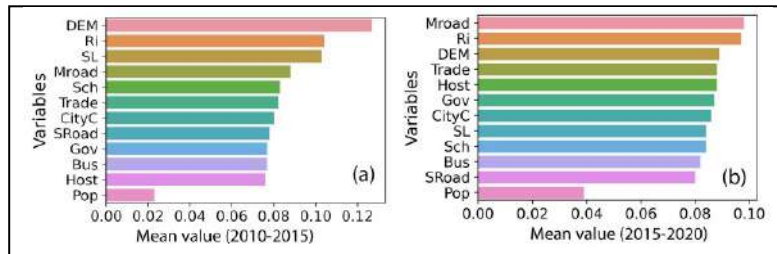


Figure 4. Spatial driving factors importance

4. CONCLUSION

This research has predicted land-use change and analyzed the importance of each spatial driving factors in Tuyen Quang city (Vietnam) by using machine learning and GIS. The ANN-CA model in MOLUSCE plug-in in QGIS 3.34.1 software was applied to predict future land-use change based on historical land use (2010, 2015, 2020) and 12 driving factors. The model demonstrated strong performance, achieving an overall accuracy of 87.58% and a Kappa coefficient of 0.83. When compared to 2020, the predicted land-use change for 2030 reveal a projected increase in residential land, administration and public services land, industrial and commercial land by 4.1%, 8.49%, and 32.29%, respectively, while agricultural land and forest land will decrease by 5.41% and 8.44%, respectively. The water and unused land are predicted to exhibit stability, with no major variations expected. Additionally, this study identified DEM, Ri, SL, Mroad, and Trade as the most significant factors influencing land-use change during the 2010–2020 period in Tuyen Quang city. Future studies will broaden the scope and can incorporate policy, environmental, pandemic and climate change factors to achieve more comprehensive results. Moreover, alongside official land-use maps, upcoming research will explore using land-use maps extracted from satellite images to validate, better assess annual land-use change and enhance the reliability of predictions.

5. ACKNOWLEDGEMENTS

PhD Candidate Bui Ngoc Tu was funded by the Master, PhD Scholarship Programme of Vingroup Innovation Foundation (VINIF), code VINIF.2023.TS.141. The authors wish to extend their gratitude to all contributors, reviewers, and editors for their valuable support.

6. REFERENCES

- Alamanos, A., 2023. A Cellular Automata Markov (CAM) model for land use change prediction using GIS and Python. Available at: https://github.com/Alamanos11/Land_uses_prediction.
- Breiman, L., 2001. Random forests. Machine Learning 45(1), 5–32.

- Camara, M., Jamil, N. R. B., Abdullah, A. F. B., and Hashim, R. B., 2020. Integrating cellular automata Markov model to simulate future land use change of a tropical basin. *Global Journal of Environmental Science and Management* 6(3).
- Du, X., Zhao, X., Liang, S., Zhao, J., Xu, P., and Wu, D., 2020. Quantitatively Assessing and Attributing Land Use and Land Cover Changes on China's Loess Plateau. *Remote Sensing* 12(3).
- Feudjio Fogang, L., Tiomo, I. F., Kamga, B. Y., Mounmemi Kpoumie, H., Tanougong Nkondjoua, A. D., Nguetsop, V. F., and Zapfack, L., 2023. Predicting land use/land cover changes in the Santchou Wildlife Reserve (Santchou, West-Cameroon) using a CA-Markov model. *Trees, Forests and People* 14, 100438.
- Hassan, M. M., and Nazem, M. N. I., 2016. Examination of land use/land cover changes, urban growth dynamics, and environmental sustainability in Chittagong city, Bangladesh. *Environment, Development and Sustainability* 18(3), 697–716.
- Isinkaralar, O., and Varol, C., 2023. A cellular automata-based approach for spatio-temporal modeling of the city center as a complex system: The case of Kastamonu, Türkiye. *Cities* 132, 104073.
- Iskandar, B., Saidah, Kurnia, A. A., Jauhari, A., and Zannah, F., 2024. Modeling Land Cover Change Using MOLUSCE in Kahayan Tengah Forest Management Unit, Kalimantan Tengah. *Jurnal Sylva Lestari* 12(2), 242–257.
- Klanreungsan, B., and Nilsonthi, P., 2024. Urban Land Use Changes Simulation with CA-ANN Model: A Case Study of Mae Sot District, Tak Province, Thailand. *International Journal of Geoinformatics*.
- Lv, J., Wang, Y., Liang, X., Yao, Y., Ma, T., and Guan, Q., 2021. Simulating urban expansion by incorporating an integrated gravitational field model into a demand-driven random forest-cellular automata model. *Cities* 109, 103044.
- McDermott, C. L., Montana, J., Bennett, A., Gueiros, C., Hamilton, R., Hirons, M., Maguire-Rajpaul, V. A., Parry, E., and Picot, L., 2023. Transforming land use governance: Global targets without equity miss the mark. *Environmental Policy and Governance* 33(3), 245–257.
- Muhammad, R., Zhang, W., Abbas, Z., Guo, F., and Gwiazdzinski, L., 2022. Spatiotemporal Change Analysis and Prediction of Future Land Use and Land Cover Changes Using QGIS MOLUSCE Plugin and Remote Sensing Big Data: A Case Study of Linyi, China. *Land* 11(3), 419.
- Petropoulos, G. P., Kalivas, D. P., Georgopoulos, I. A., and Srivastava, P. K., 2015. Urban vegetation cover extraction from hyperspectral imagery and geographic information system spatial analysis techniques: Case of Athens, Greece. *Journal of Applied Remote Sensing* 9(1), 096088.
- Ramadhan, G. F., and Hidayati, I. N., 2022. Prediction and Simulation of Land Use and Land Cover Changes Using Open Source QGIS. A Case Study of Purwokerto, Central Java, Indonesia. *Indonesian Journal of Geography* 54(3).
- Reilly, M. K., O'Mara, M. P., and Seto, K. C., 2009. From Bangalore to the Bay Area: Comparing transportation and activity accessibility as drivers of urban growth. *Landscape and Urban Planning*, 92(1), 24–33.
- Samardžić-Petrović, M., Dragičević, S., Bajat, B., and Kovačević, M., 2015. Exploring the Decision Tree Method for Modelling Urban Land Use Change. *Geomatica* 69(3), 313–325.
- Santé, I., García, A. M., Miranda, D., and Crecente, R., 2010. Cellular automata models for the simulation of real-world urban processes: A review and analysis. *Landscape and Urban Planning* 96(2), 108–122.
- The National Assembly of the Socialist Republic of Vietnam., 2024. Land law. National Political Publishing House.
- Weith, T., Barkmann, T., Gaasch, N., Rogga, S., Strauß, C., and Zscheischler, J. (Eds.), 2021. Sustainable Land Management in a European Context: A Co-Design Approach, Vol 8. Springer

International Publishing.

- Wu, F., Mo, C., and Dai, X., 2022. Analysis of the Driving Force of Land Use Change Based on Geographic Detection and Simulation of Future Land Use Scenarios. *Sustainability* 14(9), 5254.
- Wu, R., Wang, J., Zhang, D., and Wang, S., 2021. Identifying different types of urban land use dynamics using Point-of-interest (POI) and Random Forest algorithm: The case of Huizhou, China. *Cities* 114, 103202.
- Wu, X., Liu, X., Zhang, D., Zhang, J., He, J., and Xu, X., 2022. Simulating mixed land-use change under multi-label concept by integrating a convolutional neural network and cellular automata: A case study of Huizhou, China. *GIScience & Remote Sensing* 59(1), 609–632.
- Xu, Q., Zhu, A.-X., and Liu, J., 2023. Land-use change modeling with cellular automata using land natural evolution unit. *Catena* 224, 106998.
- Yang, X., Chen, R., and Zheng, X. Q., 2016. Simulating land use change by integrating ANN-CA model and landscape pattern indices. *Geomatics, Natural Hazards and Risk* 7(3), 918–932.
- Yue, W., Qin, C., Su, M., Teng, Y., and Xu, C., 2024. Simulation and prediction of land use change in Dongguan of China based on ANN cellular automata—Markov chain model. *Environmental and Sustainability Indicators* 22, 100355.
- Zhang, D., Liu, X., Wu, X., Yao, Y., Wu, X., and Chen, Y., 2019. Multiple intra-urban land use simulations and driving factors analysis: A case study in Huicheng, China. *GIScience & Remote Sensing* 56(2), 282–308.

INVESTIGATING LAND SUBSIDENCE BY PROCESSING MULTI-Temporal SAR TIME SERIES ON GOOGLE COLAB: CASE STUDY IN CAMAU CITY, MEKONG DELTA, VIETNAM

Ha Trung Khien^{1*}, Tran Van Anh², Pham Quy Nhan³, Ha Thi Hang¹, Khuc Thanh Dong¹, Tatsuya Nemoto⁴ and Venkatesh Raghavan⁴

¹Department of Geodesy, Hanoi University of Civil Engineering, 55 Giai Phong Street, Dong Tam Ward, Hai Ba Trung Dist., Ha Noi, Vietnam
Email: khienht@huce.edu.vn, hanght@huce.edu.vn, dongkt@huce.edu.vn

² Department of Geomatics and Land Administration, Hanoi University of Mining and Geology, No.18 Vien Street, Duc Thang Ward, Bac Tu Liem Dist., Hanoi, Vietnam
Email: tranvananh@humg.edu.vn

³ Hanoi University of Natural Resources and Environment (HUNRE), No 41A Phu Dien Road, Phu Dien Ward, North Tu Liem Dist., Hanoi, Viet Nam
Email: pqnhan@hunre.edu.vn

⁴ Osaka Metropolitan University, Graduate School of Science, 3-3-138 Sugimoto Sumiyoshi-ku, Osaka-shi, 558-8585, Japan
Email: tnemoto@omu.ac.jp, raghavan@omu.ac.jp

ABSTRACT

The phenomenon of land subsidence is widespread and complex in Ca Mau Province, stemming from both natural factors and human activities. Radar remote sensing technology has become an effective tool for monitoring and surveying land subsidence over large areas. The process of processing radar images to identify land subsidence not only requires specialized knowledge and experience but also necessitates powerful hardware systems to handle multi-temporal data. Therefore, this process can be costly and time-consuming. This study focuses on evaluating the application of the Google Colab online platform using the MT-SAR (Multi-Temporal Synthetic Aperture Radar) processing method to analyze a series of 24 Synthetic Aperture Radar images from January 2022 to December 2023 for Ca Mau City and surrounding areas. By comparing the results from Google Colab with field survey data, the study will assess the effectiveness and accuracy of land subsidence detection using the SBAS technique on the Google Colab platform, with results showing a correlation coefficient R² of 0.80 and RMSE of 4mm.

1. INTRODUCTION

The InSAR (Interferometric Synthetic Aperture Radar) technique is currently being explored for detecting land subsidence through various methodologies, including Differential InSAR (D-InSAR), Permanent Scatterers InSAR (PS-InSAR), and Small Baseline Subset (SBAS) techniques, as well as their combinations, across diverse global regions. Radar remote sensing was first applied to extract surface data of Venus and the Moon in 1969 (A. Rogers, 1969). By 1974, Graham removed the topographic phase from SAR images to map and detect surface displacement (Graham, 1974). Howard demonstrated that the D-InSAR method is affected by atmospheric noise and spatiotemporal conditions (H.A. Zebker, 1992). The PS-InSAR method was proposed by Ferretti et al. (A. Ferretti, 2000). However, this method has limitations when applied to areas with few stable scatterers, such as rural regions, forests, or deserts. In 2002, Berardino and colleagues introduced the SBAS method, which enables more effective monitoring in regions with rapidly changing ground conditions (P. Berardino, 2002). Since its development, SBAS has been employed for surface deformation detection across

various global locations. Notable studies include the monitoring of subsidence in Mexico City using the SBAS technique (S., 2020); the application of both PS-InSAR and SBAS technologies to detect land subsidence in Kunming City, China (Xiao, Zhao et al., 2022); Yuejuan Chen's work, which combined all three methods PS-InSAR, D-InSAR, and SBAS to identify Persistent Scatterers (PS) and Distributed Scatterers (DS) in Tongliao City, Inner Mongolia (Chen, Ding et al., 2024).

In Vietnam, the D-InSAR, PS-InSAR, and SBAS methods have also been studied and applied for land subsidence detection in several regions. Early research in Vietnam focused on monitoring subsidence in Hanoi (Van Anh, 2016; Dang, 2014; Bui, 2020). In the Mekong Delta region, including Ca Mau, a study by Erban applied InSAR technology using stacking methods to determine average phase displacement (Erban, Gorelick et al., 2014). The PS-InSAR method was utilized to detect land subsidence in the Mekong Delta (Philip S. J. Minderhoud, 2020). With the same method, Anh V.T. conducted studies in the Ca Mau area (Anh, 2021; Anh T. V., 2023).

These studies predominantly utilize software platforms such as StaMPS/MTI (Stanford Method for Persistent Scatterers/Multi-Temporal InSAR), ESA SNAP (European Space Agency's Sentinel Application Platform), and SARscape (Synthetic Aperture Radar Scape) that operate on computer systems with adequate configuration and storage capacity, particularly for processing multi-temporal radar image series over extensive areas. To overcome these limitations, online platforms leveraging server resources from major technology companies like Google and Microsoft have been developed, enhancing performance and cost-effectiveness for processing large datasets. Google Colab, a widely used online platform provided by Google, offers significant advantages for remote sensing data processing (Johary, Révillion et al., 2023). This study utilizes the SBAS method on the Google Colab platform to process a series of 24 multi-temporal radar images to monitor land subsidence in Ca Mau City and surrounding areas from January 2022 to December 2023.

2. RESEARCH METHODOLOGY

2.1 Study area

The study area includes the entire city of Ca Mau and several neighboring communes within the districts of Dam Doi, Cai Nuoc, Tran Van Thoi, U Minh, and Thoi Binh, located in Ca Mau province in the southern territory of Vietnam (Figure 1). This region is predominantly flat, with an average elevation ranging from 0.4 to 0.6 meters above sea level. Some areas have elevations around 0.2 meters in low-lying regions and between 0.8 to 1.1 meters in higher regions. The topography gently slopes from north to south and from northeast to northwest. The area features a complex network of rivers and canals, facilitating agricultural irrigation. The eastern and southern parts are mainly used for intensive and semi-intensive shrimp farming, while the northern and western parts are primarily used for double-crop rice cultivation, vegetables, and freshwater agriculture.

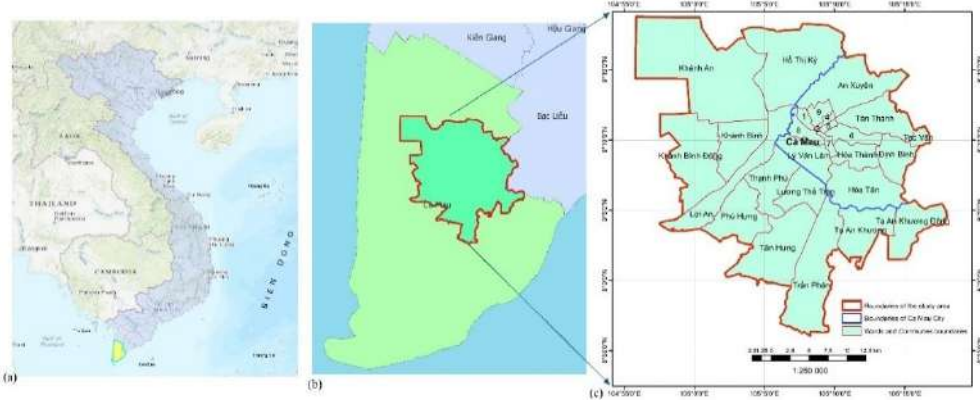


Figure 1. (a) Location of Ca Mau Province in Vietnam, (b) Location of the study area within Ca Mau Province, (c) Boundaries of wards and communes in the study area.

2.2 Data

In this paper, the dataset utilized consists of a series of 24 images from the Sentinel-1A satellite, covering the period from January 2022 to December 2023 in the Ca Mau Province region. Sentinel-1A imagery is a product of the Copernicus Earth Observation program of the European Space Agency (ESA), equipped with a C-band Synthetic Aperture Radar (SAR) with a 12-day repeat cycle in Interferometric Wide Swath (IW) mode with VV polarization (Table 1). The Sentinel-1A datasets were obtained from the Alaska Satellite Facility's database (<https://search.asf.alaska.edu/>). Additionally, the study employs SRTM DEM (Shuttle Radar Topography Mission) data provided by NASA with a ground resolution of 30 meters.

Table 1. Parameters of Sentinel-1A Satellite Images in the Study.

Parameter	Value
Flight Direction	Descending
Data Acquisition Mode	IW (Interferometric Wide Swath)
Polarization	VV
Band	C
Wavelength (cm)	5,6
Spatial Resolution	20m
Swath Width	250km
Number of Images	24
Observation Period	01/2022 – 12/2023

2.3 Proposed Method

MT-SAR (Multi-Temporal Synthetic Aperture Radar) is a method for analyzing synthetic aperture radar (SAR) data using multi-temporal observations to measure and monitor surface deformation with high accuracy. It is one of the techniques used in long-term analyses, enabling the monitoring of phenomena such as land subsidence, mountain deformation, or changes in the height of architectural structures over time. MT-SAR can estimate ground surface movement with millimeter precision. Key MT-SAR techniques include PS-InSAR (Persistent Scatterer Interferometry SAR) and SBAS (Small Baseline Subset). In this study, we focus on using the SBAS method to determine subsidence in Ca Mau City, Ca Mau Province, Vietnam.

SBAS is an advanced method used in Synthetic Aperture Radar (SAR) image processing for monitoring and measuring surface deformation, proposed by Berardino in 2002 (Berardino P, 2002). This method relies on analyzing subsets of SAR images with small baselines to minimize errors related to observational conditions and signal noise.

The process of applying SBAS technique to process multi-temporal Synthetic Aperture Radar (SAR) images for surface deformation monitoring consists of the following main steps:

(1) SAR data acquisition: Collecting 24 SAR images from the Sentinel-1A satellite from January 2022 to December 2023.

(2) SAR image pre-processing: Utilizing geometric correction methods to ensure precise alignment of all SAR images and applying filters to remove noise.

(3) Creating interferometric image pairs: Computing interferometric pairs of SAR images with small spatial and temporal baselines to minimize geometric errors. Subsequently, performing interferometric phase processing on these pairs to determine phase differences between two image scenes. Applying methods to mitigate atmospheric phase variation and geometric errors.

(4) Phase unwrapping: Employing algorithms such as SNAPHU (Statistical-Cost Network-Flow Algorithm for Phase Unwrapping) (Zebker, 2000) to unwrap the phases of the interferometric pairs, converting from wrapped phase to absolute phase.

(5) Time-series deformation analysis: Using Digital Elevation Model (DEM) data to correct for terrain effects on the interferometric pairs. Then, applying the SBAS method to analyze the time-series of unwrapped interferometric phases to determine surface deformation over time.

2.4 Google Colab online platform

Google Colab (Google Collaboratory) is a free online platform offered by Google that facilitates the editing and execution of Python code in a notebook environment. Leveraging Google's cloud infrastructure, Google Colab eliminates the need for high-performance local computing resources. Users can access this platform with a Google account and a stable internet connection, allowing them to operate it seamlessly across various devices. The processing of radar image time series is a resource-intensive and complex task. By utilizing Google Colab, users benefit from sufficient computational power and storage capacity. In this study, the PyGMTSAR library is utilized on the Google Colab platform to collect, process, and analyze

radar image series using the SBAS technique. PyGMSAR is an open-source library developed in Python, designed to support these analytical processes (Pechnikov, 2023).



The screenshot shows the CodeJuliaPyb IDE interface with the following details:

- Title Bar:** Contains the project name "CodeJuliaPyb", file tabs for "Top", "Changelog", "New", "Changelog", "Top", and "Top", and a status bar indicating "Running Python 3.8.5".
- Left Sidebar:** Shows a tree view with a root node "Top" expanded, displaying "src" and "sensor_data".
- Right Sidebar:** Includes sections for "Nhận xét" (Comments), "Chia sẻ" (Share), and "Thống kê" (Statistics).
- Code Editor:** Displays Python code for interacting with the GitHub API to clone repositories and update issues. The code includes imports for requests, os, and json, and uses GitHub's OAuth token for authentication.

Figure 2. Google Colab Online Platform.

3. RESULTS AND DISCUSSION

3.1 Subsidence detection on Google Colab

As presented in Section 2.2, the paper utilizes a dataset consisting of 24 time-series Synthetic Aperture Radar (SAR) images with a SBAS method. Below is the baseline distribution of the interferogram pairs (Figure 3).

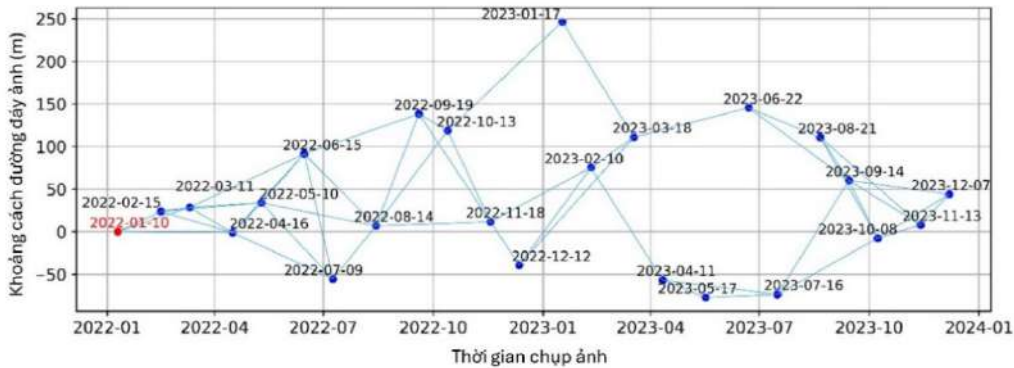


Figure 3. Distribution diagram of the baseline set of Sentinel images for study area.

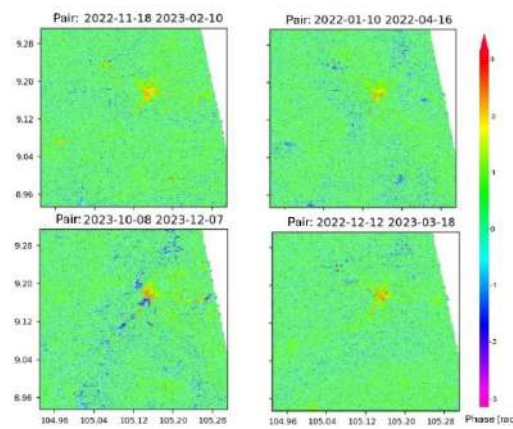


Figure 4. Typical interferogram.

Following data acquisition, the images were aligned with precise orbit files and cropped to accurately match the study area. The interferometric processing of the image pairs involved applying the Goldstein filter to mitigate noise, thereby producing clear interferograms with topographic phase effects removed. Additionally, the Minimum Cost Flow (MCF) technique was utilized for phase unwrapping. Out of the 24 image scenes, 50 filtered interferograms were generated. Figure 4 presents four selected interferograms with distinct fringes, highlighting the deformation within the study area.

After employing noise filtering techniques to obtain the clearest 50 interferograms, phase unwrapping using the Minimum Cost Flow (MCF) algorithm on the SNAPHU software, implemented on the Google server, finally utilized SBAS analysis to calculate the deformation over the 24-time series as shown in Figure 5.

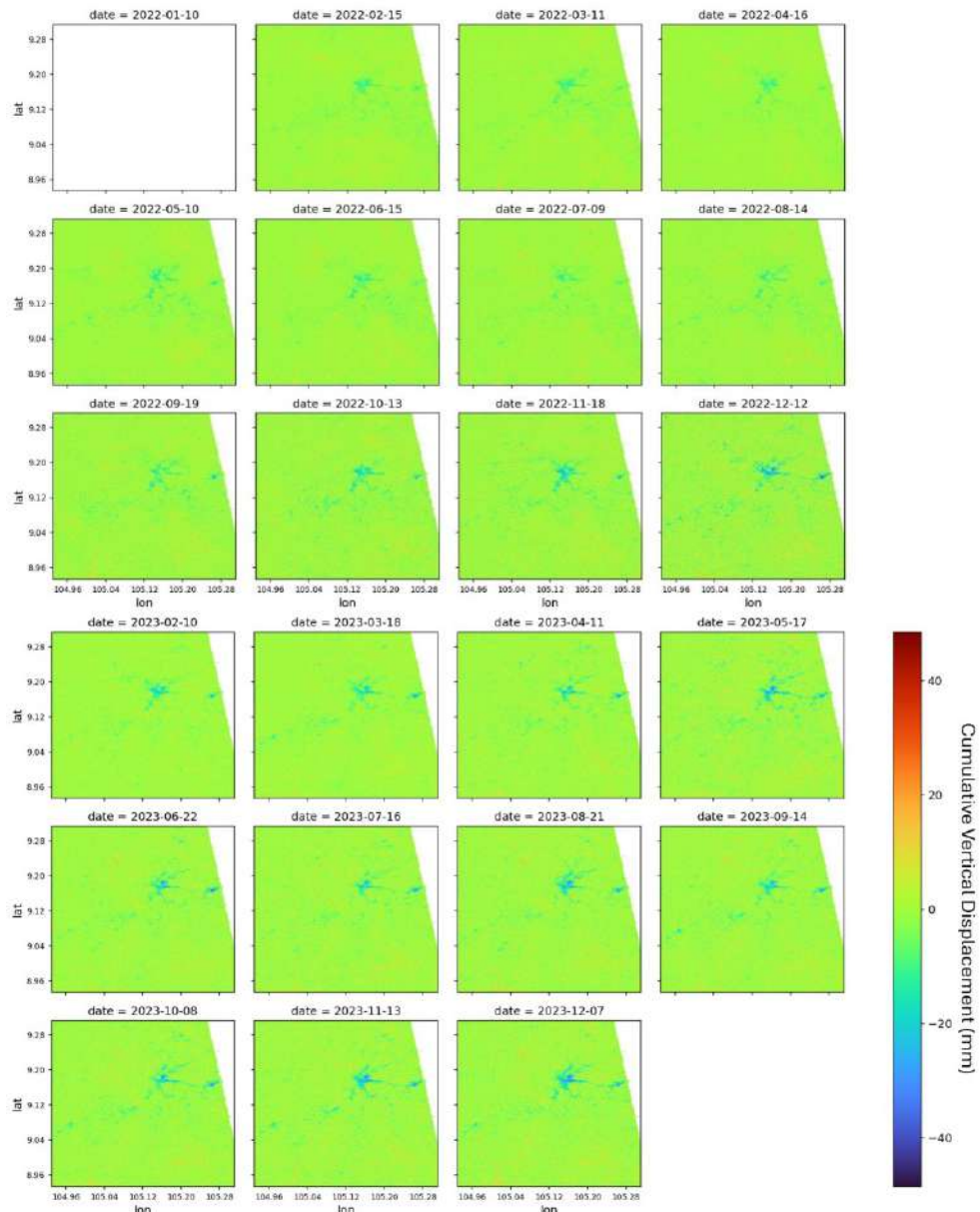


Figure 5. Deformation analysis sequence using SBAS on Google Colab.

Figure 6 shows the cumulative subsidence from January 2022 to December 2023, as synthesized and analyzed using the SBAS method. The blue areas indicate the most significant subsidence within Ca Mau City. The results from the map reveal that the main subsidence occurrences are concentrated in Wards 2 and 5, as well as in the adjacent areas of these wards with Wards 1, 4, 6, 7, 8, and 9. The maximum subsidence recorded over the entire area using SBAS is -48 mm, while the average subsidence across the study area is -20 mm.

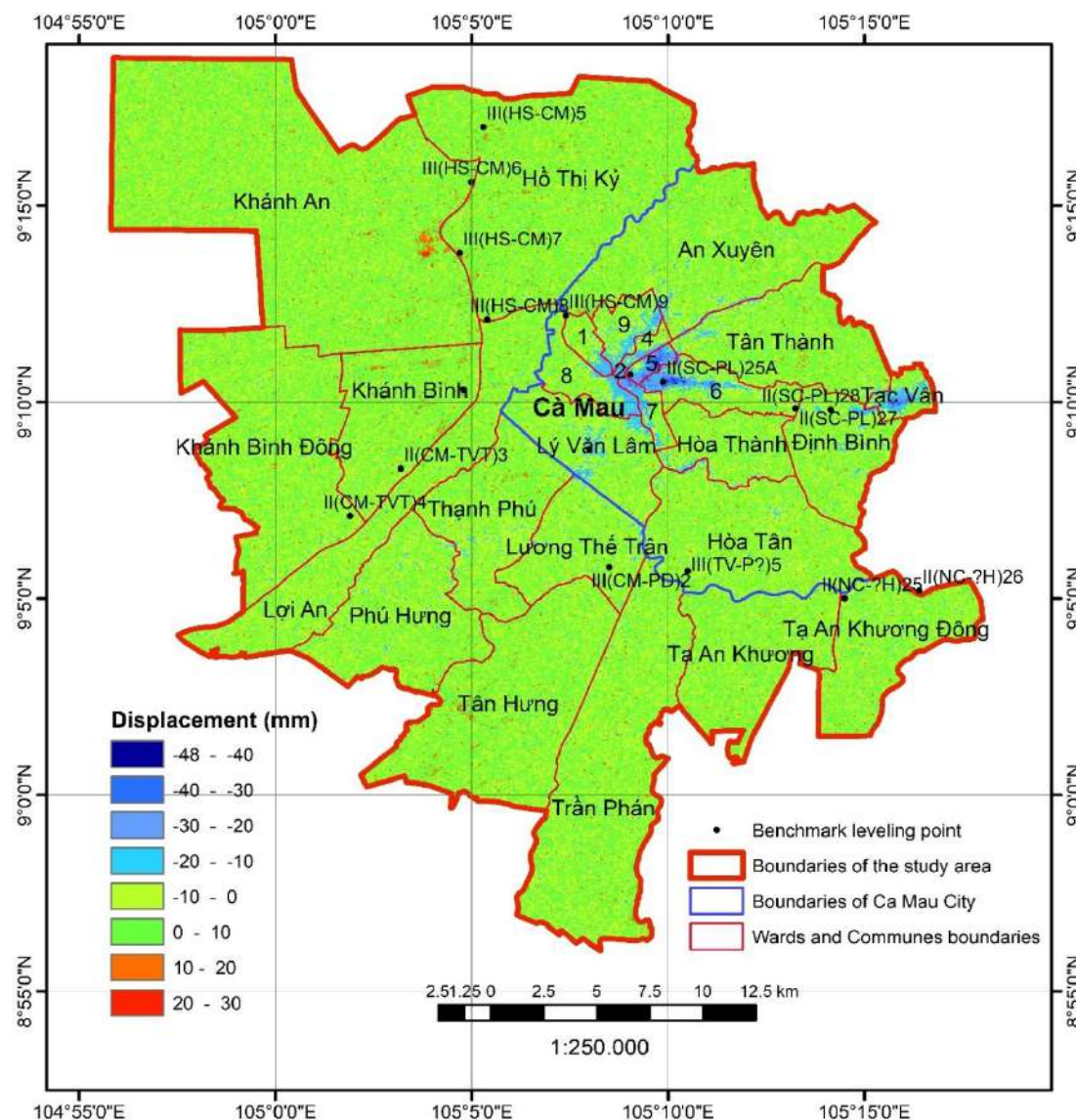


Figure 6. Map of Cumulative Vertical Displacement from January 2022 to December 2023.

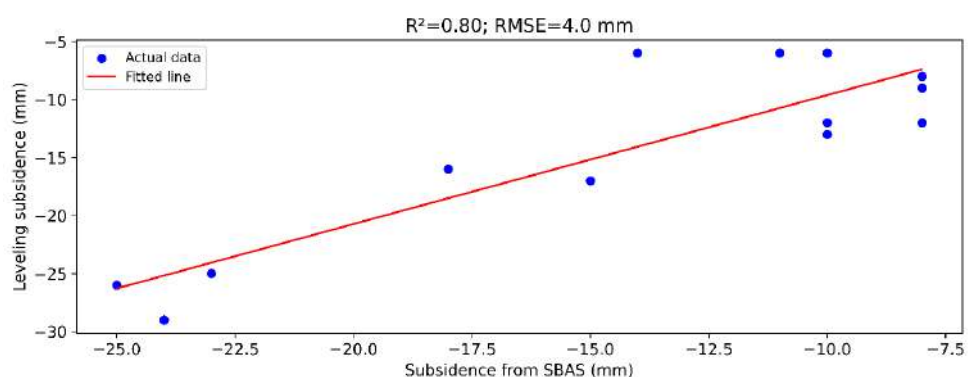
3.2 Accuracy assessment

To assess the reliability of the subsidence results determined using the SBAS method implemented on Google Colab, we compared these results with subsidence measurements at 13 benchmark points, which were determined using precise leveling methods by the Department of Survey, Mapping and Geographic Information Vietnam (Tran, 2024) (Figure 6). The comparison results are presented in Table 2, where subsidence values obtained using the SBAS method were extracted from Figure 6 at the 13 subsidence benchmarks and compared with precise leveling measurements.

Table 2. Comparison of subsidence between SBAS and levelling survey.

STT	Point name	Vertical Displacement from SBAS (mm)	Leveling-Measured Subsidence (mm)	Difference (mm)
1	II(CM-TVT)3	-6	-10	-4
2	II(CM-TVT)2	-6	-11	-5
3	II(NC-H)25	-16	-18	-2
4	II(NC-H)26	-8	-8	0
5	II(SC-PL)24	-26	-25	-1
6	II(SC-PL)25A	-25	-23	-2
7	II(SC-PL)27	-29	-24	-5
8	II(SC-PL)28	-17	-15	-2
9	III(HS-CM)5	-9	-8	-1
10	III(HS-CM)6	-12	-8	-4
11	III(HS-CM)8	-13	-10	-3
12	III(HS-CM)9	-6	-14	-8
13	III(TV-PU)5	-12	-10	-2

Using a linear regression model to assess the correlation between subsidence results obtained by SBAS and levelling survey, the study yielded $R^2 = 0.80$ and RMSE = 4 mm (Figure 7).

**Figure 7. Assessment of correlation between subsidence data from SBAS and levelling survey.**

4. CONCLUSION

The study employed the Small Baseline Subset (SBAS) method on the Google Colab

platform, utilizing 24 SAR images. The subsidence monitoring results for Ca Mau City and its surrounding communes reveal that subsidence is predominantly concentrated in the central areas of Ca Mau City, particularly in Wards 2 and 5, as well as adjacent areas including Wards 1, 4, 6, 7, 8, and 9. The average subsidence for the entire study area from January 2022 to December 2023 was found to be -20 mm. Compared to in-situ leveling measurements, the subsidence results obtained using the SBAS method on Google Colab demonstrated a high level of accuracy, with an R^2 of 0.80 and a Root Mean Square Error (RMSE) of 4 mm.

Additionally, the processing of the multi-temporal radar image series using the SBAS method on Google Colab was completed within 30 minutes, utilizing 75 GB of cloud memory provided by Google's servers. This demonstrates that Google Colab can effectively handle multi-temporal radar image processing, offering several advantages such as being free, easily accessible, and providing robust computational resources that significantly accelerate processing times. Moreover, integration with Google Drive facilitates efficient data management, and the online collaboration feature enables seamless sharing and teamwork. However, Google Colab has some limitations, including constraints on resources and runtime, as well as variable performance during peak usage periods when many users are active.

5. REFERENCES

- A. Ferretti, C. P., F. Rocca., 2000. Nonlinear subsidence rate estimation using permanent scatterers in differential SAR interferometry. *IEEE Trans. Geosci. Rem. Sens.* 38, 2202-2212.
- A. Rogers, R. V. I., 1969. Mapping the surface reflectivity by radar interferometry. *Science* 165, 797-799.
- Anh T. V. , D. K. T., Khien H. T., Hanh T. H., Nghi L. T., Hoa P. T. T., Dung N., Anh L. H., Dinh N. Q., 2023. Land Subsidence Susceptibility Mapping Using Machine Learning in the Google Earth Engine Platform. In N. Dao, Thinh, T.N., Nguyen, N.T. (editors). *Intelligence of Things: Technologies and Applications. ICIT 2023. Lecture Notes on Data Engineering and Communications Technologies*, Vol 88, Springer, Cham, Ho Chi Minh City, Vietnam.
- Anh, T. V., 2021. Monitoring subsidence in Ca Mau City and Vicinities using the multi temporal Sentinel-1 radar images. 4th Asia Pacific Meeting on Near Surface Geoscience & Engineering.
- Berardino P, F. G., Lanari R and Sansosti E, 2002. A new algorithm for surface deformation monitoring based on small baseline differential SAR interferograms. *s IEEE Transactions on Geoscience and Remote Sensing* 40, 2375–2383.
- Bui, L. K., W. Featherstone, and M. Filmer, 2020. Disruptive influences of residual noise, network configuration and data gaps on InSAR-derived land motion rates using the SBAS technique. *Remote Sensing of Environment* 247, 111941.
- Chen, Y., et al., 2024. Research on Time Series Monitoring of Surface Deformation in Tongliao Urban Area Based on SBAS-PS-DS-InSAR. *Sensors* 24, 1169.
- Dang, V. K., C. Doubre, C. Weber, N. Gourmelen, and F. Masson, 2014. Recent land subsidence caused by the rapid urban development in the Hanoi region (Vietnam) using ALOS InSAR data. *Natural Hazards and Earth System Sciences* 14, 657-674.
- Erban, L., et al., 2014. Groundwater extraction, land subsidence, and sea-level rise in the Mekong Delta, Vietnam. *Environmental Research Letters* 9, 084010.
- Graham, L. C., 1974. Synthetic interferometer radar for topographic mapping. *Engrs.* 62, 763–768.
- H.A. Zebker, J. V., 1992. Decorrelation in interferometric radar echoes. *IEEE Trans. Geosci. Rem. Sens.* 30, 950-959.

-
- Johary, A. R. F., et al., 2023. Detection of Large-Scale Floods Using Google Earth Engine and Google Colab. *Remote Sensing* 15.
- P. Berardino, G. F., R. Lanari, E. Sansosti, 2002. A new algorithm for surface deformation monitoring based on small baseline differential SAR interferograms. *IEEE Trans. Geosci. Rem. Sens.* 40, 2375-2383.
- Pechnikov, A., 2023. PyGMTSAR: Sentinel-1 Python InSAR: An Introduction. Kindle Edition.
- Philip S. J. Minderhoud, I. H., Jan Kolomaznik, and Olaf Neussner, 2020. Towards unraveling total subsidence of a mega-delta – the potential of new PS InSAR data for the Mekong delta. *Proc. IAHS.* 382, 327–332.
- S., Y., 2020. Validating InSAR-SBAS results by means of different GNSS analysis techniques in medium- and high-grade deformation areas. *Environmental Monitoring and Assessment* 192 1–12.
- Tran, A. V. B., M.A.; Ha, K.T.; Khuc, D.T.; Tran, D.N.; Tran, H.H.; Le, N.T., 2024. Land Subsidence Susceptibility Mapping in Ca Mau Province, Vietnam, Using Boosting Models. *ISPRS Int. J. Geo-Inf* 13, 161.
- Van Anh, T., Cuong, T. Q., Anh, N. D., Dinh, H. T. M., Anh, T. T., Hung, N. N., & Linh, L. T. T., 2016. Application of PSInSAR method for determining of land subsidence in Hanoi city by Cosmo-Skymed imagery. International Conference on GeoInformatics for Spatial-Infrastructure Development in Earth & Allied Sciences (GIS-IDEAS).
- Xiao, B., et al., 2022. The Monitoring and Analysis of Land Subsidence in Kunming (China) Supported by Time Series InSAR. *Sustainability* 14, 12387.
- Zebker, C. W. C. a. H. A., 2000. Network approaches to two-dimensional phase unwrapping: intractability and two new algorithms. *Journal of the Optical Society of America A* 17, 401-414.

ESTIMATE THE AMOUNT OF CARBON EMISSIONS FROM DEFORESTATION AND FOREST DEGRADATION OVER TWO DECades IN KON HA NUNG PLATEAU, GIA LAI PROVINCE, VIETNAM

**Nguyen Huu Viet Hieu^{1,2*}, Nguyen Ngoc Thach², Pham Van Manh², Nguyen Cao Tung¹,
Le Anh Hung¹, Tran Khanh Nhu¹**

¹Forest Inventory and Planning Institute (FIFI),
Ministry of Agriculture and Rural Development, Hanoi, Vietnam

Email: nguyenhiehus@gmail.com

²VNU University of Science, Vietnam National University, Hanoi
334 Nguyen Trai, Thanh Xuan, Hanoi, Vietnam

*Corresponding author. Email: nguyenhiehus@gmail.com

ABSTRACT

The Forests play an important role in reducing carbon emissions and stabilizing climate change. Research on forest status and biomass fluctuations helps us understand and evaluate factors affecting forest carbon sequestration capacity, biomass fluctuations and recovery rates. Research on assessing deforestation and natural forest degradation based on remote sensing technology with deep learning methods. In this study, we used SPOT-4 and Sentinel-2 remote sensing data to assess natural forest changes in the Kon Ha Nung Plateau, Vietnam during the period 2000 - 2022 (Overall Accuracy is 90.3%, Kappa = 0.87). Thereby, the causes of deforestation and forest degradation in Kon Ha Nung Plateau from 2000 to 2022 were assessed. The research results showed that the current forest status in the study area from 2000 to 2022 had major fluctuations, specifically: The total area of lost forest reached 56,159.9 ha, the area of degraded forest was 17,206.4 ha. From data on the developments and causes of deforestation and forest degradation, the study calculated the amount of CO₂ emissions of Kon Ha Nung Plateau in the period 2000 - 2022 with a positive value of about 658,842 tons of CO₂/year. This shows that natural forests in the study area are emitting more CO₂ than the amount of forests can absorb.

1. INTRODUCTION

Forests and forest ecosystems have been and are currently facing threat globally, particularly in tropical regions: deforestation for agriculture, logging, hunting, wildfires, climate change, and other human impacts (Corlett and Primack, 2011, Nazifah et al., 2020). The biodiversity of tropical forests is increasingly threatened by deforestation and various other impacts leading to forest degradation (Saha, 2020). The annual rate of biodiversity loss primarily from tropical rainforests is approximately 17,500 species per year (FAO, 2017). Policies regarding forestry are crucial in forest management as they guide actions of forestry practitioners or natural resource managers in specific locations within a landscape (Grebner et al., 2022). However, if policies are unreasonable and management is weak, this can lead to deforestation and forest degradation. Additionally, conflicts of interest between the rights to enjoy the values of the forest-by-forest management communities and groups using and exploiting forest resources are also causes of deforestation and forest degradation (Kane et al., 2018). To reduce deforestation and conserve forests, the United Nations has considered the REDD+ (Reducing Emissions from Deforestation and Forest Degradation and '+' for enhancing carbon stocks, conservation and sustainable management of forests) mechanism,

with conservation funding provided by developed countries to developing countries (Tacconi, 2011).

One of the most common methods for supervising and monitoring forest cover changes is the application of remote sensing technology and GIS (Hoffer, 1978). In which, the use of remote sensing images has been widely and extensively applied worldwide (Guo et al., 2022; Kalwar et al., 2022; Forkuo and Frimpong, 2012; Balaji et al., 2016).

To improve the accuracy of maps and more precisely classify types of land cover, many algorithms and auxiliary data have been applied in remote sensing studies. There are many semantic segmentation algorithms such as Random forest, U-net, Mask R-CNN, Feature Pyramid Network (FPN), etc. In this research, we will mainly focus on U-net which is one of the most well-recognized image segmentation algorithms, and many of the ideas are shared among other algorithms.

The objective of this paper is to present the results of research on creating maps of deforestation and forest degradation from 2000 to 2022 based on remote sensing and GIS data, using the U-net deep learning interpretation method. This is combined with biomass change maps from 2000 to 2022 to estimate CO₂ emissions over 22 years in the Kon Ha Nung plateau, Gia Lai province, Vietnam.

2. STUDY AREA AND MATERIAL

2.1 Study area

The Kon Ha Nung plateau area is a mountainous region in the eastern part of the Truong Son range, located in the northeast of Gia Lai province. It is about 100 km from Pleiku city via National Highway 19 and the Truong Son Dong Highway, with a total natural area of 2,429.33 km² (Figure. 1). The boundaries of the area:

- + North borders Kon Plong district (Kon Tum province).
- + East borders Quang Ngai and Binh Dinh provinces.
- + South borders An Khe town and Dak Po district.
- + West borders Chu Pah district.

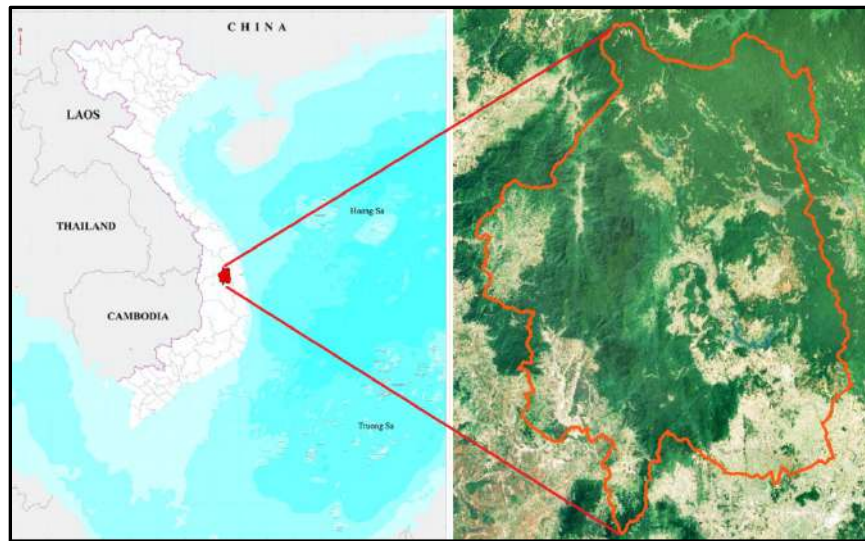


Figure 1. Location of Kon Ha Nung Plateau area

2.2 Data

In this study, we used SPOT-4 satellite images from 2000 and 2010, and Sentinel-2 from 2022 to create a land cover map of the Kon Ha Nung plateau area in Gia Lai province, Vietnam (Figure. 2).

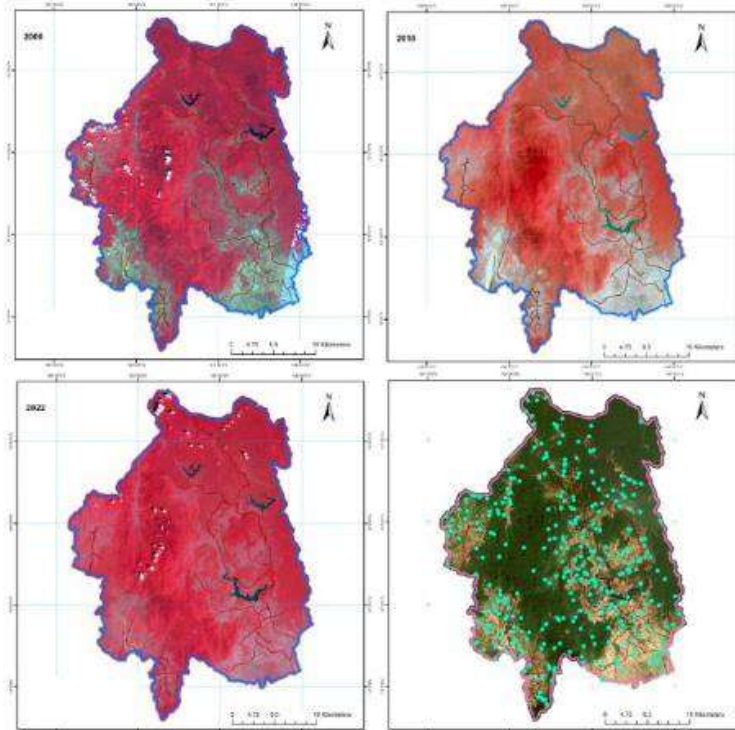


Figure 2. Multi-temporal remote sensing images of 2000, 2010, 2022, and a set of samples from 2022 in the Kon Ha Nung plateau area

2.3 Methods

- Image interpretation for creating maps of deforestation and forest degradation:

The U-net method is a deep learning neural network architecture used to create land cover maps from remote sensing data. The structure of U-net consists of two main parts: the encoder and the decoder. The essence of the U-net architecture is a Convolutional Neural Network (CNN) that encodes image information and then decodes it to predict land cover maps. The study uses a Python script for remote sensing image interpretation based on the U-net algorithm, developed by ESRI in 2021 and updated in 2024, and applied using ArcGIS Pro 3.0 software (Source: Deep learning package from Esri <https://livingatlas.arcgis.com>).

Verify the image interpretation results:

- Develop an error matrix between the classification results and the Kappa (κ) index control and evaluation sample. According to Congalton (1999), matrix tables are the most effective method for evaluating accuracy (Congalton and Green 1999).

- Overall Accuracy
- User accuracy
- Producer accuracy

The Kappa coefficient is used as a measure of classification accuracy. This is the utility coefficient of all elements from the error matrix. It is the fundamental difference between what is real about the deviation error of the matrix and the total number of changes indicated by rows and columns (McGrath 2010). The formula for determining the indicator κ is as follows:

$$\kappa = \frac{N \sum_{i=1}^r X_{ii} - \sum_{i=1}^r (X_{i+} - X_{+i})}{N^2 - \sum_{i=1}^r (X_{i+} - X_{+i})} \quad (1)$$

Where: r = Number of columns in the image matrix, X_{ii} = number of pixels observed in row i and column i (on the main diagonal), X_{i+} = Total pixels observed in row i, X = total pixels observed in column i and N = total number of pixels observed in the image matrix. According to the US Geological Survey, κ has 3 groups of values: $\kappa \geq 0.8$: high accuracy; $0.4 \leq \kappa < 0.8$: moderate accuracy; and $\kappa < 0.4$: low accuracy.

- Creating biomass change maps:

Applying linear regression to estimate carbon biomass from SPOT-4 images (2000, 2010), Sentinel-2 images (2022), and a multi-temporal standard plots system. The study inherits and uses the multi-temporal standard plots system in 2000, 2010, and 2022. Except for the 2022 data, which includes additional plots, the standard plots data for 2000 and 2010 are entirely inherited from the "National Forest Inventory (NFI)" project, Cycle III (2001-2005) and Cycle IV (2006-2010), led by the Ministry of Agriculture and Rural Development.

Determining biomass at standard plot points:

The study uses the equation developed by the authors Huy et al. (2016) for estimating biomass in the Central Highlands region (Huy et al., 2016).

$$AGB = 304.1668(D^2H^{0.7})^{0.95102} \quad (2)$$

Determining the ground biomass model for different forest types:

Based on the biomass determined at standard plots and the vegetation indices determined from remote sensing images referenced to the positions of the standard plots, the construction of biomass estimation models for the entire study area can be generally expressed as a function

$AGB = f(NDVI, LR)$, where AGB, NDVI, and LR respectively correspond with biomass, vegetation index, and forest type at each standard plot point.

Validation of the accuracy of the biomass estimation model

The Pearson correlation coefficient for two variables x, y from n samples is calculated according to the formula:

$$R^2 = \frac{\sum_{i=1}^n [(Y_i - \bar{Y}_i)(X_i - \bar{X}_i)]}{\sqrt{\sum_{i=1}^n (Y_i - \bar{Y}_i)^2} \times \sqrt{\sum_{i=1}^n (X_i - \bar{X}_i)^2}} \quad (3)$$

Where: Y_i and \bar{Y}_i are the estimated variables and their mean values
 X_i and \bar{X}_i are the measured variables and their mean values.
 n is the number of samples in the dataset.

The combination of standard errors (SE) is used to assess the quality and quantity of biomass stocks (i.e. AGC obtained from linear regression analysis) by comparing them with field-measured biomass stocks. The lower the SE value, the higher the accuracy.

This study experimentally evaluated various models and selected the following two formulas:

- The biomass estimation formula for the Kon Ha Nung Plateau area using SPOT-4 image data (2000, 2010) (Dang et al., 2022):

$$AGB = 454.59 * \log_{10}(NDVI) + 257.46 * LR + 147.38 \quad (4)$$

The formula (4) was validated with $R^2 = 0.72$ and RMSE = 22.87 (Mg/ha).

- The biomass estimation formula for the Kon Ha Nung Plateau area using Sentinel-2 image data (2022) (Dang et al., 2022):

$$\text{Log10}(AGB) = 0.44 * \text{NDVI} + 0.22 * LR + 1.74 \quad (5)$$

The formula (5) was validated with $R^2 = 0.759$ và RMSE = 19.50 (Mg/ha).

From the survey data in the sampling plot system, biomass models are used to estimate biomass, which is then used to calculate carbon and CO₂ equivalent for each plot and subsequently estimated for the forest stand. In this study, the carbon sequestration and CO₂ equivalent are calculated using the following conversion factor:

$$C = 0,47 \times AGB \quad (\text{IPCC}, 2019) \quad (6)$$

$$CO_2 = 3,67 \times C \quad (7)$$

3. RESULTS

3.1 Forest biomass fluctuation for the period 2000 – 2022

Based on the results from the selected regression models with the highest accuracy (the Lin-Log model for 2000 and 2010, and the Log-Lin model for 2022) (Dang et al., 2022), biomass estimation maps for the Kon Ha Nung Plateau area have been created and are presented in

Figure. 3, with some characteristics according to the biomass thresholds as shown in Table. 1 below.

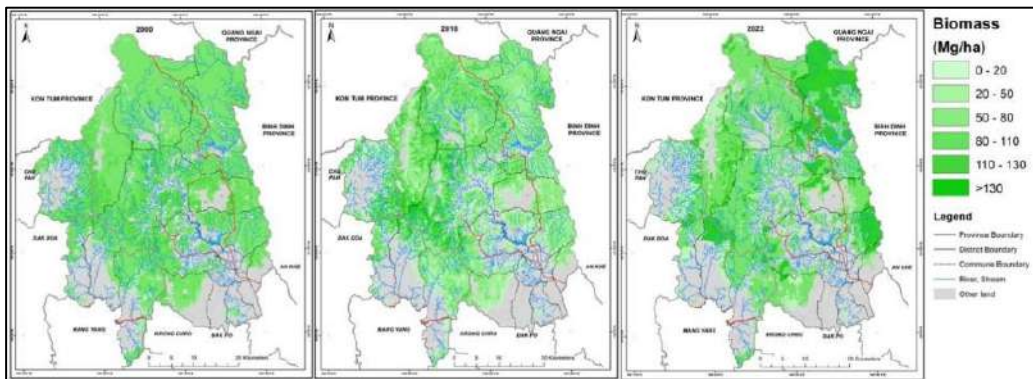


Figure 3. Biomass estimation maps for the Kon Ha Nung Plateau area in 2000, 2010 and 2022

Table 1. The results of calculating the natural forest biomass values for the Kon Ha Nung Plateau area in 2000, 2010, and 2022 (Unit: Mg/ha)

Range of biomass values	0 - 20	20 - 50	50 - 80	80 - 110	110 - 130	>130
2000	Area (ha)	2,499	4,387	8,976	40,806	68,433
	%	1.45	2.54	5.20	23.65	39.66
2010	Area (ha)	1,030	14,769	3,039	86,377	13,942
	%	0.69	9.85	2.03	58.05	9.30
2022	Area (ha)	2,375	13,733	10,191	89,242	79
	%	1.58	9.16	6.80	59.51	0.51
						22.45

For the year 2000, areas with biomass values ranging from 110 to 130 tons/ha cover over 68,000 ha, accounting for 39% of the total natural forest area, whereas areas with biomass values less than 20 tons make up only 1.45% of the total area, covering 2,499 ha. For the year 2010, areas with biomass values ranging from 80 to 110 tons/ha cover over 86,000 ha, accounting for 58% of the total natural forest area. Meanwhile, areas with biomass values ranging from 0 to 20 tons/ha have the smallest total area, with more than 1,000 ha (accounting for 0.69% of the total natural forest area). For the biomass range from 130 to 180 tons/ha, the area percentages for the years 2010 and 2022 are 20.09% and 22.45%, respectively. The biomass range from 110 to 130 tons/ha shows significant fluctuation between 2010 and 2022, decreasing from nearly 14,000 ha in 2010 to about 80 ha in 2022.

Based on the biomass estimation results for the years 2000, 2010, and 2022, and using formulas (6) and (7), carbon stock estimation maps for the years 2000 and 2022 have been created for the Kon Ha Nung Plateau area (Figure. 4).

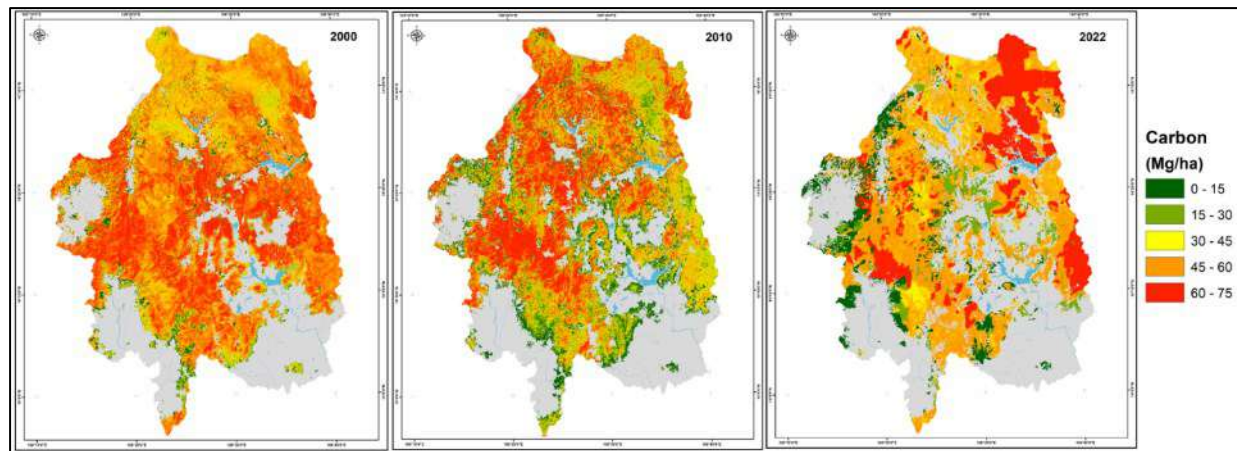


Figure 4. Carbon stock estimation maps for the Kon Ha Nung Plateau area in 2000, 2010, and 2022

Areas with carbon stocks ranging from 45 to 60 tons/ha cover over 90,000 ha, accounting for more than 60% of the total area for the year 2010 and over 46% for the year 2022. In contrast, for the year 2000, the area with these carbon stock values was about 40,000 ha (23.65%). For the year 2000, carbon stock values above 75 tons/ha were predominant, covering approximately 47,000 ha, which corresponds with 27.5% of the total area. Natural forest areas with carbon stock values ranging from 75 to 90 tons/ha increased significantly in 2022, rising from 0% to 15.83% of the total natural forest area in the Kon Ha Nung Plateau region. This increase is primarily concentrated in the core area of the Kon Chr Rang Nature Reserve (Figure. 4).

3.2 Forest biomass variation according to the classification of current forest status changes

As mentioned in the methodology section, this content presents the statistical results of biomass variation according to the areas classified by natural forest changes, including deforestation and forest degradation. The specific results are shown in Table 2.

Table 2. Natural forest changes

TT	Categories	Area change during the period 2000 - 2010 (Ha)	Area change during the period 2010 - 2022 (Ha)	Total for the period 2000 -2022 (Ha)	Average per year 2000 - 2022 (Ha)
I	Deforestation	28,560.1	27,599.8	56,159.9	2,552.7
1	TXG	1,587.9	10,522.0	12,109.9	550.5
2	TXB	14,468.7	13,038.6	27,507.3	1,250.3
3	TXN	5,645.4	3,596.5	9,241.9	420.1
4	TXP	6,858.1	442.7	7,300.8	331.9
II	Degradation	15,024.2	2,182.3	17,206.4	782.1
1	TXG-TXB	8,469.0	375.5	8,844.5	402.0
2	TXG-TXN	172.9	0.3	173.2	7.9
3	TXG-TXP	419.2	2.9	422.1	19.2
4	TXB-TXN	1,781.0	4.3	1,785.4	81.2
5	TXB-TXP	2,894.8	1,796.6	4,691.5	213.2
6	TXN-TXP	1,287.3	2.6	1,289.8	58.6

Note: TXG - Rich secondary evergreen broadleaved forest on soil mountain ;TXB - Medium secondary evergreen broadleaved forest on soil mountain; TXN - Poor secondary evergreen broadleaved forest on soil mountain; TXP - Rehabilitation secondary evergreen broadleaved forest on soil mountain.

During the period 2000 - 2022, the total deforestation area in the study area reached 56,159.9 ha, and the total area of forest degradation was 17,206.4 ha. Based on the data on natural forest changes, the total forested area, deforested area, and forest degradation area, are shown in Table 3.

Table 3. Forest biomass variation according to the classification of current forest status change areas

Categories	CO ₂ emissions during the period 2000 - 2010	CO ₂ emissions during the period 2010 - 2022	Total for the period 2000 - 2022	Average per year 2000 - 2022
Deforestation	4,916,380	7,842,813	12,759,193	579,963
Degradation	1,304,778	430,544	1,735,321	78,878
Net	6,221,157	8,273,357	14,494,515	658,842

According to the reference level (RL) calculation method of FCPF: During the period from 2000 to 2022, the total emissions from deforestation and forest degradation in the Kon Ha Nung plateau area amounted to 14,494,515 tons of CO₂. The net emission-removal in the study area is approximately 14,494,515 tons of CO₂/22 years, which is equivalent to 658,842 tons of CO₂/year.

The causes of deforestation and forest degradation in the Kon Ha Nung plateau are all influenced by economic and social factors. Economic and social development is reflected in the demand for timber, household economic development, the need for firewood, livestock development, food requirements, infrastructure development, and the expansion of commercial crops...Economic and social development is essential for every locality, especially in remote, isolated, and particularly disadvantaged areas. However, economic and social development must be linked with forest conservation and resource development. Given these challenges, the Kon Ha Nung plateau needs appropriate solutions to ensure a balance between forest conservation and the development of local livelihoods. To propose suitable solutions for forest protection and development, it is necessary to identify the economic and social factors that significantly impact deforestation and forest degradation. This understanding will help in developing appropriate solutions and policies, ensuring that the proposed programs and measures are feasible and can be effectively implemented in practice.

4. CONCLUSION

Creating a land cover status map and assessing land cover changes serve as the foundation for forest management, protection, and sustainable development in mountainous regions. Based on multi-temporal remote sensing data and integrated with field verification methods, three land cover maps for the Kon Ha Nung plateau were created for the years 2000, 2010, and 2022, with an overall accuracy of 90.3% and $\kappa = 0.87$. From 2000 to 2022, over 40,000 ha of natural forest area was lost, and more than 17,000 ha experienced degradation and reduced forest quality, primarily due to conversion to areas for perennial crops, annual crops, and planted forests. During the period 2010 - 2022, the rate of natural forest loss significantly decreased, largely due to changes in forestry policies and the prioritization of economic development linked with protection and development of forest in the region. The study has determined that

the net CO₂ emission-removal of the Kon Ha Nung plateau for the period 2000 - 2022 is approximately 14,494,515 tons of CO₂ over 22 years, which is equivalent to 658,842 tons of CO₂ per year. Human activities, along with development policies and land use policies applied in the area, are the main causes of the changes in natural forest area in the Kon Ha Nung plateau, both in short periods and throughout the 2000 - 2022 period. During the period 2000 - 2010, the effectiveness of forest protection and development policies was relatively limited. However, in the period 2010 - 2022, policies for forest protection, restoration, and expansion have started to show significant results in forest conservation and development efforts. Many policies directly impact and improve the livelihoods of ethnic minorities, through models that integrate local economic development with management and protection of forests. Therefore, based on the results of this study and the evaluation of the effectiveness of local forestry policies, it is possible to help managers develop a "Sustainable Forest Management Framework" that provides a comprehensive approach to forest management planning and sustainable forest resource conservation.

5. ACKNOWLEDGMENTS

Nguyen Huu Viet Hieu was funded by the Master, PhD Scholarship Programme of Vingroup Innovation Foundation (VINIF), code VINIF.2023.TS.036.

6. REFERENCES

- Balaji, P., Serbin, G., Cawkwell, F. and Green, S. (2016) Remote Sensing of Forest Cover Change in Ireland.
- Congalton, R. G. and Green, K. (1999) 'Assessing the accuracy of remotely sensed data: Principles and practices', in Boca Raton, FL, USA., Lewis Publishers,
- Corlett, R. and Primack, R. (2011) Tropical Rain Forests: An Ecological and Biogeographical Comparison, Second edition.
- Dang, H. N., Ba, D. D., Trung, D. N. and Viet, H. N. H. (2022) 'A novel method for estimating biomass and carbon sequestration in tropical rainforest areas based on remote sensing imagery: A case study in the Kon Ha Nung Plateau, Vietnam', Sustainability, 14(24), 16857.
- FAO (2017) Using criteria and indicators for sustainable forest management, Rome: Food and Agriculture Organization of the United Nations.
- Forkuo, E. K. and Frimpong, A. (2012) 'Analysis of Forest Cover Change Detection', International Journal of Remote Sensing Applications, 2, 82-92.
- Grebner, D., Bettinger, P., Siry, J. and Boston, K. (2022) 'Forest policies and external pressures' in, 365-386.
- Guo, J., Gong, P., Dronova, I. and Zhu, Z. (2022) 'Forest cover change in China from 2000 to 2016', International Journal of Remote Sensing, 43, 593-606.
- Hoffer, R. M. (1978) 'Biological and physical considerations in applying computer-aided analysis techniques to remote sensing', Remote sensing: the quantitative approach, 227-289.
- Huy, B., Kralicek, K., Poudel, K. P., Phuong, V. T., Van Khoa, P., Hung, N. D. and Temesgen, H. (2016) 'Allometric equations for estimating tree aboveground biomass in evergreen broadleaf forests of Viet Nam', Forest Ecology and Management, 382, 193-205.
- IPCC (2019) Refinement to the 2006 IPCC Guidelines for National Greenhouse Gas Inventories.
- Kalwar, A., Mathur, R., Chavan, S. and Narvekar, C. (2022) 'Forest Cover Change Detection Using Satellite Images' in, 565-573.

-
- Kane, S., Dhiaulhaq, A., Sapkota, L. M. and Gritten, D. (2018) 'Transforming forest landscape conflicts: the promises and perils of global forest management initiatives such as REDD+', *Forest and Society*, 2(1), 1-17.
- McGrath, R. (2010) 'Kappa Coefficient' in.
- Nazifah, N., Yarni, M. and Nasution, M. (2020) 'Indonesian government policy in forest fire handling', *Jurnal Komunikasi Hukum (JKH)*, 6, 210.
- Saha, N. (2020) 'Tropical Forest and Sustainability: An Overview' in, 1052-1059.
- Tacconi, L. (2011) 'POLICY Palatable forest conservation', *Nature Climate Change*, 1, 143-14

EXTRACTING TRAVEL DISTANCE AND SLOPE FAILURE HEIGHT USING ORIENTED BOUNDING BOXES

Tatsuya Nemoto¹, Taiga Yamada² and Venkatesh Raghavan¹

¹Graduate School of Science, Osaka Metropolitan University
3-3-138 Sugimoto, Sumiyoshi-ku, Osaka 558-8585, Japan
Email: tnemoto@omu.ac.jp

²Faculty of Science, Osaka City University
3-3-138 Sugimoto, Sumiyoshi-ku, Osaka 558-8585, Japan

ABSTRACT

A method was developed to simply extract travel distance and relative height from polygon data of slope failure areas and digital elevation model using Oriented Bounding Boxes. Using this method, they can be obtained instantly.

The accuracy of the values obtained by this method was verified using slope failures occurred during the 2004 Niigata Prefecture Chuetsu Earthquake. The result showed that the proposed method was generally effective.

1. INTRODUCTION

In order to reduce the damage caused by slope failure, it is important to predict the distance it will travel. It can be predicted from the travel distance, relative height of past slope failures. Moriwaki (1987) showed that the ratio of slope failure slope and relative height/travel distance has a linear relationship. Sakai *et al.* (2020) investigated the relationship between area and travel distance for earthquake-activated slope failures and showed that travel distance can be predicted probabilistically. However, manually measuring them from a topographic map requires a huge amount of time and effort.

In this study, a method has been developed to simply extract travel distance and relative height from polygon data of slope failure areas and digital elevation model using Oriented Bounding Boxes. Values extracted by this method were compared with manually measured values to verify their accuracy.

2. EXTRACTION METHOD

An Oriented Bounding Box (OBB) is a rectangle surrounding the object, rotated so that it has the minimum area. In this method, the slope failure polygon is surrounded by OBB, and the travel distance L and height H are extracted from the slope failure polygon and Digital Elevation Model (DEM) using the following steps (Figure 1).

Step 1: Let the midpoints of long sides and short sides of OBB be MP1 and MP3, MP2 and MP4, respectively, and obtain the x and y coordinates of each midpoint (Figure 2).

Step 2: Obtain the z coordinate (elevation value) of each midpoint from DEM.

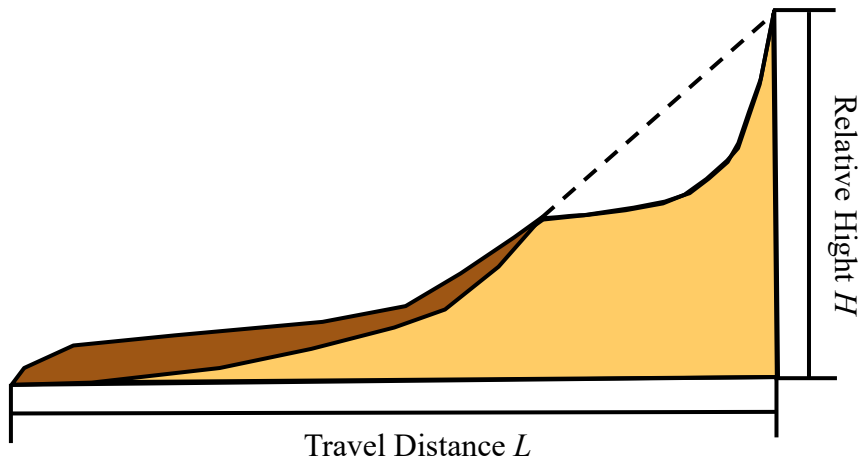


Figure 1. Travel distance and relative height of slope failure.

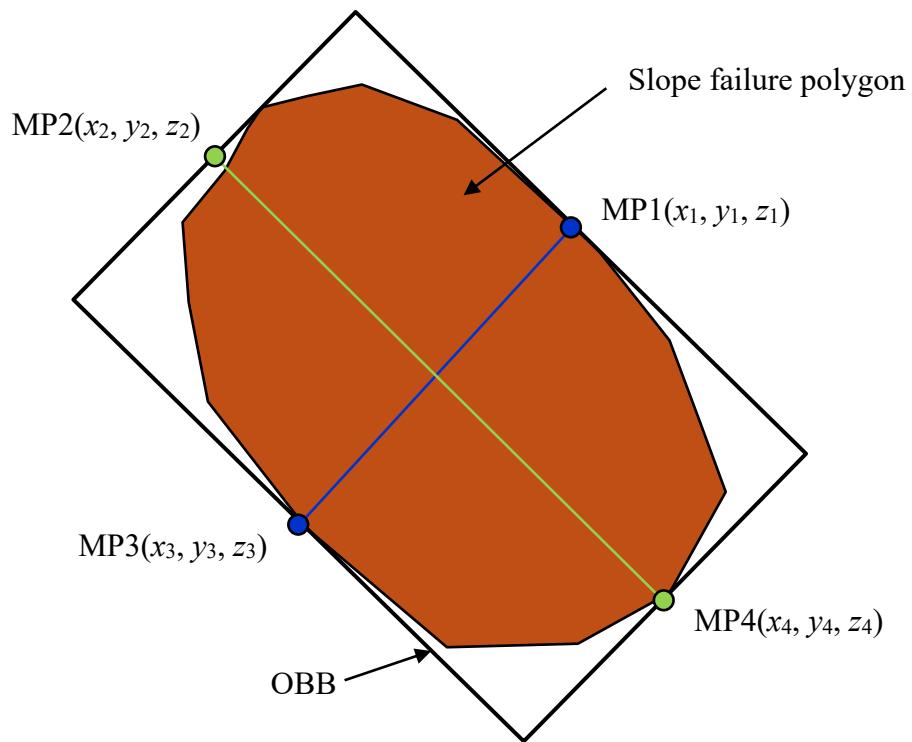


Figure 2. Slope failure polygon and OBB.

Step 3: If the elevation difference between $MP1$ and $MP3$ is smaller than that between $MP2$ and $MP4$, the target slope failure is classified as *Long*, otherwise it is classified as *Wide*.

Step 4: If the target slope failure is *Long*, the horizontal distance between $MP2$ and $MP4$ is the travel distance L , and the difference in elevation between them is the relative height H . If the target is *Wide*, the horizontal distance between $MP1$ and $MP3$ is the travel distance L , and the elevation difference is the relative height H .

In this study, an R language program was created to extract L and H .

3. RESULTS AND EVALUATION

From the 81 slope failure polygons that occurred during the 2004 Niigata-ken Chuetsu Earthquake, Japan (Yagi *et al.*, 2007) and 10 m mesh DEM, the travel distance L and relative height H were extracted using this method (Figure 3).

In order to verify the accuracy of the extraction result, the travel distance L and relative height H were manually measured based on 10 m interval contour lines (Figure 4). Figure 5 shows the relationship between L and the travel distance measured manually. Figure 6 shows the relationship between H and relative height measured manually. Two scatter plots show that the results obtained by this method roughly match the results obtained by manual measurement. The average error rate for travel distance L is 2.9%, and the average error is 4.59 m. The average error rate for the relative height H was 5.6%, and the average error was 9.58 m. Histograms of the error rate for L and H are shown in Figures 7 and 8, respectively. Since both error rates are generally within the range of $\pm 10\%$, we infer that this method is effective.

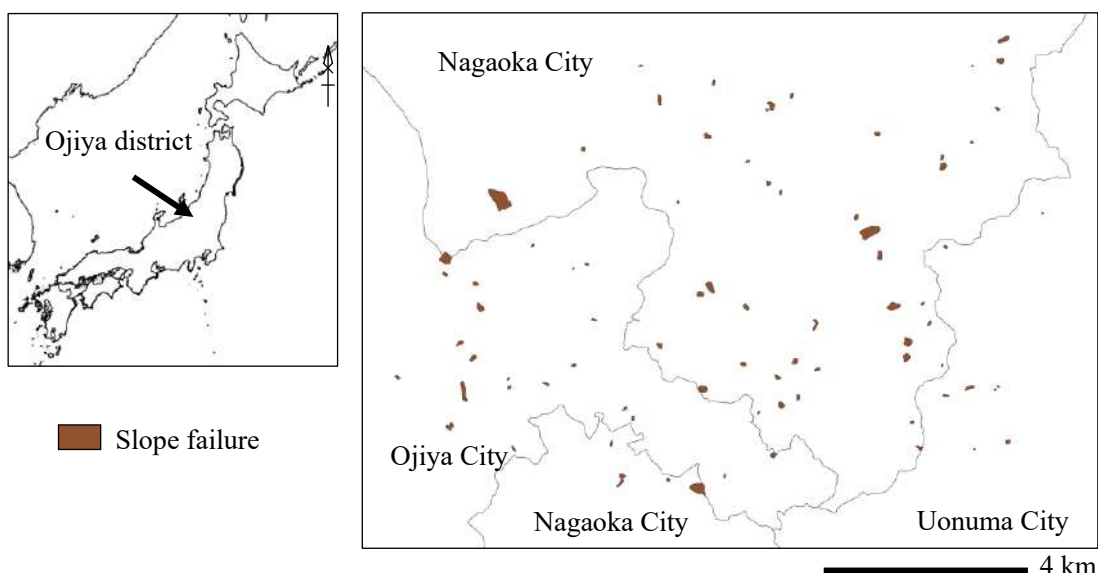


Figure 3. Slope failures in Ojiya district, Niigata Prefecture, Japan.

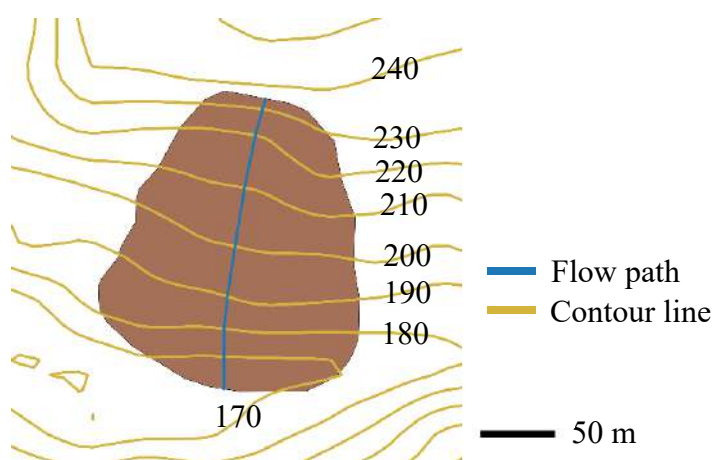


Figure 4. Example of Manual Measurement.

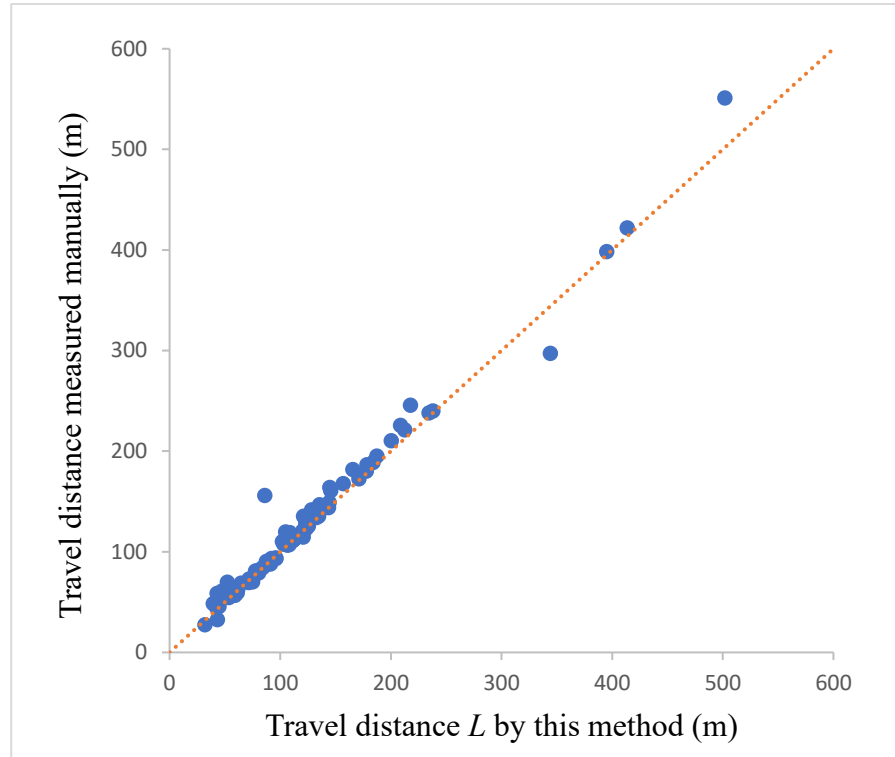


Figure 5. Relationship between travel distance L by this method and manual measurement.

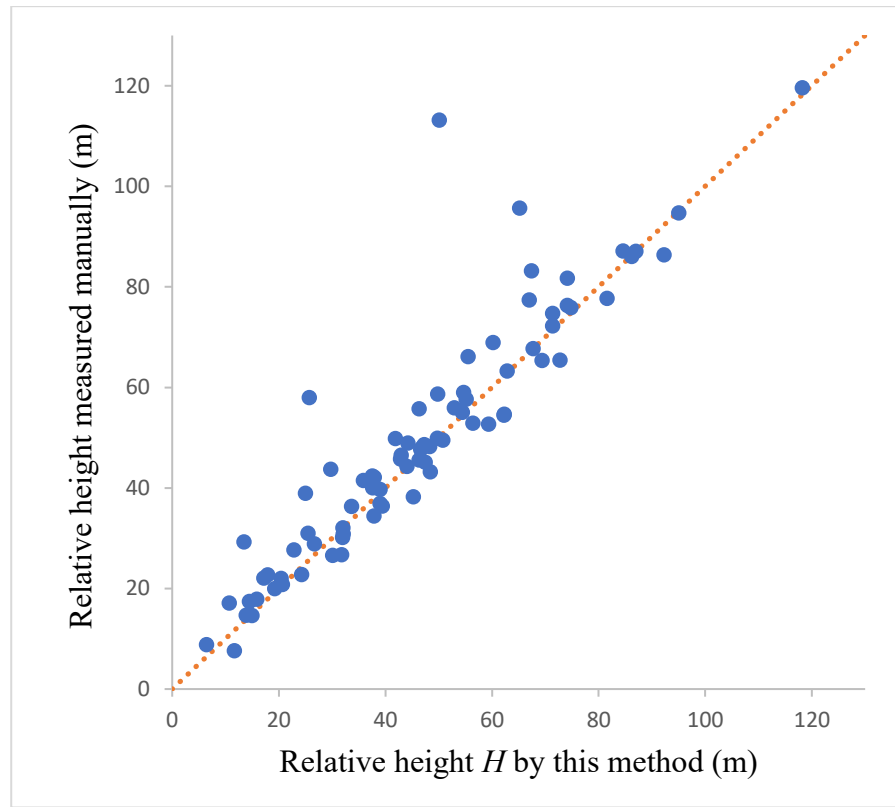


Figure 6. Relationship between relative height H by this method and manual measurement.

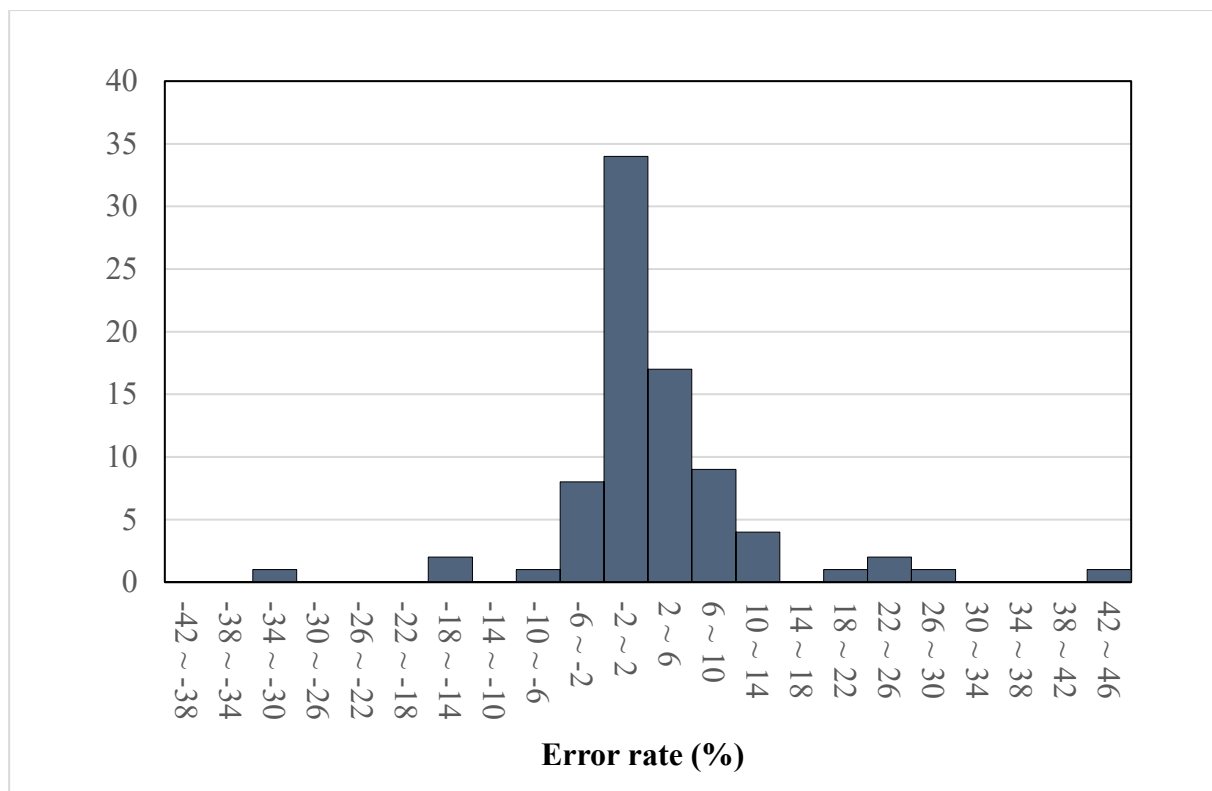


Figure 7. Histograms of the error rate for travel distance L .

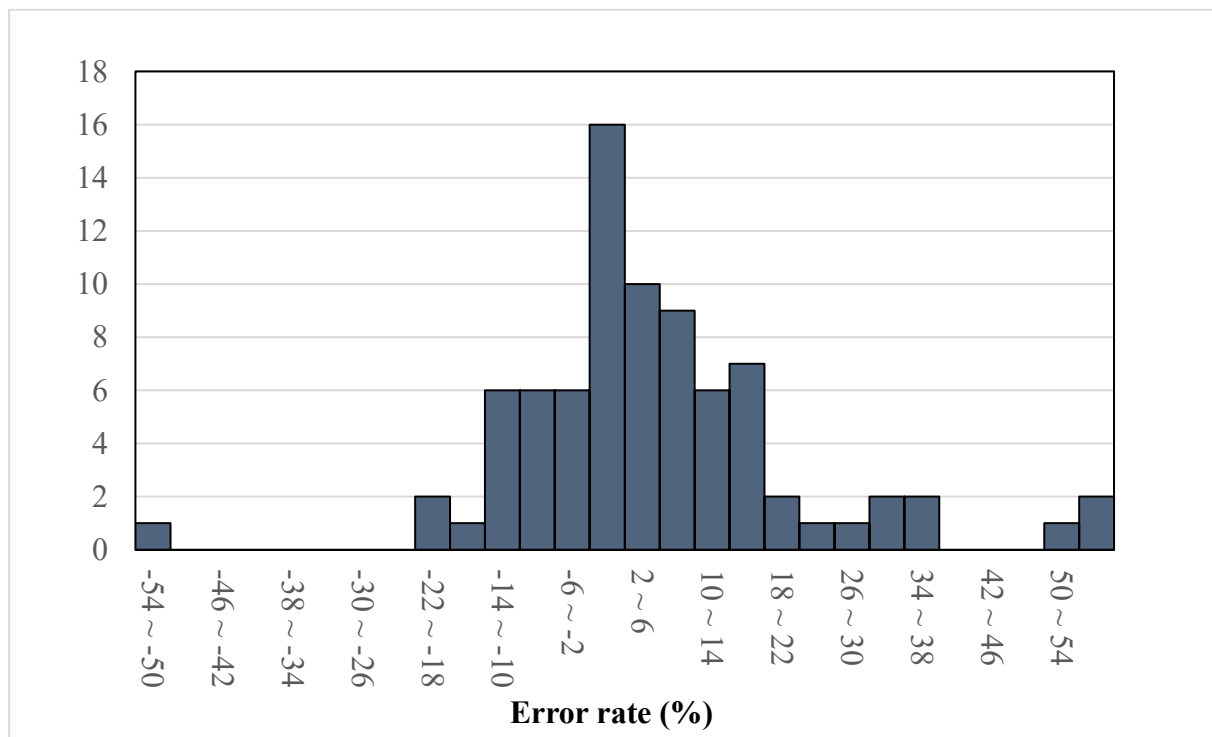


Figure 8. Histograms of the error rate for relative height H .

4. CONCLUSION

In this study, the method was developed to simply extract travel distance L and relative height H from polygon data of slope failure areas and digital elevation model using OBB. By using this method, L and H can be obtained instantly.

The results of comparing the values obtained by this method and those obtained by manual measurement showed that this method is effective. However, if the actual flow path is in the diagonal direction of OBB, the error rate tends to be large. In order to further improve accuracy, it is necessary to develop a method for extracting L and H along the flow path.

5. REFERENCES

- Moriwaki, H., 1987. A prediction of the runout distance of a debris. *Journal of Japan Landslide Society*, 24, 10-16.
- Sakai, Y., Uchida, T., and Hirata, I., 2020. Proposal of probabilistic prediction method of travel distance in an earthquake-induced landslide. *Journal of the Japan Society of Erosion Control Engineering*, 73, 3-14.
- Yagi, H., Yamasaki, T., and Arsumi, M. (2007) Feature and distribution of landslides induced by the Mid Niigata Prefecture Earthquake in 2004, Japan. <https://www.sciencebase.gov/catalog/item/5b5a0840e4b0610d7f4dcbb5b>

A STUDY ON THE DISTRIBUTION OF VILLAGE NAMES DERIVED FROM VEGETATION IN NORTHEASTERN THAILAND, CAMBODIA, AND LAOS

Nagata Yoshikatsu

Graduate School of Informatics, Osaka Metropolitan University
3-3-138 Sugimoto, Sumiyoshi, Osaka 558-8585, Japan
Email: nagatay@omu.ac.jp

ABSTRACT

The place names of villages use words that are suitable for describing the land in a straightforward manner. Words that evoke landmarks such as valleys and hills, as well as rivers and ponds that are suitable locations for obtaining water resources, are used very often. Words derived from plants useful for life are also frequently used, either alone or in combination with words describing the topographical environment.

This report examines the frequency and distribution of words derived from vegetation used in village-level place names in northeastern Thailand, Cambodia, and Laos, which are located in continental Southeast Asia. “Mango” and “lotus” are representative examples of words that are widely used in a large number of cases in the study area. ‘Sadao’ and ‘chanuan’ in Thai are words that can be observed to have a northern boundary in their usage.

The consideration of local vernacular names in village names expressed in local languages is an essential issue for the progress of this study.

1. INTRODUCTION

The place names of villages often use words that are appropriate to describe the land in a straightforward manner. Words such as “river” and “pond” evoke a place with easy access to water resources that are essential for life. Words such as “valley” and “hill” also evoke landforms that are landmarks. Words derived from plants useful for life are also often used, either alone or in combination with words describing the topographical environment.

In the previous conference, the occurrence and distribution of vegetation-derived words in village names in northeastern Thailand and northern Cambodia was overviewed (Nagata, 2023). In this report, it was introduced that the word “lotus” was most frequently used in northeastern Thailand and the word “mango” in northern Cambodia. It was also pointed out that village names using the word “bamboo,” which is common in northern Cambodia, are extremely rare in northeastern Thailand.

Since the previous report, the collection of village place names has been extended to include all of Cambodia and Laos, which has close historical ties to northeastern Thailand and Cambodia, in order to broaden this discussion of frequency of use and spatial distribution. This report examines the frequency and distribution of vegetation-derived words used in village-level place names in northeastern Thailand, Cambodia, and Laos, one region and two countries contiguous to continental Southeast Asia.

2. MATERIALS

An overview of the location of the three regions shows that northeastern Thailand and Cambodia are north-south neighbors with the Dangrek Mountains in between, and that the Mekong River borders most of northeastern Thailand and Laos.

The number of village-level place names analyzed is approximately 29,000 for northeastern Thailand, 13,200 for Cambodia, and 11,600 for Laos. The place name data for northeastern Thailand are based on the KCC2K surveys conducted by the Ministry of the Interior of Thailand around 1990 and do not include urban centers (CDD Thailand, 1993), and the location data were obtained mainly from the L7017 series of topographic maps produced in the 1980s (Nagata, 1996). For Cambodia, the place name data are based on 1:50,000 topographic maps published in the 1960s, and therefore only representative place names for urban areas are included. In Laos, village names were extracted from the 1995 census and include urban areas. Their geographic locations were identified on 1:100,000 maps published in the 1980s. Thus, although the age and the range of data collected is not homogeneous from region to region, it is sufficient material to study the occurrence of words of vegetation origin as a first step toward an overview.

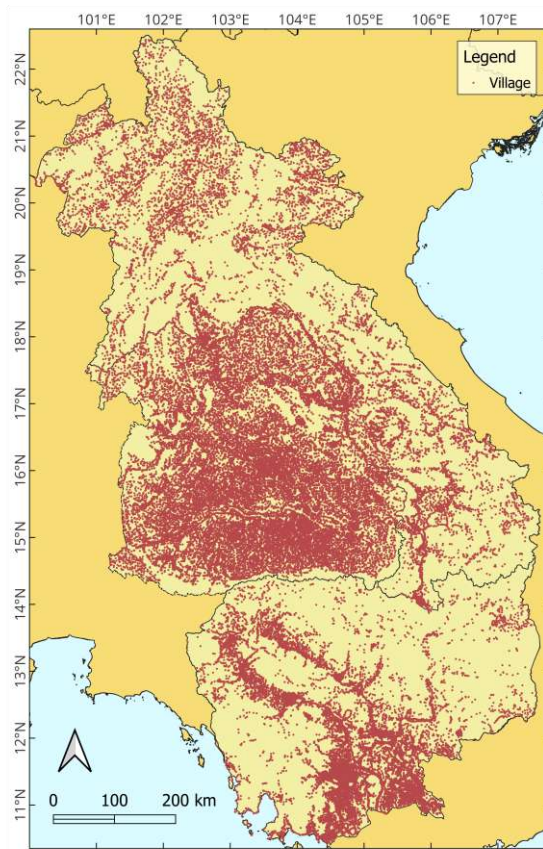


Figure 1. Villages in the study area.

Figure 1 shows the spatial distribution of all villages in the study area. In northeastern Thailand, villages are located almost everywhere, while in Cambodia they are unevenly distributed along the major rivers in the south-central region. In Laos, villages are much more sparsely distributed than in northeastern Thailand.

Table 1. Frequency of words in village names.

Word *1	N.E. Thailand	Cambodia	Laos
bua / chhuk / bua : lotus	511 (1.76%)	76 (0.58%)	69 (0.59%)
muang / svay / muang : mango	436 (1.50%)	389 (2.96%)	73 (0.63%)
makham / ampil / makkham : tamarind	312 (1.07%)	122 (0.93%)	51 (0.44%)
sakae / sangke / kae	169 (0.58%)	54 (0.41%)	16 (0.14%)
samrong / samraong / samhong	151 (0.52%)	145 (1.10%)	6 (0.05%)
tan / tnaot / tan : sugar palm	90 (0.31%)	99 (0.75%)	44 (0.38%)
khilek / angkanh / khilek	72 (0.25%)	8 (0.06%)	1 (0.01%)
madua / lovea / makdua : fig	60 (0.21%)	67 (0.51%)	27 (0.23%)
maphok / thlok / phok	52 (0.18%)	71 (0.54%)	7 (0.06%)
pradu / thnung / du	48 (0.17%)	51 (0.39%)	22 (0.19%)
sano / snoao / sano	42 (0.14%)	32 (0.24%)	13 (0.11%)
sadao / sdau / kadao	36 (0.12%)	33 (0.25%)	1 (0.01%)
takhro / pongro / kho : Ceylon oak	30 (0.10%)	62 (0.47%)	30 (0.26%)
sompoi / sambuor / sompoi	25 (0.09%)	36 (0.27%)	0 (0.00%)
chanuan / snuol / padong	7 (0.02%)	40 (0.30%)	1 (0.01%)
maiphai / russei / maiphai : bamboo	2 (0.01%)	152 (1.15%)	16 (0.14%)

*1) Word in Thai / Khmer / Lao : English, respectively. Romanized scripts of non-English are for reference only.

3. VEGETATION-DERIVED WORDS

No specific criteria were used in the selection of words of vegetation origin. The selection was based on an overview of place names and an examination of the meanings of frequently occurring words. In addition, since this study is an extension of last year's report, words that occur frequently in both Cambodia and northeastern Thailand were selected for consideration. Table 1 shows the words, and their frequency of occurrence discussed in this

report. Word names are given in Romanized Thai, Khmer, and Lao, in that order, with English names added if they are familiar to the public.

3.1 Words commonly used in the study area

The most common word derived from vegetation is “mango,” an edible fruit tree. It occurs in about 3% of village names in Cambodia. It occurs in about 1.5% and 0.6% of village names in northeastern Thailand and Laos, respectively. Although Laos and northeastern Thailand are closely related as the basin of the Mekong River, there is a large difference in the frequency of occurrence. One of the reasons for this is that the Lao language is the mother tongue of about half of the total Lao population. It is possible that there are many place names with words derived from languages other than Lao. The distribution of villages containing the word “mango” is shown in Figure 2(a).

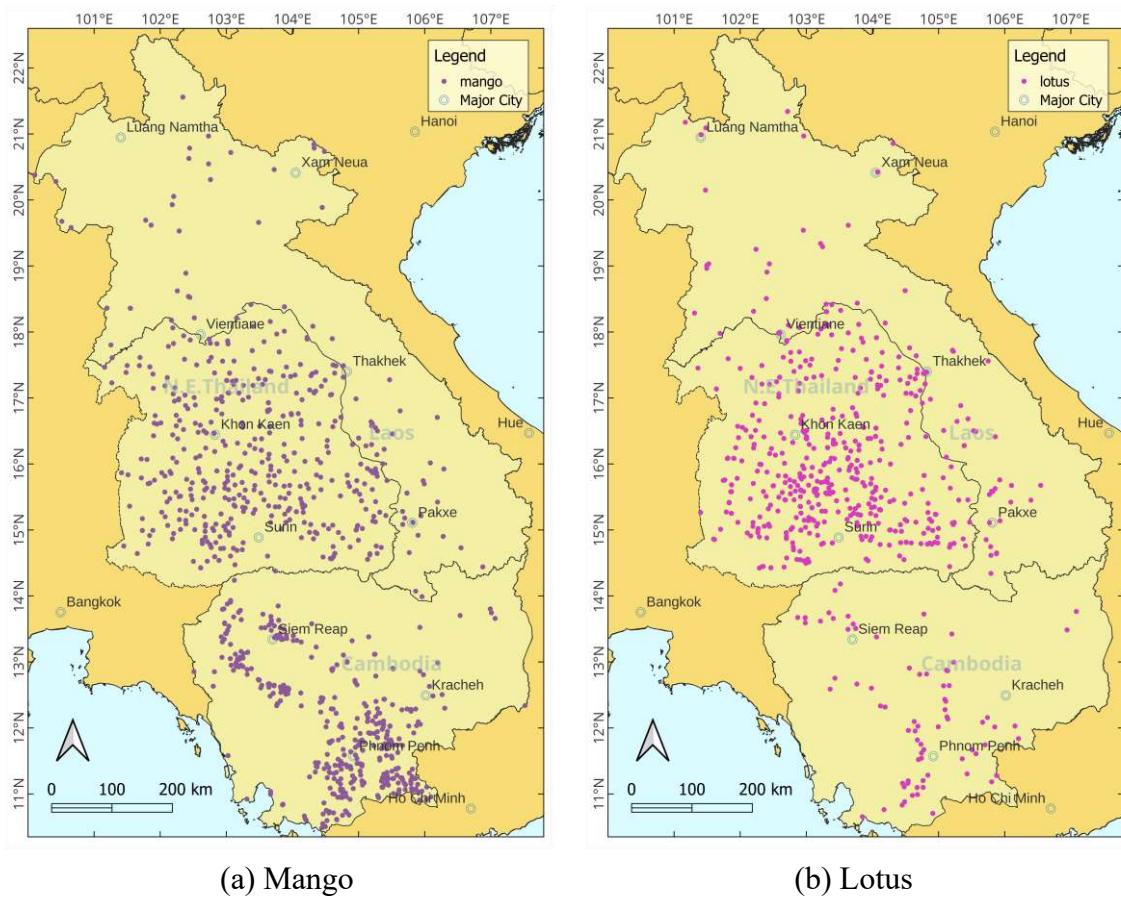


Figure 2. Words commonly used in the study area.

In northeastern Thailand, “lotus” is the most common word, appearing in about 1.8% of the village names. It appears in about 0.6% of village names in both Cambodia and Laos. Lotus is a word that reminds people of beautiful bodies of water, not only for food but also for scenery. The distribution of villages containing the word “lotus” is shown in Figure 2(b).

Although not as common as “lotus” or “mango,” the words “sugar palm” and “fig” are commonly used in the names of villages in the region. These four words are familiar to the locals as food. The sugar palm can be a symbol tree of a village, easily recognizable from afar.

3.2 Limited to south of 17 degrees north latitude

The distribution of villages using the word for a medium-sized shrub of the Fabaceae family, called ‘chanuan’ or ‘sanuan’ in northeastern Thailand, is limited to south of 17 degrees north latitude, as far as examples known at this time are concerned. A similar example of a word whose northern limit is 17°N is the tree name ‘sadao’ in Thai. In English it is called neem or Indian lilac. The distribution of villages using these two words is shown in Figure 3.

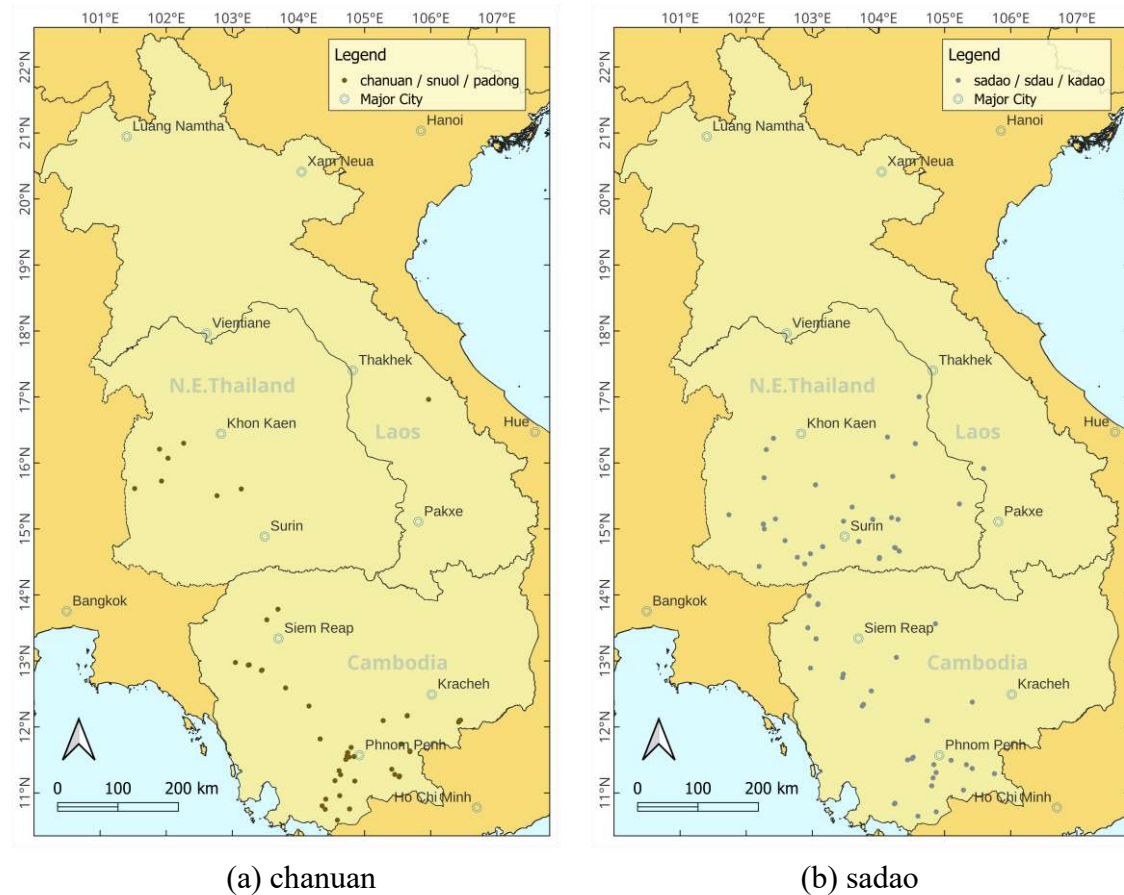


Figure 3. Words whose use is limited to south of 17 degrees north latitude.

Although it is not known to the author whether the northern limit of distribution of these two species in the actual vegetation distribution is 17 degrees north latitude or not, it is very interesting that the extent of their recognition as village symbols is so far.

3.3 Uneven distribution in northeastern Thailand

Figure 4(a) shows the distribution of ‘takhro’ in northeast Thailand, which is unevenly distributed in the southwestern part of the region. On the other hand, a study (Cruz-Garcia and Price, 2011) conducted in Kalasin province, located in the central northeast of Thailand, recorded ‘kho’ as the name of Ceylon oak. The word ‘kho’ is also used in Thai to refer not only to Ceylon oak but also to plants of the genus *Livistona* (Tomita, 1990), making it a polysemous word. The possibility that ‘kho’ is used as a name for Ceylon oak in the empty areas of northeastern Thailand needs to be investigated.

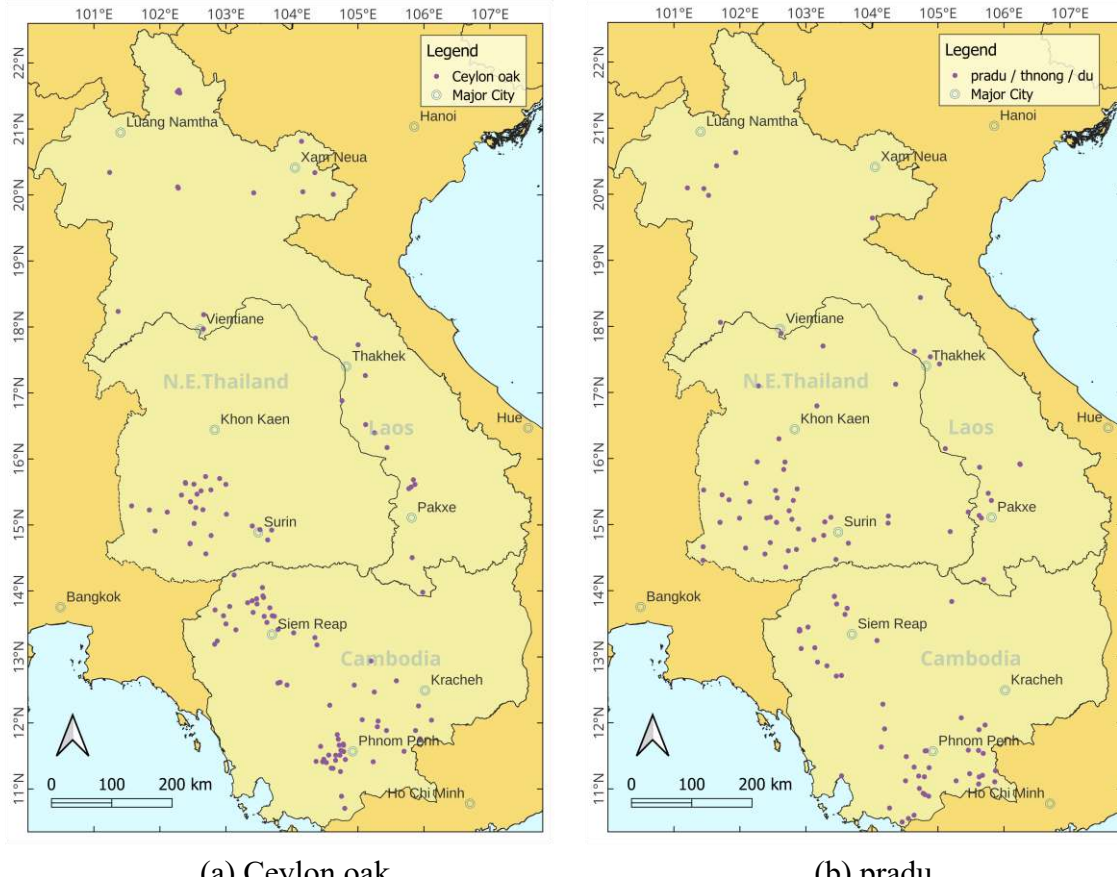


Figure 4. Words with uneven distribution in Northeastern Thailand.

Figure 4(b) shows the distribution of villages with the tree name ‘pradu’ in Thai. Similar to the Ceylon oak, village names containing the word ‘pradu’ are rare in all but the southwestern part of northeastern Thailand. The possibility that other names than ‘pradu’ may be used in the blank areas needs to be investigated, but the author does not have sufficient information at this time.

3.4 Appropriateness of words

An overview of the examples of use and distribution as village names reveals several words that suggest the need for detailed research.

In Cambodia, the word for bamboo is the second most frequently used in village names after mango, as shown in Table 1. In northeastern Thailand, however, there are only two examples. Although bamboo is a widely observed plant in northeastern Thailand and is widely used in daily tools, the author cannot explain why the frequency of use in village names is extremely low compared to that in Cambodia. As a useful resource closely related to daily life and close at hand, it is necessary to consider the possibility that there are expressions of which the author is unaware of. For example, bamboo shoots could be considered as a word derived from bamboo, but even so, only one other example was found. The distribution of villages using “bamboo” is shown in Figure 5(a).

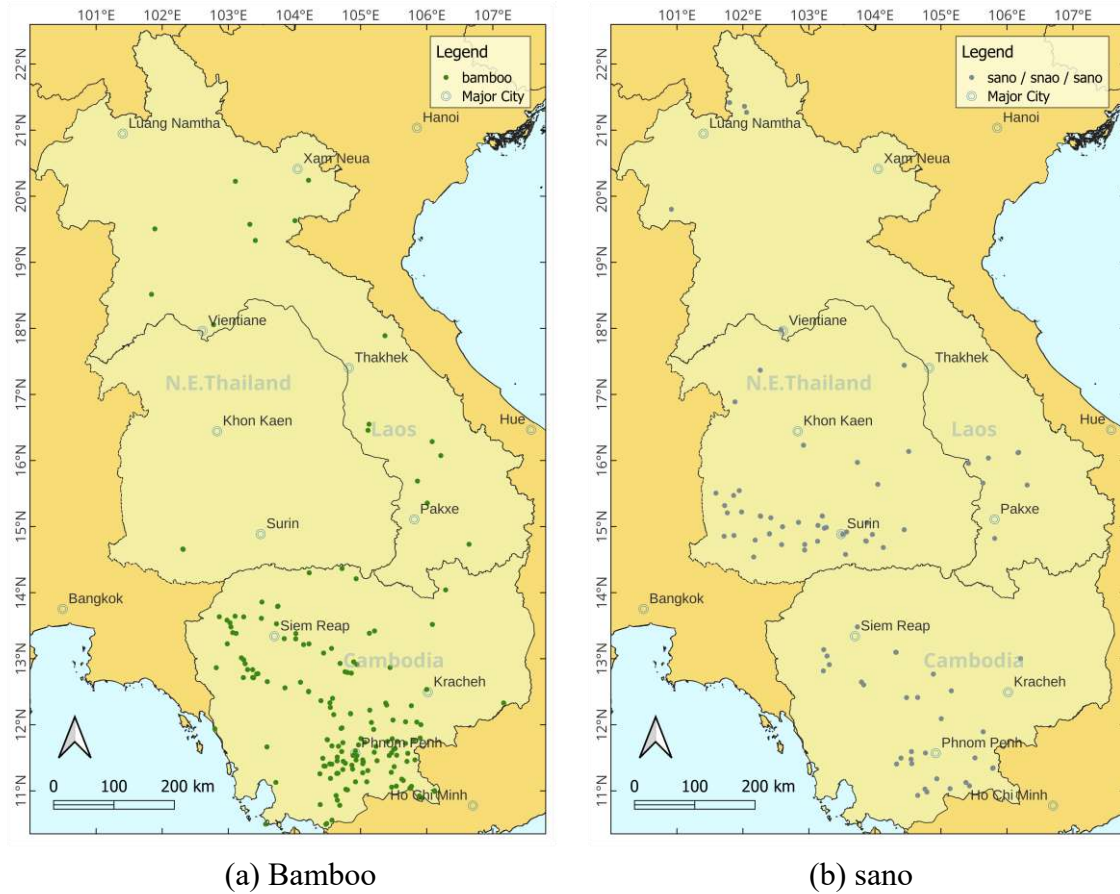


Figure 5. Words that require further investigation for appropriateness.

The word ‘sano’ in Thai shown in Figure 5(b) is not significantly more common than the other words shown in this report, although there are examples of its use in village names in all regions. The fact that there is one place where the use of ‘sano’ is clustered near the northernmost part of Laos suggests that it should be investigated whether ‘sano’ in Lao is a word that refers to the same tree species as words in other regions.

4. CONCLUSION

This study focuses on the analysis of vegetation-derived words and their occurrence in place names. The words used in place names depend on the language used in the village. Therefore, the local common name of a tree is not always the same as the standard language. This study is primarily relied on general word dictionaries such as (Headley 1997), (Phinthong 1989), and (Tomita 1990), a checklist of plants (Inthakoun and Delang 2008), and botanical dictionaries that can be searched in each language to confirm the meaning of words appearing in place names. If a word is used differently from its common name in the standard language, there is a possibility that the distribution of word use may be omitted from the study, as in the case of Ceylon oak and ‘pradu’ shown in this report. The accuracy of the analysis is compromised by a number of issues, including the failure to sufficiently take into account local names for plants that are familiar in local communities. Nevertheless, it was demonstrated that place names denoting small communities at the village level contain information that reveals aspects of the vegetation environment and lifestyle culture that are common across countries

and regions. As described in (Nagata 2022), numerous villages in Thailand have words of Khmer origin, while villages in the Mekong River basin in Cambodia have words of Thai or Lao origin expressed in Khmer script. The persistence of diverse ethnic cultures across national boundaries is also a significant insight conveyed by place names.

Given that a considerable number of research findings on the utilization of useful plants contain not only their scientific names but also their common names from a variety of geographical regions, it would be beneficial to incorporate these findings in a sequential manner in order to extend the study on the correlation between place names and vegetation.

5. ACKNOWLEDGEMENT

Much of the cartographic material referred to in this study is based on the Library of Congress collection. I am grateful for the opportunity to view many of them. This study was supported by JSPS KAKENHI Grant Number JP19K12700. Any opinions, findings, and conclusions or recommendations expressed in this material are those of the author and do not necessarily reflect the views of the author's organization, JSPS or MEXT.

6. REFERENCES

- CDD Thailand, 1993. *Muban chonnabot Thai pi 2535* [Villages of the Rural Areas of Thailand, 1992].
- Cruz-Garcia, G.S., Price, L.L., 2011. *Ethnobotanical investigation of 'wild' food plants used by rice farmers in Kalasin, Northeast Thailand*, Journal of Ethnobiology and Ethnomedicine 2011, 7-33.
- Headley, R.K., 1997. *Cambodian-English Dictionary*, Catholic University of American Press.
- Inthakoun, L., Delang, C.O., 2008. *Lao Flora, A checklist of plants found in Lao PDR with scientific and vernacular names*, Lulu Press.
- Nagata, Y., 1996. Mapping the Village Database: Spread of Economic Growth to Rural Areas of Northeast Thailand, *Southeast Asian Studies*, 33(4), 138-156.
- Nagata, Y., 2022. A Spatio-Temporal Study on the Community Level Place Names of around the Dangrek Mountains Area, *Proceedings of the 2022 Pacific Neighborhood Consortium Annual Conference and Joint Meetings*, 27-32.
- Nagata, Y., 2023. Geospatial overview of the vegetation environment suggested by community level place names in the area of northeastern Thailand and northern Cambodia, *Proceedings of the GIS-IDEAS 2023*, 160-164.
- Phinthong, P., 1989. *Sara Nukrom Phasa Isan-Thai-Angkrit* [Isan-Thai-English Dictionary], Siritham Press.
- Tomita, T., 1990. *Tai-nichi Jiten* [Thai-Japanese Dictionary], Yotokusha.

APPLYING GEOINFORMATICS TECHNOLOGY FOR BUILDING WEBGIS TO SUPPORT DRAINAGE MANAGEMENT IN NINH KIEU AND CAI RANG DISTRICTS OF CAN THO CITY

Nguyen Thanh Ngan^{1,2} and Nguyen Hieu Trung²

¹Ho Chi Minh City University of Natural Resources and Environment (HCMUNRE)

236B Le Van Sy Street, Ward 1, Tan Binh District, HCM City

Email: ntngan@hcmunre.edu.vn

²Can Tho University (CTU)

Campus II, 3/2 Street, Xuan Khanh Ward, Ninh Kieu District, Can Tho City

Email: nhtrung@ctu.edu.vn

ABSTRACT

Ninh Kieu and Cai Rang are central urban districts of Can Tho City, playing an important role in the socio-economic development of the entire region. In the current period, these two districts are strongly affected by climate change and sea level rise, making urban flooding in these areas increasingly complex and serious. To overcome the flood situation that has lasted for many years in Ninh Kieu and Cai Rang districts, managers and scientists need to find appropriate solutions to improve the effectiveness of urban drainage management. Applying geoinformatics technology is a feasible solution to overcome limitations and improve the effectiveness of urban drainage management and flood reduction. This paper introduces the results obtained in building WebGIS to support drainage management in Ninh Kieu and Cai Rang districts. WebGIS helps managers implement drainage management more easily and effectively, thereby improving the performance of the drainage system, contributing to reduce the negative impacts of urban flooding, improving the quality of life of people in the study area.

Keywords: geoinformatics technology, WebGIS, drainage management, Can Tho City.

1. INTRODUCTION

Ninh Kieu and Cai Rang are two district-level administrative units of Can Tho City. Both districts are important socio-economic centers, located in the southeast of the city. This area is strongly affected by climate change and natural disasters. These factors combined with rapid urbanization have created great pressure on drainage management activities in Ninh Kieu and Cai Rang districts. For the above reason, this area often experiences urban flooding during the rainy season, especially when heavy rains and high tides have occurred in recent years. This phenomenon has caused many difficulties, damage and reduced the quality of life of communities in Ninh Kieu and Cai Rang districts.

To overcome the flood situation, managers and scientists need to find appropriate solutions to improve the effectiveness of drainage management. Applying geoinformatics technology to build WebGIS to support drainage management is a feasible and effective solution. This solution has been successfully applied in many cities around the world and in Vietnam (Yang et al., 2006; Mishra and Bhatnagar, 2012; Tran Trong Duc, 2016; Ajwaliya et al., 2017; Tran Trong Duc, 2019; Kang, et al., 2021; Palla and Gnecco, 2021). This research was implemented to build WebGIS to support drainage management in Ninh Kieu and Cai Rang districts. This WebGIS is a useful tool to help managers improve the efficiency of drainage management in the central area of Can Tho City.

2. METHODS AND DATA

2.1 Research methods

The WebGIS to support drainage management is built through five main steps: (1) gathering and synthesizing relevant data, (2) analyzing and processing data, (3) creating spatial database, (4) building WebGIS, (5) evaluating results and proposing solutions. The process of creating spatial database plays an important role in the entire project implementation process because it directly affects the accuracy and suitability of data when represented on WebGIS. The spatial database on drainage management is built in SpatiaLite format, allowing use on many GIS software systems. The steps of the entire research process are shown briefly in Figure 1.

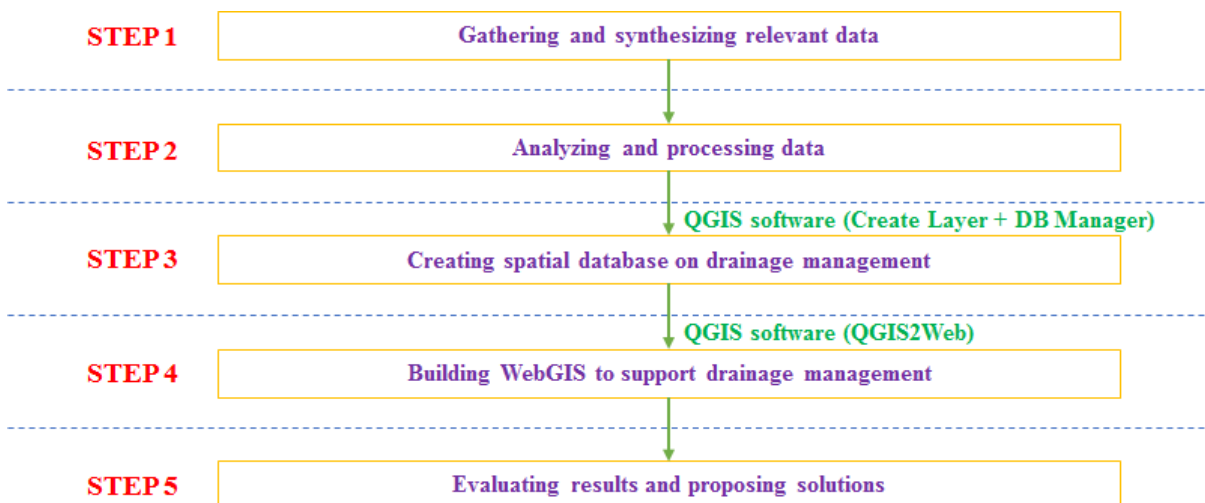


Figure 1. The steps of research process.

2.2 Research data

The WebGIS to support drainage management is built on the basis of two main types of data: (1) digital maps, (2) reports and statistics. Digital map data is in vector form (CAD file and shapefile), including five categories: (1) administrative boundaries, (2) roads, (3) terrain elevation, (4) houses and buildings, (5) drainage networks. The boundaries of these digital maps cover the entire area of Ninh Kieu and Cai Rang districts. Figure 2 demonstrates the spatial extent of the study area.

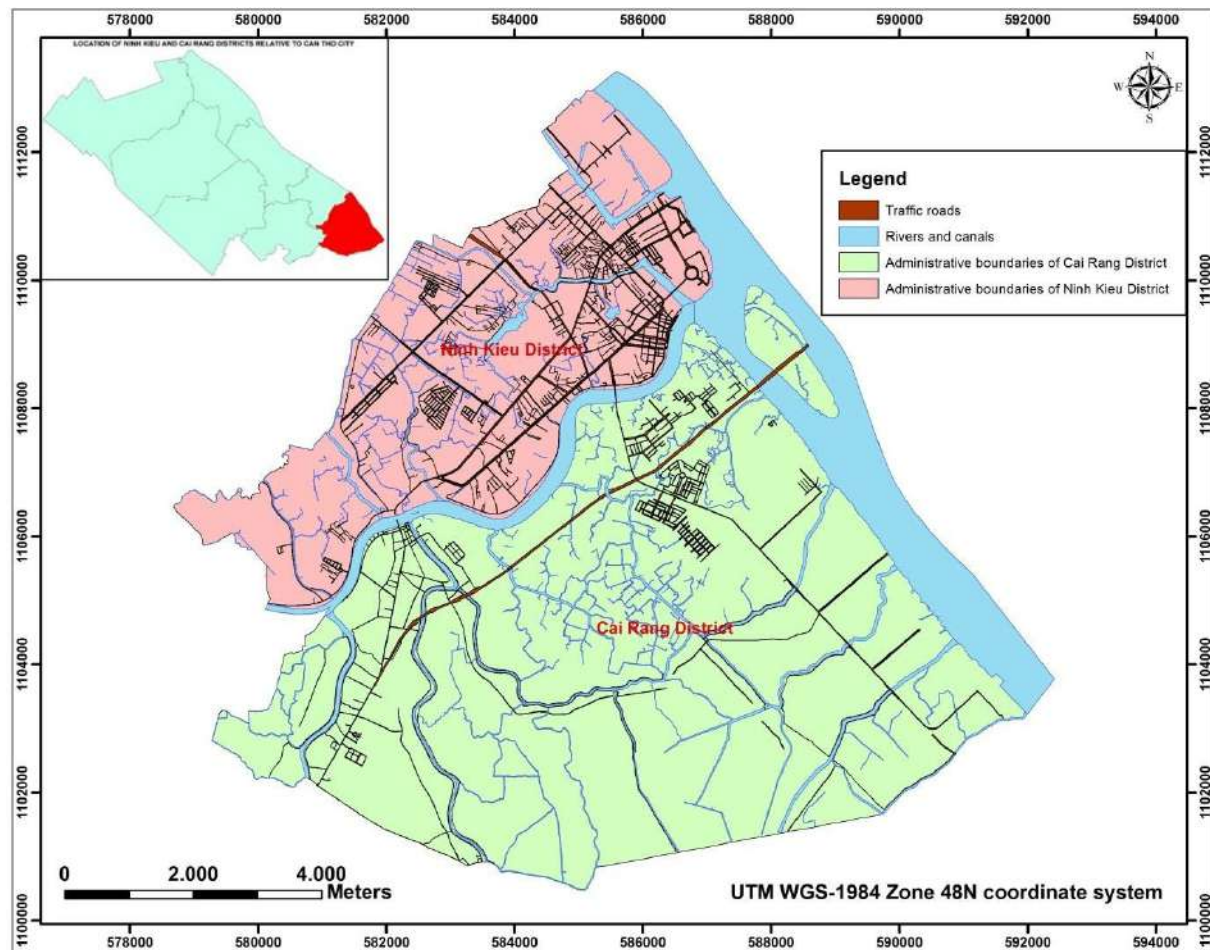


Figure 2. The spatial extent of the study area.

3. RESULTS AND DISCUSSION

3.1 The spatial database on drainage management

The data component of the WebGIS to support drainage management is derived from the spatial database built for Ninh Kieu and Cai Rang districts. Digital maps are collected, preprocessed and converted to the same coordinate system before being used to create a spatial database. The spatial database on drainage management includes two components: topographic background data and thematic data. This spatial database is created in the SpatiaLite format using tools on QGIS software. The entire spatial database on drainage management is divided into five data groups and 24 data layers. The topographic background data component has four data groups and 16 vector layers, while the thematic data component on drainage management has one data group and eight vector layers. Data layers in this spatial database are built on the UTM WGS-1984 Zone 48N coordinate system. The structure of the spatial database on drainage management is depicted in Figure 3.

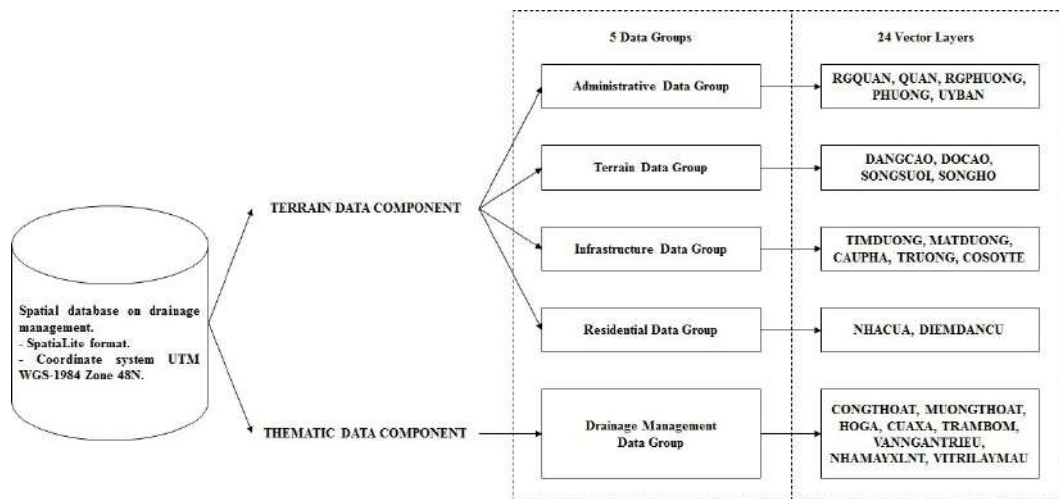


Figure 3. The structure of the spatial database on drainage management.

3.2 The WebGIS to support drainage management

The WebGIS to support drainage management is built on QGIS software with tool QGIS2Web. This WebGIS is designed according to a three-tier architecture model including:

- (1) Web Browser, (2) Web Server, (3) Map Server (Alesheikh et al., 2002).

Web Browser: an application for accessing a website with a predefined design (Internet Explorer, Chrome, Mozilla Firefox).

Web Server: Internet Information Services (IIS) software created by Microsoft.

Map Server: QGIS software and spatial database in SpatiaLite format.

The WebGIS to support drainage management has four main functions: (1) displaying digital maps, (2) interacting with digital maps, (3) displaying object attributes, (4) querying and searching for information. In the WebGIS interface, each function of the system is called and executed through one or several tools. These tools are represented as icons on the work screen. Windows and dialog boxes that appear during interaction with WebGIS are floating windows. Figure 4 presents the interface of the WebGIS to support drainage management.



Figure 4. The interface of the WebGIS to support drainage management.

4. CONCLUSIONS AND RECOMMENDATIONS

The research has built a WebGIS to support drainage management for Ninh Kieu and Cai Rang districts, contributing to improving the efficiency and professionalism of local management. This WebGIS is also a useful tool in preventing harmful effects of urban flooding and improving the quality of life of Can Tho City residents. During the research process, a spatial database on drainage management in SpatiaLite format was also built. This spatial database includes five data groups and 24 vector layers that can be used for many purposes in urban management in Ninh Kieu and Cai Rang districts. In the future this WebGIS will be supplemented with more functions and necessary data layers to better serve managers in the study area in particular and Can Tho City in general.

5. ACKNOWLEDGMENTS

The authors would like to thank the ValBGI Project and Assoc. Prof. Dr. Le Van Trung for providing data support for this research.

6. REFERENCES

- Yang, C. T., Ye, L., and Yu, J., 2006. *A framework of web-gis for urban drainage network system*. College of Information and Electronic Engineering, Zhejiang University of Science and Technology, Hangzhou, China, 35-41.
- Mishra, R., and Bhatnagar, S., 2012. WEB GIS for disaster management: Flood scenario. *International Journal of Advanced Information Science and Technology* 8(8), 11-14.
- Tran Trong Duc, 2016. Khai thác dữ liệu không gian về hệ thống hạ tầng thoát nước thông qua Internet. *Tạp chí Phát triển Khoa học và Công nghệ* 19(K4), 67-74, doi:10.32508/stdj.v19i2.669.
- Ajwaliya, R. J., Patel, S., and Sharma, S. A., 2017. Web-GIS based application for utility management system. *Journal of Geomatics* 11(1), 86-97.
- Tran Trong Duc, 2019. Phát triển hệ WebGIS cho phép khai thác dữ liệu mạng lưới thoát nước thông qua Internet. *Tạp chí Khoa học Đô đạc và Bản đồ* 41, 43-49, doi:10.54491/jgac.2019.41.293.
- Kang, X., Liang, H., Luo, W., and Xu, W., 2021. WebGIS System of Kunming Public Drainage Pump Station. *Journal of Physics: Conference Series* 1972, 012047, doi:10.1088/1742-6596/1972/1/012047.
- Palla, A., and Gnecco, I., 2021. The web-gis trig eau platform to assess urban flood mitigation by domestic rainwater harvesting systems in two residential settlements in Italy. *Sustainability* 13(13), 7241, doi:10.3390/su13137241.
- Alesheikh, A. A., Helali, H., and Behroz, H. A., 2002. *Web GIS: technologies and its applications*. In Symposium on Geospatial Theory, Processing and Applications, Ottawa, Canada, Vol 15, Hannover, Germany: ISPRS, 213-222.

3D URBAN GEOLOGICAL INFORMATION DEVELOPMENT FOR RESILIENT SOCIETY

Susumu Nonogaki

¹Geological Survey of Japan, National Institute of Advanced and Industrial Science and Technology
Central 7, 1-1-1 Higashi, Tsukuba, Ibaraki, 305-8567, Japan
Email: s-nonogaki@aist.go.jp

ABSTRACT

Geological information plays an important role in evaluating earthquake-induced geohazard risk, such as ground motion amplification and liquefaction/subsidence. Recently, as part of the intellectual infrastructure development by the national government, cooperating with local governments, Geological Survey of Japan (GSJ) has been working on creating three-dimensional (3D) geological maps of urban areas that represent the shallow subsurface geological conditions. The 3D maps are given as surface-based 3D geological model constructed by stacking the shapes of geological boundary surfaces estimated using elevation data set of geological boundaries obtained from stratal analysis of huge number of borehole data, considering the stratigraphic relationship of strata. In addition, GSJ also has been developing a web-based system for browsing geological information including the 3D geological maps. The web-based system allows us to visualize geological structures in 2D/3D as well as to create geological cross-sections along arbitrary line on web browser. To date, the 3D geological maps of the northern area of Chiba Prefecture and central Tokyo, Japan have been completed and are available for free on the GSJ website. These 3D geological information will help to enhance the accuracy of geo-risk assessment and subsurface environmental assessment and improve the efficiency of city planning, thereby contributing to the achievement of resilient cities and communities and other goals set forth in the SDGs.

1. INTRODUCTION

To achieve a safe, resilient and sustainable society, it is necessary to develop reliable intellectual infrastructures, such as basic research, ideas, and general-purpose technologies, and share it in an easy-to-use form. Geological information is one of the key intellectual infrastructures in the field of disaster management. In Japan, various intellectual infrastructures related to subsurface geological conditions have been developed and provided as thematic maps on the Web by national organizations under the jurisdiction of ministries. For example, Geospatial Information Authority of Japan (GSI), which is also under the jurisdiction of the Ministry of Land, Infrastructure, Transport and Tourism (MLIT), has released the “GSI Maps” [URL1] that provides topographic maps, photographs, elevations, topographic classifications, and other information on the land of Japan (Mogi, 2019). National Research Institute for Earth Science and Disaster Resilience (NIED), which is under the jurisdiction of the Ministry of Education, Culture, Sports, Science and Technology (MEXT), has released the “J-SHIS Map” [URL2] that provides the national seismic hazard maps for Japan which consist of the Probabilistic Seismic Hazard Maps (PSHM) and the Scenario Earthquake Shaking Maps (SESM). In addition, Geological Survey of Japan (GSJ), which is under the jurisdiction of Ministry of Economy, Trade and Industry (METI), provides the “GeomapNavi” [URL3] that enables geological information of various types and scales developed by GSJ to be viewed (Naito, 2020).

The thematic maps are useful for national-scale analyses based on the general information about subsurface geology but are difficult to use for city-scale analyses that require higher accuracy. The purpose of this study is to raise public awareness of disaster management and promote the effective use of underground space in urban areas. To achieve these goals, we are developing three-dimensional (3D) urban geological maps that show the distribution patterns of strata in shallow subsurface in detail, which is necessary for city planning. In this paper, we describe the method of creating 3D geological maps, web browsing system, features and issues of 3D geological maps.

2. 3D GEOLOGICAL MODELING

The 3D urban geological maps are created by surface-based 3D geological modeling using borehole data and some geospatial data, such as Digital Elevation Models (DEMs) and aerial photos. Figure 1 shows a flow diagram of 3D geological modeling. In the following, the three processes essential for 3D geological modeling are described.

2.1 Analysis of borehole data

The positions of geological boundaries are determined for borehole data. Two types of borehole data are used: those created for stratigraphic studies by GSJ and those created for public construction works. The former is typified by detailed geological information, such as radiocarbon dates, fossils, and pollens, that can be used as a reference for stratal correlation and analysis of geological structure. The latter is typified by the availability of tens of thousands of data in de facto standard format in Japan determined by MLIT (2016). These borehole data are usually provided by local governments or downloaded from the websites of national organizations like the “KuniJiban” [URL4] by the Public Works Research Institute (PWRI), which is under the jurisdiction of MLIT. In this study, we use borehole data by GSJ as reference data to determine the positions of the geological boundaries in other borehole data and create an elevation dataset for next process.

2.2 Estimation of geological boundary surfaces

The shape of geological boundary surfaces is estimated using the elevation dataset obtained from stratal correlation for borehole data. In urban plains areas, the strata formed in relatively recent geological times are distributed up to the depth of several tens of meters. These layers are often slightly dipping and have good continuity in the horizontal direction. In addition, the positional accuracy of borehole data produced for public construction works is lower than that of borehole data produced for stratigraphic studies and often has errors of tens of centimeters in the vertical direction. Therefore, we use the spline fitting technique by Nonogaki *et al.* (2012) which can consider both the goodness of fit and the smoothness of surface to estimate the shape of the geological boundary surfaces.

2.3 Construction of 3D geological models

A 3D geological model is constructed by stacking the shapes of the estimated geological boundaries, considering the stratigraphic relationships of the strata. Firstly, a logical model of geological structure (LMGS) (Shiono *et al.*, 1998), which defines the order of strata formation and the positional relationship between geological bodies and geological boundary surfaces, is

created using attribute information on the surfaces, such as conformity and unconformity. Next,

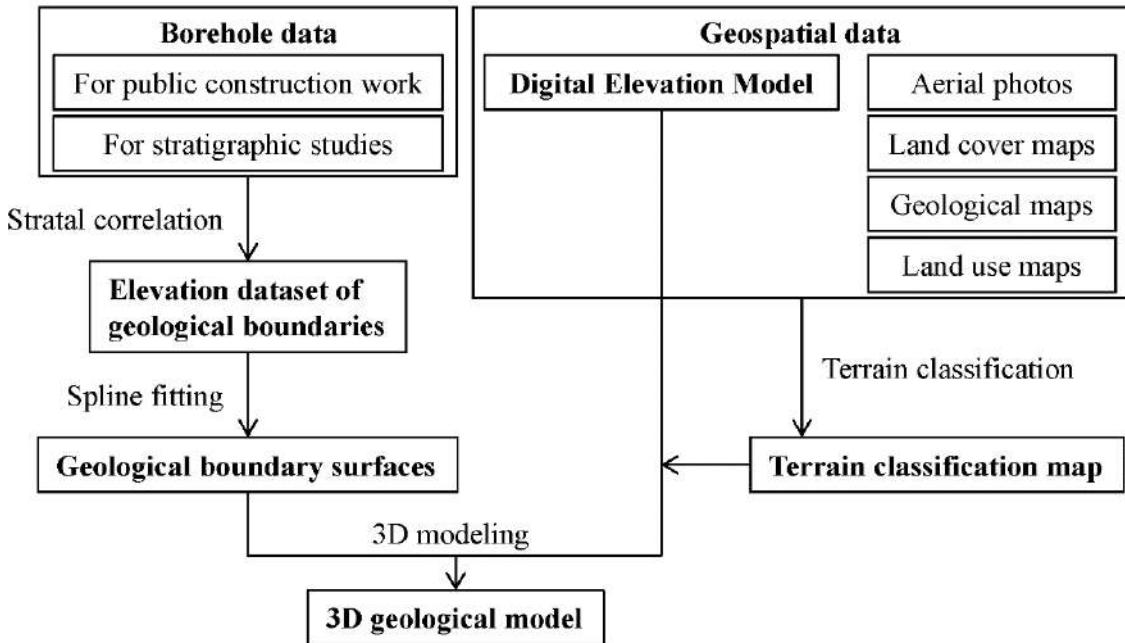


Figure 1. Flow diagram for 3D geological modeling.

following Masumoto *et al.* (2004), the distribution range of each geological boundary surface is determined based on the LMGS using Geographic Information System (GIS). Finally, a surface-based 3D geological model is virtually constructed by combining the shapes of the geological boundary surfaces with the shape of the ground surface that has the terrain classification information.

For data publication, all surfaces used for the 3D geological model are saved as raster grid data in GeoTIFF format and in original ASCII format. Moreover, contour maps and PNG tile maps of the geological boundary surfaces, which can be browsed on web browsing system for geological information described in the next chapter, are created using GDAL [URL5].

3. WEB BROWSING SYSTEM DEVELOPMENT

A web system has been developed for browsing the 3D geological model mentioned above, so that anyone can understand the detailed distribution of strata with high disaster risk. In the following, an overview of the geological information available on this system: two-dimensional (2D) and 3D maps, and geological cross-section is described. In addition, Figure 2 shows visualization examples of each geological information.

3.1 2D maps

Two types of 2D maps are available: one is geological maps that show the distribution of strata on the ground, like paper-based geological maps, and another is contour maps of the geological boundary surfaces that comprise the 3D geological model. These 2D maps are all given as PNG tile map. It is also possible to get the attribute information of the displayed map by mouse click. For geological maps, the name of the strata can be taken, and for contour maps, the elevation of the geological boundary surfaces can be taken.

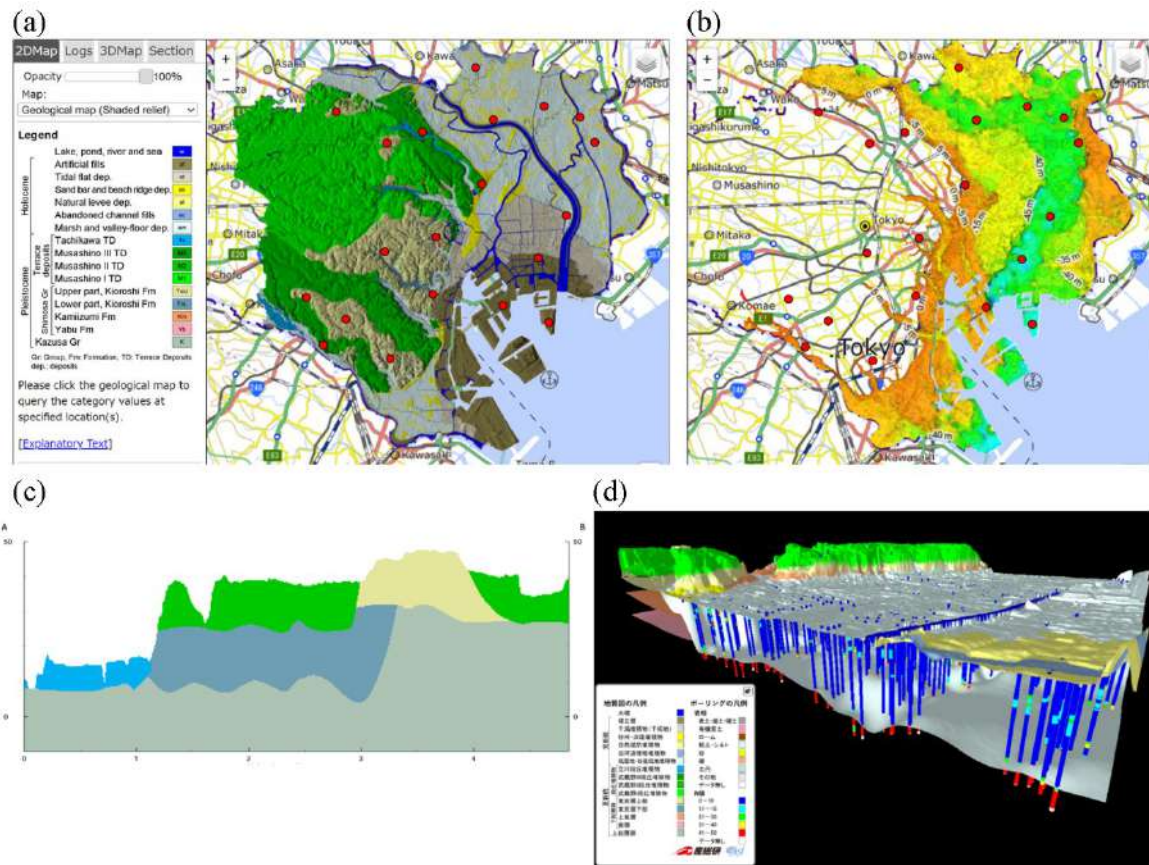


Figure 2. Geological information available in the web system. (a) 2D geological map, (b) contour map of geological boundary surface, (c) geological cross-section, and (d) 3D geological map.

3.2 Geological cross-sections

The user can create a geological cross-section along a line between any two points specified by mouse operation. In cross-sectional mapping, it is also possible to specify the vertical-to-horizontal ratio and the base elevation of the cross-section. To obtain a cross-section of a folded path, it is necessary to create a cross-section for each of the line segments that make up the path.

3.3 3D maps

The 3D geological maps are provided in small blocks to reduce its data size. For rendering each 3D map, the visualization tool for shallow subsurface geology (Nonogaki and Nakazawa, 2023), which allows the user to switch show/hide mode of geological boundary surfaces and borehole objects as well as to adjust the vertical-to-horizontal ratio of 3D rendering space and position of light source, is used.

4. DISCUSSIONS

4.1 Advantages of 3D urban geological maps

One of the advantages of 3D geological maps is the high visibility of the subsurface geological conditions. The 3D maps allow anyone to easily understand the detailed shapes of strata and thus confirm the distribution of soft layers that have earthquake-induced geohazard risk and hard layers that become the foundations of buildings, thereby raising users' disaster awareness.

Another advantage is that the shape of strata can be given as numerical data. As 3D geological maps can be easily applied to computer analyses, it is possible to simulate various seismic hazards, such as ground motion amplification and earthquake-induced liquefaction/subsidence. In addition, by combining 3D geological maps with building models, they can also contribute to infrastructure development in urban areas. Figure 3 shows an example of overlaying 3D geological map and 3D urban model "PLATEAU" [URL6] developed by MLIT in Tokyo Digital Twin Project [URL7]. In this example, it is easy to see on which geological layer the building is constructed.

4.2 Future challenges

The reliability of the geological boundary surfaces, which are key components of the surface-based 3D geological model, is important in applying the 3D models to geohazard risk evaluation and infrastructure development. Reliability is often discussed as uncertainty when geostatistical methods such as kriging are used for surface estimation, but not when spline fitting techniques are used, because the geological boundary surfaces almost always satisfy the elevation data obtained by stratal correlations. To facilitate the use of 3D geological models in the future, especially in the field of civil engineering where reliability often needs to be discussed, it is necessary to provide data on the reliability of the geological boundary surfaces in addition to the two data currently provided: the shape and estimation errors of the geological boundary surfaces.

In surface-based 3D geological models, there is no attribute information between geological boundary surfaces. However, many subsurface analyses use the distribution of physical properties such as soil types and SPT N-values within strata. For this reason, the current 3D geological maps are not directly applicable to these analyses. To promote the use of 3D geological models, it will also be necessary to estimate the distribution of physical properties in the future.

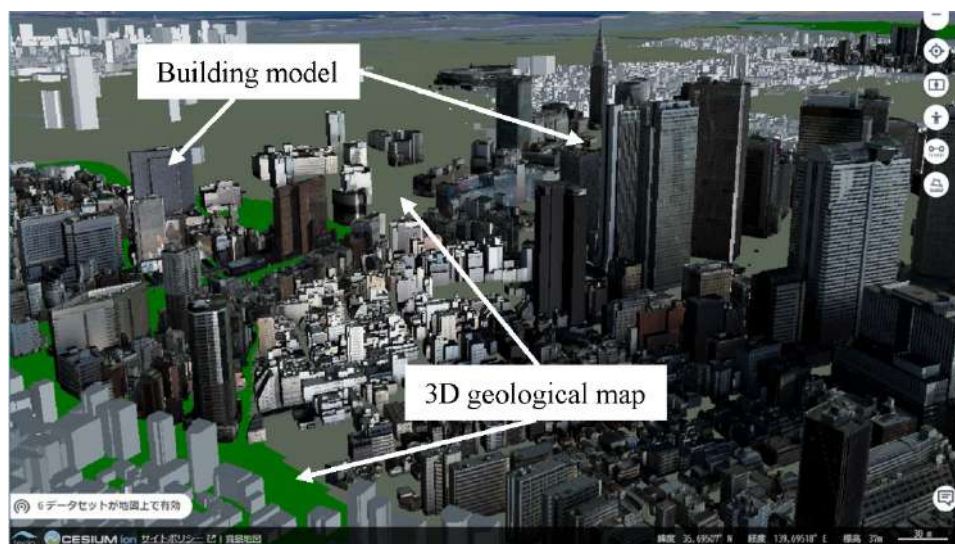


Figure 3. Application example of 3D geological map in digital twin.

5. CONCLUSIONS

The 3D urban geological maps are available for free on the website “Urban Geological Map” by GSJ [URL8]. The 3D geological information is an important intellectual infrastructure and will assist in a better understanding of geo-risk and the subsurface environment. Thus, it contributes to the development of a safe and resilient society, and other goals set forth in the SDGs. In the future, we plan to solve the problems mentioned above and expand the coverage of the 3D geological maps.

6. REFERENCES

- Masumoto, S., Raghavan, V., Yonezawa, G., Nemoto, T., and Shiono, K., 2004, Construction and visualization of a three-dimensional geologic model using GRASS GIS. *Transaction in GIS*, **8**(2), 211–223.
 DOI: <https://doi.org/10.1111/j.1467-9671.2004.00176.x>
- Ministry of Land, Infrastructure, Transport and Tourism, 2016, *Guideline on electronic delivery of the results of soil investigation and geological survey*. Ministry of Land, Infrastructure, Transport and Tourism, 50p. (in Japanese)
- Mogi, H., 2019. The advancement of utilizing geospatial information via GSI Maps. *Abstr. Int. Cartogr. Assoc.*, 1, 252.
 DOI: <https://doi.org/10.5194/ica-abs-1-252-2019>.
- Naito, K., 2020. Information platform for dissemination of geological information: GeomapNavi, *Journal of the Japan society of photogrammetry and remote sensing*, **59**, 1, 18–21. (in Japanese with English abstract)
 DOI: <https://doi.org/10.4287/jsprs.59.18>
- Nonogaki, S., Masumoto, S., and Shiono K., 2012. Gridding of geological surfaces based on equality-inequality constraints from elevation data and trend data. *International Journal of Geoinformatics*, **8**, 49–60.
- Nonogaki, S. and Nakazawa, T., 2023. Web-based visualization tool for 3D geological structures in shallow subsurface in urban areas. *Proceedings of GIS-IDEAS 2023*, 208–212.
- Shiono K., Masumoto S., and Sakamoto M., 1998. Characterization of 3D Distribution of Sedimentary Layers and Geomapping Algorithm – Logical Model of Geologic Structure –. *Geoinformatics*, **9** (3), 121–134. (in Japanese with English abstract)
 DOI: https://www.jstage.jst.go.jp/article/geoinformatics1990/9/3/9_3_121
- [URL1] GSI Maps, Geospatial Information Authority of Japan.
https://maps.gsi.go.jp/index_m.html (Last confirmed date: Sep. 14, 2024)
- [URL2] J-SHIS Maps, National Research Institute for Earth Science and Disaster Resilience.
<https://www.j-shis.bosai.go.jp/map/?lang=en> (Last confirmed date: Sep. 14, 2024)
- [URL3] GeomapNavi, Geological Survey of Japan.
<https://gbank.gsj.jp/geonavi/?lang=en> (Last confirmed date: Sep. 14, 2024)

[URL4] Kunijiban, Public Works Research Institute.

<https://www.kunijiban.pwri.go.jp/jp/> (Last confirmed date: Sep. 14, 2024)

[URL5] GDAL, Warmerdam F., Rouault E., and others.

<https://gdal.org/en/latest/> (Last confirmed date: Oct. 22, 2024)

[URL6] PLATEAU, Ministry of Land, Infrastructure, Transport and Tourism, Japan.

<https://www.mlit.go.jp/plateau/> (Last confirmed date: Sep. 14, 2024)

[URL7] Tokyo Digital Twin Project, Tokyo Metropolitan Government, Japan.

<https://info.tokyo-digitaltwin.metro.tokyo.lg.jp/> (Last confirmed date: Sep. 14, 2024)

[URL8] Urban Geological Map, Geological Survey of Japan.

https://gbank.gsj.jp/urbangeol/index_en.html (Last confirmed date: Sep. 14, 2024)

RELATIONSHIP BETWEEN COMPOUND EXTREME INDICES AND ATMOSPHERIC CIRCULATION PATTERNS IN THAILAND

Teerachai Amnuaylojaroen¹, Atsamon Limsakul², Wuttichai Paengkaew², Nidalak Aroonchan², Jerasorn Santisirisomboon³, Ratchanan Srisawadwong³, and Lin Wang⁴

¹School of Energy and Environment, University of Phayao
19 19, Mae Ka, Mueang Phayao District, Phayao 56000, Thailand
Email: teerachai4@gmail.com

² Department of Climate Change and Environment (DCCE)
49 Rama VI Rd. Soi 30, Phaya Thai, Phaya Thai, Bangkok 10400, Thailand
Email: atsamonl@gmail.com, wutthichai9577@gmail.com, nidalak_oil@hotmail.com

³ Center of Regional Climate Change and Renewable Energy, Ramkhamhaeng University
2086 Ramkhamhaeng Rd, Khwaeng Hua Mak, Khet Bang Kapi, Bangkok 10240, Thailand.
Email: jerasorn@ru.ac.th, nick.ratchanan@gmail.com

⁴ Institute of Atmospheric Physics, Chinese Academy of Sciences
Beijing, Chaoyang, Beichen W Rd, 100017, China
Email: linwang@mail.iap.ac.cn

ABSTRACT

This study examines the correlation between compound extreme indices and atmospheric circulation patterns in Thailand from 1970 to 2023. The aim of this study is to examine the consequences of various atmospheric indices, including the Pacific Decadal Oscillation (PDO), Southern Oscillation Index (SOI), Niño indices (3.4, 1+2, 3), Global Mean Sea Surface Temperature (GMST), Quasi-Biennial Oscillation (QBO), Pacific Warm Pool (PACWARM), and the Trans-Niño Index (TNI), on compound extreme weather events. Composite analyses were performed to compare the average values, as well as the high and low extreme values, during periods of compound extreme heat and precipitation, as well as extreme conditions of Tmax35-SPI5day. The results suggest that the PDO and Niño indices typically have negative mean values during low extremes, indicating an outbreak of stronger La Niña conditions. During periods of extreme conditions, the Southern Oscillation Index (SOI) experiences an increase, which suggests the existence of stronger La Niña signals. The Global Mean Surface Temperature (GMST) exhibits a consistent and continuous upward trend during periods of high extremes, thus emphasizing the ongoing phenomenon of global warming. During periods of high extremes, the Quasi-Biennial Oscillation (QBO) experiences substantial declines, whereas the Pacific Warm Pool (PACWARM) index shows an increase. Conversely, during periods of low extremes, the PACWARM index decreases. The TNI exhibits variations in ENSO phases, declining during periods of high extremes and rising during periods of low extremes. The results reveal the dynamic characteristics of atmospheric circulation patterns and their vital effect on climate patterns and compound extreme events in Thailand.

1. INTRODUCTION

The frequency and intensity of extreme weather events have increased as a result of climate change. This poses substantial risks to ecosystems, economies, and human health worldwide (IPCC, 2021). Due to its complex climate and geographical characteristics, Thailand is especially susceptible to such extreme events (Amnuaylojaroen, 2021). Understanding the connection between compound extreme indices and atmospheric circulation patterns is essential for planning and mitigating the effects of these events.

Compound extreme indices, which analyze the simultaneous occurrence of multiple extreme weather events, enable a more comprehensive evaluation of climate extremes in comparison to indices that focus on individual events (Zscheischler et al., 2018). These indices

can measure complicated connections among different meteorological variables, such as temperature, precipitation, and wind, which frequently influence the intensity of extreme events (De Luca et al., 2017). Thailand has experienced severe weather events such as heavy rainfall, droughts, and heatwaves, which have resulted in significant socio-economic disruptions. These events emphasized the importance of establishing better predictive models and adaptive strategies (Singhrattna et al., 2005; Limsakul and Singhruck, 2016).

Large-scale climatic forces, such as the El Niño-Southern Oscillation (ENSO), the Indian Ocean Dipole (IOD), and the Madden-Julian Oscillation (MJO), drive atmospheric circulation patterns that have a significant impact on weather extremes in regional scales (Wu et al., 2012). These patterns have an impact on the propagation and severity of temperature and rainfall, which in turn affects the frequency of severe weather events (Yang et al., 2018). The ENSO phenomenon has been associated with both droughts and heavy rainfall events in Southeast Asia, including Thailand (Singhrattna et al., 2005).

Although it is crucial to understand these connections, there is a scarcity of research that combines compound extreme indices with Thailand's specific atmospheric circulation patterns. Previous studies have primarily examined specific extreme events or conducted broad regional analyses, potentially neglecting the localized impacts and interactions (Hao et al., 2018). Therefore, the objective of this study is to examine the correlation between compound extreme indices and atmospheric circulation patterns in Thailand.

2. METHODOLOGY

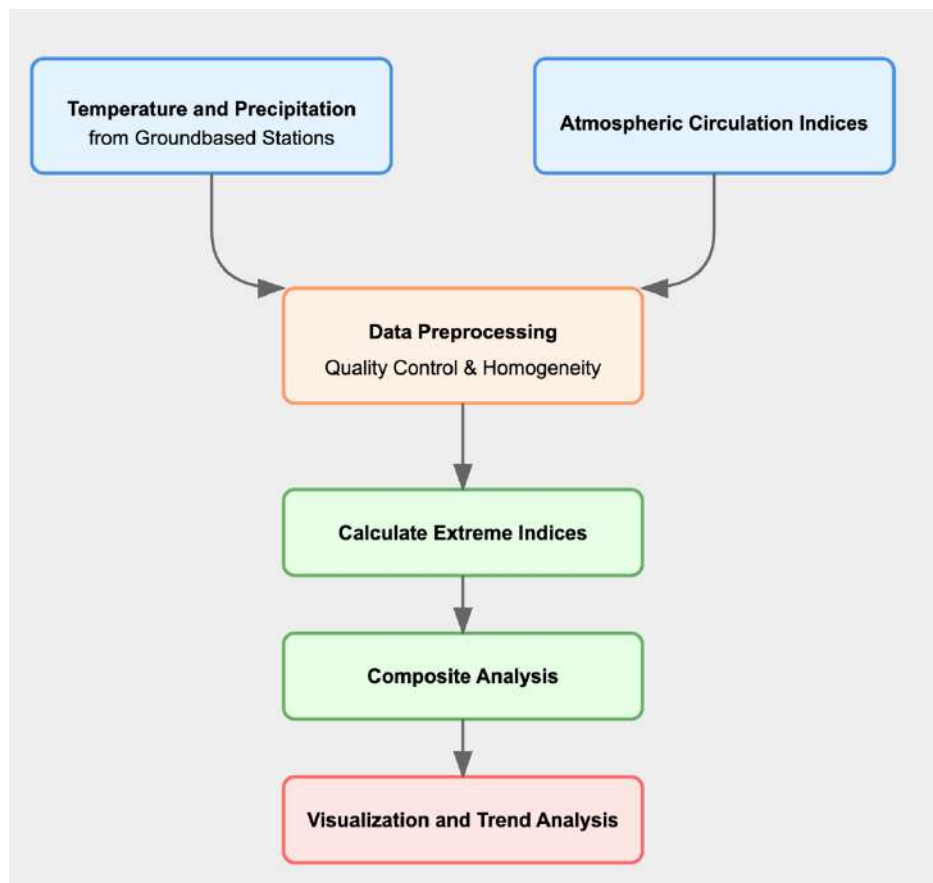


Figure 1 Data analysis process for this study.

This study uses a data analysis process for studying climate and weather patterns. It begins with

two parallel data sources: temperature and precipitation measurements from 120 ground-based stations, and atmospheric circulation indices from National Oceanic and Atmospheric Administration (NOAA). These data streams undergo preprocessing, which includes quality control checks and homogeneity testing to ensure data reliability. The process then moves to calculating extreme indices to identify significant weather events, followed by composite analysis to study patterns and relationships.

2.1 Compound extreme indices

Many extreme weather and climate events are often caused by the interaction of multiple hazards and drivers, known as compound events, that comprise two or more extreme events occurring concurrently, coincidentally or successively (Hao et al., 2018a; AghaKouchak et al., 2020; Zscheischler et al., 2020). Compound extreme heat-precipitation events (CEHPEs) and compound extreme heat-drought events (CEHDEs) are the most important compound extremes, posing severe impacts on human health, and societal and ecological systems (Hao et al., 2018; Ning et al., 2022). The empirical method as a statistical approach has been commonly used to explore and analyse multiple variables or components of compound extremes (Hao et al. 2018a; Zscheischler et al. 2020; Yu et al. 2022). It was executed by counting the number of two or more different extremes occurring coincidentally or sequentially within a certain window of time. The individual extreme was first defined, followed by calculating the quantity of compound extremes based on the concurrent or consecutive occurrence of individual extremes (Hao et al. 2018a; Yu et al. 2022). In this study, GIS software was utilized during the preprocessing stage to standardize station data coordinates, ensuring consistent spatial projections and accurate alignment of each station's geographic location. By minimizing spatial errors, this approach improved the quality and reliability of the datasets before statistical analysis. The CEHPEs were calculated from daily Tmax and daily precipitation for each station individually. Percentile-based extreme indices developed by the ETCCDI, it was first analysed for extreme precipitation and heat events (Klein Tank et al. 2009; Zhang et al. 2011). Extreme precipitation and heat events were defined as when daily precipitation or daily Tmax was larger than 90th percentile values for the reference period of 1970-2005 (Hao et al. 2018a; Ning et al. 2022). GIS was further employed to integrate multiple spatial datasets, including temperature, precipitation, and atmospheric indices data from each station. This integration within a GIS framework ensured alignment across spatial and temporal dimensions, facilitating a cohesive analysis of compound extreme events across varied geographic settings. The CEHPEs were then counted if heat events occur within three days prior to the starting day of the extreme precipitation event (Hao et al. 2018a; Ning et al. 2022). Droughts were identified using 1-month Standardised Precipitation Index (SPI). The thresholds were set to CEHDEs when daily Tmax greater than 90th percentile occurring in the month with severe drought ($SPI < -1.5$). Both compound indices were calculated based on 65 station data of daily Tmax and precipitation that had been passed the quality control and homogeneity test.

2.2 Atmospheric circulation indices

This study obtained atmospheric circulation index data from the National Oceanic and Atmospheric Administration (NOAA), which included the Pacific Decadal Oscillation (PDO), Southern Oscillation Index (SOI), El Niño-Southern Oscillation (ENSO), Global Mean Sea Surface Temperature (GMSST), Niño, Quasi-Biennial Oscillation (QBO), Pacific Warm Pool (PACWARM), and Trans-Niño Index (TNI). PDO induces enduring changes in the Pacific Ocean, impacting climate fluctuations and weather patterns over decades, especially in North America. The Southern Oscillation Index (SOI) quantifies the variations in atmospheric pressure between Tahiti and Darwin. It is an essential indicator for monitoring the El Niño-

Southern Oscillation (ENSO) phenomenon, which has significant effects on global weather patterns. The Niño indices (3.4, 1+2, 3) represent deviations from normal sea surface temperatures in the equatorial Pacific. These indices are important for understanding the different phases of the El Niño-Southern Oscillation (ENSO) phenomenon, which has a substantial impact on global climate patterns. GMSST provides a comprehensive representation of average ocean surface temperatures across the globe, emphasizing global trends. QBO, short for Quasi-Biennial Oscillation, refers to the periodic changes in the direction and speed of winds in the equatorial stratosphere. These variations have a significant impact on weather patterns, such as monsoons and hurricanes. PACWARM, the warmest oceanic region in the western Pacific, has a crucial impact on global atmospheric circulation and the formation of tropical weather systems. Finally, the TNI quantifies the variations in temperature between the central and eastern Pacific regions, facilitating comprehension of the shifts between El Niño and La Niña occurrences and their effects on climate. These indices combined enhance our understanding of the dynamic interactions within the Earth's climate system and emphasize the significance of ongoing monitoring for climate impact assessments.

2 Composite analysis

In this study, we apply a composite analysis to assess how atmospheric circulation indices respond to different categories of compound extreme events. The variables used in this analysis are defined including Overall Mean (OM) represents the overall mean value of each atmospheric index across the entire dataset, regardless of the occurrence of extreme events. This serves as a baseline to compare variations during extreme conditions. High Extreme Mean (HEM) is the mean value of each atmospheric index during periods identified as "high extremes." High extremes are defined by the occurrence of specific compound events where the index values exceed the 90th percentile threshold, reflecting unusually high conditions, such as elevated temperature or intense precipitation events. Low Extreme Mean (LEM) represents the mean value of each atmospheric index during periods identified as "low extremes." Low extremes refer to instances where the index values fall below the 10th percentile threshold, indicating unusually low or diminished conditions, such as reduced temperatures or minimal precipitation levels during the study period.

These variables, OM, HEM, and LEM, are calculated to enable comparisons among average conditions (OM), high extreme conditions (HEM), and low extreme conditions (LEM) for each atmospheric index. Such comparisons reveal how indices like the PDO, SOI, Niño indices, and others shift in response to extreme events, thereby providing insights into the behavior of atmospheric patterns under varying climate extremes.

Composite analysis is a statistical method used to understand the behavior of atmospheric variables under specific compound extreme indices in this study (Von Storch and Zwiers, 2002). It typically involves calculating the average values of atmospheric indices during specific extreme conditions. Here are the related equations:

$$OM = \frac{1}{N} \sum_{i=1}^N x_i ,$$

where N is the total number of observations and X_i is the value of the index at time i.

$$HEM = \frac{1}{n_h} \sum_{i \in H} x_i ,$$

where n_h is the number of observations in the high extreme category and H represents the set of high extreme indices.

$$LEM = \frac{1}{n_h} \sum_{i \in L} x_i,$$

where n_h is the number of observations in the high extreme category and L represents the set of low extreme indices.

Composite analysis is particularly suited for this research because it allows us to capture patterns and trends by averaging atmospheric conditions during extreme weather events. By focusing on 'high' and 'low' extremes separately, we can identify how specific conditions (like strong La Niña or El Niño patterns) influence extreme weather events in Thailand. This approach enables us to distinguish between typical conditions and those that occur during unusual weather patterns, providing deeper insights into the link between atmospheric patterns and extreme events.

3. RESULT

3.1 Time series analysis

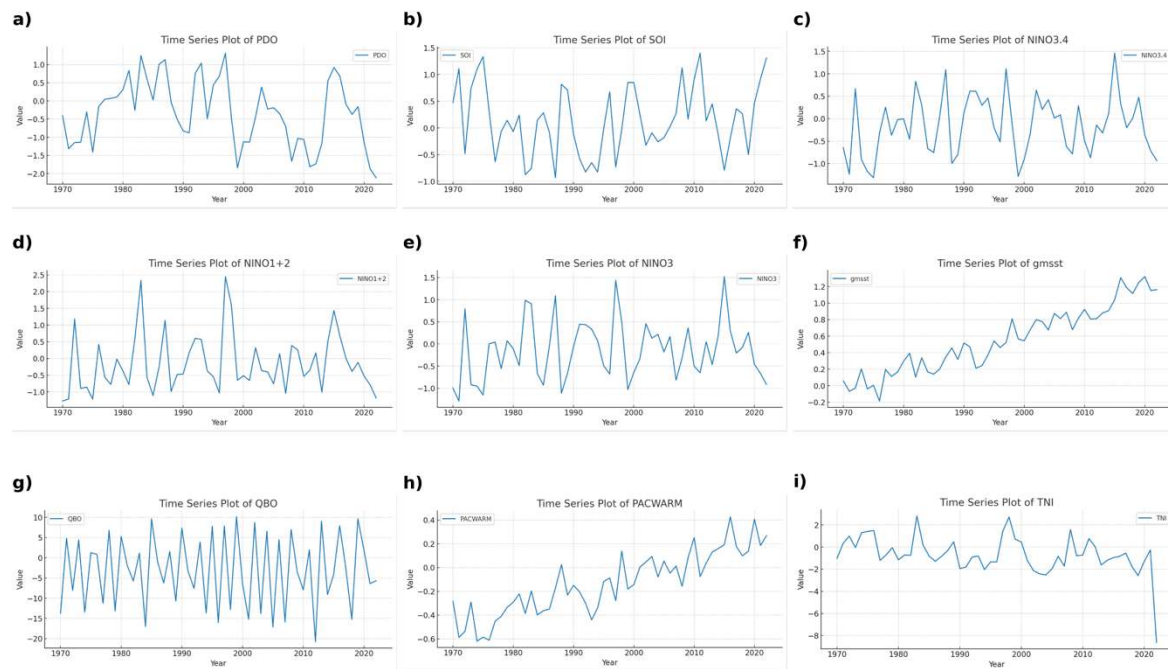


Figure 1 Time series plots of various atmospheric circulation modes from 1970 to 2023 for a) PDO, b) SOI, c) Niño 3.4, d) Niño 1+2 , (e) Niño 3 , (f), GMSST (g) QBO, h) PACWARM, and i) TNI.

The time series plots in Figure 1 demonstrate substantial variations and patterns in different atmospheric circulation modes between 1970 and 2023. The PDO shows long-term changes over several decades, whereas the SOI and Niño indices (3.4, 1+2, 3) emphasize the significant fluctuations linked to El Niño and La Niña events, which are crucial for understanding ENSO phenomena. The GMSST and PACWARM indices exhibit a consistent upward pattern, indicating the continuation of global warming. QBO demonstrates consistent oscillations in the stratospheric wind, while TNI indicates a transitional pattern between different phases of ENSO.

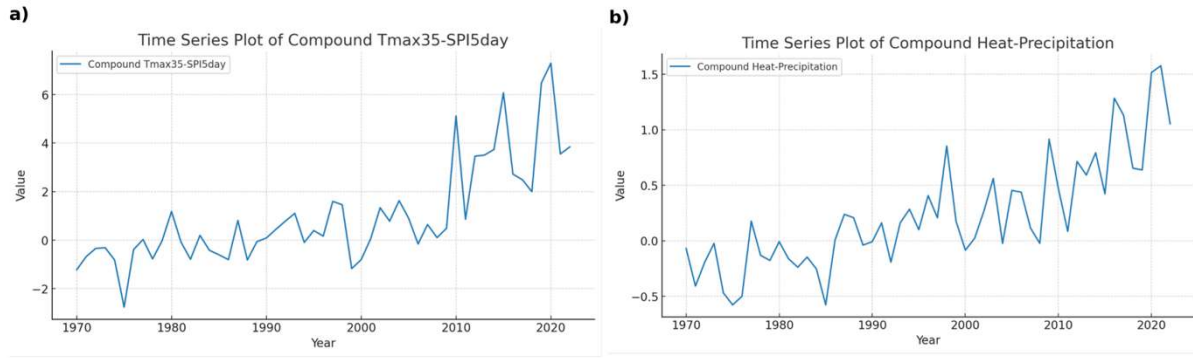


Figure 2 Time series plots of various atmospheric circulation modes from 1970 to 2023 for a) Tmax35-SPI5day index, b) compound between heat and precipitation index.

Figure 2 displays time series plots of composite indices covering from 1970 to 2023, indicating extreme temperature and precipitation conditions. Figure 2a illustrates the Tmax35-SPI5day index, which represents the combined influence of maximum temperature exceeding 35°C and short-term deviations in precipitation. The plot exhibits a consistent upward trend, suggesting a notable increase in both the frequency and intensity of these extreme events throughout the given time period. Figure 2b displays the compound heat-precipitation index, which demonstrates the relationship between extreme heat and precipitation events. This index also indicates a consistent upward pattern, indicating that the frequency of compound heat and precipitation events has increased.

3.2 Composite analysis

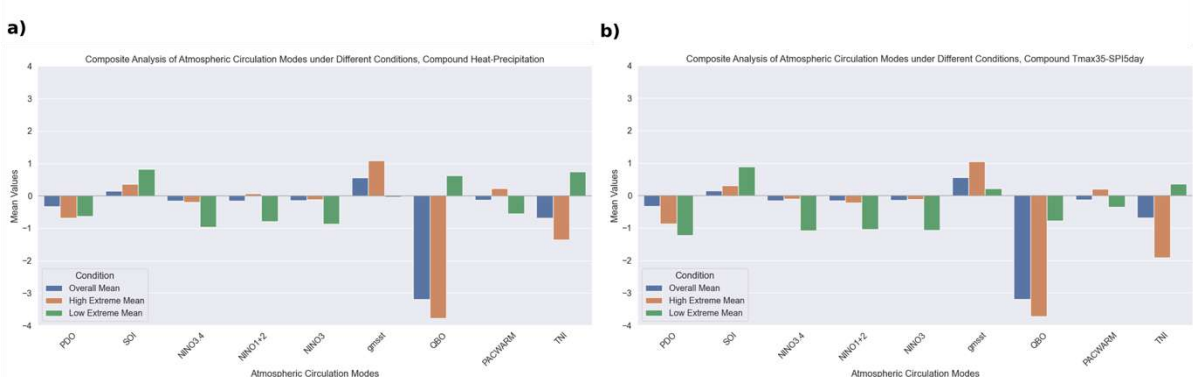


Figure 3 Composite analyses of atmospheric circulation modes under different conditions of compound extremes for (a) compound heat and precipitation index, and (b) compound Tmax5 and SPI6day index.

Figure 3 shows composite analyses of atmospheric circulation modes across various conditions of compound extremes. Figure 3a examines the composite heat and precipitation index, specifically comparing the mean, high extreme, and low extreme values for each atmospheric circulation mode. Figure 3b analyzes the composite Tmax5 and SPI6day index, yet again comparing the mean, maximum extreme, and minimum extreme values. They represent the response of various atmospheric circulation modes to extreme conditions. The

findings show significant variations in atmospheric responses during periods of high and low extremes.

Table 1. Composite Analysis of Average Atmospheric Circulation Modes During Extreme Compound Heat and Precipitation, and Tmax35- SPI5day Conditions

Index	Overall Mean	High Extreme Mean		Low Extreme Mean	
		Heat+Prep.	Tmax35-SPI5day	Heat+Prep.	Tmax35-SPI5day
PDO	-0.329	-0.689	-0.864	-0.631	-1.220
SOI	0.145	0.358	0.306	0.828	0.886
NINO 3.4	-0.151	-0.201	-0.102	-0.962	-1.082
NINO 1+2	-0.152	0.068	-0.226	-0.794	-1.047
NINO 3	-0.144	-0.113	-0.110	-0.865	-1.061
GMST T	0.553	1.083	1.050	-0.030	0.210
QBO	-3.198	-3.769	-3.723	0.622	-0.779
PACW ARM	-0.132	0.231	0.197	-0.553	-0.350
TNI	-0.686	-1.356	-1.914	0.746	0.366

Table 1 displays an analysis of the average patterns of atmospheric circulation during occurrences of extreme combined heat and precipitation, as well as compound extreme Tmax35-SPI5day conditions. The analysis compares the mean, maximum and minimum values for each index. PDO shows a significant decrease in the mean during both high and low extremes, with the lowest values occurring during low extremes. The SOI exhibits an increase during periods of extreme conditions, which is indicative of a stronger La Niña signal. The Niño indices (3.4, 1+2, 3) typically exhibit negative mean values, with more significant declines during low extremes, indicating stronger La Niña conditions. The GMST increases significantly during periods of high extremes and experiences a slight increase during periods of low extremes, which suggests a continuous warming trend. QBO exhibits a significant decrease in the mean during periods of high extremes, while experiencing a less noticeable decrease during periods of low extremes. The PACWARM index increases during periods of high extremes and decreases during periods of low extremes. TNI exhibits a decrease during periods of high extremes and an increase during periods of low extremes, indicating changes in the phases of ENSO. The results emphasize the unique reactions of

atmospheric circulation patterns during various extreme conditions, emphasizing their crucial influence on climate effects. The evidence suggests that there is an apparent increase in extremes during low extremes, indicating a change in ENSO phases.

4. DISCUSSION

The findings of this study provide the behavior of different atmospheric circulation patterns during compound extreme conditions. The variations and patterns in significant indicators such as the PDO, SOI, and Niño indices (3.4, 1+2, 3) are crucial for understanding ENSO. The PDO exhibits long-term changes over several decades, whereas the SOI and Niño indices emphasize the significant variations linked to El Niño and La Niña episodes. This variability corresponds to a previous study that has shown the substantial impact of these indices on global climate patterns (Mantua and Steven, 2002; Johnson et al., 2020). The increasing patterns observed in the GMST and PACWARM indices indicate the continuous occurrence of global warming, which is consistent with the conclusions reached from various climate studies (Mantua and Steven, 2002). QBO and TNI exhibit periodic oscillations and transitional patterns between different ENSO phases, indicating their substantial influence on interactions between the stratosphere and the Earth's surface climate (Mantua and Steven, 2002). The analysis of compound indices focuses mainly on extreme temperature and precipitation conditions. The Tmax35-SPI5day index and the compound heat-precipitation index exhibit upward trends, suggesting an increase in the occurrence and severity of these extreme events. The observed pattern corresponds with the increasing frequency of compound climate extremes resulting from global warming (Mantua and Steven, 2002). The analysis of atmospheric circulation patterns during extreme heat and precipitation events reveals notable shifts in the PDO, SOI, and Niño indices. Specifically, the PDO and Niño indices tend to display negative values, indicating an increased occurrence of La Niña conditions. The GMST increases significantly during periods of high extremes, indicating a warming trend. In contrast, the QBO and PACWARM indices show considerable variability. The TNI exhibits a transition in ENSO phases, declining during periods of high extremes and increasing during periods of low extremes. The analysis also shows that during extreme Tmax35-SPI5day conditions, the PDO experiences a significant decrease in both high and low extremes, with the lowest values observed during low extremes. The SOI and Niño indices continue to indicate a more increased occurrence of La Niña conditions during extreme events. The GMST continues to demonstrate an increase during periods of high extremes, indicating a continuing pattern of warming. Additionally, the QBO and PACWARM indices indicate significant changes. TNI exhibits significant variability, characterized by a decline during periods of high extremes and a moderate rise during periods of low extremes. These findings are consistent with prior research that emphasizes the complicated connection between these atmospheric indices and extreme climate events (Mantua and Steven, 2002).

The findings of this study have practical implications for enhancing weather forecasting models. By identifying how indices like PDO and SOI behave during extreme weather events, meteorologists can better predict compound climate events in Thailand. For example, recognizing a pattern in PDO or SOI during extreme heat-drought events could be used in developing early warning systems, helping to anticipate severe weather seasons and enabling proactive responses. The insights from this study could support climate adaptation policies in Thailand. By understanding the link between atmospheric indices and compound extreme events, policymakers can better anticipate which regions are at risk and allocate resources accordingly. These findings could inform the prioritization of infrastructure projects, such as

water management systems or heat-resilient urban planning, particularly in areas identified as vulnerable to extreme heat-drought or heat-precipitation events.

Furthermore, this study's results are valuable for disaster preparedness efforts, as identifying patterns in atmospheric indices during extreme events can help with the strategic allocation of resources. For instance, if La Niña phases (indicated by a rise in SOI) coincide with increased compound heat-drought events, early resource mobilization can mitigate impacts, ensuring timely assistance to affected communities.

5. CONCLUSION

While this study provides valuable insights into the relationship between compound extreme indices and atmospheric circulation patterns in Thailand, several areas warrant further investigation. Future research could explore additional atmospheric indices beyond those analyzed here, to gain a more comprehensive understanding of other factors influencing compound extreme events. Additionally, incorporating higher-resolution spatial analyses could offer more localized insights, identifying specific areas within Thailand that are particularly susceptible to extreme events. There is also potential for advancing predictive models that integrate both atmospheric indices and compound extreme indices, improving early warning systems and climate resilience planning. These future directions would enhance our understanding of complex climate dynamics and support adaptation strategies to mitigate the impacts of extreme weather events in Thailand and similar regions.

6. REFERENCES

- Amnuaylojaroen, T. 2021. Projection of the precipitation extremes in Thailand under climate change scenario RCP8. 5. *Frontiers in Environmental Science* 9, 106.
- De Luca, P., Hillier, J. K., Wilby, R. L., Quinn, N. W., and Harrigan, S., 2017. Extreme multi-basin flooding linked with extra-tropical cyclones. *Environmental Research Letters* 12(11), 114009.
- Hao, Z., Singh, V. P., and Xia, Y., 2018. Seasonal drought prediction: Advances, challenges, and future prospects. *Reviews of Geophysics* 56(1), 108-141.
- IPCC, 2021. Climate Change 2021: The Physical Science Basis. Contribution of Working Group I to the Sixth Assessment Report of the Intergovernmental Panel on Climate Change.
- Johnson, Z. F., Chikamoto, Y., Wang, S. Y. S., McPhaden, M. J., and Mochizuki, T., 2020. Pacific decadal oscillation remotely forced by the equatorial Pacific and the Atlantic Oceans. *Climate Dynamics* 55, 789-811.
- Limsakul, A., and Singhruck, P. 2016. Long-term trends and variability of total and extreme precipitation in Thailand. *Atmospheric Research*, 169, 301-317.
- Mantua, N. J., and Hare, S. R., 2002. The Pacific decadal oscillation. *Journal of Oceanography* 58, 35-44.
- Singhrattna, N., Rajagopalan, B., Kumar, K. K., and Clark, M., 2005. Interannual and interdecadal variability of Thailand summer monsoon season. *Journal of Climate* 18(11), 1697-1708.
- Von Storch, H., and Zwiers, F. W. 2002. *Statistical analysis in climate research*. Cambridge university press.

-
- Wu, B., Li, T., and Zhou, T., 2010. Relative contributions of the Indian Ocean and local SST anomalies to the maintenance of the western North Pacific anomalous anticyclone during the El Niño decaying summer. *Journal of Climate* 23(11), 2974-2986.
- Yang, S., Li, Z., Yu, J. Y., Hu, X., Dong, W., & He, S. 2018. El Niño–Southern Oscillation and its impact in the changing climate. *National Science Review*, 5(6), 840-857.
- Zscheischler, J., Westra, S., van den Hurk, B. J., Seneviratne, S. I., Ward, P. J., Pitman, A., and Zhang, X., 2018. Future climate risk from compound events. *Nature Climate Change* 8(6), 469-477.
- AghaKouchak, A., F. Chiang, L.S. Huning, C.A. Love, I. Mallakpour, O. Mazdiyasni, H. Moftakhari, S.M. Papalexiou, E. Ragno, and M. Sadegh, 2020. Climate Extremes and Compound Hazards in a Warming World. *Annu. Rev. Earth Planet. Sci.*, 48, 519-548.
- Zscheischler, J., O. Martius, S. Westra, E. Bevacqua, C. Raymond, R.M. Horton, B. van den Hurk, A. AghaKouchak, A. Jézéquel, M.D. Mahecha, D. Maraun, A.M. Ramos, N.N. Ridder, W. Thiery, and E. Vignotto, 2020. A Typology of Compound Weather and Climate Events. *Nat. Rev. Earth Environ.*, 1, 333-347.
- Ning, G., M. Luo, W. Zhang, Z. Liu, S. Wang, and T. Gao, 2022. Rising Risks of Compound Extreme Heat-Precipitation Events in China. *Int. J. Climatol.*, 42, 5785-5795.
- Yu, H., N. Lu, B. Fu, L. Zhang, M. Wang, and H. Tian, 2022. Hotspots, Co-Occurrence, and Shifts of Compound and Cascading Extreme Climate Events in Eurasian Drylands. *Environ. Int.*, 169, 107509. <https://doi:10.1016/j.envint.2022.107509>.
- Zhang, X., L. Alexander, G.C. Hegerl, P. Jones, A.K. Tank, T.C. Peterson, B. Trewin, and F.W., 2011. Indices for Monitoring Changes in Extremes based on Daily Temperature and Precipitation Data. *WIREs Clim. Change.*, 2(6), 851-870.
- Klein Tank, A., F. Zwiers, and X. Zhang, 2009. Guidelines on analysis of extremes in a changing climate in support of informed decisions for adaptation, 53 pp
- Hao, Z., V.P. Singh, and F. Hao, 2018a. Compound Extremes in Hydroclimatology: A Review. *Water*, 10(6), 718. <https://doi:10.3390/w10060718>.

PROCESSING AND ANALYZING MULTI-SOURCE, MULTI-RESOLUTION GEOSPATIAL DATA ON CLOUD PLATFORMS FOR SOME ENVIRONMENTAL AND DISASTER APPLICATIONS

Tran Van Anh^{1*}, Ha Trung Khien², Tran Hong Hanh¹, Khuc Thanh Dong², Truong Xuan Quang³, Tatsuya Nemoto⁴ and Venkatesh Raghavan⁴

¹ Hanoi University of Mining and Geology, Department of Geomatics and Land Administration, No.18 Vien Street, Duc Thang Ward, Bac Tu Liem, Hanoi, Vietnam

Email: tranvananh@humg.edu.vn; tranhonghanh@humg.edu.vn

² Hanoi University of Civil Engineering, Department of Geodesy, 55 Giai Phong street, Dong Tam, Hai Ba Trung, Ha Noi, Vietnam

Email: khienht@huce.edu.vn; dongkt@huce.edu.vn

³ Faculty of Architecture, Urbanism and Sustainable Science, School of Interdisciplinary Sciences and Arts, Vietnam National University, Hanoi 144 Xuan Thuy, Cau Giay, Hanoi, Vietnam

Email : txquang@vnu.edu.vn

⁴Osaka Metropolitan University, Graduate School of Science, 3-3-138 Sugimoto Sumiyoshi-ku, Osaka-shi, 558-8585, Japan

Email: tnemoto@omu.ac.jp; raghavan@omu.ac.jp

ABSTRACT

Recently, our earth has been facing increasingly severe conditions due to various climate change phenomena. Natural disasters such as storms, floods, and landslides have become more frequent. Monitoring changes or deformations in the land surface has thus become more crucial. While processing data over large areas often provides a comprehensive view for assessing the extent of changes and damage caused by natural and human factors, it requires handling vast amounts of data. Fortunately, cloud computing platforms have become more powerful and are now supporting numerous studies in earth science and environmental monitoring. This article provides an overview of how two cloud computing platforms, Google Earth Engine (GEE) and Google Colab (GC), are utilized to process large datasets for monitoring and forecasting land surface changes in various regions of Vietnam. Four examples of applications using GEE and Google Colab include: analyzing open-pit coal mine changes using Sentinel-1 and Sentinel-2 satellite images on the GEE platform; predicting landslides using Support Vector Machine (SVM), Random Forest (RF), and Gradient Boosting (GB) machine learning models on the GEE platform; monitoring landslides from Sentinel-1 Radar image series using PyGMTSAR on Colab, and last is forecasting land subsidence using a subsidence value series from 2015 to 2023 showcasing the capabilities of these platforms.

1. INTRODUCTION

In recent years, the use of satellite image processing for applications related to natural resources, the environment, and natural disasters has become increasingly widespread. Combining satellite imagery with geospatial data has enhanced the accuracy of land cover interpretation and the monitoring of surface changes. Machine learning models and artificial intelligence, when integrated with multi-source data, have been instrumental in forecasting natural disasters such as floods, landslides, and subsidence, thereby helping to mitigate risks to human life.

Given the large volume of imagery and geospatial data, the diversity of sources and formats, and their growing accessibility, these datasets can be classified as "big data" (Laney 2001, Diebold 2012). Cloud computing platforms, which function as virtual supercomputers, provide access to vast processing and computational resources for various data types. In

addition, cloud computing allows flexible data storage, enabling more efficient post-processing.

Several current cloud computing platforms are relevant to natural resources and environmental applications. Amazon Web Services (AWS) offers access to the largest suite of machine learning and artificial intelligence (AI) services. AWS hosts various satellite imagery datasets, including Sentinel-1, Sentinel-2, Landsat 8, and the National Oceanic and Atmospheric Administration's (NOAA) High-Resolution Rapid Refresh (HRRR) Model. Google Cloud Platform (GCP), introduced by Google in 2008, is a public cloud-based service designed for developing and hosting web applications in Google-managed data centers on a pay-as-you-go basis. GCP offers services such as data storage, analytics, machine learning tools, and enterprise mapping services (Krishnan and Gonzalez 2015).

In 2010, Microsoft launched Azure, a cloud computing platform for building, testing, deploying, and managing applications and services via Microsoft-managed data centers (Wilder 2012). Azure provides machine learning services and hosts satellite data products such as Landsat, Sentinel-2 for North America (from 2013 to present), and MODIS imagery (from 2000 onwards).

More recently, Google Earth Engine (GEE) has emerged as a prominent platform for big data processing in geospatial applications. GEE is a cloud-based platform that enables parallel processing of geospatial data at a global scale using Google's cloud infrastructure (Gorelick, Hancher et al. 2017). GEE is a free platform hosting petabyte-scale archives of over 40 years of remote sensing data, including Landsat, MODIS, Sentinel 2, 3, and 5-P, as well as meteorological datasets like NOAA AVHRR and radar satellite data from ALOS PalSAR 1, 2, and Sentinel-1 (Gorelick et al., 2017). GEE also includes geospatial datasets related to climate, weather, and geophysics, and offers ready-to-use products such as monthly and daily rainfall data from satellite and ground-based rain gauges, and the Normalized Difference Vegetation Index (NDVI) (Kumar and Mutanga 2018).

GEE's notable strength lies in its ability to process large-scale satellite data without requiring users to download data locally, thanks to Google's powerful server infrastructure. This infrastructure allows users to access millions of optical and radar satellite images, as well as environmental data from various sources. GEE provides robust tools for processing and analyzing satellite data, including image operations, time series analysis, and the generation of environmental maps and indices. Additionally, GEE offers a code editor via a web-based Integrated Development Environment (IDE), enabling users to write, develop, and execute complex scripts using JavaScript APIs (Kumar and Mutanga, 2018).

However, while GEE is a powerful tool for processing and analyzing satellite data, it has limitations when it comes to applying advanced data analysis methods, such as artificial intelligence (AI), machine learning, and deep learning. GEE primarily focuses on image data processing and offers direct support for only a limited range of machine learning algorithms, which may restrict users from conducting more detailed analyses. This is where Google Colab becomes essential.

Google Colab is an online notebook environment that strongly supports Python and data analysis libraries such as TensorFlow, PyTorch, and scikit-learn. It allows users to perform advanced data analysis and build machine learning or deep learning models without worrying about hardware limitations.

The combination of GEE and Colab creates a more efficient data analysis workflow. Users can leverage GEE to retrieve and process large-scale satellite data and then export the data to Colab to apply AI and machine learning algorithms to uncover deeper patterns and insights. For instance, after generating environmental indicators from satellite data in GEE, users can use Colab to develop and train machine learning models to analyze environmental changes or predict future trends.

In this paper, we aim to explore the capabilities of GEE in analyzing multi-source satellite data over time and integrate it with machine learning algorithms to predict surface changes such as the expansion of open-pit mining Thai Nguyen and landslide prediction in a mountainous region of Vietnam. Additionally, we will show a landslide monitoring study using a multi-temporal Sentinel-1 complex image series for the 2019-2020 period, as well as a land subsidence forecast for a small area in the Mekong Delta of Vietnam.

2. METHODOLOGY

2.1 Google Earth Engine (GEE) Applications

As presented in the introduction, GEE is a cloud computing platform with large data sources related to satellite image data and geospatial data. Below is a summary of some of the functions of GEE (Tamiminia, Salehi et al. 2020)

Table 1. Some algorithms and features available in the Google Earth Engine Code Editor.

Order	Package	Capabilities	Order	Package	Capabilities
1	Machine learning	<ul style="list-style-type: none"> - Supervised Classification - Unsupervised Classification - Regression 	4	Geometry Feature	<ul style="list-style-type: none"> -Filtering - Mapping
2	Image	<ul style="list-style-type: none"> - Image Visualization - RGB composites - Color plates - Masking - Mosaicking - Clipping - Rendering categorical maps - Thumbnail 	5	Image Collection	<ul style="list-style-type: none"> - Histograms - Image Regions charts - Time-series in Image Regions - Charts by image classes - Iterating over an image collection

3	Charts	Time-series charts	6	Specialized algorithms	- Landsat algorithms	
					- Sentinel-1 algorithms	
					- Resampling and Reducing Resolution	

As discussed, the remote sensing data processing capabilities of GEE have encouraged researchers to leverage this technology for various environmental applications (Table 1). GEE's ability to store geospatial datasets, along with its features for coding, sharing, processing, and visualizing data, has made it a standout competitor among existing cloud platforms. Although several studies have explored geospatial big data analytics, they have primarily focused on its characteristics, existing tools, and applications (Chi, Plaza et al. 2016); (Tamiminia, Salehi et al. 2020). In the fields of remote sensing and spatial data analytics, a Google Scholar search returns approximately 356,000 results that related to the GEE, underscoring the effectiveness of GEE's tools and functionality in meeting the demands of image and geospatial data analysis and processing. Figure 1 below shows the GEE interface.

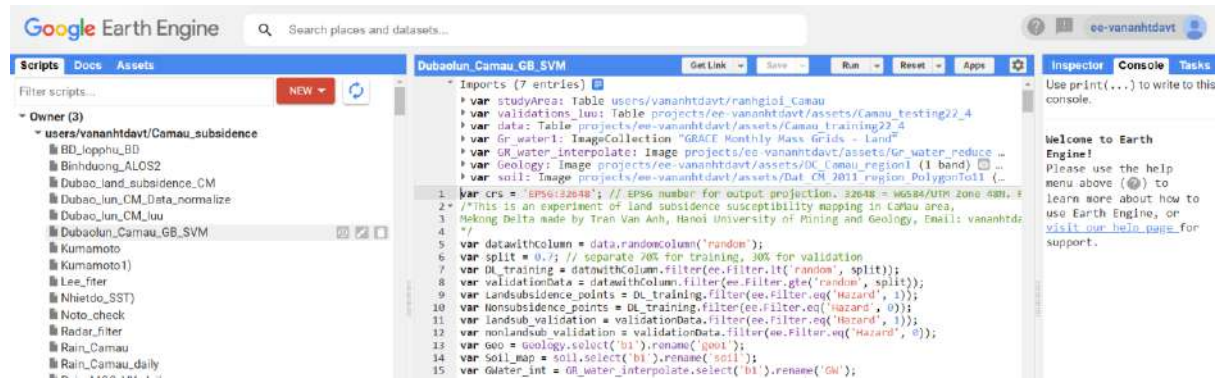


Figure 1. Google Earth Engine Platform

2.2 Applications of the Google Colab Platform

The Google Colab cloud platform is a web-based service that provides users with a coding environment equipped with powerful computing resources, tools, and functions, enabling complex analyses on large datasets. These resources, including storage and high-

performance servers, are hosted by the provider and accessed by users through a web browser. With the exponential growth in data and increasingly complex analytical methods used by researchers and businesses, cloud platforms are becoming more advantageous. The availability of GPUs and TPUs, accessible from a user's personal computer, allows for advanced analysis to be performed without the need for expensive hardware. Additionally, many cloud services offer analytics-ready data or access to datasets via APIs, making it faster and easier to collect and utilize diverse data types.

Unlike GEE, Google Colab supports running machine learning and deep learning algorithms from various libraries and can integrate with other platforms like Kaggle, Jupyter, or GEE for advanced Earth observation and geospatial data analysis. Google Colab uses Python, a widely popular language for geospatial data analysis. Figure 2 below shows the Google Colab interface.

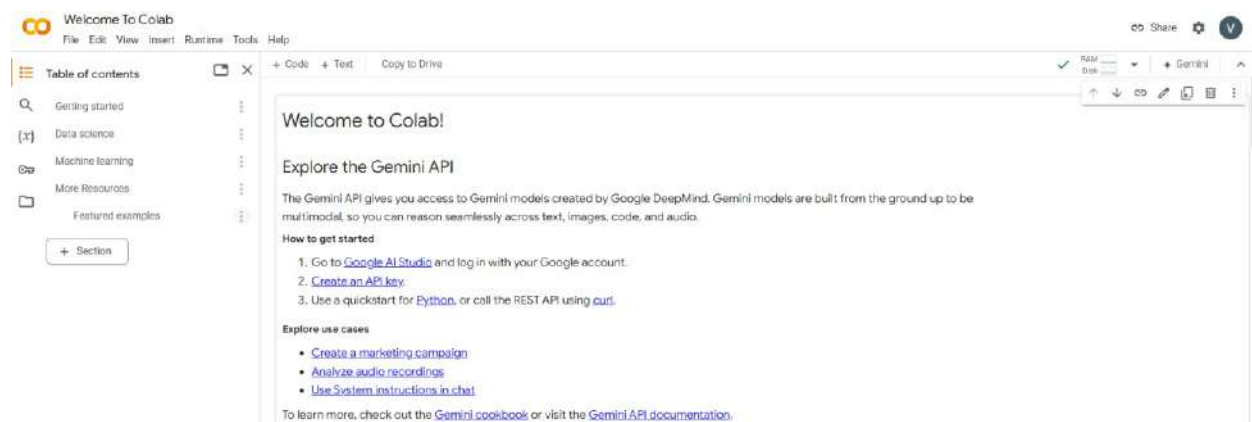


Figure 2. Google Colab Platform

3. UTILIZING CLOUD COMPUTING PLATFORMS FOR ENVIRONMENTAL AND RESOURCE DATA ANALYSIS AND PROCESSING

3.1 Application of Google Earth Engine (GEE) to determine the expansion of open-pit coal mines through the use of optical satellite imagery, radar data

The study focuses on the Minh Tien coal mine, located in the communes of Minh Tien and Na Mao in Thai Nguyen province, Vietnam. Licensed in 2014 with an approved extraction capacity of 8,500 tons per year, the mine began open-pit operations in 2018, significantly increasing its output beyond the licensed limit. As the mining areas have expanded, waste material from the mine has been deposited near agricultural lands, posing environmental risks and threatening the livelihoods of local residents. This study monitors the mine's expansion using satellite data available on Google Earth Engine, including both radar Sentinel-1 images and Sentinel-2 optical images. Figure 3 is Flowchart of data processing.

The processing for multi temporal Sentinel-1 images in both ascending and descending directions and Sentinel-2 to calculate the Normalized Difference Vegetation Index (NDVI) series to control the different trends from 2016 to 2021. NDVI is then employed to mask the areas with vegetation that witness no abrupt changes in the land cover. This NDVI also acts as the basis for collecting samples for Random Forest classification of the Sentinel-2 images. The results from Sentinel-1 and Sentinel-2 combined with MASK from NDVI have determined the

expansion area of the Minh Tien coal mine. The results are compared with those published on the website of Thai Nguyen Portal and have a significant similarity (Van Anh, Hanh et al. 2022).

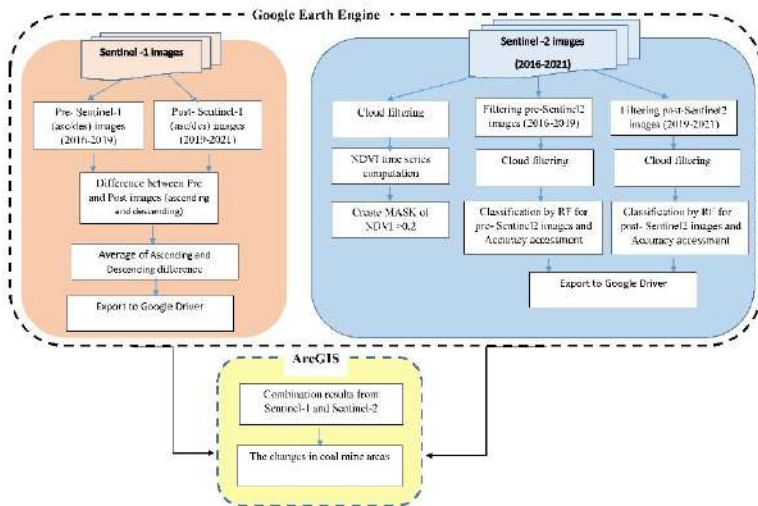


Figure 3. Flowchart of data processing

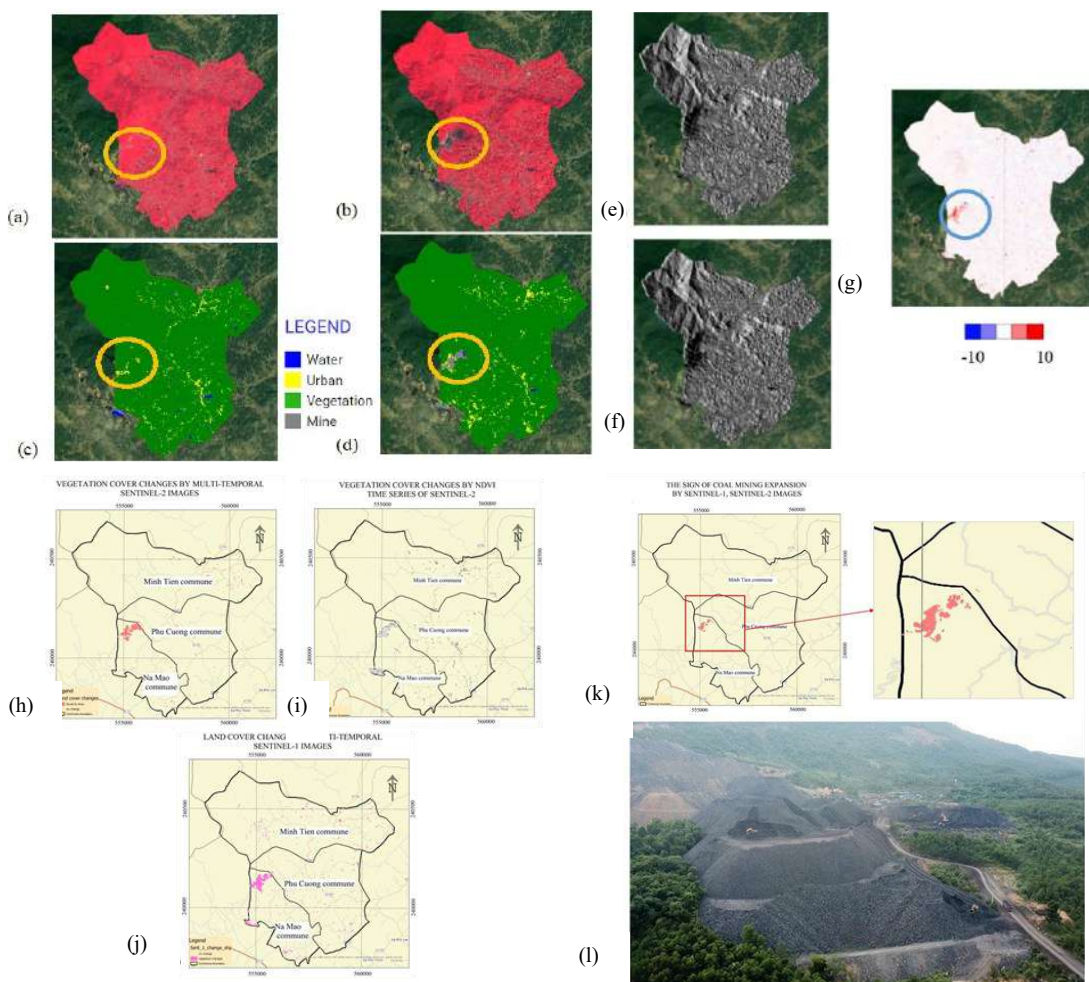


Figure 4. (a) Sentinel-2 image (2016-2019) median filter, (b) Sentinel-2 images (2019-2021) median filter, (c) RF classification image (2016-2019), (d) RF classification image

(2019-2021), (e) Sentinel-1 image before 2019, (f) Sentinel-1 image after 2019, (g) subtraction between the two times of Sentinel-1 images, (h) Land cover changes by Sentinel-2, (i) NDVI MASK, and (j) land cover changes by Sentinel-1 images. (k) Result of expansion of coal mine area from 2016 to 2021, (l) a photo at the location of the Minh Tien coal mine taken in September 2021

3.2 Building a landslide susceptibility map using SVM, RF and GB on GEE platform

Our study focuses on some of the capabilities of GEE in landslide prediction modeling. We tested three algorithms for the Van Yen area, Yen Bai, Vietnam. The study employed data from 13 factors influencing landslides, along with field survey data and PSI-InSAR analysis of Sentinel-1 imagery, to develop landslide susceptibility maps using Support Vector Machine (SVM), Random Forest (RF), and Gradient Boosting (GB) machine learning models. (Tran, Khuc et al. 2024)

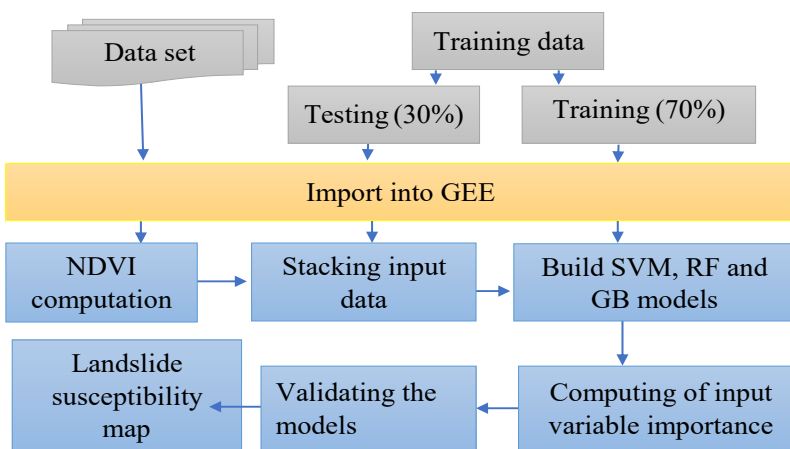


Figure 5. Flowchart of model building for landslide prediction

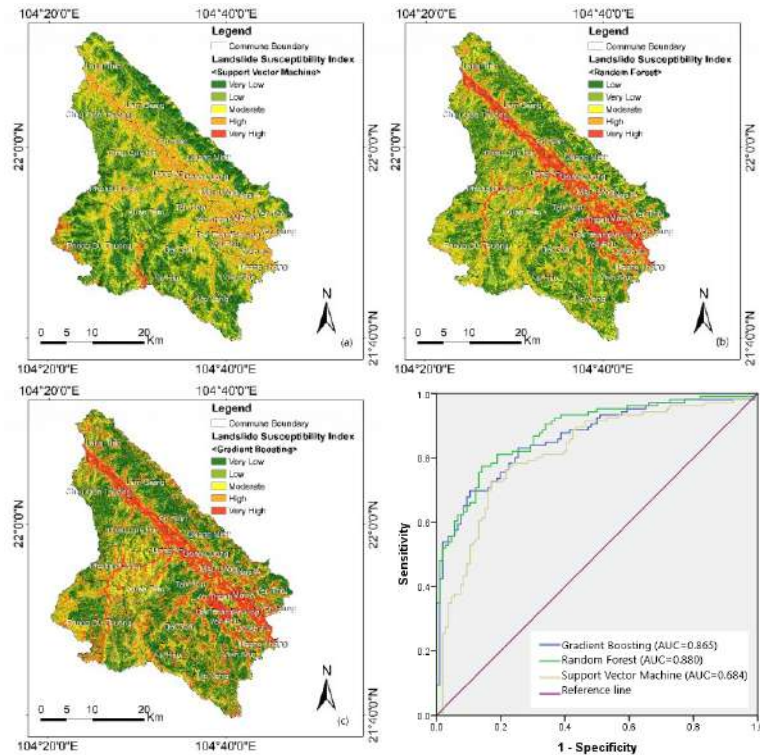


Figure 6. Landslide susceptibility map predicted by models: (a) SVM, (b) RF, (c) GB

The findings revealed that areas with high landslide susceptibility were concentrated along major transportation routes in the districts of Chau Que Ha, Phong Du Ha, and Phong Du Thuong. The results showed that the combination of models improved the accuracy of landslide susceptibility maps, with the Random Forest model outperforming Gradient Boosting and Support Vector Machine, achieving AUC values of 0.880, 0.865, and 0.684, respectively. Additionally, the Google Earth Engine (GEE) cloud platform proved highly effective by integrating vast cloud-based datasets and applying efficient machine learning algorithms to build predictive models.

3.3 Landslide monitoring on Colab GMTSAR platform based on Sentinel-1 Radar image series in the period 2019-2020

As mentioned above, GEE has the ability to obtain and process satellite image data and geospatial database sources quite well, however, for complex Radar images, GEE is not capable. PyGMTSAR was developed by Dr. Eric Fielding and his team at the Jet Propulsion Laboratory (JPL), part of the California Institute of Technology (Caltech), as part of their initiative to create accessible and efficient tools for processing and analyzing SAR data within the scientific community. PyGMTSAR is an open-source, Python-based software package designed for studying Earth's surface deformation through synthetic aperture radar (SAR) data. It integrates with GMT5SAR, another SAR data processing toolkit, and provides various features and utilities for SAR analysis. A new use case for PyGMTSAR, focusing on SBAS analysis by Alexey Pechnikov (Pechnikov 2024), is now available on Google Colab

In this study, we processed data for 18 Sentinel-1 images of Van Yen area, Yen Bai province, Vietnam to monitor landslides during the period from 2019-2020. The processing procedure is as shown in figure 6.

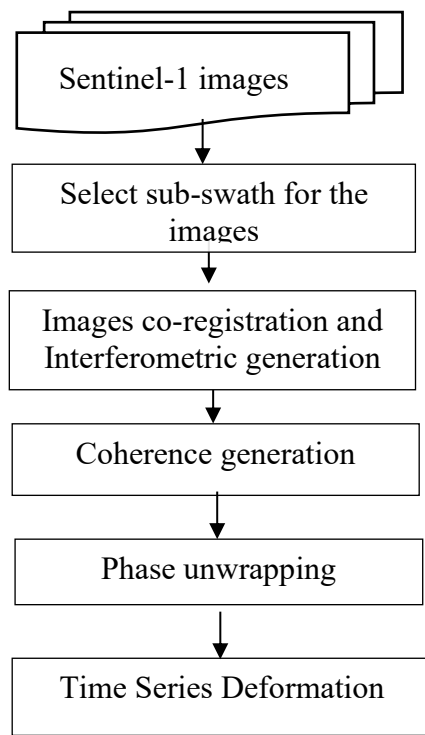


Figure 7. Flowchart of landslide monitoring on PyGMTSAR on Google Colab

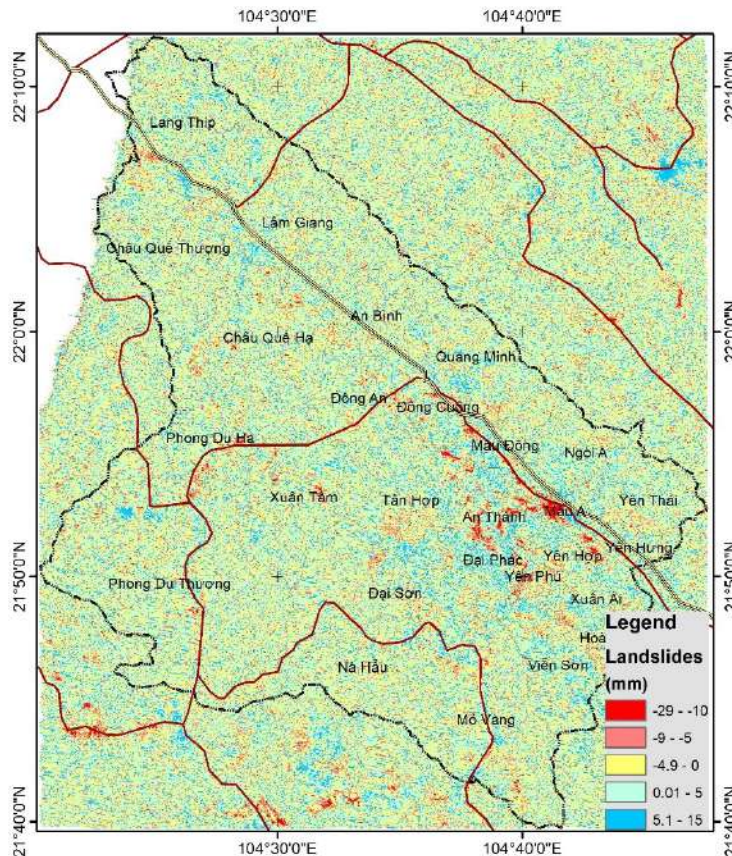


Figure 8. Landslide monitoring in Van Yen, Yen Bai, Vietnam by PyGMTSAR on Google Colab

3.4 Land Subsidence Forecasting on Google Colab Using Data Series Processed from Sentinel-1 Radar Images

As discussed above, GEE offers significant benefits by allowing us to access and process available data without the need to download it to our personal computers. However, specialized processing tools, such as machine learning and deep learning, are somewhat limited in GEE. In contrast, Google Colab, with its support for Python programming, is a valuable tool that integrates with various open-source libraries, making it effective for generating forecast maps. In this application, we highlight the use of the XGBoost machine learning algorithm for forecasting land subsidence based on results from multi-temporal radar image processing of the area around Ca Mau city from 2015 to 2023. Unlike our previous studies that used the Boosting Model to predict subsidence susceptibility, this study focused on estimating the subsidence values one year after the end of the subsidence data series (Tran, Brovelli et al. 2024), (Tran, Khuc et al. 2023). The figure 9 illustrates a subsidence forecast flowchart generated on Google Colab.

To forecast subsidence, we utilized the subsidence value series generated by the PSInSAR method for the period from 2015 to 2023. This time series included 92 subsidence data columns used as input data. A total of 5,290 PS points were selected to build the subsidence forecast model for this area. The set of points was divided, with 70% used for training the model and 30% used for accuracy evaluation. Figure 10 shows the results of land subsidence prediction interpolated by the Kriging algorithm.

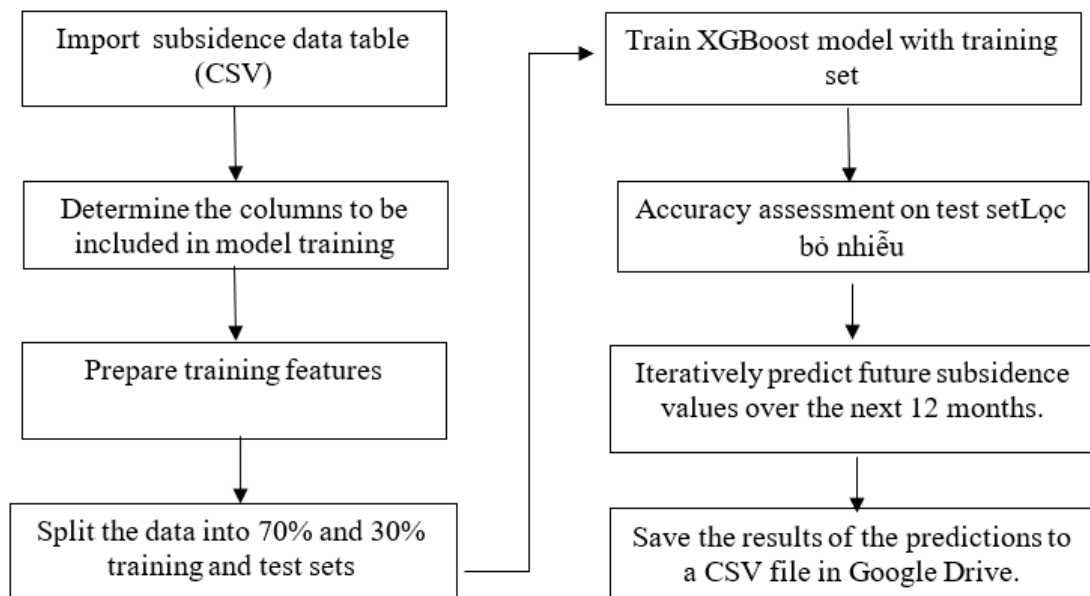


Figure 9. Subsidence forecasting diagram made on Google Colab

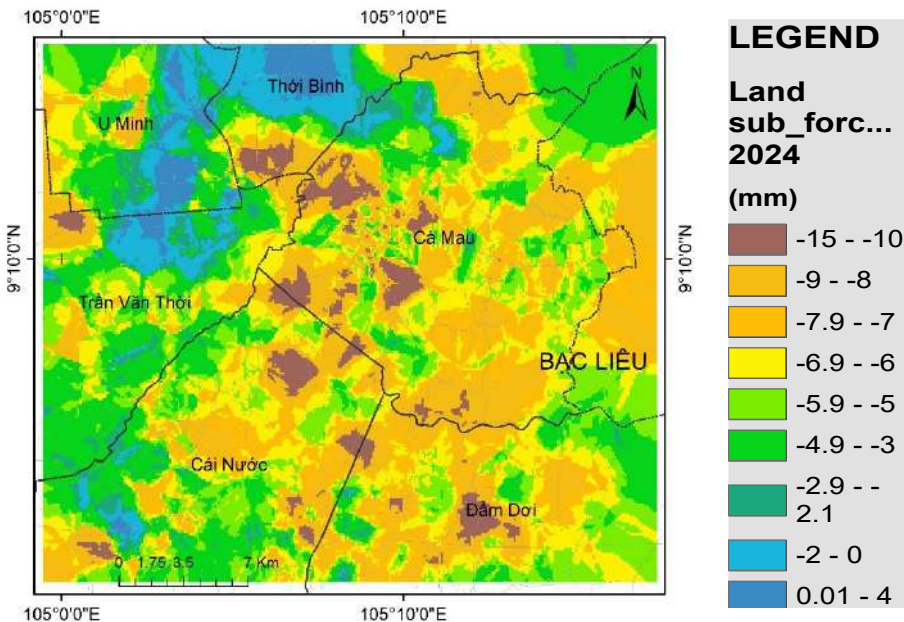


Figure 10. Subsidence forecasting map for 2024 using XGBoost algorithm

The settlement forecast was calculated for the 12 months leading up to the end of the data series, from May 2022 to May 2023. The purpose was to use this 12-month period to assess accuracy before proceeding with the forecast for the following 12 months. A total of 4,232 points were included in the forecast. Statistical metrics such as RMSE, MAE, and R² were employed to assess the accuracy. The RMSE, MAE, and R² of 12 months under assessment is presented in the table below.

Table 2. Evaluation error for 12 columns of test data

Month	RMSE (mm)	MAE (mm)	R ²
1	4.13	2.25	0.992
2	3.76	2.34	0.992
3	3.94	2.36	0.991
4	4.44	2.76	0.991
5	4.63	2.87	0.989
6	4.49	2.74	0.989
7	4.70	2.87	0.990
8	4.46	2.72	0.991
9	4.53	2.82	0.989
10	5.33	3.31	0.986
11	5.44	3.45	0.985
12	3.31	1.64	0.994
Average	4.43	2.6775	0.989

The forecasted subsidence over the 12-months was compared with the final time point in the data series from May 2023. The results indicated that the most significant subsidence occurred around Ca Mau city, with additional points around Cai Nuoc district, Tran Van Thoi,

and a few in U Minh district. Over one year, the highest recorded subsidence was -14 mm, primarily concentrated in Ca Mau city and the Cai Nuoc area.

4. CONCLUSION

In this study, four applications using the GEE and Google Colab platforms were highlighted: (1) monitoring coal mine expansion in Thai Nguyen, Vietnam, (2) creating a landslide susceptibility map with machine learning on the GEE platform in Van Yen district, Yen Bai province, Vietnam, using SVM, RF, and GB algorithms, (3) monitoring landslides from Sentinel-1 radar image series using PyGMTSAR on Colab, and (4) forecasting land subsidence using a subsidence value series from 2015 to 2023. These applications demonstrate the strengths of both GEE and Google Colab. By utilizing them, users can leverage GEE's capabilities in processing large-scale datasets and Colab's advanced data analysis tools. This combination not only streamlines workflows but also unlocks new possibilities for research and applications across various fields

5. REFERENCES

- Chi, M., A. Plaza, J. A. Benediktsson, Z. Sun, J. Shen and Y. Zhu., 2016. Big data for remote sensing: Challenges and opportunities. *Proceedings of the IEEE* 104(11): 2207-2219.
- Diebold, F. X., 2012. On the Origin (s) and Development of the Term'Big Data'.
- Gorelick, N., M. Hancher, M. Dixon, S. Ilyushchenko, D. Thau and R. Moore., 2017. Google Earth Engine: Planetary-scale geospatial analysis for everyone. *Remote sensing of Environment* 202: 18-27.
- Krishnan, S. and J. L. U. Gonzalez., 2015. Building your next big thing with google cloud platform: A guide for developers and enterprise architects, *Springer*.
- Kumar, L. and O. Mutanga., 2018. Google Earth Engine applications since inception: Usage, trends, and potential. *Remote sensing* 10(10): 1509.
- Laney, D., 2001. 3D data management: Controlling data volume, velocity and variety. *META group research note* 6(70): 1.
- Pechnikov, A., 2024. PyGMTSAR: Sentinel-1 Python InSAR. An Introduction.
- Tamiminia, H., B. Salehi, M. Mahdianpari, L. Quackenbush, S. Adeli and B. Brisco., 2020. Google Earth Engine for geo-big data applications: A meta-analysis and systematic review. *ISPRS journal of photogrammetry and remote sensing* 164: 152-170.
- Tran, A. V., M. A. Brovelli, K. T. Ha, D. T. Khuc, D. N. Tran, H. H. Tran and N. T. Le., 2024. Land Subsidence Susceptibility Mapping in Ca Mau Province, Vietnam, Using Boosting Models. *ISPRS International Journal of Geo-Information* 13(5): 161.
- Tran, V. A., T. D. Khuc, X. Q. Truong, A. B. Nguyen and T. T. Phi., 2024. Application of potential machine learning models in landslide susceptibility assessment: A case study of Van Yen district, Yen Bai province, Vietnam. *Quaternary Science Advances* 14: 100181.
- Tran, V. A., T. D. Khuc, T. K. Ha, H. H. Tran, T. N. Le, T. T. H. Pham, D. Nguyen, H. A. Le and Q. D. Nguyen., 2023. Land subsidence susceptibility mapping using machine learning in the Google Earth Engine platform. International conference on intelligence of things, Springer.
- Van Anh, T., T. H. Hanh, N. Q. Nga, L. T. Nghi, T. X. Quang, K. T. Dong and T. T. Anh .,2022. Determination of illegal signs of coal mining expansion in Thai Nguyen Province, Vietnam from a combination of radar and optical imagery. *International Conference on Geo-Spatial Technologies and Earth Resources*, Springer.
- Wilder, B., 2012. Cloud architecture patterns: using Microsoft azure, O'Reilly Media, Inc..

GEOLOGICAL CONSIDERATION FOR DEVELOPMENT IN BANDING ISLAND, MALAYSIA USING REMOTE SENSING AND GIS

Mohammad Firuz Ramli¹, Zulkifle Abd Latif² and Nasyairi Mat Nasir³

Department of Environment, Faculty of Forestry and Environment, Universiti Putra Malaysia, Malaysia

ABSTRACT

Development in steep hilly area is consistently at risk of landslides. Banding Island in Malaysia was originally a summit of a hill with steep slopes on both sides, but became an island after the surrounding areas was inundated, turning it into parts of Temenggor Dam. The main objective of this study was to investigate the effect of development to landslide occurrences in Banding Island, Malaysia utilising archived remote sensing data within the geographical information system (GIS) environment. Free archived Landsat imagery had been used to illustrate the development history of the area and its relationship to the landslide occurrences. The results indicated that slopes cleared for road construction were more prone to landslides compared to the areas that were not cleared. This paper demonstrates that integrating remote sensing and GIS is effective for incorporating geological consideration in planning development in hilly area.

MAPPING SOIL POLLUTION IN CAMAU CITY, VIETNAM

Ho Dinh Duan

³Corresponding author, Mien Trung Institute for Scientific Research, Hue, Vietnam
Corresponding Email: duanhd@gmail.com

ABSTRACT

Camau city is located in far south of Vietnam, and recently experienced a fast social-economic development, in the same rhythm of the Mekong delta region. As a result, an environmental degradation has been seen. This paper focuses on the heavy metal soil pollution, which comes from various factors, including industrialization, as well as agricultural and fishery activities. Soil and water samples from surveys carried out by the provincial Department of Natural Science and Environment (Camau DONRE) in 2021 and 2022 were used for assessment of typical heavy metal contamination: Cu, Pb, Zn, Cd and As. The IDW spatial interpolation was employed for building the pollution map. In addition, we have based on the point source of pollution map to verify the contamination map just created and classify the level of harmful affects caused by these potential sources. For this purpose, the Dice coefficient was used to assess the dissimilarity between two subsets in an image. The findings of this study may help the local government regulate and mitigate the environmental degradation in this area.

Keywords: Heavy metal, soil pollution, IDW interpolation, point source pollution, Dice coefficient, Camau city

IDENTIFICATION OF MORPHOLOGICAL FEATURES IN SLOPE FAILURE AREAS DUE TO HEAVY RAINFALL USING CHANGE VECTOR ANALYSIS AND RANDOM FOREST CLASSIFIER

Mitsunori Ueda, Nemoto Tatsuya, Venkatesh Raghavan

Identification of slope failure areas is essential for solving geological hazard problems such as disaster prevention, urban planning and land development. Slope failure areas are identified by human interpretation using aerial photographs and satellite images. However, manual interpretation has the problem of requiring a lot of time and labor. Furthermore, objectivity is insufficient due to differences in human interpretation. Therefore, there is a need for development of technology to automatically detect slope failure areas. Also, in order to understand the characteristics of the slope failure, it is necessary to investigate the relationship between the structures inside the slope failure areas, such as the scarp and main body. Slope failure is a phenomenon that creates spatially irregular terrain in a short time. In this study, we automatically identified slope failure areas with focus on temporal changes. Change Vector Analysis (CVA) and Random Forest Classifier (RFC) were used to identify scarp and main body in slope failure areas from changes in the Digital Elevation Models (DEMs) during two periods. CVA compares paired images from two different time periods and numerically analyzes the changes between the two periods by expressing them as the vector. In this study, changes in pairs of topographic features were analyzed using CVA. RFC was used to extract slope failure areas using change vectors as training data. The study area is located in a part of Tamba city in Hyogo prefecture, Japan. The target to be identified is the slope failure that occurred due to heavy rainfall in 2014. In this research, 1 m DEMs were generated from airborne laser survey data acquired before and after slope failure event. Topographical characteristics were calculated from the DEMs at the two time periods and the pairs of each topographical features were combined. The results of the CVA showed different characteristics depending on the strength and direction of the change vector. The strength of the change vector suggested the possibility of determining the slope failure areas from the histograms. The direction of the change vector indicated that they could be useful for classifying scarp and main body in slope failure from the distribution of values. As the result of RFC, the learning features which contributed most to learning were the pair of terrain normal vectors and their variances, the second was the pair of elevation and Laplacian and the third was the pair of elevation and slope angle. The feature importance in RFC revealed that the geometric characteristics of the terrain significantly contributed to the classification, while the terrain conditions had a minimal impact on the learning process. The extraction accuracy was verified using the Cohen's kappa statistic. The result of accuracy was 0.75, which corresponds to "Substantial". The results of extraction using the RFC were generally good. However, there were misinterpretations in the rivers and non-slope failure areas. This study focused on the changes in topographical characteristics from DEMs acquired before and after the event and identified scarp and main body in the slope failure areas. Identification of slope failure areas using topographical changes is useful for quickly generating the inventory maps of slope failure. Also, allows geological hazard mapping and updating, including location, shape, and morphology information of slope failure. Furthermore, revealing morphology of slope failure will be useful in predicting slope failures. The methodology described in this paper can be applied to pre and post failure DEM derived from InSAR or high-resolution global DEM such as AW3D.

INVESTIGATION OF MACHINE LEARNING MODELS FOR SLOPE FAILURE SUSCEPTIBILITY ZONATION IN PARTS OF YEN BAI PROVINCE, VIETNAM

Tran Tung Lam, Tatsuya Nemoto, Venkatesh Raghavan, Xuan Quang Truong

GIS-IDEAS Oral Presentation

Yen Bai Province in northern Vietnam, especially Mu Cang Chai (MCC) and Van Yen (VY) districts, are highly susceptible to slope failure due to rugged terrain, high rainfall and anthropogenic activities . In this research MCC was used as an area for training and testing the machine learning models, while VY serves model validation due to similar topographic and geological conditions.

The methodology treats the slope failure prediction as a binary classification task (landslide/no-landslide). A balanced dataset of 286 landslide and 286 non-landslide points in MCC, along with 16 contributing factors, including topographic, geologic, hydrologic, anthropogenic and vegetation factors calculated from open data sources and made use from existing databases and from previous research on the area. Principal Component Analysis (PCA) and Pearson Correlation Coefficients refine the dataset by evaluating correlated factors and removing the least important ones, the size of the training dataset can be reduced while ensuring the performance of the ML models. Four ML models: Random Forest (RF), Support Vector Machine (SVM), Logistic Regression (LR), and Extreme Gradient Boosting (XGBoost) are trained and evaluated to select the best hyperparameter tuning for each model. Model accuracy is assessed via confusion matrices, accuracy score, ROC (Receiver operating characteristic) curves and AUC (Area under the ROC Curve).

Results show the models perform effectively in MCC with the average accuracy of all models being 0.74. The trained ML models with tuned hyper-parameters after running on MCC data, was validated on datasets for VY. The VY data also consists of 16 factors, with a data set of 308 landslide/non-landslide points. RF and XGBoost have the highest accuracy for both training and testing area (MCC) and Validation area (VY), with XGBoost showing a slightly higher accuracy score of 0.83 while RF scores 0.80.

The XGBoost model produces good results and could be further optimized to achieve even better zonation in future studies. The machine learning workflow can be applied on other areas that are prone to slope failures. Other geologic and weathering factors could be included in the analysis to further improve the model.

ADVANCING GEOSCIENCE AND GEOSPATIAL AWARENESS THROUGH EDUCATIONAL OUTREACH: THE CERG STORY

Natraj Vaddadi; Keynote Talk
Centre for Education & Research in Geosciences, Pune, India

Geoscience and geospatial knowledge are foundational to understanding the Earth's processes and addressing many environmental challenges humanity faces today. In an effort to promote geoscience literacy, a variety of outreach activities have been developed by The Centre for Education and Research in Geosciences (CERG), India. These programs, aimed at both laypeople and students, emphasize the importance of Earth Science in daily life and foster an appreciation of the interdisciplinary nature of geoscience. This abstract highlight several key outreach initiatives designed to inspire the next generation of geoscientists and raise awareness about the importance of geospatial techniques.

The Key programs include:

- **Geoween Celebration:** An annual event with activities like mineral, fossil, and poster exhibits, contests, workshops, and film screenings to explore Earth Science's influence on everyday life.
- **Geoquest:** An interschool Earth Science quiz fostering curiosity about Earth processes and environmental challenges.
- **Geolab Project Contest:** A platform for students to present innovative geoscience-related solutions, often incorporating fields like IT, data science, and biology.
- **Geotrails:** Guided field trips for school children to observe volcanic and geomorphic features in Pune, Maharashtra.
- **Jal Katha:** An international short film festival focused on water conservation and responsible water use.
- **Maps & Me Workshop:** Introducing students to geospatial technologies and open-source mapping tools for real-world problem-solving.

Overall, CERG's outreach programs serve as powerful tools for building geoscience and geospatial awareness among the public, particularly schoolchildren. By offering a range of interactive, interdisciplinary, and engaging activities, these programs help cultivate a new generation of environmentally conscious individuals who understand the importance of Geosciences in addressing the pressing challenges of today's world. Through hands-on learning and real-world applications, these initiatives are fostering a deeper appreciation of Earth Science and inspiring young students to consider careers in this vital field. As the need for geospatial awareness and geoscience literacy continues to grow, these outreach activities provide a blueprint for how education and public engagement can be successfully intertwined to build a more informed and responsible society.

ESTABLISHMENT OF GROUNDWATER DATABASE IN THE COASTAL AREA OF SOC TRANG PROVINCE BY USING QGIS

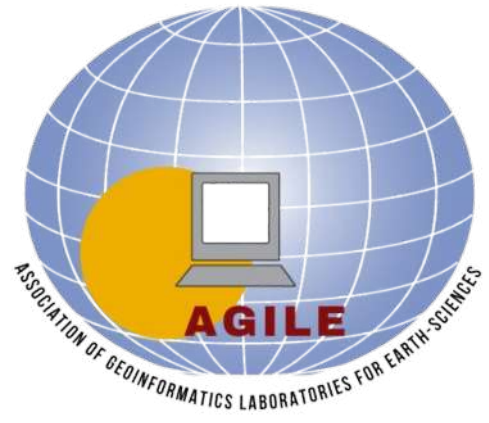
Nguyen Vo Chau Ngan

GIS-IDEAS Oral Presentation

The research was conducted to support the management of exploitation and use of underground water for Ward 2, Vinh Chau town, Soc Trang province, Vietnam. A total of 1,504 households with wells were interviewed directly about water use. In addition, water samples from 9 wells were also collected and measured for quality parameters. Survey information was compiled and then established into a database using QGIS software. Households exploit groundwater for daily life and crop irrigation with 73.54% and 72.54%, respectively. Additionally, households use groundwater for the purpose of aquaculture. Most households do not treat water used for daily life purposes. The water used to irrigate crops increases in the dry season, causing difficulties for households using conventional water pumps. Households must upgrade water pumps through the most common forms: syringes, air pumps, and rocket pumps. Water source quality is still within allowable standards for pH and TDS parameters. Several specific maps have been built with the database built with QGIS software, and users can retrieve information according to personal requirements. Research results have been transferred to authorities to exploit and support the management of underground water resources.

AGILE

The **Association of Geoinformatics Laboratories for Earthsciences (AGILE)** is a professional organization focused on advancing education, research, and international collaboration in geoinformatics, particularly within the field of Earth sciences. Headquartered in Osaka City, AGILE fosters the development and dissemination of geoinformatics knowledge and technology through a variety of targeted activities.



Objectives

AGILE seeks to:

1. Provide advanced professional education and promote the dissemination of geoinformatics technologies.
2. Enhance global and mutual collaboration among researchers in Earth sciences through the presentation and discussion of scientific research.
3. Promote the development and adoption of open-source software, open data, and related technologies.
4. Support the international growth of geoinformatics through partnerships with academic and professional institutions worldwide.

Key Activities

To achieve its mission, AGILE engages in the following core activities:

1. **Academic Events:** Organizing and supporting conferences, research meetings, and symposiums to facilitate the exchange of ideas and research findings.
2. **Publications:** Producing academic journals and other materials to disseminate cutting-edge knowledge.
3. **Workshops:** Conducting hands-on workshops to promote skill development in geoinformatics.
4. **International Collaboration:** Building bridges with academic societies and institutions globally to foster innovation and shared learning.
5. **Auxiliary Activities:** Undertaking additional initiatives aligned with its primary goals, ensuring continuous progress in the field.

AGILE stands as a dynamic platform for advancing geoinformatics in Earth sciences, prioritizing open knowledge, international collaboration, and professional growth.

THE GIS-IDEAS JOURNAL



The GeoInformatics for Spatial-Infrastructure Development in Earth & Allied Sciences (GIS-IDEAS) Journal, hereafter referred to as "The GIS-IDEAS Journal," traces its origins to the biennial international conference organized under the aegis of the Japan-Vietnam Geoinformatics Consortium (JVGC) since 2002.

In response to growing interest and continued patronage, we have undertaken the initiative to launch the Open Access GIS-IDEAS Journal under the tutelage of the Association of GeoInformatics Laboratories for Earthsciences (AGILE), the new name adopted by JVGC as of August 1, 2024.

The GIS-IDEAS Journal aims to promote academic exchanges through the publication of high-quality, peer-reviewed research articles and review papers in the field of Geoinformatics. It will be managed by an International Editorial Board comprising scholars who have been closely involved in organizing the GIS-IDEAS Conference Series.

The inaugural issue (Vol. 1, No. 1) is scheduled for release in the first quarter of 2025, with subsequent issues to be published quarterly. Further details about the journal will be announced during the GIS-IDEAS 2024 event.

The GIS-IDEAS Journal (TGIJ) will be a peer reviewed journal published by the Association of GeoInformatics Laboratories for Earthsciences (AGILE) . TGIJ is issued 4 times a year in electronic form, publishes Original Research Articles and Review Papers in all aspects of result research in the field of GeoInformatics. We encourage all interested contributors to submit their work for consideration.

Focus and Scope

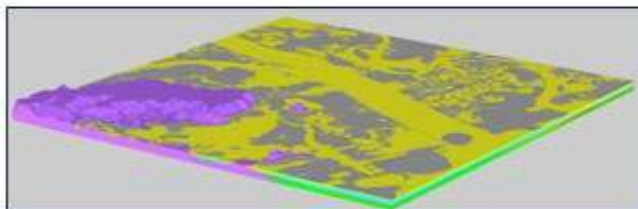
Journal of GIS Ideas is dedicated to publishing high-quality research papers and reviews on terrestrial and marine topics, including geomatics, geophysics, geography, geology, geographic information systems, remote sensing, cartography, oceanography, hydrography, and marine science and technology.

The GIS-IDEAS Journal (TGIJ) focuses on theoretical, empirical, and applied research in geoinformatics and geosciences.

We look forward to your continued support in establishing the GIS-IDEAS Journal as a respected publication within the Geoinformatics community.

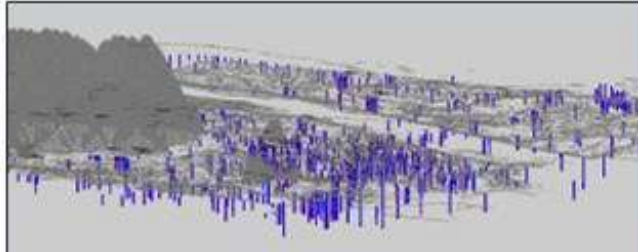
UTILISING JAPAN'S OPEN GEO-INFORMATION DATA TO PROTECT THE LAND FROM DISASTERS

TOPOGRAPHIC & GEOLOGICAL MAPS

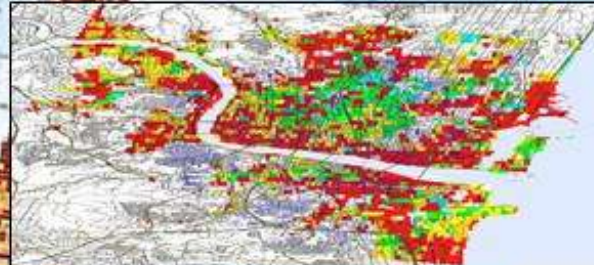


OPEN GEO-TECHNICAL DATABASE By NGIC

UTILISATION OF GEO-TECHNICAL DATA



EXTRACTION OF HAZARDS



RECONSTRUCTION TOWN PLANNING



Japan Geotechnical Consultants Association (ZENCHIREN)
1-5-13, Uchikanda, Chiyoda-ku, Tokyo, 101-0047, Japan
TEL : +81-3-3518-8873 FAX : +81-3-3518-8876



Map Solution Innovative ally for your business

Modern Geomatics Platform

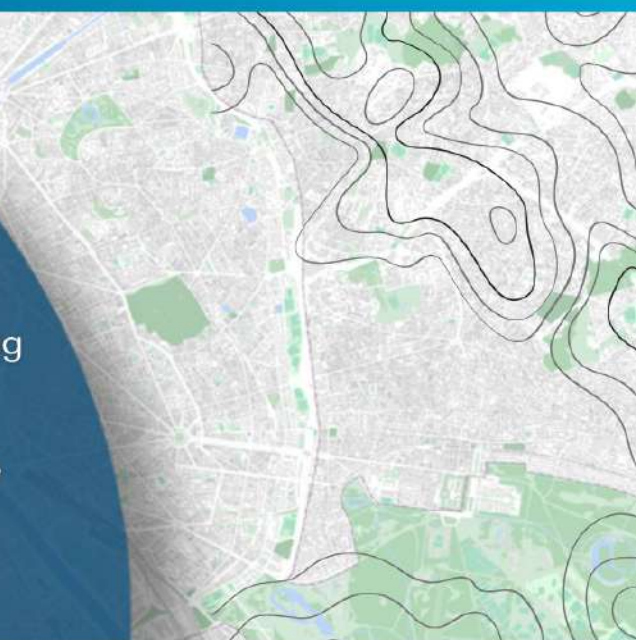
 vallarismaps.com ↗





OUR SERVICES

- ▶ **1** Provides consulting services in the field of GIS and open source IDS, and offers technical support services on some open source software.
- ▶ **2** GeoLabs puts all its expertise at your service during technical training in geomatics and open source webmapping.
- ▶ **3** GeoLabs has advanced skills in computer science and geomatics that it mobilizes to design innovative solutions.
- ▶ **4** GeoLabs hosts your GIS or IDS and optimizes the performance of your web infrastructures.



FLAGSHIP PRODUCTS

ZOO-Project

ZOO-Project is a WPS (Web Processing Service) implementation written in C, Python and JavaScript. It is an open source platform which implements the WPS 1.0.0 and WPS 2.0.0 standards edited by the Open Geospatial Consortium (OGC).

Download

Install

Execute



WPS Server

ZOO-Kernel is a powerful server-side C Kernel able to manage and chain WPS services



WPS Services

ZOO-Services is a collection of ready to use WPS services based on open source libraries.



WPS API

ZOO-API is a server side Javascript API for creating and chaining WPS Services.



WPS Client

ZOO-Client is a JavaScript library for interacting with WPS Services from web applications.

- **WPS Standards (1.0.0 and 2.0.0)**
- **OGC API - Processes - Part 1: Core Standard**
- **OGC API - Processes - Part 2: Deploy, Replace, Undeploy draft specification**
- **OGC API - Processes - Part 3: Workflow draft specification (cc: remote-processes)**

zoo-Project provides a developer-friendly framework for creating and chaining services (processes). Its main goal is to provide generic and standard-compliant methods for using existing open source libraries.



MapMint

MapMint4Me



Manage your **Geoportal** on your **browser**. only a few clicks away...

Monitor ... **Transform** ... **Map** ... **Publish** ... **Share** ...



Fast & easy to use

MapMint is designed to help individuals and organizations to publish quality web maps. No coding required.



Highly customizable

MapMint provides numerous features to design quality maps and publish advanced webmapping applications.



Standards-compliant

MapMint implements various geospatial and web standards and provides an interoperable and extensible architecture.

- Advanced geospatial analytics
- WPS, WMS, WFS, WCS and WMTS auto setup
- Users and groups management
- +100 GIS data formats supported
- Convert, reproject, encode and query vector data
- Convert, reproject and process raster data
- Powerful mapfile-based project manager
- Advanced layer manager, editor and styler
- Create base layers from your data



GeoLabs SARL

Futur Building 1
1280, Avenue des Platanes
34970 LATTES FRANCE



+ (33) 670082539



Osaka
Metropolitan
University



Open
Geospatial
Consortium



contact@geolabs.fr



www.geolabs.fr



This work is licensed under a Creative Commons Attribution 4.0 International License. Re-users are allowed to copy, distribute, and display or perform the material in public. Adaptations may be made and distributed.

ISBN: 978-4-99140-750-5

A standard linear barcode representing the ISBN number 978-4-99140-750-5.

9 784991 407505

NOT FOR SALE